



**Development and Verification of Injection  
Systems for Proton Transfer Reaction  
Mass Spectrometry (PTR-MS) Analysis of  
Diverse Volatile Organic Compounds**

Thesis submitted for the degree of

Doctor of Philosophy

at the University of Leicester

By

Milan Ashvinbhai Patel

Department of Chemistry

University of Leicester

January 2015

## **Statement of Originality**

This thesis is based on work conducted by the author in the Department of Chemistry at the University of Leicester mainly during the period of October 2006 and April 2013.

All the work recorded in this thesis is original unless otherwise acknowledged in the text or by references.

.....

M. A. Patel

January 2015

# Direct Injection Proton Transfer Reaction Time of Flight Mass Spectrometer

Milan Ashvinbhai Patel

## Abstract

The PTR-MS is the well-established technique in the field of analysis of volatile compounds from air, food and breath. The principal advantage of the technique is real time analysis, high sensitivity and less fragmentation. However, this technique requires the samples in the gas phase and therefore, liquid samples cannot be analysed directly. The leading focus of this thesis was to develop a technique that will enable the use of the aqueous sample to extend the application of the PTR-MS.

This thesis documents the design and calibration of the sample inlet systems and subsequent application development. The initial work dedicated to develop and calibrate the heated inlet system (HIS) to inject the aqueous sample, volatile organic solvent sample and headspace above the liquid sample. The subsequent development and calibration of the capillary inlet system (CIS) for the continuous injection of the aqueous sample is documented in this thesis. Applications for the environmental, food and diagnostic field were developed.

In the environmental field, identification and calibration of the pesticide compounds from the water was performed. Acceptable sensitivity and limit of quantification ( $\sim 1.0 \mu\text{g/mL}$ ) was achieved for organophosphate pesticides used in the experiments. Further work is required to improve the sensitivity and lower the limit of quantification to  $\text{ng/mL}$  levels instead of  $\mu\text{g/mL}$  levels. Additional work is required for the detection and quantification for the chlorinated pesticides, as PTR-ToF-MS instrument used in this thesis is not able to detect these pesticides. For the food field, Scotch whiskies were successfully characterised based on their VOC profiles. Lastly, for the diagnostic field, urine headspace from five volunteers was analysed, to identify and to quantify different VOCs. Different VOCs (different ketones and aldehydes) were successfully identified and quantified. The precision of the measurement for acetone and acetaldehyde was 13.7% and 15.6%, respectively. Further work with bigger pool of volunteers, and a technique in which urine samples can be injected directly is required to establish the database for the VOCs and to improve the sensitivity of VOCs. Lastly, a two-stage technique was developed to identify isobaric compounds that are chemically different but have a similar mass. For example, butanal which is an aldehyde and butanone, which is a ketone, are chemically different but both compounds have a mass of 72 amu.

In this thesis, as stated above, it is documented that liquid samples can be analysed by using PTR-MS, but further work is required to resolve the issues like contamination and handling of large sample volume.

## Acknowledgements

I would first like to thank my supervisors Professor Andrew M Ellis and Professor Paul M Monks for giving me the opportunity to work on such an interesting project, and for their advice and assistance throughout my Ph.D. It has been a pleasure to work within the Atmospheric Chemistry group over the past few years. I would also like to thank the other members of the group, with whom I was fortunate enough to work alongside Kevin Wyche, Kerry Wills, Rebecca Cordell, Ian White, Zoë Fleming, Karun Arunasalam, Shane Barber, Ian Goodall and Sharmilah Kuppusami. I would also like to thank the staff within the Department of Chemistry workshops for their valuable technical support.

I must say a special thank you to Robert Blake for all the help and expertise, received throughout my PhD, which was always greatly appreciated.

On a more personal note, I am extremely grateful to my employer to give me the time and encouragement to pursue for my PhD. My final and greatest thanks go to my family for their constant love and support throughout the whole of my academic career and without whom none of this would have been possible, so I thank and dedicate this thesis to my mother Chandrakantaben Patel, my wife Bhoomi Patel and, my brother Snehal Patel.

## TABLE OF CONTENTS

### Chapter 1: An Introduction to the Direct Injection Mass Spectrometry

1.1	Introduction and thesis outline .....	18
1.2	KEY TECHNOLOGIES .....	23
1.2.1	MS-e-noses .....	24
1.2.2	APCI .....	25
1.2.3	PTR-MS and SIFT-MS.....	27
1.2.4	PTR-MS.....	28
1.2.5	SIFT-MS .....	30
1.2.6	DART (Direct Analysis in Real Time).....	32
1.3	APPLICATIONS.....	34
1.3.1	Environmental measurement.....	34
1.3.2	Food analysis.....	35
1.3.3	Diagnostic analysis .....	38
1.4	SUMMARY .....	40
1.5	REFERENCES:.....	40

### Chapter 2: Proton Transfer Reaction Time of Flight Mass Spectrometry: Instrumentation and Operation

2.1	Introduction .....	48
2.2	PROTON TRANSFER REACTION MASS SPECTROMETRY .....	48
2.2.1	Instrumentation .....	48
2.2.2	Proton transfer reaction .....	53
2.2.3	Cluster ion chemistry .....	55
2.2.4	Time-of-Flight Mass Spectrometry .....	56
2.3	The Leicester PTR-ToF-MS Instrument .....	61

2.3.1	Overview .....	61
2.3.2	Gas inlet system .....	62
2.3.3	Ion source and drift tube .....	63
2.3.4	Mass analyser and detection .....	65
2.3.5	Data collection, processing and normalisation.....	66
2.3.6	PTR-ToF-MS mass spectrum and mass resolution..	68
2.4	REFERENCES: .....	69

### **Chapter 3: Calibration of Standards in Liquid and Liquid Headspace by Heated Inlet Source (HIS)**

3.1	Introduction .....	73
3.2	Source design .....	76
3.3	Experimental procedure .....	79
3.3.1	HIS and PTR-ToF-MS Settings.....	79
3.3.2	Reagent .....	79
3.3.3	Preparation of Liquid Standards .....	80
3.3.4	Sample Injection .....	81
3.3.5	Liquid headspace analysis.....	82
3.4	Results and discussion .....	83
3.4.1	Dynamics of Liquid Injections .....	83
3.4.2	Analytical tests and calibrations .....	87
3.5	Conclusions .....	99
3.6	REFERENCES .....	101

### **Chapter 4: Calibration of Standards Solutions Using a Capillary Inlet Source (CIS)**

4.1	Introduction .....	104
4.2	SOURCE DESIGN .....	106

4.2.1	Overview .....	106
4.2.2	Source construction .....	107
4.2.3	Source heating .....	109
4.3	EXPERIMENTAL .....	112
4.3.1	PTR-ToF-MS.....	112
4.3.2	Gases and reagent .....	112
4.3.3	Liquid Standards.....	113
4.3.4	Sample Injection .....	113
4.4	RESULTS.....	115
4.4.1	Effect on Hydronium Ion.....	115
4.4.2	Calibration of Different VOCs .....	117
4.5	CONCLUSION.....	121
4.6	References .....	123

## **Chapter 5: Characterisation of Whiskey Using PTR-TOF-MS**

5.1	INTRODUCTION.....	124
5.2	EXPERIMENTAL .....	127
5.2.1	Experimental set-up.....	127
5.2.2	Whisky and other reagent used for the experiments.....	128
5.2.3	Sample preparation .....	129
5.2.4	Ethanol standard solutions .....	130
5.2.4.1	Direct injection and headspace .....	130
5.2.5	Data collection and analysis.....	131
5.3	RESULTS AND DISCUSSION .....	131
5.3.1	Ion chemistry and effect of ethanol on hydronium .....	131
5.3.2	Analyte Identification.....	137

5.3.3	Precision of the measurement of ethanol from Whisky samples.....	141
5.3.4	Whisky Discrimination .....	142
5.4	CONCLUSION.....	145
5.5	REFERENCES:.....	147

## **Chapter 6: Headspace and Direct Analysis of Urine by HIS-PTR-TOF-MS**

6.1	Introduction .....	152
6.2	EXPERIMENTAL .....	155
6.2.1	Experimental set-up.....	155
6.2.2	Sample collection, storage and reagents.....	155
6.2.3	Sample preparation .....	156
6.2.4	Headspace and direct injections.....	157
6.2.5	Calculations.....	158
6.3	RESULTS AND DISCUSSION .....	158
6.3.1	Comparison of VOC profiles from direct injection and headspace analysis.....	158
6.3.2	Influence of salt, acid and base.....	161
6.3.3	VOC characterisation .....	163
6.3.4	Ammonia.....	168
6.3.5	Ketones .....	170
6.3.6	Aldehydes.....	174
6.3.7	Acetonitrile .....	178
6.3.8	Dimethyl amine and Trimethyl amine .....	180
6.3.9	Benzene and toluene .....	182
6.3.10	Alcohols.....	184
6.3.11	Urine headspace analysis vs. Breath analysis.....	186
6.4	CONCLUSION.....	187

6.5	REFERENCES: .....	189
-----	-------------------	-----

## **Chapter 7: Detection and Analysis of Semi-Volatile Pesticide Compounds From Water by HIS-PTR-TOF-MS**

7.1	Introduction .....	197
7.2	EXPERIMENTAL .....	200
7.2.1	Instrumental set-up .....	200
7.2.2	Sample Preparation .....	200
7.2.2.1	Reference material and reagent .....	200
7.2.2.2	Liquid-liquid extraction and direct water injection. ... .....	202
7.3	RESULTS AND DISCUSSION .....	203
7.3.1	Extraction solvent and effect of sample on Hydronium .....	203
7.3.2	Direct injection vs. Liquid-liquid extraction .....	208
7.3.3	Pesticides identification by PTR-MS .....	209
7.3.4	Limit of Detection of Pesticides by PTR-MS .....	211
7.3.5	Parathion and Methyl parathion .....	213
7.3.6	Diazinon .....	215
7.3.7	Fenthion .....	217
7.3.8	Triazophos .....	219
7.3.9	Pirimiphos-methyl .....	221
7.3.10	Phorate and Atrazine .....	223
7.4	CONCLUSION .....	224
7.5	REFERENCES .....	228

## **Chapter 8: Two-stage Proton Transfer Reaction Time of Flight Mass Spectrometry**

8.1	Introduction .....	232
8.2	EXPERIMENTAL .....	234
8.3	RESULTS.....	237
8.3.1	Two-Stage PTR-MS.....	237
8.3.2	Butanal and Butanone .....	238
8.3.3	Methacrolein and methyl vinyl ketone.....	240
8.3.4	Hexanal/2-hexanone/3-hexanone.....	241
8.3.5	Quantification of isobaric components .....	243
8.4	CONCLUSION.....	245
8.5	REFERENCES:.....	246

## **Chapter 9: Summary and future direction**

9.1	INTRODUCTION.....	249
9.2	INLET SOURCES AND LIQUID INJECTION FOR PTR-MS .....	249
9.3	CHARACTERISATION OF WHISKY .....	252
9.4	HEADSPACE AND DIRECT ANALYSIS OF URINE ....	253
9.5	ANALYSIS OF SEMI-VOLATILE COMPOUNDS .....	254
9.6	TWO-STAGE PTR-MS.....	256
9.7	FINAL COMMENTS .....	256
9.8	REFERENCES:.....	257

## LIST OF TABLES

Table 1.1	Comparison of the main characteristics of the typical implementations of the on-line DIMS methods considered [1].	28
Table 2.1	Proton affinity of different compounds.	50
Table 3.1	The limit of detection (pmol/l) for different compounds when injected in different matrix.	91
Table 3.2	The sensitivity (pmol/l) for different compounds when injected in different matrix.	94
Table 4.1	The sensitivity (pmol/l) for different compounds when injected in different matrix.	115
Table 4.2	The limit of detection (pmol/l) for different compounds when injected in different matrix.	116
Table 5.1	The precision data for ethanol from five whisky samples.	141
Table 6.1	The precision of the measurement for the VOCs.	166
Table 6.2	The bias of the measurement for the VOCs.	167
Table 6.3	Concentration of ammonia in nmol/Litre from the urine of five healthy volunteers.	169
Table 6.4	Concentration of ketones in $\mu\text{mol/Litre}$ from the headspace analysis of urine from five healthy volunteers.	172
Table 6.5	Concentration of aldehydes in nmol/l from the headspace analysis of urine from five healthy volunteers.	176
Table 6.6	Concentration of acetonitrile in $\mu\text{mol/Litre}$ from the headspace analysis of urine from five healthy volunteers.	179
Table 6.7	Concentration of DMA and TMA in nmol/Litre from the headspace analysis of urine from five healthy volunteers.	181
Table 6.8	Concentration of Benzene and Toluene in nmol/Litre from the headspace analysis of urine from five healthy volunteers.	183
Table 6.9	Concentration of Methanol, Ethanol and Propanol in nmol/Litre from the headspace analysis of urine from five healthy volunteers.	185
Table 7.1	Physical property of the pesticides.	201
Table 7.2	Proton affinity of neutral molecules and anions.	207

Table 7.3	Limit of detection	210
Table 8.1	Comparison of aldehyde and ketone proton affinities relevant to this work.....	237
Table 8.2	Outcome of hexanal proton affinity bracketing experiments.....	242
Table 8.3	Quantitative experiment results on a mixture of MA and MVK.....	245

## LIST OF FIGURES

Figure 1.1	Diagram of MS-e-nose approach [1].....	25
Figure 1.2	Diagram of APCI source .....	26
Figure 1.3	Schematic diagram of Ionicon PTR-MS.....	30
Figure 1.4	Principles of SIFT-MS, image taken from [1].....	31
Figure 1.5	Schematic diagram of the DART ion source [1] .....	34
Figure 2.1	Diagram to show the basic components and principles of a linear ToF-MS system (adapted from Wyech (2008)) [4]. .....	57
Figure 2.2	Photograph showing the Leicester PTR-ToF-MS instrument .....	62
Figure 2.3	A schematic diagram of the PTR-ToF-MS instrument .....	62
Figure 2.4	A schematic diagram of the drift tube. E1 – E6 represents electrodes 1 – 6 and R1 – R6 represents resistors 1 – 6, of which R1 – R5 are fixed a 1 M $\Omega$ and R6 is variable between 0 – 1 M $\Omega$ . S1, V1, PG and PO refer to the sample and vapour inlets, pressure gauge and pump outlet respectively. The main drift cell region is located between E1 and E6 and the collision cell between E6 and ground (G); the two regions can be operated at different E/N values (Diagram adapted from Wyech (2008)) [4]. .....	64
Figure 2.5	Comparison of raw (top) and processed (bottom) PTR-ToF-MS mass spectrum [5]. .....	68
Figure 3.1	A schematic diagrams of HIS.....	77
Figure 3.2	Photograph of the heated inlet source.....	77
Figure 3.3	The original HIS source with at least 80 – 100 cm long exposed Teflon tubing.....	78
Figure 3.4	Final design of HIS.....	78
Figure 3.5	Response of the PTR-ToF-MS instrument when injecting water with the original setup at no injection, injection starts and reaching a stable signal. The time between start of the injection and reaching a stable signal can be estimated to be about 40 seconds.....	84
Figure 3.6	Response of the PTR-ToF-MS instrument when injecting water with new set up (shorter inlet tube). The time between start of the injection and reaching a stable signal is about 10 s. ....	85

Figure 3.7	Response of the PTR-ToF-MS instrument when injecting hexane into HIS with original setup and new setup.....	86
Figure 3.8	Plots of a signal for protonated methanol, acetonitrile, acetaldehyde, acetone and 2-butanone vs. concentration in water with new set up.....	89
Figure 3.9	Plots of signal for protonated methanol, acetonitrile, acetaldehyde, acetone and 2-butanone versus concentration in hexane.....	90
Figure 3.10	Plots of signal for protonated methanol, acetonitrile, acetaldehyde, acetone and 2-butanone versus concentration in hexane.....	91
Figure 3.11	Plots of signal for protonated methanol, acetonitrile, acetaldehyde, acetone and 2-butanone vs. concentration in headspace above water standards .....	92
Figure 3.12	Plots of signal for protonated methanol, acetonitrile, acetaldehyde, acetone and 2-butanone vs. concentration in headspace above water standards .....	93
Figure 3.13	Plots of 2-butanone, acetone, acetonitrile and acetaldehyde signals as a function of concentration in hexane and analysed on GC-MS. ....	96
Figure 3.14	Plots of 2-butanone, acetone, acetonitrile and acetaldehyde signals as a function of concentration in hexane and analysed on GC-MS. ....	97
Figure 4.1	Schematic diagram of the Capillary inlet source .....	106
Figure 4.2	Complete CIS source .....	107
Figure 4.3	Sample inlet probe purchased from AB Sciex UK Limited, Cheshire, UK .....	107
Figure 4.4	Top flange showing the sample inlet and gas inlet connections.....	108
Figure 4.5	Photograph of the bottom flange.....	109
Figure 4.6	A photograph of metal jacket heater .....	110
Figure 4.7	Side view of the heating unit .....	111
Figure 4.8	Diagram of Capillary Inlet Source system. A calibration solution in syringe is connected to the inlet of the CIS through T-piece.....	115

Figure 4.9	Response of the $\text{H}_3\text{O}^+$ (un-normalised) when introducing pure water sample at 1.0 $\mu\text{l/s}$ flow rate for 180 s run from CIS.....	116
Figure 4.10	Calibration curve for 2-butanone in water over the concentration range of 10 to 60 pm/l .....	117
Figure 4.11	Calibration curve for acetonitrile in water over the concentration range of 10 to 60 pm/l .....	118
Figure 4.12	Calibration curve for acetone in water over the concentration range of 10 to 60 pm/l .....	118
Figure 5.1	The full scheme of the ion chemistry reaction system of $\text{H}_3\text{O}^+$ with ethanol and water vapour.....	133
Figure 5.2	PTR-MS mass spectra for ethanol/water solution (a) 5%, (b) 10%, (c) 50% and (d) 100%.....	135
Figure 5.3	Injection was made in the absence of the water vapour. MW 19 was observed due the residual moisture in the drift tube. After injecting the ethanol, stable $\text{H}_3\text{O}^+$ was observed after 10 s where no stable signal was observed for ethanol and its fragments at MW 47, 93 and 139 .....	136
Figure 5.4	Typical mass spectrum from the direct injection of whisky samples with and without the addition of the ethanol (Dominant $\text{H}_3\text{O}^+$ signal at $m/z$ 19 was removed from the graph for better representation of other VOCs).....	137
Figure 5.5	Abundances of ions with significant differences between whisky varieties .....	143
Figure 6.1	Full scan mass spectrum observed from the direct injection of urine and urine headspace from the urine sample collected from the one volunteer.....	159
Figure 6.2	Difference from direct injection to headspace injection on major VOCs .....	160
Figure 6.3	Effect of salt in urine on the VOCs emitted .....	162
Figure 6.4	A presentation of level of ammonia at three different pH levels from the headspace analysis of the urine sample from one volunteer .....	169
Figure 6.5	Levels of ketones from urine headspace from five healthy volunteer.....	171
Figure 6.6	A presentation of level of acetone, pentanone acid and heptanone at three different pH levels from the headspace analysis of the urine sample from one volunteer .....	172

Figure 6.7	Aldehyde levels measured for five volunteers .....	176
Figure 6.8	A presentation of level of different aldehydes at three different pH levels from the headspace analysis of the urine sample from one volunteer.....	176
Figure 6.9	A presentation of level of acetonitrile at three different pH levels from the headspace analysis of the urine sample from one volunteer. ....	179
Figure 6.10	A presentation of level of DMA and TMA at three different pH levels from the headspace analysis of the urine sample from one volunteer.....	180
Figure 6.11	A presentation of level of benzene and toluene at three different pH levels from the headspace analysis of the urine sample from one volunteer.....	183
Figure 6.12	Level of methanol, ethanol, propanol and phenol at three different pH values from the headspace analysis of the urine sample from one volunteer.....	184
Figure 7.1	Response of the PTR-ToF-MS instrument when 10.0 $\mu$ L of hexane/toluene (5/1, v/v) was injected. ....	206
Figure 7.2	Compound identification data generated by injecting the reference standard solution prepared in hexane into HIS .....	210
Figure 7.3	Chemical structure of (a) parathion and (b) methyl parathion .....	213
Figure 7.4	Calibration plot for parathion from the liquid-liquid extraction method .....	214
Figure 7.5	Chemical structure of Diazinon.....	216
Figure 7.6	Calibration plot for diazinon from the liquid-liquid extraction method .....	217
Figure 7.7	Chemical structure of fenthion.....	218
Figure 7.8	Calibration plot for fenthion from the liquid-liquid extraction method .....	219
Figure 7.9	Chemical structure of Triazophos.....	220
Figure 7.10	Calibration plot for triazophos from the liquid-liquid extraction method .....	220
Figure 7.11	Chemical structure of pirimiphos-methyl.....	221
Figure 7.12	Calibration plot for primiphos-methyl from the liquid-liquid extraction method .....	222

Figure 7.13 Chemical structure of (a) phorate, (b) atrazine .....	223
Figure 8.1 (A) University of York PTR-ToF-MS (B) Two stage PTR ion source .....	236
Figure 8.2 (a) Signal seen for protonated butanal (monitored at the fragment peak at $m/z$ 55) as the proton source is switched between $H_3O^+$ and protonated acetone. (b) Corresponding results for butanone, in this case monitored at $m/z$ 73. The switch from $H_3O^+$ to $H^+$ . Acetone brings about a roughly threefold drop in the $m/z$ 73 .....	239
Figure 8.3 (A) Signal seen for protonated methacrolein as the proton source is switched between $H_3O^+$ , protonated acetone and protonated butanone. (B) Signal levels seen for protonated methyl vinyl ketone (MVK) as the proton source is switched between $H_3O^+$ , protonated acetone and protonated butanone. ....	241
Figure 8.4 Calibration plots obtained for methacrolein (MA) and methyl vinyl ketone (MVK) using hydronium and protonated acetone as proton donors. Permeation tubes were used as VOC2 sources .....	244

# **CHAPTER 1: AN INTRODUCTION TO THE DIRECT INJECTION MASS SPECTROMETRY**

---

## **1.1 INTRODUCTION AND THESIS OUTLINE**

The rapid, non-invasive and direct on-line measurement of volatile organic compounds (VOCs) and biogenic VOCs (BVOCs) plays an increasingly relevant role in various fundamental and applied research fields. Numerous (biological) processes and products constantly release (B) VOCs, but their presence in the gas phase is often at trace levels. Nevertheless, these BVOCs are important because many can be linked to important characteristics and properties of processes and products, they also provide relevant, transparent information on biological, safety and quality aspects (e.g., environment or food) [1].

In environmental studies and atmospheric chemistry, the origin of VOCs is typically characterised as either “biogenic” or, the opposite, “anthropogenic”. Therefore, the term “biogenic VOCs (BVOCs)” is more typical in environmental studies. The BVOC originates from various biological organisms and plays an important role in biological, environmental, food and health science. The plants are the dominant source of BVOCs into the atmosphere. The air concentration of BVOCs is in the ppbv-pptv range. The atmospheric lifetime of these BVOCs varies from minutes to hours. The BVOCs interfere with the atmospheric reactions and they have an impact on the global temperature [2, 3].

The BVOCs and VOCs also have a greater impact on the human health and for the early detection of diseases [4]. Breath analysis has great potential for non-invasive diagnosis and monitoring of number disease states. Headspace analyses of urine, feces, and

blood and skin volatiles have been attempted. Probert *et al.* [5] have reviewed the potential of fecal volatile compounds for diagnosis of gastrointestinal disease using GC-MS.

The origin of both aroma and flavour of food controls the human sensory perception of food. For example, the smell is caused by the appealing scent of fresh fruit, while the flavours released during eating or drinking [6]. The VOCs in food produced and released at different stages of food production. They also create an interesting link to atmospheric studies, in several regions, BVOC emissions are, at least for certain species, dominated by emission from crops [7]. Direct BOVC and VOC monitoring is therefore an important non-invasive tool for product characterisation and process monitoring.

An ideal analytical technique for detecting (B)VOCs would be non-invasive, non-destructive, selective and capable of real time detection in complex mixtures at trace concentrations. Such a technique would allow new approaches for rapid process monitoring and control and fast characterisation of products. It would also allow timely assessment of environmental, medical and nutritional conditions that allows fundamental processes and permits immediate corrective re-actions in applications, some of the most important of which are [1]:

- atmospheric and environmental chemistry
- medical sciences
- biotechnology
- metabolomics
- biological research
- food and flavour science and technology
- homeland security
- waste incineration and waste-disposal monitoring

- industrial process monitoring
- outdoor and indoor air quality monitoring

Analytical technologies for rapid (B)VOC monitoring in all the above-mentioned areas will bring new perspectives and are of clear benefit. For example, food technology, in particular quality control in food production, requires the need for rapid, high-throughput measurement of large sample sets, preferably without affecting the sample and without interfering with the production process. Environmental chemistry and plant studies need to exploit fast response times to follow rapidly varying processes, while the analysis of exhaled breath of human beings, called “breath analysis”, would benefit from a similar high rate of response.

Direct-injection mass spectrometry (DIMS) is the term used for the different technique where samples are directly introduced to the mass spectrometer without any pre-treatment *e.g.* sample clean up or pre-concentration. Some of the technologies used for the DIMS approaches are discussed in this chapter. VOC monitoring of the above-mentioned applications not only relies on high time resolution, but also takes advantage of the high sensitivity provided by most DIMS technologies. Rapid monitoring does not allow for pre-concentration and the compounds of interest may well be present in the gas phase in the sub-parts per trillion (ppt) range, for both environmental and medical applications. For these types of application, very high sensitivity achieved by state-of-the-art DIMS techniques, allows direct monitoring of (B)VOCs in the gas phase.

An additional qualifying feature of on-line DIMS techniques is the large dynamic range that is required for certain applications. An exemplary case is the measurement of BVOCs released from food matrixes, where simultaneously compounds in the range parts per million (ppm) (*e.g.* alcohols), parts per billion (ppb)

(*e.g.* esters) and ppt or below (*e.g.* sulfur compounds) are present [8, 9]. Another example is the measurement of biological matrices such as human breath or urine [10]. Similar situations occur in process monitoring, where a large number of compounds over a large range of concentrations need to be monitored simultaneously.

The analysis of VOCs is thus challenging for various reasons:

- (1) They are often embedded in complex, volatile mixtures
- (2) Their concentrations may evolve rapidly with time
- (3) They may be present on a wide range of concentration and often also in trace amounts

Routine MS-based analytical techniques such as LC-MS, LC-MS/MS, GC-MS and GC MS/MS are hardly suited to address these analytical challenges. Samples have to be introduced via a gas-handling system and the atmospheric pressure sample has to be diluted to vacuum conditions necessary for operating a mass spectrometer (indirect gas injection).

In classical analytical chemistry, the mass spectrometer is usually preceded, in VOC detection, by a gas chromatography (GC) separation step, and GC-based methods [11] are the standard analytical technique used for (B)VOC identification and quantification. Although highly valuable, they are not designed to examine the rapid changes of VOC concentrations occurring in fast processes. Often, a necessary sampling and pre-treatment phase [11] introduces time averages of the concentration of the measured mixture. Because of these drawbacks, other methods have been developed over the years to complement GC-based methods with simplified, high sensitivity, fast and direct on line monitoring of (B)VOCs, with a high (even sub-second) time resolution.

Among the various options to address these needs, from spectroscopic methods to solid state gas sensors arrays [12], advanced DIMS has proved to be a high-performance technology and a valuable complement to existing methods. A number of methods have been developed, aiming to exploit the potential of MS (high sensitivity, fast monitoring) while avoiding the drawbacks inherent in chromatographic separation and sample pre-treatment methods. A number of methods have been developed to utilise the potential of MS for direct injection technology [13, 14].

The greatest difficulties arising in DIMS are the need to interface directly atmospheric pressure samples to the vacuum. It was also needed for a proper functioning of a mass spectrometer and to identify the observed peaks. Since there can be the results of overlapping signals from the mix of (B)VOCs present in the sample: no preceding separation takes place with DIMS.

Some of the most important and widespread approaches used for the DIMS is discussed in Section 1.2. The different technologies discussed in this chapter are, MS e noses, atmospheric pressure chemical ionization (APCI) [13, 15], proton transfer reaction MS (PTR-MS), selected ion flow tube-MS (SIFT-MS) and direct real time analysis (DART).

The main aim of the work described in this thesis was to develop a direct injection proton transfer reaction mass spectrometry technique, particularly for liquid samples, as its application in the analysis of the VOCs from the atmosphere [16, 17] and breath analysis [18] is well documented. In this chapter, general DIMS techniques and its applications are discussed. This leads on to Chapter 2, which focuses on the PTR-TOF-MS technique. The theoretical principles and instrumental arrangements are described along with the setup of the University of Leicester's

PTR-TOF-MS instrument, which was used for the majority of the work presented in this Thesis.

Chapters 3 and 4 of this thesis focus on the design and development of the inlet systems for the introduction of aqueous, solvent and headspace samples into PTR-MS. The heated inlet source (HIS) described in Chapter 3 is designed for aqueous, solvent and headspace samples. In Chapter 4, new capillary inlet source (CIS) was developed for the aqueous samples.

Chapter 5, 6 and 7 of this thesis detail some of the applications explored. In Chapter 5, different whiskies were characterised by their brand and the blend by measuring the VOC profile by headspace and direct sample analysis. In Chapter 6, different VOCs were measured and quantified from the headspace of human urine while in Chapter 7 organophosphate pesticides were detected and measured by injecting the solvent samples generated by liquid-liquid extraction.

In Chapter 8, the focus is shifted from direct liquid analysis, to the study of isobaric compounds. In particular two stage PTR-MS technique has been tested for the measurement and discrimination of isobaric compounds. Finally, Chapter 9 summarises the work performed and discusses the possible future direction.

In the remainder of this chapter, a general introduction to DIMS techniques is provided, along with brief descriptions of applications in the food industry, in environmental measurement and in diagnostics research.

## **1.2 KEY TECHNOLOGIES**

A number of different approaches to DIMS have been developed over past decades. While they all share the fact that sample gas

is directly introduced into the device, they vary significantly in terms of sampling, inlet and ionization/detection principles.

### 1.2.1 MS-e-noses

An electronic nose has been described as “an instrument which comprises an array of electronic, chemical sensors with partial specificity and an appropriate pattern recognition system, capable of recognizing simple or complex odours” [19]. Its name stresses the fact that it mimics the behaviour of human olfaction and this is why its main fields of application are food and flavour sciences, where the substitution of proper sensory analysis, difficult and time consuming, with instrumental methods, is a long hoped-for objective. The idea is that the output of a series of unspecific sensors can be used to build models to classify products or processes, by means of Chemometrics or data mining [20, 21].

The headspace (HS) sample is the gas space above the sample in a container and volatile sample components diffuse into the gas phase forming the headspace. Headspace analysis is therefore the analysis of the volatile compounds present in that gas. The analysis of HS samples by a mass spectrometer operated in the electron ionisation mode without any GC separation. The feasibility of the method is demonstrated by various applications and this is often referred to as a “MS-based electronic nose” or an “MS e-nose”. The MS-e-nose approach is illustrated in Figure 1.1. The mass pattern obtained, considered as fingerprint of the sample analysed.

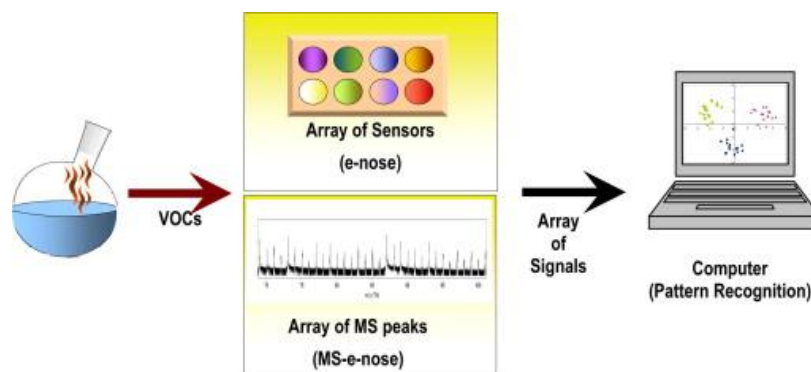


Figure 1.1 Diagram of MS-e-nose approach [1]

However, e-noses suffer from several drawbacks, including sensor poisoning, high sensitivity to moisture, poor linearity, poor reproducibility on different instruments and sensor drift. When an MS-e-nose is used with EI, it suffers from severe fragmentation, leading to complex spectra with many overlapping fragments, and little chemical information can be obtained.

Besides EI, other ionization methods are increasingly being introduced, some of which are promising in terms of both portability and robustness. They can be termed collectively “MS fingerprinting” approaches, and provide rapid, efficient tools for the characterization of samples. The fingerprint has been used to set up classification models [22], and for calibration models to predict the characteristics of food products [9]. In particular, coupling with ToF mass analysers further offers increases in speed and information entangled in rapid fingerprinting [23, 24].

### 1.2.2 APCI

Atmospheric Pressure Chemical Ionisation (APCI) is an ionisation technique that uses gas-phase ion-molecule reaction at atmospheric pressure. In this technique, primary ions are produced by a corona discharge across a solvent spray. APCI is mainly used for polar compounds with molecular weights up to

about 1500 amu [25]. The principle for an APCI source is shown in the Figure 1.2.

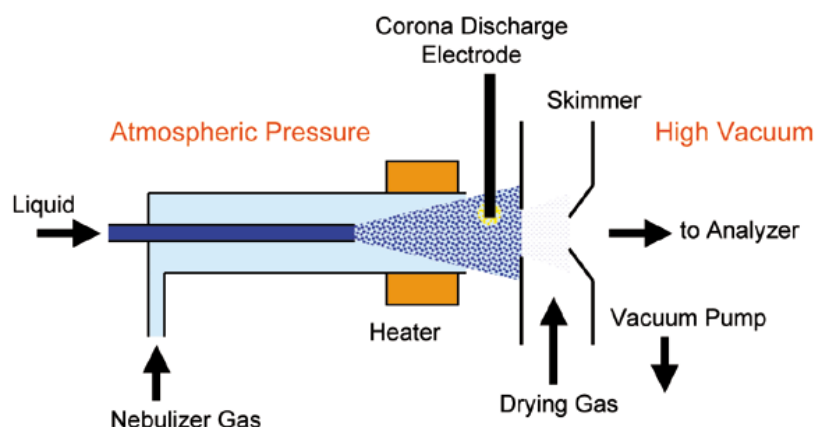


Figure 1.2 Diagram of APCI source

The analyte in solution comes from a direct inlet probe or a liquid chromatography elutes. It is directly introduced into a pneumatic nebulizer where it is converted into a thin fog by a nebulizer gas. Normally nitrogen is used as a nebulizer gas. Droplets are then displaced by the gas flow through a heated quartz tube called a desolvation chamber. The heat transferred to the spray droplets allows the vaporisation of the mobile phase and of the sample in the gas flow. The temperature of this chamber is controlled. After the desolvation, the mixture is carried past a corona discharge electrode, where ionization occurs. The ionisation process is similar to the process taking place in standard chemical ionisation but occur under atmospheric pressure. In the positive mode, either proton transfer or adduction of reactant gas ions occurs to produce the ions of molecular species, depending on the relative proton affinities of the reactant ions and gaseous analyte molecule. In the negative mode, the ions of the molecular species are produced by either proton abstraction or adduct formation.

However, APCI ionization is rather complex due to the presence of many possible ionization agents. Other problems are the suppression of ionization in the source, leading to non-quantitative results, difficulties in the unequivocal identification of compounds solely based on their  $m/z$  values and the relatively low ionization efficiency. All these potential shortcomings were recently discussed from the point of view of flavour analysis [28]. These potential shortcoming can be in some cases, be resolved if experiments are run under carefully controlled conditions [28].

For several years, APCI has been the reference technique in on-line monitoring of flavour compounds, especially for breath-to-breath analysis of in vivo release [28]. Because of its long history and its availability in most analytical laboratories, APCI remains a vital DIMS method, in spite of the development of other techniques, described below, with higher sensitivity (e.g. PTR-MS) or simpler ionisation (e.g. SIFT-MS) as demonstrated by its continuing development [31].

### 1.2.3 PTR-MS and SIFT-MS

Proton Transfer Reaction Mass Spectrometry (PTR-MS) and Selected Ion Flow Tube Spectrometry (SIFT-MS) are popular for the detection the VOCs at trace levels from a variety of matrices. The SIFT technique is also very effective in the investigation of ion-molecules reactions. A comparison of the main characteristics of the PTR-MS, SIFT-MS and APCI is provided in Table 1.1.

Main technological philosophies between PTR-MS and SIFT-MS are:

(1) PTR-MS, is based on the realisation of pure and intense ion sources that do not need further ion filtering; and,

(2) SIFT-MS is more closely related to the ion-mobility reaction set-up, allowing a higher purity of the parent-ion beam and the possibility to select it easily, at the cost of a reduced sensitivity.

Specific detailed about each of these types are provided in the next two sections.

Table 1.1 Comparison of the main characteristics of the typical implementations of the on-line DIMS methods considered [1].

	APCI	PTR-MS	SIFT-MS
Source	Corona discharge	Hollow-cathode/radioactive discharge	Microwave-discharge plasma
Precursor Ion	$(\text{H}_2\text{O})\text{nH}^+$	$\text{H}_3\text{O}^+$ , $\text{NO}^+$ , $\text{O}_2^+$	$\text{H}_3\text{O}^+$ , $\text{NO}^+$ , $\text{O}_2^+$
Precursor-ion selection	None	None	Quadrupole
Thermalizing precursor ions	Declustering tube	Neutral gases form sample	Helium
Extra dilution	Dry nitrogen	None	Necessary to reduce clustering
Analyte introduction	Direct introduction	Direct introduction	Direct introduction
Reaction region	None	Drift tube	Flow tube
Mass analyser	Quadruple/Quadruple	Quadrupole or ToF or Iontrap	Quadruple or ToF
Product-ion detection	Secondary electron multiplier	Secondary electron multiplier	Secondary electron multiplier

#### 1.2.4 PTR-MS

Lindinger and co-workers in the mid-1990s first introduced the PTR-MS technique. The technique has been reviewed several times in literature, the first being by Lindinger [26] that presents a clear description of PTR-MS fundamentals and potential.

Reviews that are more recent are presented in [27] and [28].

The main constituents of a PTR-MS apparatus are the ion source, a reaction region and a mass analyser. In most instruments, the  $\text{H}_3\text{O}^+$  primary-ion beam is produced by a hollow cathode ion source [26] or by a radioactive material [16, 17]. This setup

presents some advantages as no mass selection is applied and all the reagent ions are directly feed into the reaction chamber. This setup simplifies the system and allows for better sensitivity. Alternative designs of the source have been tested to reduce impurities and back streaming from the reaction chamber [29] at the cost of sensitivity [30].

More recently, other ions have been studied [31-33] and, recently, a marketed commercial system from Ionicon Analytik (see Figure 1.3 for Ionicon PTR-MS diagram) allows for rapid switching between different ions e.g.  $\text{H}_3\text{O}^+$ ,  $\text{NO}^+$  and  $\text{O}_2^+$ . The literature on this recent development is limited, but it appears very promising, as there is a chance for a better compound identification by bracketing with different parent ions as described in for isobaric aldehydes and ketones also discussed in Chapter 9 of this Thesis. The second part of a PTR-MS apparatus is the short drift region, where the parent ions driven by an electric field and eventually interact with the neutral species to be detected. The process is controlled by drift-tube temperature (typically 50–100°C), pressure ( $\sim 200$  Pa) and electric potential. PTR technique and property of drift tube and the reactions happens in the draft tubes are discussed in detail in Chapter 2 of this thesis.

The last part of a PTR-MS system is the mass analyser. Linear quadrupoles are one of the widely used mass analysis in PTR-MS system. They are robust and relatively cheap, but it is slow, and typically provide only unit mass resolution. Two alternatives have been used and they are discussed in literature:

(1) Prazeller *et al.* [34] has used the ion-trap mass analyser with their PTR system. Ion trap mass analyser stores the ions for a given time, thus increasing the instrument sensitivity and allowing collision-induced dissociation experiments to identify isobaric compounds [35].

(2) The second is the coupling with a ToF mass detector [16, 17, 36, 37] and has its strong points in the very rapid spectra acquisition and high mass resolution.

PTR-MS technique and University of Leicester PTR-TOF-MS instrument used for the majority of work in this thesis is discussed in detail in Chapter 2.



Figure 1.3 Schematic diagram of Ionicon PTR-MS

### 1.2.5 SIFT-MS

SIFT-MS developed by Španěl and Smith [38], who have reviewed the fundamentals and several applications [39]. Further applications and recent developments have also been reviewed [40].

In SIFT-MS, the parent ions are generated by microwave plasma or by an electron impact ion source, and the primary ions are then selected from the ion mixture by a quadrupole mass filter. The basic principles of the SIFT-MS technique is explained in this section with reference to the diagram shown in Figure 1.4.

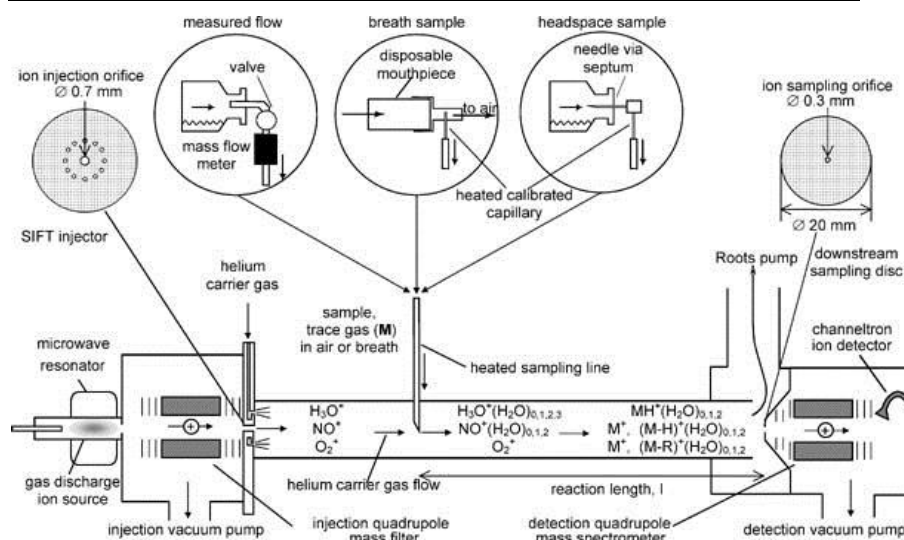


Figure 1.4 Principles of SIFT-MS, image taken from [1]

Positive ions are created in a microwave discharge ion source containing a mixture of water vapour and air at a relatively high pressure. The ions then enter the low-pressure chamber through a small orifice. A current of ions of a given mass-to-charge ratio,  $m/z$ , is extracted from the mixture of ion species using a quadrupole mass filter. The current of primary ions is then injected into a fast flowing inert carrier gas stream by the pump. The ions are carried along the flow tube as a thermalised ion swarm and are sampled via a pinhole at the downstream end of the flow tube where the sampled ions pass into a differentially pumped, quadrupole mass spectrometer.

The sample of air to be studied is introduced into the SIFT-MS instrument via a sample inlet port in the flow tube at a measured flow rate. Trace gases in the air sample can react with the primary ions and the product ions formed are detected and quantified by the downstream detector system.

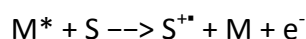
Accurate quantification is possible with the SIFT-MS because the reaction time of the primary ions with the trace gas molecules is precisely defined in the SIFT, and the rate coefficients for the ion-molecule reactions can be measured accurately in separate

SIFT experiments if they are not already known. From such SIFT experiments, a large database of rate co-efficient has been created, which is critical for the quantification [41]. The primary ions are chosen so that they do not react significantly with the major components of the air or breath sample ( $N_2$ ,  $O_2$ ,  $H_2O$ , or  $CO_2$ ) which would result in them being rapidly lost from the ion swarm. However, they must react efficiently with the trace gases to produce identifiable product ions in order to be detected. In the case of VOC detection the hydronium ion  $H_3O^+$ ,  $O_2^+$  and  $NO^+$  fulfil these criteria. In SIFT-MS, the choice is for softer ionization and higher flexibility at the cost of less sensitivity and a more complex set-up when compare to PTR-MS.

### 1.2.6 DART (Direct Analysis in Real Time)

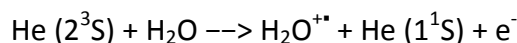
DART is an atmospheric pressure ion source that instantaneously ionises gases, liquids and solids in the open air under ambient conditions [42]. It was developed in 2005 by Laramée and Cody and is now marketed by JEOL and Ionsense. DART was among the first ambient ionisation techniques not requiring sample preparation, so solid and liquid material can be analysed by a mass spectrometer in their native state. Ionization can take place directly on the sample surface, be it, currency bills, tablets, bodily fluids (blood, saliva and urine), glass, plant leaves, fruits & vegetables and even clothing. Liquids are analysed by dipping an object (such as a glass rod) into the liquid sample and then presenting it to the DART ion source. Vapours are introduced directly into the DART gas stream [42].

The ionization involves an interaction between the analyte molecule (S) and electronically excited atoms or vibronically excited molecules (metastable species -  $M^*$ ) [43]:

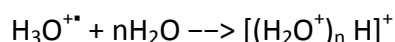
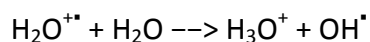


Upon collision between the excited gas molecule ( $M^*$ ) and the surface of the sample, an energy transfer takes place, from the excited gas molecule ( $M^*$ ) to the neutral analyte molecule (S). This causes an electron to be released from the analyte molecule, producing a radical cation. The cation then ejected from the sampling surface and travels to the mass analyser along with the gas stream (typically  $N_2$  or Ne). The reaction presented above called Penning ionisation. In this ionisation process to take place, the energy of the excited state gas molecule must be higher than the ionisation potential of the neutral molecule.

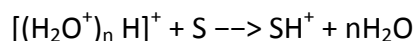
When helium (He) used as the carrier gas, the ionization process occurs by the following sequence: First, an excited He atom collides with a water molecule and ionises it:



The ionized water molecule then undergoes several reactions with other neutral water molecules resulting in the formation of a protonated water cluster:



The water cluster, then interacts with the analyte molecule (S) generating a protonated molecule.



DART can also operate in the negative ion mode. The mechanism by which negative ions form is under current discussion and investigation. DART's reaction with water is extremely efficient and its performance is not affected by high humidity. A schematic diagram of the DART is shown in Figure 1.5.

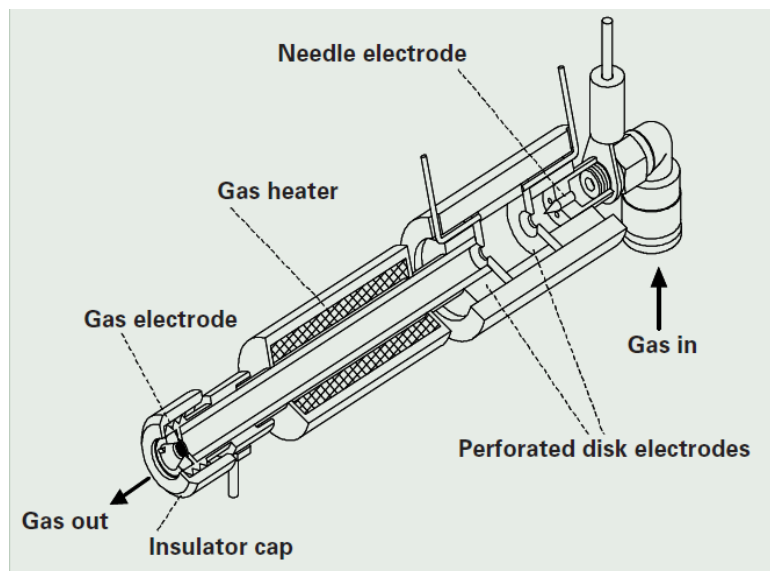


Figure 1.5 Schematic diagram of the DART ion source [1]

The DART ion source has been used to analyse an extremely wide range of analytes, including drugs [44], explosives and arson accelerants, chemical weapons, environmentally important compounds [15], inks and dyes and papers [45], food [46, 47] and medicine [48]. An important benefit of DART is that materials can be analysed directly on surfaces.

## 1.3 APPLICATIONS

### 1.3.1 Environmental measurement

Environmental monitoring, atmospheric chemistry and plant biology need, in field campaigns and in the laboratory-based studies, proper identification and quantification of VOCs always at low concentrations and often on the short time scales. Plant-emitted VOCs (*e.g.* isoprene, monoterpenes, and sesquiterpenes) and oxygenated compounds [49] are involved in many physiological and ecological functions. They react with other species in the atmosphere and have a major impact on atmospheric chemistry [3]. In the atmosphere, VOCs are important because they may affect the photochemical ozone

formation, particulate formation, stratospheric ozone depletion, and climate [13, 50]. There is a wide range of anthropogenic VOC sources driven by combustion processes; the production, treatment, storage, and distribution of fossil fuels; and organic solvents, industrial production processes, and agriculture, and DIMS have been used successfully for the real-time measurement. PTR-MS has proven to be quite useful technique for these as numbers of publications are available in the literature for the urban and suburban VOC measurements [51-53]. Many VOCs are also toxic and/or carcinogenic, and in establishing their effect on human health, it is vital to be able to monitor their concentrations in a wide range of environments. DIMS is important for this application as most of these VOCs have short lifetime [54] and real-time analysis may be required. DIMS can be applied to other situations that, in a more general sense, can be considered examples of environmental monitoring: indoor and outdoor air-quality monitoring. On one hand, chemical contamination of indoor air is a contributing factor for many diseases and the need of portable, rapid, high-sensitivity techniques to assess indoor exposure to VOCs [55, 56] is becoming increasingly urgent.

DIMS application in measurement of real time detection of explosive and chemical warfare agent has also researched [57]. Emissions from industrial processes is another area, because airborne molecular contamination is a concern for any high technology, manufacturing process, especially in the microelectronics, bioprocessing and chemical industry.

### 1.3.2 Food analysis

The emission of organic gases from food, whether through decay or through digestion or through manufacturing, is important in the food industry. DIMS plays an important role in

the food and agricultural industries for the measurement of VOCs [58] as they control flavour perception and strongly influence consumers' preferences and, in general, they are key constituents of raw materials and processed foodstuffs. Moreover, almost any step in the food-processing chain has an effect on the VOC profile by altering the compounds originally present or even generating new ones. Thus, BVOC monitoring may constitute a means to investigate, *in vivo*, flavour stimuli, to control food quality [59, 60] or to determine its geographic origin [61, 62] or to characterise the different brand [[63, 64], Chapter 5]. PTR-MS to date has been used successfully for this application [57-60]. The majority of the applications for the PTR-MS is in flavour studies and in the assessment of food quality.

The importance of mass spectrometric techniques in flavour studies has long been recognized. When foods are consumed, flavour compounds are released from the food matrix and are transported to receptors in the mouth and nose. The release of VOCs into the nasal cavity, generating a characteristic aroma, plays a key role in the perception of flavour. The release of VOCs can be influenced by a wide variety of factors, such as saliva content, the mastication process, food fat content, and food texture. Consequently, a better understanding of the concept of flavour perception and how it is affected by the food matrix and the consumption process requires the investigation of VOC emission from foods. Analytical approaches that quantify VOCs in food matrices by traditional volatile-sampling techniques are necessary to characterise flavours released from food, but they cannot provide information on the fraction of VOCs that are effectively available for perception in a real situation of food consumption. The most direct method to address this issue is the monitoring of the nose-space concentration of VOCs during

food consumption. There are several analytical challenges related to this application:

- (1) Time resolution, since measurement must be fast enough to resolve the rapid variation in the nose-space concentration at least at a frequency higher than the breath tidal, and that rules out GC-based methods;
- (2) High sensitivity, since the human olfactory threshold can be very low, down to pptv for key aroma compounds;
- (3) No interferences from clean air constituents humidity; and,
- (4) The possibility of quantitative analysis of a component in a mixture.

DIMS methods appear an ideal approach to address these issues, particularly if the compounds of interest are known in advance and only monitoring, not identification, is needed or whole profile for VOCs is required for analysis.

Taylor, Linforth, and co-workers have used APCI [65] for in vivo analysis of volatile release. Usually, APCI instruments for flavour release are equipped with quadrupole analysers. To reach a sufficient time resolution and sensitivity, they need to be run in the multiple-ion-detection mode that limits the measurable number of traces to 5–10; moreover, APCI ionization is intrinsically affected by humidity and source temperature. This is particularly relevant in the case of nose-space analysis because the relative humidity varies. Another possible issue with an APCI is suppression of the signal in the presence of a dominant species. One such example ethanol in alcoholic beverages, as alcoholic beverages has higher proportion of ethanol compare to other VOCs. A possible solution is to saturate the sample with ethanol, so that ethanol becomes the effective proton donor.

One of the challenges for DIMS, particularly for PTR-MS, in an analysis of VOCs from a foodstuff is to be able to successfully identify the full range of active compounds. Not only is there the possibility of isobaric interferences, but fragmentation can complicate the analysis when a series of similar compounds are explored. This is a significant issue in flavour studies, where a variety of compound types, such as aldehydes, ketones, alcohols, and esters, might contribute to the flavour profile. Comparisons with the extensive work on the reactions between  $\text{H}_3\text{O}^+$  and various classes of organic compounds from SIFT-MS is a useful guide but is not definitive because of the higher collision energies encountered in PTR-MS.

In this thesis, PTR-TOF-MS was used for the characterisation of the whiskeys samples. The VOC profile from the direct injection of whiskey sample and headspace injection was collected. As discussed above, to avoid the suppression from the ethanol, whiskey samples were diluted with ethanol and VOC profile was collected. Multivariate analysis was performed on the data to characterise the whiskey sample.

### 1.3.3 Diagnostic analysis

On-line breath analysis, the on-line monitoring of the (B)VOCs in the air exhaled during respiration, is attracting growing interest as a possible medical research and diagnostic tool [18, 40, 66, 67]. Urine analysis [68, 69], in vivo human skin studies [70] and occupational health exposure in medical/laboratory environments [71-73] are other examples where non-invasive diagnostic analysis may be beneficial. Although there is not yet a clear answer regarding the most suitable approach for fast, non-invasive breath analysis, DIMS methods are certainly interesting in terms of time resolution and sensitivity, and evaluated in parallel with a GC and spectroscopic methods that are the traditional alternative technologies.

Monitoring VOCs in exhaled human breath have attracted considerable attention because of its potential as a technique that is non-invasive and painless to patients. It is already used in the diagnosis of several health disorders and pathologies (e.g. lung cancer and inflammatory lung diseases) [10, 35, 62, 63].

PTR-MS and SIFT-MS have been particularly applied for the breath analysis. For example, it is possible, with reduced effort, to screen a large population of healthy volunteers and to describe the expected distribution of major breath BVOCs (e.g. ammonia, acetone, methanol, ethanol and isoprene). A further step is to characterise population segments with specific characteristics (age) or habits (smokers and non-smokers).

In the case of halitosis, SIFT-MS has been used to measure concentrations of both in mouth and in-nose VOCs to differentiate systemic and orally generated compounds [35] (e.g. acetone, methanol and isoprene are mostly systemic, while ethanol is mostly produced in the mouth). Breath isoprene has been shown to be related to blood cholesterol levels and it has been found to be enhanced in end-stage renal disease patient following dialysis. SIFT-MS [74] has been used successfully for the measurement of breath isoprene. PTR-MS has been used for real time breath monitoring of the intravenous anaesthetic agent propofol and its volatile metabolites in patients undergoing surgery [75, 76]. PTR-MS also has seen a number of other medical applications that do not involve breath measurements. For example, it has been used to assess the concentration of acetonitrile in the urine of habitual cigarette smokers and in non-smokers as a quantitative marker of recent smoking behaviour [69]. The results showed a significant enhancement of acetonitrile concentration in the urine of the heavy smokers. Chapter 6 of this thesis describes the analysis of

the headspace of urine sample to monitor the different VOCs from the smoker and non-smokers.

The possibility of following metabolic processes in real time is also a useful application of DIMS in health sciences. APCI is also a widely used method and extensive literature is available but due to complex ionisation process caused by the presence of different precursor species (water clusters, in particular). It is not an ideal technique.

### **1.4 SUMMARY**

This chapter has introduced the field of DIMS and different techniques that are being used on the regular basis. This chapter also introduced the application of the DIMS to the field environmental analysis, food analysis and diagnostic analysis. This thesis aims to demonstrate that the even though majority of the application of the DIMS is based on the sample requires being in the gas phase, direct injection is also possible to the aqueous samples. In an effort to develop the direct injection application for the PTR-TOF-MS, new inlet source is designed for the introduction of the aqueous samples and new applications for the aqueous samples have been developed. The details of the CIR-MS technique and the assessment of its performance in breath research follows in Chapter 2.

### **1.5 REFERENCES:**

1. Biasioli, F., Chahan, Y., Tilmann, M., D, Dewulf, J., Langenhove, V., Direct-injection mass spectrometry adds the time dimension to (B)VOC analysis. *TrAC Trends in Analytical Chemistry*, 2011. 30(7): p. 1003-1017.
2. Dewulf, J. and H. Van Langenhove, Biogenic volatile organic compounds. *TrAC Trends in Analytical Chemistry*, 2011. 30(7): p. 935-936.
3. Peñuelas, J. and M. Staudt, BVOCs and global change. *Trends in Plant Science*, 2010. 15(3): p. 133-144.

4. Dummer, J., Storer, M., Swanney, M., McEwan, M., Scott-Thomas, A., Bhandari, S., Chambers, S., Dweik, R., Epton, M., Analysis of biogenic volatile organic compounds in human health and disease. *TrAC Trends in Analytical Chemistry*, 2011. 30(7): p. 960-967.
5. Probert, C.S.J., Ahmed, F., Khaild, T., Johnson, E., Smith, S., Ratcliffe, N., Volatile organic compounds as diagnostic biomarkers in gastrointestinal and liver diseases. *Journal of Gastrointestinal and Liver Diseases*, 2009. 18(3): p. 337-343.
6. Biasioli, F., Gasperi, F., Yeretian, C., Mark, T.D., PTR-MS monitoring of VOCs and BVOCs in food science and technology. *TrAC Trends in Analytical Chemistry*, 2011. 30(7): p. 968-977.
7. Karl, M., Guenther, A., Koble, R., Leip, A., Seufert, G., A new European plant-specific emission inventory of biogenic volatile organic compounds for use in atmospheric transport models. *Biogeosciences*, 2009. 6(6): p. 1059-1087.
8. Yeretian, C., A. Jordan, and W. Lindinger, Analysing the headspace of coffee by proton-transfer-reaction mass-spectrometry. *International Journal of Mass Spectrometry*, 2003. 223–224(0): p. 115-139.
9. Aprea, E., Biasioli, F., Gasperi, F., Mott, D., Marini, F., Mark, T.D., Assessment of Trentingrana cheese ageing by proton transfer reaction-mass spectrometry and chemometrics. *International Dairy Journal*, 2007. 17(3): p. 226-234.
10. Buszewski, B., Keszy, M., Ligor, T., Amann, A., Human exhaled air analytics: biomarkers of diseases. *Biomedical Chromatography*, 2007. 21(6): p. 553-566.
11. Dewulf, J., H. Van Langenhove, and G. Wittmann, Analysis of volatile organic compounds using gas chromatography. *TrAC Trends in Analytical Chemistry*, 2002. 21(9–10): p. 637-646.
12. Brunner, C., Szymczak, W., Hollriegl, V., Mortl, S., Oelmez, H., Bergner, A., Huber, R.M., Hoeschen, C., Oeh, U., Discrimination of cancerous and non-cancerous cell lines by headspace-analysis with PTR-MS. *Analytical and Bioanalytical Chemistry*, 2010. 397(6): p. 2315-2324.
13. Badjagbo, K., S. Sauvé, and S. Moore, Real-time continuous monitoring methods for airborne VOCs. *TrAC Trends in Analytical Chemistry*, 2007. 26(9): p. 931-940.
14. Cevallos-Cevallos, J.M., et al., Metabolomic analysis in food science: a review. *Trends in Food Science & Technology*, 2009. 20(11–12): p. 557-566.

15. Badjagbo, K., Picard, P., Moore, S., Sauve, S., Direct Atmospheric Pressure Chemical Ionization-Tandem Mass Spectrometry for the Continuous Real-Time Trace Analysis of Benzene, Toluene, Ethylbenzene, and Xylenes in Ambient Air. *Journal of the American Society for Mass Spectrometry*, 2009. 20(5): p. 829-836.
16. Wyche, K.P., Development, Characterisation and Implementation of Chemical Ionisation Reaction Time-of-Flight Mass Spectrometry for the Measurement of Atmospheric Volatile Organic Compounds. Thesis: University of Leicester, 2008.
17. Blake, R.S., Monitoring tropospheric composition using time of flight chemical ionisation mass spectrometric techniques. Thesis: University of Leicester, 2005.
18. Willis, K.A., Development of Chemical Ionisation Reaction Time-of-Flight Mass Spectrometry for the Analysis of Volatile Organic Compounds in Exhaled Breath. Thesis: University of Leicester, 2009.
19. Gardner, J.W. and P.N. Bartlett, Brief history of electronic noses. *Sensors and Actuators, B: Chemical*, 1994. B18(1 -3 pt 1): p. 211-220.
20. Cynkar, W., Cozzolino, D., Damberg, B., Janik, L., Gishen, M., Feasibility study on the use of a headspace mass spectrometry electronic nose (MS e\_nose) to monitor red wine spoilage induced by *Brettanomyces* yeast. *Sensors and Actuators B: Chemical*, 2007. 124(1): p. 167-171.
21. Montuschi, P., Santonico, C. Mondino, G. Pennazza, G. Mantini, E. Martinelli, R. Capuano, G. Ciabattoni, R. Paolesse, C. Di Natale, P. J. Barnes and A. D'Amico, Diagnostic Performance of an Electronic Nose, Fractional Exhaled Nitric Oxide, and Lung Function Testing in Asthma. *CHEST Journal*, 2010. 137(4): p. 790-796.
22. Granitto, P.M., Biaxioli, F., Apera, E., Mott, D., Furlanello, C., Mark, T.D., Gasperi, F., Rapid and non-destructive identification of strawberry cultivars by direct PTR-MS headspace analysis and data mining techniques. *Sensors and Actuators B: Chemical*, 2007. 121(2): p. 379-385.
23. Fabris, A., Biasioli, P. M. Granitto, E. Aprea, L. Cappellin, E. Schuhfried, C. Soukoulis, T. D. Märk, F. Gasperi and I. Endrizz, PTR-ToF-MS and data-mining methods for rapid characterisation of agro-industrial samples: influence of milk storage conditions on the volatile compounds profile of Trentingrana cheese. *Journal of Mass Spectrometry*, 2010. 45(9): p. 1065-1074.
24. Cappellin, L., Biasioli, F., Granitto, P.M., Schuhfried, E., Soukoulis, C., Costa, F., Mark, T.D., Gasperi, F., On data

- 
- analysis in PTR-TOF-MS: From raw spectra to data mining. *Sensors and Actuators B: Chemical*, 2011. 155(1): p. 183-190.
25. Covey, T.R., B.A. Thomson, and B.B. Schneider, Atmospheric pressure ion sources. *Mass Spectrometry Reviews*, 2009. 28(6): p. 870-897.
26. Lindinger, W., J. Hirber, and H. Paretzke, An ion/molecule-reaction mass spectrometer used for on-line trace gas analysis. *International Journal of Mass Spectrometry and Ion Processes*, 1993. 129(0): p. 79-88.
27. Blake, R.S., P.S. Monks, and A.M. Ellis, Proton-transfer reaction mass spectrometry. *Chemical Reviews*, 2009. 109(3): p. 861-896.
28. De Gouw, J. and C. Warneke, Measurements of volatile organic compounds in the earth's atmosphere using proton-transfer-reaction mass spectrometry. *Mass Spectrometry Reviews*, 2007. 26(2): p. 223-257.
29. Hanson, D.R., et al., Proton transfer mass spectrometry at with a circular glow discharge: Sensitivities and applications. *International Journal of Mass Spectrometry*, 2009. 282(1-2): p. 28-37.
30. Inomata, S., Tanimoto, H., Aoki, N., Hirokawa, J., Sadanaga, Y., A novel discharge source of hydronium ions for proton transfer reaction ionization: Design, characterization, and performance. *Rapid Communications in Mass Spectrometry*, 2006. 20(6): p. 1025-1029.
31. Norman, M., A. Hansel, and A. Wisthaler, O<sub>2</sub><sup>+</sup> as reagent ion in the PTR-MS instrument: Detection of gas-phase ammonia. *International Journal of Mass Spectrometry*, 2007. 265(2-3): p. 382-387.
32. Jordan, A., Haidacher, S., Hanel, G., Hartungen, E., Herbig, J., Mark, L., Schottkowsky, R., Seehauser, H., Sulzer, P., Mark, T.D., An online ultra-high sensitivity Proton-transfer-reaction mass-spectrometer combined with switchable reagent ion capability . *International Journal of Mass Spectrometry*, 2009. 286(1): p. 32-38.
33. Wyche, K.P., Blake, R.S., Willis, K.A., Monks, P.S., Ellis, A.M., Differentiation of isobaric compounds using chemical ionization reaction mass spectrometry. *Rapid Communications in Mass Spectrometry*, 2005. 19(22): p. 3356-3362.
34. Prazeller, P., Palmer, P.T., Boscaini, E., Jobson, T., Alexander, M., Proton transfer reaction ion trap mass spectrometer. *Rapid Communications in Mass Spectrometry*, 2003. 17(14): p. 1593-1599.
35. Warneke, C., de Gouw, J.A., Lovejoy, E.R., Murphy, P.C., Kuster, W.C., Fall, R., Development of Proton-Transfer Ion Trap-Mass Spectrometry: On-line Detection and

- Identification of Volatile Organic Compounds in Air. *Journal of the American Society for Mass Spectrometry*, 2005. 16(8): p. 1316-1324.
36. Ennis, C.J., Reynolds, J.C., Keely, B.J., Carpenter, L.J., A hollow cathode proton transfer reaction time of flight mass spectrometer. *International Journal of Mass Spectrometry*, 2005. 247(1–3): p. 72-80.
37. Jordan, A., Haidacher, S., Hanel, G., Hartungen, E., Mark, L., Seehauser, H., Schottkowsky, R., Sulzer, P., Markt, T.D., A high resolution and high sensitivity proton-transfer-reaction time-of-flight mass spectrometer (PTR-TOF-MS). *International Journal of Mass Spectrometry*, 2009. 286(2–3): p. 122-128.
38. Španěl, P., M. Pavlik, and D. Smith, Reactions of H<sub>3</sub>O<sup>+</sup> and OH<sup>-</sup> ions with some organic molecules; applications to trace gas analysis in air. *International Journal of Mass Spectrometry and Ion Processes*, 1995. 145(3): p. 177-186.
39. Smith, D. and P. Španěl, Selected ion flow tube mass spectrometry (SIFT-MS) for on-line trace gas analysis. *Mass Spectrometry Reviews*, 2005. 24(5): p. 661-700.
40. Španěl, P. and D. Smith, Progress in SIFT-MS: Breath analysis and other applications. *Mass Spectrometry Reviews*, 2011. 30(2): p. 236-267.
41. Cappellin, L., Probst, M., Limtrakul, J., Biasoli, F., Schuhfried, E., Soukoulis, C., Mark, T.D., Gasperi, F., Proton transfer reaction rate coefficients between H<sub>3</sub>O<sup>+</sup> and some sulphur compounds. *International Journal of Mass Spectrometry*, 2010. 295(1–2): p. 43-48.
42. Cody, R.B., J.A. Laramée, and H.D. Durst, Versatile New Ion Source for the Analysis of Materials in Open Air under Ambient Conditions. *Analytical Chemistry*, 2005. 77(8): p. 2297-2302.
43. Cody, R.B., Laramée, James A., Nilles, J. Michael, Durst, H. Dunpont, Direct Analysis in Real Time (DART) Mass Spectrometry. [www.jeolusa.com](http://www.jeolusa.com).
44. Jagerdeo, E. and M. Abdel-Rehim, Screening of Cocaine and Its Metabolites in Human Urine Samples by Direct Analysis in Real-Time Source Coupled to Time-of-Flight Mass Spectrometry After Online Preconcentration Utilizing Microextraction by Packed Sorbent. *Journal of the American Society for Mass Spectrometry*, 2009. 20(5): p. 891-899.
45. Adams, J., Analysis of printing and writing papers by using direct analysis in real time mass spectrometry. *International Journal of Mass Spectrometry*, 2011. 301(1–3): p. 109-126.

46. Chernetsova, E.S. and G.E. Morlock, Assessing the capabilities of direct analysis in real time mass spectrometry for 5-hydroxymethylfurfural quantitation in honey. *International Journal of Mass Spectrometry*, 2012. 314(0): p. 22-32.
47. Vaclavik, L., Cajka, T., Hrbek, V., Hajslova, J., Ambient mass spectrometry employing direct analysis in real time (DART) ion source for olive oil quality and authenticity assessment. *Analytica Chimica Acta*, 2009. 645(1–2): p. 56-63.
48. Zhu, H., Wang, C., Song, F., Liu, Z., Liu, S., Rapid quality assessment of Radix Aconiti Preparata using direct analysis in real time mass spectrometry. *Analytica Chimica Acta*, 2012. 752(0): p. 69-77.
49. Loreto, F. and J.-P. Schnitzler, Abiotic stresses and induced BVOCs. *Trends in Plant Science*, 2010. 15(3): p. 154-166.
50. Monks, P.S., Gas-phase radical chemistry in the troposphere. *Chemical Society Reviews*, 2005. 34(5): p. 376-395.
51. Filella, I. and J. Peñuelas, Daily, weekly, and seasonal time courses of VOC concentrations in a semi-urban area near Barcelona. *Atmospheric Environment*, 2006. 40(40): p. 7752-7769.
52. Holzinger, R., Kleiss, B., Donoso, L., Sanhueza, E., Aromatic hydrocarbons at urban, sub-urban, rural (8°52'N; 67°19'W) and remote sites in Venezuela. *Atmospheric Environment*, 2001. 35(29): p. 4917-4927.
53. Miyakawa, Y., S. Kato, and Y. Kajii, Calibration of the Proton Transfer Reaction Mass Spectrometry (PTR-MS) Instrument for Oxygenated Volatile Organic Compounds (OVOCs) and the Measurement of Ambient Air in Tokyo. *Journal of Japan Society for Atmospheric Environment / Taiki Kankyo Gakkaishi*, 2005. 40(5): p. 209-219.
54. Demarcke, M., et al., History effect of light and temperature on monoterpenoid emissions from *Fagus sylvatica* L. *Atmospheric Environment*, 2010. 44(27): p. 3261-3268.
55. Mulligan, C.C., Justes, D.R., Noll, R.J., Sanders, N.L., Laughlin, B.C., Cooks, R.G., Direct monitoring of toxic compounds in air using a portable mass spectrometer. *Analyst*, 2006. 131(4): p. 556-567.
56. Huang, G., Gao, L., Duncan, J., Harper, J.D., Sanders, N.L., Ouyang, Z., Cooks, R.G., Direct Detection of Benzene, Toluene, and Ethylbenzene at Trace Levels in Ambient Air by Atmospheric Pressure Chemical Ionization Using a Handheld Mass Spectrometer.

- Journal of the American Society for Mass Spectrometry, 2010. 21(1): p. 132-135.
57. Mayhew, C.A., Sulzer, P., Petersson, F., Haidacher, S., Jordan, A., Mark, L., Watts, P., Mark, T.D., Applications of proton transfer reaction time-of-flight mass spectrometry for the sensitive and rapid real-time detection of solid high explosives. *International Journal of Mass Spectrometry*, 2010. 289(1): p. 58-63.
58. Maarse, H., *Volatile compounds in food and beverages*. 1991, New York: Marcel Dekker.
59. Ragaert, P., Devlieghere, F., Loos, S., Dewulf, J., Van Langenhove, H., Foubert, I., Vanrolleghem, P.A., Debevere, J., Role of yeast proliferation in the quality degradation of strawberries during refrigerated storage. *International Journal of Food Microbiology*, 2006. 108(1): p. 42-50.
60. Nosedá, B., Ragaert, P., Pauwels, D., Anthierens, T., Van Langenhove, H., Dwulf, J., Devlieghere, D., Validation of selective ion flow tube mass spectrometry for fast quantification of volatile bases produced on atlantic cod (*gadus morhua*). *Journal of Agricultural and Food Chemistry*, 2010. 58(9): p. 5213-5219.
61. Maçatelli, M., Akkermans, W., Koot, A., Buchgraber, M., Paterson, A., van Ruth, S., Verification of the geographical origin of European butters using PTR-MS. *Journal of Food Composition and Analysis*, 2009. 22(2): p. 169-175.
62. Araghpour, N., et al., Geographical origin classification of olive oils by PTR-MS. *Food Chemistry*, 2008. 108(1): p. 374-383.
63. Rocha, S.M., et al., Rapid tool for distinction of wines based on the global volatile signature. *Journal of Chromatography A*, 2006. 1114(2): p. 188-197.
64. Dragone, G., et al., Characterisation of volatile compounds in an alcoholic beverage produced by whey fermentation. *Food Chemistry*, 2009. 112(4): p. 929-935.
65. Taylor, A.J., Linforth, R.S.T., Harvey, B.A., Blake, A., Atmospheric pressure chemical ionisation mass spectrometry for in vivo analysis of volatile flavour release. *Food Chemistry*, 2000. 71(3): p. 327-338.
66. Lirk, P., F. Bodrogi, and J. Rieder, Medical applications of proton transfer reaction-mass spectrometry: ambient air monitoring and breath analysis. *International Journal of Mass Spectrometry*, 2004. 239(2-3): p. 221-226.
67. Amann, A., Poupart, G., Telser, S., Ledockowski, M., Schmid, A., Mechtcheriakov, S., Applications of breath

- gas analysis in medicine. *International Journal of Mass Spectrometry*, 2004. 239(2–3): p. 227-233.
68. Abbott, M.S., The development and application of SIFT-MS to explore the trace gases in urine and breath and their association with malignancy. PhD Thesis, Keele University, 2008.
69. Pinggera, G.M., Lirk, P., Bodogri, F., Herwig, ., Steckel-Berger, G., Bartsch, G., Rieder, J., Urinary acetonitrile concentrations correlate with recent smoking behaviour. *BJU Int*, 2005. 95(3): p. 306-9.
70. Steeghs, M.M.L., Moeskops, B.W.M., van Swam, K., Cristescu, S.M., Scheepers, P.T.J., Harren, F.J.M., On-line monitoring of UV-induced lipid peroxidation products from human skin in vivo using proton-transfer reaction mass spectrometry. *International Journal of Mass Spectrometry*, 2006. 253(1–2): p. 58-64.
71. Alegretti, A.P., F.V. Thiesen, and G.P. Maciel, Analytical method for evaluation of exposure to benzene, toluene, xylene in blood by gas chromatography preceded by solid phase microextraction. *Journal of Chromatography B*, 2004. 809(1): p. 183-187.
72. Rieder, J., Prazeller, P., Boehler, M., Lirk, P., Lindinger, W., Amann, A., Online monitoring of air quality at the postanesthetic care unit by proton-transfer-reaction mass spectrometry. *Anesth Analg*, 2001. 92(2): p. 389-92.
73. Rieder, J., Keller, C., Brimacomber, J., Gruber, G., Lirk, P., Summer, G., Amann, A., Monitoring pollution by proton-transfer-reaction mass spectrometry during paediatric anaesthesia with positive pressure ventilation via the laryngeal mask airway or uncuffed tracheal tube. *Anaesthesia*, 2002. 57(7): p. 663-6.
74. Hryniuk, A. and B.M. Ross, Detection of acetone and isoprene in human breath using a combination of thermal desorption and selected ion flow tube mass spectrometry. *International Journal of Mass Spectrometry*, 2009. 285(1–2): p. 26-30.
75. Critchley, A., Elliott, T.S., Harrison, G., Mayhew, C.A., Thompson, J.M., Worthington, T., The proton transfer reaction mass spectrometer and its use in medical science: applications to drug assays and the monitoring of bacteria. *International Journal of Mass Spectrometry*, 2004. 239(2–3): p. 235-241.
76. Harrison, G.R., Critchley, A.D., Mayhew, C.A., Thompson, J.M., Real-time breath monitoring of propofol and its volatile metabolites during surgery using a novel mass spectrometric technique: a feasibility study. *Br J Anaesth.*, 2003. 91(6): p. 797-9.

## **CHAPTER 2: PROTON TRANSFER REACTION TIME-OF-FLIGHT MASS SPECTROMETRY: INSTRUMENTATION AND OPERATION**

---

### **2.1 INTRODUCTION**

The primary focus of this thesis is the development and the application of a heated inlet source (HIS) for coupling with Proton Transfer Reaction Time-of-Flight Mass Spectrometry (PTR-TOF-MS). The Leicester instrument employed is sometimes known as the Chemical Ionisation Reaction Time-of-Flight Mass Spectrometer (CIR-TOF-MS) because it is able to use several different CI reagents [1, 2], although  $\text{H}_3\text{O}^+$  remains the main CI reagent and the one used exclusively in the work in this thesis. The Leicester instrument has been well characterised, particularly with regard to atmospheric measurement [3, 4] and breath analysis [5].

This chapter begins with some general material on PTR-MS and is then followed by a brief description of the Leicester instrument and its operating principle.

### **2.2 PROTON TRANSFER REACTION MASS SPECTROMETRY**

#### **2.2.1 Instrumentation**

For any sample to be analysed by mass spectrometry, the neutral molecules must first be ionised. Proton transfer as an ionisation source was first introduced by Munson and Field in 1966 [6] as an alternative to the traditional electron ionisation (EI) method. In an EI source, the interaction between high-energy electrons in the region of 70 eV and the gaseous analyte results in the ejection of an electron from the latter to

form a cation [7, 8]. In this process energy in excess of the ionisation energy of the molecule, which is typically around 10 eV for VOCs, is transferred. The excess energy often results in extensive fragmentation of the molecular ion. Characteristic fragmentation patterns can be used to determine analyte identity, but identification becomes very complicated when analysing complex mixtures. In comparison, proton transfer is based on gas phase ion-molecule reactions between the analyte and a primary reagent ion. As a result, proton transfer is described as a “soft” ionisation technique as it produces a protonated ion with little excess energy, resulting in little or no fragmentation. Often, only a single analyte ion is produced, so the resulting mass spectra are greatly simplified when compared with electron impact ionisation.

The type of ion-molecule reaction is dependent upon the chemical properties of both the CI reagent used and the individual analyte species, but generally, ionisation will proceed via one of four reactions: proton transfer, charge transfer, anion abstraction or association [9]. Proton transfer reactions have become the most widely used, and forms the basis of the PTR-MS technique. Typical reagent gases and the corresponding reagent ions for proton transfer include methane/ $\text{CH}_5^+$ , ammonia/ $\text{NH}_4^+$  and water/ $\text{H}_3\text{O}^+$  [10]. Proton transfer for a compound will only occur if its proton affinity is higher than the reagent ion, which has to be taken into account when selecting a suitable reagent. Table 2.1 provides proton affinities for a selection of different compounds.

Table 2.1 Proton affinity of different compounds

Classification	Molecule	$\infty$ Proton affinity/kJ mol <sup>-1</sup>
Inorganic gases	O <sub>2</sub>	421
	N <sub>2</sub>	494
	CO <sub>2</sub>	541
	O <sub>3</sub>	626
	H <sub>2</sub> O	691
	NH <sub>3</sub>	854
	alkanes	methane
ethane		596
propane		626
<i>i</i> -butane		678
alkenes	ethene	641
	propene	752
alkynes	acetylene	641
	propyne	748
aromatics	benzene	750
	toluene	784
	phenol	817
	aniline	883
other organics	chloromethane	647
	formaldehyde	713
	acetaldehyde	769
	ethanol	776
	acetone	812
	acetonitrile	779

<sup>∞</sup> Taken from the compilation by Hunter and Lias [1].

All PTR-MS instruments feature the following components: (1) an ion source for the production of the reagent ions, (2) a drift tube that acts as the reaction chamber where proton transfer between the reagent ions and neutral analytes takes place, and (3) a mass analyser/detection system. The majority of PTR-MS instruments reported in the literature are commercially available Ionicon Analytik systems [12], most of which feature a hollow cathode discharge (HCD) ion source coupled to a quadrupole mass analyser.

In an HCD ion source containing water vapour the discharge process causes the ionisation of water vapour to produce ions such as  $O^+$ ,  $H^+$ ,  $H_2^+$ ,  $OH^+$  and  $H_2O^+$ , all of which react further with neutral water molecules to subsequently produce  $H_3O^+$  ions, either in the discharge region itself or the small source drift region that follows [13]. High concentrations of  $H_3O^+$  ions are produced (often as high as > 99% purity) without the need for pre-selection of ions before entering the drift tube, as opposed to SIFT-MS, which employ a mass filter to select a single reagent. Some  $O_2^+$  and  $NO^+$  impurity ions are formed because of back diffusion of air from the drift tube into the ion source, an unwanted occurrence since these ions can also react with VOCs [14]. HCD sources normally operate between 2 – 3 mbar, and  $H_3O^+$  count rates of  $10^6$  counts  $s^{-1}$  at the downstream mass spectrometer are routinely achieved [15]. Radioactive ion sources ( $^{241}Am$ ,  $^{210}Po$ ) have been employed as an alternative to discharge sources and can operate at higher pressures (up to 13 mbar) [16, 17]. Higher drift tube pressures can translate into higher instrument sensitivity [15, 16, and 18]. Reagent ions from the ion source are drawn into the drift tube that consists of a series of ring electrodes and insulating spacers, and is normally 5 – 15 cm in length [19]. The sample is continuously introduced into the drift tube, with the air containing the trace analyte species acting as the buffer gas. The potential gradient over the drift tube directs the ions towards the exit and into the analyser. As previously stated, the majority of PTR-MS instruments use quadrupole analysers, which act as mass filters that only allow the transmission of ions of a particular mass to the detector at any given time. This means that while dwelling on one mass value, ions in all other mass channels are not detected. The duty cycle for a quadrupole analyser is inversely proportional to the number of mass channels monitored (assuming the same dwell

time for each channel). For the analysis of complex samples, quadrupole instruments achieve high sensitivity over a complete mass range when sufficient sampling times are available.

However, to achieve comparable sensitivity on short timescales quadrupoles are typically operated so that only a small number of preselected mass channels are monitored at the expense of losing information on other components. Detection at the pptv level has been reported for dwell times of 1 – 10 seconds [20]. Another limitation of quadrupole analysers is the relatively low mass resolution [16].

Some instruments with alternative analysers, namely ion trap (IT) and time-of-flight (TOF) systems have been developed offer the prospect of simultaneously measuring of ions of all masses. The first PTR-IT\_MS instrument was reported by Prazeller *et al.*, which coupled the IT analyser to a standard hollow cathode ion source and drift tube [21]. Similar instruments have been reported subsequently [22]. One specific advantage of IT-MS over quadrupole analysers is a higher duty cycle, up to 95 – 99% compared to 1 – 10% with a quadrupole in a typical operating mode. In addition, the IT-MS is ideally suited to MS/MS experiments, whereby collision-induced dissociation is performed on ions of a single mass after the ejection of all others from the trap [19]. This tandem mass spectrometry can be exploited in several ways, *e.g.* to help to distinguish isobaric compounds. The detection limit of PTR-IT-MS systems are not yet as good as that of quadrupole instruments, but sub-ppbv levels have been achieved [23].

Since the first publication of the Leicester time-of-flight instrument [24], a few other PTR-ToF-MS systems have been reported.

### 2.2.2 Proton transfer reaction

Exothermic proton transfer reactions between  $\text{H}_3\text{O}^+$  and VOCs occur for those compounds with a proton affinity greater than that of water, resulting in the production of protonated pseudo-molecular ions (Equation 2.1).



M represents the neutral analyte compound,  $\text{MH}^+$  its protonated product ion and  $k$  is the proton transfer reaction rate coefficient. The reaction rate coefficient indicates the intrinsic speed of the reaction, and exothermic proton transfer will proceed at or near the collision rate, *i.e.* proton transfer occurs on every collision [10].

The measurement of ion signals by the mass spectrometer in PTR-MS provides a means for determining the absolute concentration of a specific constituent of a gas mixture. With  $\text{H}_3\text{O}^+$  as the proton source and assuming reaction with only a single organic gas, designated M, the proton transfer reaction is shown in equation 2.1. This reaction is a second-order elementary reaction and satisfy the rate equation.

$$-\frac{d[\text{H}_3\text{O}^+]}{dt} = k[\text{H}_3\text{O}^+][\text{M}] \quad (2.2)$$

Assuming that  $[\text{M}] \gg [\text{H}_3\text{O}^+]$ , which is reasonable since M is a neutral gas (even if present at trace levels), then [M] is constant (the reaction is pseudo first order) and equation 2.2 can be integrated to yield

$$[\text{H}_3\text{O}^+]_t = [\text{H}_3\text{O}^+]_0 e^{-k[\text{M}]t} \quad (2.3)$$

The reaction time  $t$  is the time it takes for the reagent ion, in this case  $\text{H}_3\text{O}^+$ , to travel from the point where it is first mixed with the analyte to the end of the drift tube (beyond which reaction

essentially stops). The concentration of  $\text{H}_3\text{O}^+$  can be related to that of  $\text{MH}^+$  by

$$[\text{MH}^+]_t = [\text{H}_3\text{O}^+]_0 - [\text{H}_3\text{O}^+]_t \quad (2.4)$$

Substituting equation 2.3 into equation 2.4 gives:

$$[\text{MH}^+]_t = [\text{H}_3\text{O}^+]_0 [1 - e^{-k[\text{M}]t}] \quad (2.5)$$

The final assumptions yield a particularly simple expression.

First, we assume that conditions are chosen such that only a small proportion of  $\text{H}_3\text{O}^+$  is consumed by the reaction, that is,  $[\text{H}_3\text{O}^+]_0 \approx [\text{H}_3\text{O}^+]_t$ , or equivalently  $[\text{MH}^+]_t \ll [\text{H}_3\text{O}^+]_0$ .

If  $k[\text{M}]t \ll 1$ , which is usually true providing  $\text{M}$  is present at well below the parts per million level, then a Taylor expansion of the exponential term in equation 2.5 and retaining only the first term in the Taylor expansion of  $e^{-k[\text{M}]t}$  leads to the following:

$$\frac{[\text{MH}^+]_t}{[\text{H}_3\text{O}^+]_0} = \frac{i(\text{MH}^+)}{i(\text{H}_3\text{O}^+)} = k[\text{M}]t \quad (2.6)$$

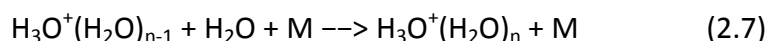
In equation 2.6,  $i(\text{MH}^+)$  is the protonated analyte ion signal,  $i(\text{H}_3\text{O}^+)$  is the hydronium reagent ion signal,  $[\text{M}]$  is the analyte concentration in the sample and  $t$  is the reaction time, which is taken as the time that the ions spend in the drift tube. If  $k$  and  $t$  are known, the concentration of a specific analyte can be determined through the measurement of the  $\text{MH}^+/\text{H}_3\text{O}^+$  signal ratio. However, the accuracy of compound concentrations determined in this way can be limited for several reasons. These reasons includes the uncertainties associated with the rate coefficient, uncertainty in the reaction time, variation in ion transmission through the mass spectrometer, differing mobility of reagent and analyte ions, and the fact that equation (2.6) does not account for additional processes such as fragmentation [19, 25]. Equation (2.6) modified to take some of these factors into account, but for determining reliable analyte

---

concentrations, calibration with a specific gas standard is preferred.

### 2.2.3 Cluster ion chemistry

As a result of unreacted neutral water vapour molecules in the drift tube,  $\text{H}_3\text{O}^+$  ions can react to form  $\text{H}_3\text{O}^+(\text{H}_2\text{O})_n$  cluster ions via the process:



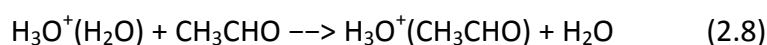
Where, M is a third body. Water vapour in the analyte gas can also enhance the formation of  $\text{H}_3\text{O}^+(\text{H}_2\text{O})_n$ . In PTR-MS, attempts are made to minimize the proportion of  $\text{H}_3\text{O}^+(\text{H}_2\text{O})_n$  ions ( $n \geq 1$ ) relative to  $\text{H}_3\text{O}^+$  in the drift tube (for reasons explained below) through the use of collision-induced dissociation. Nevertheless, despite these efforts, hydrated hydronium ions still frequently observed in mass spectra from the PTR-MS and so it is important to beware of the impact they may have on the ion chemistry. The extent of water cluster ion formation increases as the humidity of the sample increases, so for some of the types of samples analysed later in this thesis, *i.e.* urine headspace, whiskey or the direct injection of water samples, it can become very significant.

The water cluster ion can complicate interpretation of mass spectra. Hydrated hydronium cluster ions also possess higher proton affinity than the bare water molecule ( $691 \pm 3 \text{ kJ mol}^{-1}$ ). For example, the water dimer,  $(\text{H}_2\text{O})_2$ , has a proton affinity of  $808 \pm 6 \text{ kJ mol}^{-1}$ [26]. The higher proton affinity is the result of the added stability of the  $\text{H}_3\text{O}^+$  brought about by sharing the positive charge with additional water molecule. As more water molecule added, the proton affinity increases, but the incremental effect decline in magnitude as the cluster grows.

There are two important consequences of water cluster ion formation. First, the increased proton affinity means that some

---

reactions that occur with  $\text{H}_3\text{O}^+$  do not occur with  $\text{H}_3\text{O}^+(\text{H}_2\text{O})_n$ . An example is acetaldehyde, whose proton affinity lies between those of  $\text{H}_2\text{O}$  and  $(\text{H}_2\text{O})_2$ . Secondly, with hydrated hydronium ions proton transfer is not the only possible reaction channel. In the case of acetaldehyde, it is known that reaction with  $\text{H}_3\text{O}^+$  does indeed proceed by proton transfer and occurs at the collision limiting rate. However, as shown by flowing afterglow and SIFT studies [27], reaction of  $\text{H}_3\text{O}^+(\text{H}_2\text{O})$  with acetaldehyde also occurs at the collision-limiting rate, but in this case proceeds via so-called ligand switching:



If the ligand-switching reaction proceeds at the collision limited rate, the presence of  $\text{H}_3\text{O}^+(\text{H}_2\text{O})_n$  ions in PTR-MS is not necessarily a problem, since product ions containing the analyte molecule will still be formed. However, the presence of additional product channels of hydrated hydronium ions increases the complexity of data analysis and is best avoided if possible [19].

#### 2.2.4 Time-of-Flight Mass Spectrometry

Following its generation within the drift cell, the ion beam is passed into the Kore MS-200 ToF-MS for mass analysis. In this section the basic principles and components of ToF-MS is discussed, as this is the type of mass analyser used in all of the work presented in this thesis.

Many substantial reviews on the ToF-MS technique and its underlying theoretical principals have been conducted [28], and so only, a basic overview is provided here.

Stephenson [29] first introduced ToF mass analysers in 1946 for use in experiments in nuclear physics. Wiley and McLaren [30] have developed a two-stage acceleration zone to improve the resolution. The main principle at the heart of the ToF-MS

technique is the separation of ions in time rather than in space, where the latter is the norm for most other mass spectrometers.

For example, consider a distribution of ions covering a range of masses. If each ion within this pool is given an equal amount of kinetic energy by accelerating the ion 'packet' over a finite distance, the ions will travel through a field free region with a terminal velocity proportional to their mass-to-charge ratio ( $m/z$ ). This is demonstrated in Figure 2.1, where ions A and B have equal charges and masses  $m_A$  and  $m_B$ , respectively ( $m_B > m_A$ ), are accelerated over a distance  $P_L$ ; Ion A will acquire a greater velocity because of its lower mass relative to ion B and hence the former will have the shorter time-of-flight to detector. If the distance that the ions travel in the field free region,  $F_L$ , is fixed and well known, each ion of specific mass-to-charge ratio will have its own characteristic time-of-flight (TOF). Consequently, the measurement of an ion's TOF can be employed to determine its  $m/z$ .

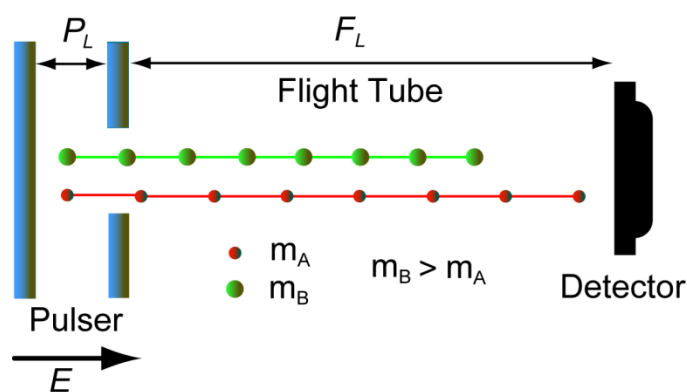


Figure 2.1 Diagram to show the basic components and principles of a linear ToF-MS system (adapted from Wyech (2008)) [4].

A ToF-MS instrument is composed of four distinct regions which are (i) an ion extraction/acceleration region (or so called pulser), (ii) x and y steering plates, (iii) a field free flight tube and (iv) a

detector. All components of the ToF-MS reside under high vacuum ( $< 10^{-6}$  mbar), as collisions with gas molecules will cause scattering of the ion beam and perturbation of the ion flight. The arrangement of some of these components in a ToF-MS system is shown diagrammatically in Figure 2.1.

In continuous beam systems, once the ion beam exits the ion source it often undergoes some form of focusing on a transfer region within the ToF-MS before being passed to the pulsed ion extraction region. In its most simple form, the pulse extraction region, or the pulser, consists of two electrodes separated by a distance,  $P_L$ , over which a pulsed potential difference is applied.

Independent of the ionisation method, the electric charge  $q$  of an ion of mass  $m_i$  is equal to an integer number  $z$  of electron charges  $e$ , and thus  $q = ez$ . The energy uptake  $E_{el}$  by moving through a voltage  $U$  is given

$$E_{el} = qU = ezU \quad (2.9)$$

Thereby, the former potential energy of a charged particle in an electric field is converted into kinetic energy  $E_{kin}$ , i.e. into translational motion

$$E_{el} = ezU = \frac{1}{2} m_i v^2 = E_{kin} \quad (2.10)$$

Assuming the ion was at rest before, which is correct in a first approximation, the velocity ( $v$ ) attained is obtained by rearranging equation 2.10 into

$$v = \sqrt{\frac{2ezU}{m_i}} \quad (2.11)$$

*i.e.*  $v$  is inversely proportional to the square root of mass.

Having acquired their terminal velocity, the ions enter a field free flight tube, in which they are isolated from any external

forces. The ions will travel the length of the flight tube distance ( $s$ ) after having been accelerated by a voltage  $U$ . The relationship between velocity and drift time  $t_d$  needed to travel the distance  $s$  is

$$t_d = \frac{s}{v} \quad (2.12)$$

Which upon substitution of  $v$  with equation 2.11 becomes

$$t_d = \frac{s}{\sqrt{\frac{2ezU}{m_i}}} \quad (2.13)$$

Equation 2.13 delivers the time needed for the ion to travel the distance  $s$  at contact velocity, *i.e.* in a field-free environment after the process of acceleration is completed.

It is also obvious from equation 2.13 that the time to drift tube through a fixed length of field-free space is proportional to the square root of  $m_i/z$ .

$$t_d = \frac{s}{\sqrt{2eU}} \sqrt{\frac{m_i}{z}} \quad (2.14)$$

Thus, the time interval  $\Delta t$  between the arrival times of ions of different  $m_i/z$  is proportional to  $s \times (m_i/z_1^{1/2} - m_i/z_2^{1/2})$ .

If there were no other factors to consider, equation 2.10 would give the final flight time of the ions. Other factor that might also require consideration is the time taken for the ions to undergo acceleration.

The ion acceleration time equated by,

$$F = Eq \quad (2.15)$$

Where,  $E$  is electric field and  $q$  is charge

$$F = m_i a \quad (2.16)$$

Where,  $m_i$  is mass and  $a$  is acceleration

$$a = Eq/m \quad (2.17)$$

The velocity and time require it reach it is calculated by,

$$a = dv/dt \quad (2.18)$$

After substituting equation 2.17 and 2.18, gives

$$v = \int \frac{Eq}{m} t \quad (2.19)$$

When initial velocity ( $v_0$ ) is added to equation 2.19,

$$v = v_0 + \left(\frac{Eq}{m}\right) t_a \quad (2.20)$$

Re-arranging the equation 2.20, will give the time that ion is accelerating from initial velocity ( $v_0$ ) to drift velocity ( $v$ )

$$t_a = \frac{v-v_0}{E} \left(\frac{m}{q}\right) \quad (2.21)$$

The drift time  $t_d$  as calculated by means of equation 2.13 is not fully identical to the total time-of-flight. The time needed for acceleration of ions  $t_a$  calculated by means of equation 2.21 has to be added. Furthermore, a short period of time  $t_0$  in which ion begins to accelerate is typically in the order of few nanoseconds also has to be added. Thus, total time-of-flight ( $t_{total}$ ) is given by [28],

$$t_{total} = t_0 + t_a + t_d \quad (2.20)$$

From the basic principles of ToF-MS described above, it is clear that only one 'packet' of ions may be extracted from the continuous source beam for analysis at any one instant. This

means that whilst each ion packet is ‘in flight’ the continuous ion beam not under analysis is simply unused. That fraction of ions which are extracted for analysis is known as the duty cycle of the instrument ( $D_c$ ). The duty cycle of a ToF-MS is defined by three parameters: (i) the size of the extraction aperture of the extraction electrode ( $X_1$ ), (ii) the speed of ions within the continuous ion beam ( $u_c$ ) and (iii) the repetition frequency of the scan ( $f$ ) [18]:

$$D_c = \frac{X_1 f}{u_c} \quad (2.21)$$

In typical modern ToF mass spectrometers, the duty cycle rarely exceeds  $\sim 2\%$ , meaning 98% of the generated ion beam is simply lost. Consequently, the low instrument duty cycle of ToF-MS results in its major drawback, i.e. limited sensitivity.

## **2.3 The Leicester PTR-ToF-MS Instrument**

### **2.3.1 Overview**

Full details of the development and characterisation of the PRT-ToF-MS instrument can be found in the PhD theses of R. S. Blake [3] and K. P. Wyche [4], and so here, details are kept to a minimum. The instrument consists of a radioactive ion source and drift tube that were built in-house, coupled to a commercial orthogonal acceleration reflectron time-of-flight mass spectrometer (Kore Technology Limited, Ely, UK). The main features of the PTR-MS instrument is shown below.

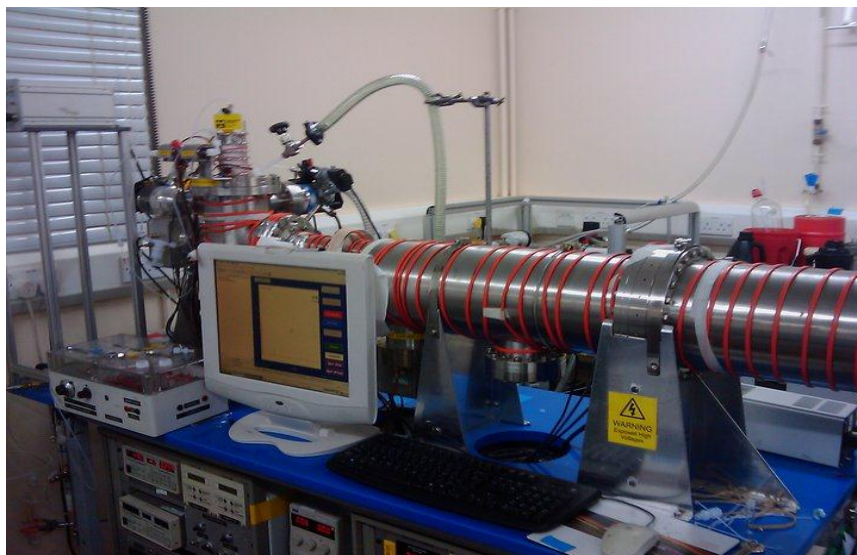


Figure 2.2 Photograph showing the Leicester PTR-ToF-MS instrument

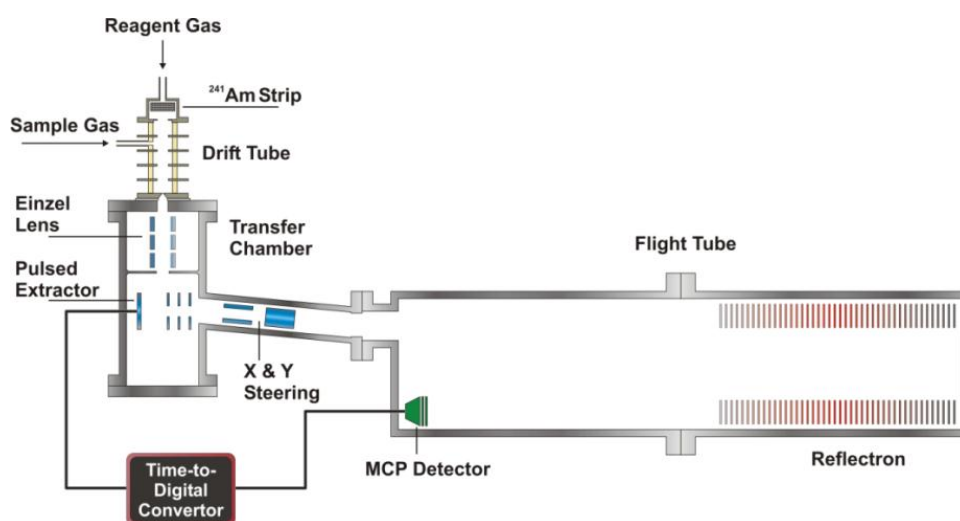


Figure 2.3 A schematic diagram of the PTR-ToF-MS instrument

### 2.3.2 Gas inlet system

The gas inlet system supplies the ion source/drift tube with a constant flow of water vapour and analyte gas. Mass flow controllers (MFCs) (Tylan FC260) controlled the flow rate of gas. To minimise memory effects, all gas lines are made of perfluoroalkoxy (PFA) polymer tubing (Swagelok, Manchester,

UK), and all fittings of the gas inlet system are made of either PFA (Galtek integral ferrule fittings, Entegris) or stainless steel (Swagelok). Gas line between the MFCs and the ion source/drift tube is maintained at 40°C with heating wire. This prevents condensation in the lines when analysing a humid sample.

Water vapour is generated by bubbling high-purity nitrogen (grade N6.0, BOC Special Gases) through a glass vessel containing high-purity deionised water (15 MΩ). The nitrogen flow through the vessel is regulated by a needle valve.

### 2.3.3 Ion source and drift tube

The radioactive ion source and drift tube (Figure 2.3) are based on a design by Hanson *et al.* [13]. The ion source consists of a radioactive strip of  $^{241}\text{Am}$  (NRD, Grand Island, NY, USA) mounted inside a stainless steel ring and housed in a stainless steel surround. The radioactive strip emits  $\alpha$ -particles with an energy around 5 MeV. A continuous flow of water vapour enters the top of the ion source at a set flow rate of 30 sccm (sccm: standard cubic centimetres per minute). Water molecules are ionised by the  $\alpha$ -particles to form  $\text{H}_3\text{O}^+$  ions, which are assumed to proceed via the mechanism shown in the following equations [31].



The drift tube, situated directly below the ion source, is approximately 11 cm in length and consists of a series of 6 stainless steel ring electrodes (0.2 cm thickness) separated by 2 cm thick insulating Semitron spacers. Viton O-rings sit in a groove in the upper and lower surface of the spacers to enable a vacuum-tight seal to be made. A thin spacer (Tufnol, 0.17 cm) separates the last electrode from the base flange. The small

region before the exit of the drift tube is referred to as the collision dissociation cell (CDC) and is 0.8 cm in length.

The analyte gas is continuously introduced at a flow rate of 220 sccm into the upstream end of the drift tube, through the wall of the spacer located between E2 and E3. The combined sample and vapour flows result in a drift tube pressure of 6 mbar measured by either a Baratron (MKS) or Pirani (Leybold) pressure gauge. The downstream end of the drift tube is evacuated using a rotary vane pump ( $5 \text{ m}^3 \text{ h}^{-1}$ , Edwards RV5). If lower sample and vapour flows are required, the amount of gas removed by the rotary pump can be restricted by partially closing an in-line tap, thus maintaining the drift tube pressure. The drift tube temperature kept constant using a heating wire, which is coiled around the outside and maintains a temperature of  $40^\circ\text{C}$

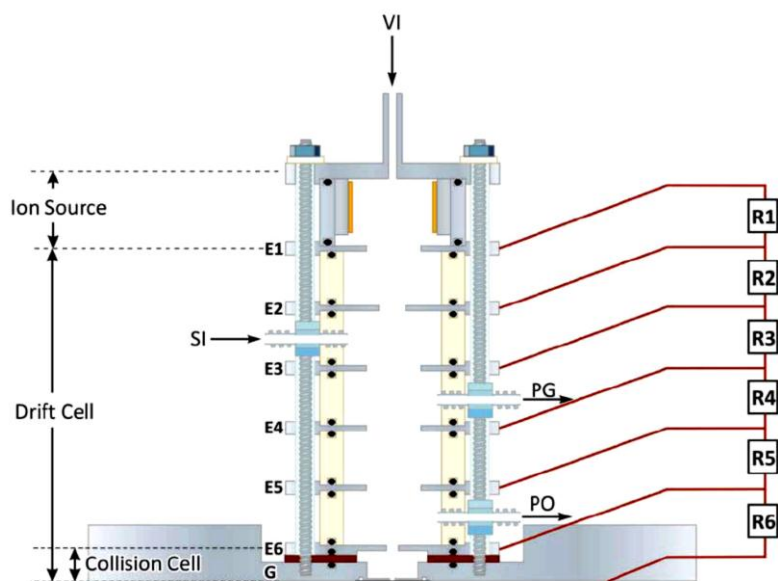


Figure 2.4 A schematic diagram of the drift tube. E1 – E6 represents electrodes 1 – 6 and R1 – R6 represents resistors 1 – 6, of which R1 – R5 are fixed a  $1 \text{ M}\Omega$  and R6 is variable between 0 –  $1 \text{ M}\Omega$ . S1, V1, PG and PO refer to the sample and vapour inlets, pressure gauge and pump outlet respectively. The main drift cell region is located between E1 and E6 and the collision cell between E6 and ground (G); the two regions can be

operated at different  $E/N$  values (Diagram adapted from Wyech (2008)) [4].

The electrodes are connected to a resistor chain consisting of five 1 M $\Omega$  resistors and one variable resistor. The first electrode is held at a typical value of +1330 V, and the resistor chain then create a voltage gradient that draw the reagent ions along the drift tube. The main section of the drift tube experiences a constant electric field, a typical value being 110 V cm<sup>-1</sup>, whilst the chosen setting of the variable resistor over the CDC results in a higher electric field of 239 V cm<sup>-1</sup>, which helps to collisionally dissociate any cluster ions prior to detection. Using the operating conditions described, the number density within the drift tube has been calculated to be 1.388 × 10<sup>17</sup> cm<sup>-3</sup>. The drift tube voltage and variable resistor setting given above provide the desired  $E/N$  value of 100/200 Td, where 1 Td = 1 Townsend = 10<sup>-7</sup> cm<sup>2</sup> V<sup>-1</sup>.

The sample ions exit the drift tube via a 200  $\mu$ m aperture. The size of the aperture dictates the flow of gas from the drift tube into the mass spectrometer; a smaller aperture here would allow higher pressures in the drift tube whilst maintaining acceptable pressures downstream in the analyser, but would reduce the ion transmission. The 200  $\mu$ m aperture provides a compromise between the ion transmission and the drift tube pressure.

### 2.3.4 Mass analyser and detection

After passing through the aperture, ions enter the transfer chamber containing an Einzel lens for focussing the ion beam.

Two turbo pumps (70 l s<sup>-1</sup>, Varian V70) evacuated this chamber. A rotary pump backed each turbo pumps. The ion beam than passes into a secondary chamber containing the pulsed

extraction system for injecting small packets of ions into the orthogonally positioned reflectron ToF-MS. This chamber is evacuated by a  $255 \text{ l s}^{-1}$  large turbo pump (BOC Edwards EXT 255) backed by a rotary pump, positioned at the base of the chamber. The system is differentially pumped throughout such that when a relatively high pressure exists in the drift tube, the low pressure required in the analyser is still achieved. The pressure inside the ToF-MS under typical operating conditions is close to  $1.0 \times 10^{-6}$  mbar as measured by a cold cathode pressure gauge (MKS Series 943).

Inside the flight tube of the TOF-MS, ions are separated according to their mass and detected by a micro-channel plate (MCP) detector. The output from the MCP is sent via a pre-amplifier to a time-to-digital converter (TDC). The TDC is responsible for triggering the pulsed extractor and recording ion arrival times at the detector.

### 2.3.5 Data collection, processing and normalisation

The mass spectral data collection is controlled through the supplied GRAMS/AI software (Thermo Scientific). GRAMS/AI converts the time data from the TDC into mass-to-charge ratios ( $m/z$ ) using Equation 2.21, displaying the raw spectra as a plot of recorded signal in counts against  $m/z$ .

$$\frac{m}{z} = \left( \frac{t - t_0}{C_b} \right)^2 \quad (2.24)$$

In the above equation,  $t$  is the arrival time of the ion and  $t_0$  and  $C_b$  are conversion parameters determined by the software after calibration to two peaks of known mass. Approximate values for  $t_0$  and  $C_b$  are 0.39 and 5.58, respectively, under normal experimental settings.

The time taken to acquire a single mass spectrum is about 80  $\mu\text{s}$  for a mass range up to 200 amu, so around 104 scans  $\text{s}^{-1}$  can be achieved. Many scans are necessary to obtain meaningful data since the ions are detected using a pulse counting system. Each successive scan was added to the previous one to build up a satisfactory signal-to-noise ( $S/N$ ) ratio. Most of the results employed in this thesis involve continuous data collection of one minute, with the exception of some of the whiskey and urine experiments where data were acquired for several minutes. Experimental parameters such as mass range, experiment length (integration time) and the number of experiments are set in the collect options of GRAMS/AI.

For the data to be processed and analysed outside of the GRAMS/AI software, two separate programs are used, MaxiSum and MaxiGroup. Firstly, the MaxiSum program transforms the raw mass spectral data through a summing process, effectively integrating the area under each peak over a defined window on either side of each nominal mass value ( $\pm 0.3$  amu). This produces an integrated signal for every mass channel. The MaxiGroup program then outputs the data as an Excel-readable file and has the optional function of summing the data to effectively model the larger integration times.

Using the convention described by Warneke *et al.*, data are normalised to 106 reagent ion counts per second, whereby 'reagent ion' are classed as both  $\text{H}_3\text{O}^+$  and  $\text{H}_3\text{O}^+(\text{H}_2\text{O})$ , using the following equation.

$$i(\text{MH}^+)_{\text{ncps}} = i(\text{MH}^+)_{\text{cps}} \times \left( \frac{10^6}{i(\text{H}_3\text{O}^+)_{\text{cps}} + i(\text{H}_3\text{O}^+(\text{H}_2\text{O}))_{\text{cps}}} \right) \quad (2.25)$$

$i(\text{MH}^+)_{\text{ncps}}$  is normalised analyte signal.  $i(\text{MH}^+)_{\text{cps}}$ ,  $i(\text{H}_3\text{O}^+)_{\text{cps}}$  and  $i(\text{H}_3\text{O}^+(\text{H}_2\text{O}))_{\text{cps}}$  are the raw signals of protonated analyte,  $\text{H}_3\text{O}^+$  ion and  $\text{H}_3\text{O}^+(\text{H}_2\text{O})$  ion respectively. The normalisation process tries to account for any changes in the hydronium ion signal [3].

### 2.3.6 PTR-ToF-MS mass spectrum and mass resolution

Figure 2.8 shows an example of a raw PTR-MS mass spectrum, displaying the signal intensity against  $m/z$ , in comparison to that obtained after data processing, *i.e.* after peak integration.

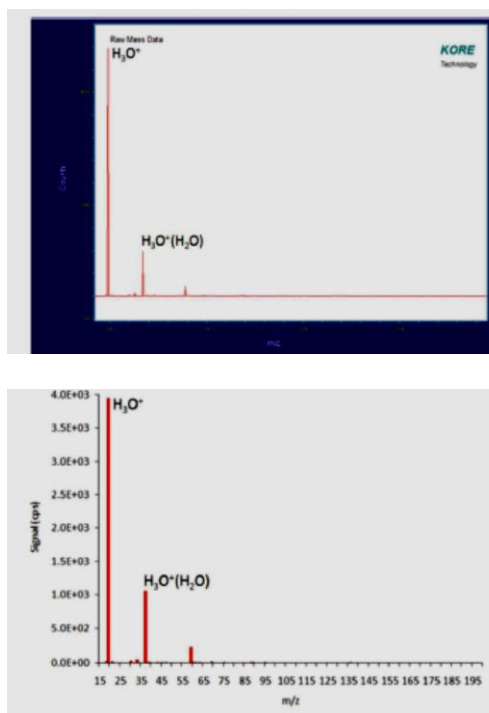


Figure 2.5 Comparison of raw (top) and processed (bottom) PTR-ToF-MS mass spectrum [5].

The dominant peak at  $m/z$  19 represents the  $H_3O^+$  reagent ion signal and the secondary peak is derived from  $H_3O^+(H_2O)$ . As PTR-ToF-MS instruments produce only singly charged ions, the  $m/z$  scale treated as a mass scale. Raw integrated  $H_3O^+$  count rates of  $2 - 4 \times 10^3$  counts  $s^{-1}$  (cps) are typically acquired while scanning at 12 – 200 amu mass range.

In mass spectrometry, the term mass resolution defines the ability of the instrument to distinguish between two ions of similar mass. Because of instrument limitations, ultimately there will always be some degree of 'spread' in the energy distribution of ions within a single ion packet. Due to this energy spread, a peak in the TOF mass spectrum will not comprise a single

discrete signal; instead, it will be composed of a range of signals with a roughly Gaussian distribution. Hence, for a single peak with no spectral interference, the resolution,  $R$ , of a mass spectrometer can be quantified by taking the ratio of the peak mass ( $m$ ) to the peak width ( $\Delta m$ ) at half the height of the peak, *i.e.* the full width half maximum (*FWHM*) mass:

$$R = \frac{m}{\Delta m} \quad (2.26)$$

The mass resolution ( $m/\Delta m$ ) of the PTR-ToF-MS instrument under standard operating conditions was determined to be in excess of 1000 over the majority of the mass range [4]. This is an order of magnitude greater than that reported for quadrupole PTR-MS instruments [16] and a linear-PTRTOF system [17], both of which quoted  $\sim 100$

## 2.4 REFERENCES:

1. Blake, R.S., Wyche, K.P., Ellis, A.M., Monks, P.S., Chemical ionization reaction time-of-flight mass spectrometry: Multi-reagent analysis for determination of trace gas composition. *International Journal of Mass Spectrometry*, 2006. 254(1–2): p. 85-93.
2. Wyche, K.P., Blake, R.S., Willis, K.A., Monks, P.S., Ellis, A.M., Differentiation of isobaric compounds using chemical ionization reaction mass spectrometry. *Rapid communications in mass spectrometry : RCM*, 2005. 19(22): p. 3356-3362.
3. Blake, R.S., Monitoring tropospheric composition using time of flight chemical ionisation mass spectrometric techniques. Thesis: University of Leicester, 2005.
4. Wyche, K.P., Development, Characterisation and Implementation of Chemical Ionisation Reaction Time-of-Flight Mass Spectrometry for the Measurement of Atmospheric Volatile Organic Compounds. Thesis: University of Leicester, 2008.
5. Willis, K.A., Development of Chemical Ionisation Reaction Time-of-Flight Mass Spectrometry for the Analysis of Volatile Organic Compounds in Exhaled Breath. Thesis: University of Leicester, 2009.

6. Munson, B., Chemical ionization mass spectrometry: ten years later. *Analytical Chemistry*, 1977. 49(9): p. 772A-775A.
7. Edmond de Hoffmann, V.S., *Mass Spectrometry: Principles and Applications*, 3rd Edition. 2007: John Wiley & Sons: Chichester.
8. Munson, M.S.B. and F.H. Field, Chemical Ionization Mass Spectrometry. I. General Introduction. *Journal of the American Chemical Society*, 1966. 88(12): p. 2621-2630.
9. J. R. Chapman, *Practical Organic Mass Spectrometry: A Guide for Chemical and Biochemical Analysis*, 2nd Edition. 1993: John Wiley & Sons: Chichester.
10. Lindinger, W., A. Hansel, and A. Jordan, On-line monitoring of volatile organic compounds at pptv levels by means of proton-transfer-reaction mass spectrometry (PTR-MS) medical applications, food control and environmental research. *International Journal of Mass Spectrometry and Ion Processes*, 1998. 173(3): p. 191-241.
11. E. P. L. Hunter, S.G.L., Evaluated gas phase basicities and proton affinities of molecules: an update. *Journal of Physical and Chemical Reference Data*, 1998. 27(3): p. 413-656.
12. Analytik, I., [www.ptrms.com](http://www.ptrms.com)
13. Hansel, A., Jordan, A., Holzinger, R., Prazeller, P., Vogel, W., Lindinger, W., Proton transfer reaction mass spectrometry: on-line trace gas analysis at the ppb level. *International Journal of Mass Spectrometry and Ion Processes*, 1995. 149–150(0): p. 609-619.
14. de Gouw, J. and C. Warneke, Measurements of volatile organic compounds in the earth's atmosphere using proton-transfer-reaction mass spectrometry. *Mass Spectrometry Reviews*, 2007. 26(2): p. 223-257.
15. Hewitt Cn Fau - Hayward, S., A. Hayward S Fau - Tani, and T. A, - The application of proton transfer reaction-mass spectrometry (PTR-MS) to the monitoring and analysis of volatile organic compounds in the atmosphere. *J Environ Monit*, 2003. 5(1): p. 1-7.
16. Hanson, D.R., Greenberg, J., Henry, B.E., Kosciuch, E., Proton transfer reaction mass spectrometry at high drift tube pressure. *International Journal of Mass Spectrometry*, 2003. 223–224(0): p. 507-518.
17. Tanimoto, H., Aoki, N., Inomata, S., Hirokawa, J., Sadanaga, Y., Development of a PTR-TOFMS instrument for real-time measurements of volatile organic compounds in air.

- International Journal of Mass Spectrometry, 2007. 263(1): p. 1-11.
18. Inomata, S., Tanimoto, H., Kameyama, S., Tsunogai, U., Irie, H., Kanaya, Y., and Wang, Z., A novel discharge source of hydronium ions for proton transfer reaction ionization: design, characterization, and performance. *Rapid Communications in Mass Spectrometry*, 2006. 20(6): p. 1025-1029.
  19. Blake, R.S., P.S. Monks, and A.M. Ellis, Proton-Transfer Reaction Mass Spectrometry. *Chemical Reviews*, 2009. 109(3): p. 861-896.
  20. Warneke, C., van der Veen, C., Luxembourg, S., de Gouw, J. A., and A. Kok, Measurements of benzene and toluene in ambient air using proton-transfer-reaction mass spectrometry: calibration, humidity dependence, and field intercomparison. *International Journal of Mass Spectrometry*, 2001. 207(3): p. 167-182.
  21. Prazeller, P., Palmer, P.T., Boscaini, E., Jobson, T., Alexander, M., Proton transfer reaction ion trap mass spectrometer. *Rapid Communications in Mass Spectrometry*, 2003. 17(14): p. 1593-1599.
  22. Steeghs, M.M.L., Sikkens, C., Crespo, E., Cristescu, S.M., Harren, F.J.M., Development of a proton-transfer reaction ion trap mass spectrometer: Online detection and analysis of volatile organic compounds. *International Journal of Mass Spectrometry*, 2007. 262(1-2): p. 16-24.
  23. Warneke, C., de Gouw, J.A., Lovejoy, E.R., Murphy, P.C., Kuster, W.C., Fall, R., Development of Proton-Transfer Ion Trap-Mass Spectrometry: On-line Detection and Identification of Volatile Organic Compounds in Air. *Journal of the American Society for Mass Spectrometry*, 2005. 16(8): p. 1316-1324.
  24. Blake, R.S., Whyte, C., Hughes, C.O., Ellis, A.M., Monks, P.S., Demonstration of Proton-Transfer Reaction Time-of-Flight Mass Spectrometry for Real-Time Analysis of Trace Volatile Organic Compounds. *Analytical Chemistry*, 2004. 76(13): p. 3841-3845.
  25. Keck, L., U. Oeh, and C. Hoeschen, Corrected equation for the concentrations in the drift tube of a proton transfer reaction-mass spectrometer (PTR-MS). *International Journal of Mass Spectrometry*, 2007. 264(1): p. 92-95.
  26. Goebbert, D. and P. Wentold, Water dimer proton affinity from the kinetic method: dissociation energy of the water dimer. *European Journal of Mass Spectrometry*, 2004. 10(6): p. 837-846.

27. Dotan, I., A.J. Midey, and A.A. Viggiano, Rate constants for the reactions of Ar<sup>+</sup> with CO<sub>2</sub> and SO<sub>2</sub> as a function of temperature (300–1500 K). *Journal of the American Society for Mass Spectrometry*, 1999. 10(9): p. 815-820.
28. Guilhaus, M., Special feature: Tutorial. Principles and instrumentation in time-of-flight mass spectrometry. Physical and instrumental concepts. *Journal of Mass Spectrometry*, 1995. 30(11): p. 1519-1532.
29. Stephenson, W.E., A Pulsed Mass Spectrometer with Improved Resolution. *Physical Reviews*, 1946. 69(11-12): p. 674-691.
30. Wiley, W.C. and I.H. McLaren, Time-of-Flight Mass Spectrometer with Improved Resolution. *Review of Scientific Instruments*, 1955. 26(12): p. 1150-1157.
31. Lagg, A., Taucher, J., Hansel, A., Lindinger, W., Applications of proton transfer reactions to gas analysis. *International Journal of Mass Spectrometry and Ion Processes*, 1994. 134(1): p. 55-66.

## **CHAPTER 3: DYNAMIC CALIBRATION OF LIQUID STANDARDS USING HEATED INLET SOURCE (HIS)**

---

### **3.1 INTRODUCTION**

Proton-transfer-reaction mass spectrometry is a well-established technique for online quantification of trace volatile organic compounds in air [1-4]. Over the past 15 years, since its inception, several improvements in the technique have been achieved [5]. These include increasing the detection sensitivity, coupling the PTR technique to high resolution mass spectrometry [6] and the introduction of switchable reagent ions [1], which makes it possible to switch between the commonly used  $\text{H}_3\text{O}^+$  primary ion and additionally  $\text{NO}^+$  and  $\text{O}_2^+$  ions [7].

All the above and many other improvements in PTR-MS means that the technique has a rapidly growing and expanding field of applications, ranging across atmospheric chemistry [8], food testing [9] and medical diagnosis (by breath analysis) [10]. However, one drawback of PTR-MS is that it is only possible to measure compounds that are present in the gas phase.

Headspace above the liquid surface is the only way to detect the trace compounds from liquid samples. In terms of the application of PTR-MS to aqueous samples, a membrane inlet system [11, 12], direct aqueous injection [13] and dynamic solution injection [14] techniques have been developed and tested.

Srinivasan *et al.* [15] have discussed membrane inlet mass spectrometry (MIMS). Four different types of sample introduction systems have been widely used for MIMS. (1) sheet

direct insertion membrane probe, (2) capillary direct insertion membrane probe, (3) dual membrane probes, and (4) membrane/ jet separator system. A capillary, direct insertion, membrane probe technique permits the use of tubular membranes, which typically have more surface area than the sheet membrane and results in enhanced analyte permeation and sensitivity. Alexander *et al.* [11] employed this approach in the first use of a membrane inlet in PTR-MS.

In their study, a hollow fibre membrane (Silastic TM (Dow Corning)) was inside a sealed stainless steel tube. The interior of the membrane was directly attached to the drift tube and sample air drawn into the membrane assembly at atmospheric pressure and flows around the outside of the membrane. Boscaini and Alexander *et al.* [12] used a similar set up to measure VOCs in water. This study performed direct and quantitative analysis of VOCs in water without pre-sampling or pre-concentration procedures. However, this technique suffers from the cross-contamination between different samples, as the same membrane used for the analysis of multiple samples to keep the cost of analysis affordable.

As an alternative to a membrane inlet, direct aqueous injection (DAI), system developed by Jurschik *et al.* [13] for analysing liquid samples by PTR-MS. In this DAI system, a carrier airstream generated by a diaphragm pump passes first through an activated charcoal and then a cooling trap to reduce the humidity prior to analyte injection. After this step, a mass flow controller used to control the flow of air to the injection region. The temperature maintained at 70°C to avoid condensation. The sample injected through a T-piece directly into the carrier gas stream. A linear signal response as a function of concentration achieved for the three VOCs used in their experiments.

Jardine *et al.* [14] developed a dynamic solution injection (DSI) system for the calibration and analysis of VOCs by PTR-MS from an aqueous sample. The DIS system consists of a liquid pump, a calibration solution vial and a mixing vial. A syringe-free stepper motor drive pump was used to control the injection flow. The liquid standards were placed in the calibration solution vial, which was sealed, one end of the tube was submerged in the sample, and the other end was connected to the pump. From the pump outlet, another tube was pierced through the septum of a mixing glass vial while N<sub>2</sub> flowed into the mixing vial via a separate tube. The mass flow controller controlled the flow rate of nitrogen. For analysis, PTR-MS was attached to the outlet of the mixing chamber.

The heated inlet source (HIS) is a simple and efficient design. The HIS described in this chapter has been developed in such a way that the neither it requires a complicated set up or flushing of the tubing to avoid the cross-contamination. The real time and the headspace analysis are also possible with HIS. The HIS is inexpensive to build and use, as it does not require any expensive pumps or fibres. Additionally, experiment set-up is simple with HIS compared to DSI, DAI and MIMS. Both DAI and DSI suffers from a complicated set-up. In DSI, a syringe pump is required to inject the sample and external heat source is required to heat the carrier gas and PTR source. In DAI, not only the dual channel pump for sample introduction but additional heat source similar to DSI is need as a part of the instrument set-up. The real-time analysis with both DSI and DAI might not be possible due to the delay time required between the two injections to flush the sample from the tube. With MIMS, even though source can be attached to the PTR, it requires the expensive fibres, which not only increases the cost but also increases the chances of contamination.

In this chapter, HIS was coupled with a PTR-MS instrument and its operating parameters were established. In addition, the effect of different matrices on the stability of the sensitivity of  $\text{H}_3\text{O}^+$  was investigated. Calibration standards were injected to calibrate the HIS and the calibration plots generated from these experiments were compared to calibration plots generated from the established GC-MS.

### **3.2 SOURCE DESIGN**

The heated inlet source (HIS) is a very simple and inexpensive design for the introduction of liquid and liquid headspace samples into a PTR-MS instrument. The HIS was made from a glass tube, which is 10 cm long and 2 cm in a diameter with 2 inlets and 1 outlet. The Department of Chemistry workshop at the University of Leicester constructed the HIS source. One of the two inlets used for the introduction of the carrier gas while the second inlet was used for the sample introduction. The outlet of the HIS was connected to the PTR-ToF-MS instrument. To heat the samples, heated metal jacket covered the HIS source. A normal temperature range of 50 – 130°C was used in the study. Figure 3.1 shows a schematic diagram of the source, while Figure 3.2 shows a photograph of the device.

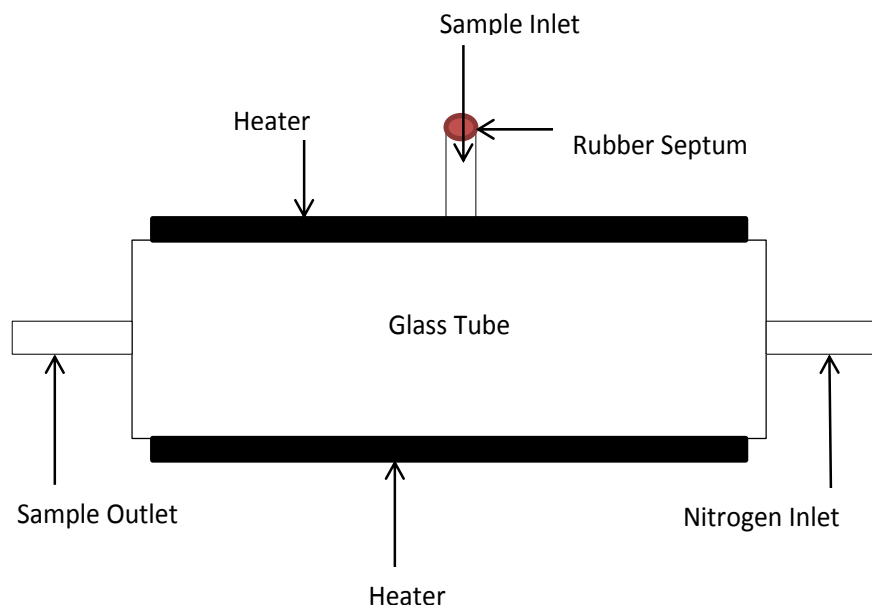


Figure 3.1 A schematic diagrams of HIS



Figure 3.2 Photograph of the heated inlet source

In Figure 3.3, where original setup is shown, the HIS was housed horizontally next to the drift tube on a metal plate that connects the drift tube to the time of flight mass spectrometer (ToF). Nitrogen was used as a carrier gas and its flow was controlled via a mass flow control unit. Teflon tubing and connectors (1/8 inch diameter) were used for the connection. Nitrogen was transported through a T-piece to one side of the source while the other side was connected to the top of the PTR-MS analyte inlet. The analyte inlet was covered with a rubber septum to prevent the loss of vacuum integrity during sample introduction. The out-let from the HIS source was connected to the drift tube

by a Teflon tube, which also made it possible to monitor any condensation through visual inspection. Due to this set-up long Teflon tube were required for the connection.

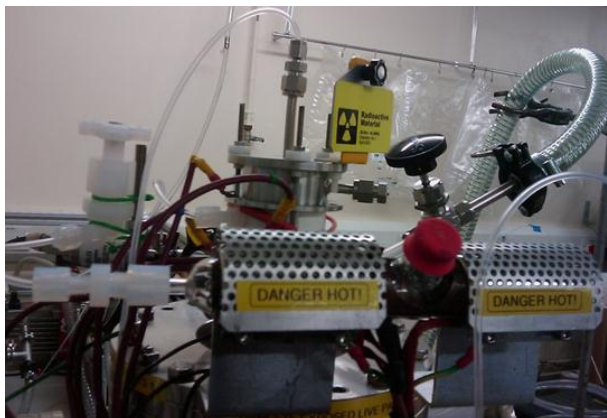


Figure 3.3 The original HIS source with at least 80 – 100 cm long exposed Teflon tubing

In the updated setup shown in Figure 3.4, two metal rods were attached to the metal plate which connected the drift tube to the TOF-MS. The HIS was mounted on these metal rods. By using this setup, a much shorter Teflon tube was required to connect the HIS outlet to the drift tube inlet. All the other connections are as per the original setup which are discussed in the above paragraph.

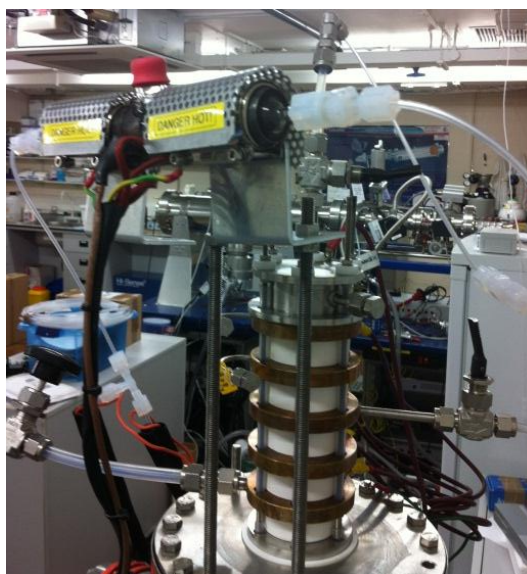


Figure 3.4 Final design of HIS

The temperature of the HIS source was maintained in the range of 70 °C to 130 °C, depending on the nature of the matrix.

Normally, the temperature was set above 100 °C for water samples and below 100 °C for more volatile solvents to ensure the complete vaporisation of the samples.

Once all connections have been made the source was heated to the require temperature with the carrier gas flowing through for at-least 30 minutes prior to analysis in order to ensure that a constant temperature was achieved for the particular experiment. For a sample introduction Hamilton gas tight syringes were used as an injector and samples were introduced into the HIS source by piercing through the rubber septum.

### **3.3 EXPERIMENTAL PROCEDURE**

The section describes the experimental parameters used during the experiments. Section 3.1 focuses the PTR-ToF-MS settings used in the study. Section 3.2 details the reagents used, while section 3.3 details the calibration standards preparation.

Sections 3.4 and 3.5, describe the injection technique, use of the aqueous and headspace samples, respectively.

#### **3.3.1 HIS and PTR-ToF-MS Settings**

Chapter 2 details the PTR-ToF-MS instrument used in the experiments.

For the PTR-ToF-MS the drift tube voltage was set at 2500V, gas flow setting of 225 lit/minute and the temperature on the drift tube was set at 40°C and pressure at 6 mbar. The data collection time was 60 s per experiment.

#### **3.3.2 Reagent**

High purity nitrogen (BOC; 99.999%) was used as a carrier gas in all experiments. Other chemicals used for the experiments were acetone (HPLC grade Sigma, UK), acetaldehyde (HPLC grade

Sigma, UK), acetonitrile (HPLC grade Sigma, UK), 2-butanone (Sigma, UK), methanol (HPLC grade Sigma, UK) and hexanol (HPLC grade Fisher, UK) and de-ionised water (in-house prepared).

### 3.3.3 Preparation of Liquid Standards

The compounds were selected based on their physical properties, *e.g.* volatile, in liquid form, readily soluble in water and does not fragment under the experimental condition. On this basis, the compounds selected for the study were acetone, 2-butanone, acetonitrile, methanol and acetaldehyde. Prior to making a calibration standard, experiments were performed by injecting a different solution prepared at different concentration levels to find out at what was the lowest level a sufficient sensitivity can be observed. The acceptable sensitivity was observed at 10.0 picomol/litter (pmol/l) therefore lowest calibration standard was prepared at 10.0 pmol/l. Standard aqueous solutions were prepared with concentrations of 10.0, 20.0, 30.0, 40.0, 50.0 and 60.0 pmol/l. To prepare the calibration standards in water, a stock solution for each compound was prepared at 20.0 nmol/l and then the serial dilution was performed to prepare the calibration standard.

Stock solutions were prepared in a separate laboratory to the one where the PTR-ToF-MS instrument was located in order to minimise any risk of contamination of the surroundings. All the solutions were prepared in glass volumetric flasks and were stored in a refrigerator when not in use. All the controlled standard addition to the water sample was done by Hamilton gas tight syringe. All the syringes were cleaned with hexane and sonicated prior to and after the preparation of the stocks and calibration standards. GC-MS standards were prepared in hexane.

### 3.3.4 Sample Injection

Prior to the start of each experiment, background signals were acquired from the first 10 experiments of similar duration to the normal experiment cycles without the introduction of any sample. After the background check, blank samples (VOC free samples) were injected to monitor any source contamination. Blank samples were also injected between experiments and at the end of the experiment to monitor the contamination and any possible carry-over effect.

To allow accurate measurement, background signals measured from the first 10 experiments prior to the start of the calibration experiments were subtracted from the analyte signal.

Three different matrices were used in the experiments:

1. Aqueous samples
2. Headspace above aqueous sample
3. Samples in organic solvent.

The headspace above aqueous sample was used to establish the calibration of the HIS when it is used in the application where headspace above the liquid is required. Chapter 6 of this thesis details the application where headspace above the urine sample was analysed and different VOCs were quantified.

The use of the volatile organic solvent is sometime important in the analysis when a small quantity of the compound from the large quantity of sample is required for the analysis and injecting a large amount of aqueous samples of the instrument is not practical. The organic solvent is also useful to dissolve a compound of interest that is not soluble in water for a calibration or analysis purposes. In this study, the organic solvents that are immiscible with water are used. Chapter 7 of this thesis details the use of volatile organic solvent for the

extraction and analysis of semi-volatile pesticide compounds from water.

The temperature of the HIS was set at 80 – 100 °C for volatile organic solvents and in the range of 100 – 130 °C for aqueous samples. The vaporisation efficiency of the sample was dependent not only on temperature but also on the injection volume. It was therefore important to observe complete vaporisation of the sample and the time it takes for 100% vaporisation. If complete vaporisation is not achieved quickly than the total scan time of the experiment required to be increased to ensure that entire sample introduced into HIS has been vaporised and all the data point are collected. The un-vaporised sample left inside the source can contaminate the HIS. In the HIS source samples are introduced at a single time, *i.e.* at the start of the experiment instead of a small, steady flow throughout the run, thus there is a possibility that the vaporised samples could enter the PTR source as a pulse. Because of this, it was very important to measure the effect of vaporised sample on  $\text{H}_3\text{O}^+$  and to check how long it takes to settle down. For this measurement different amount of water and organic solvent was injected into the HIS and consecutive 1 s scans were performed for 360 s. Data from these experiments are discussed in the Results section.

### 3.3.5 Liquid headspace analysis

1 ml of calibration standard was aliquoted in a screw-capped GC vials. These vials were heated to 30 °C for 15 minutes on a hot plate. A 50  $\mu\text{L}$  aliquot of headspace from the vial was then injected into the heated inlet tube.

## 3.4 RESULTS AND DISCUSSION

The most crucial parameter affecting the performance of the HIS inlet system when aqueous and organic solvent samples were injected was the injection volume and the time it takes for complete vaporisation. In a normal analytical situation, when more sample is injected, generally a bigger signal is observed therefore greater sensitivity can be achieved. But, in the HIS, when more aqueous sample was injected into the system, a lower detection sensitivity and a higher inaccuracy was observed due to less dilution of the vapour by the airstream and longer duration for complete vaporisation. Therefore, it was necessary that 100% of the injected liquids vaporised immediately.

### 3.4.1 Dynamics of Liquid Injections

Firstly, the impact of water and organic solvent on  $\text{H}_3\text{O}^+$  was evaluated by injecting different sample volumes.

The instrumental setup shown in Figure 3.2 was used in this study. This setup has almost 100 cm of exposed Teflon tubing, which was used to connect the HIS outlet to drift tube inlet. To measure the effect of aqueous sample used for the preparation of calibration standard on the  $\text{H}_3\text{O}^+$ , a 10  $\mu\text{l}$  and 50  $\mu\text{l}$  of the sample was injected into the HIS source and data were collected for 360 s. Data obtained from this experiment are presented in Figure 3.5. It was observed that when a 10  $\mu\text{L}$  of the sample was injected, there was a drop in hydronium ion signal after 10 s of a sample injection; this was possibly due to the temporary loss of the vacuum in the drift tube. The signal of hydronium ion started increasing from 15 s and a steady signal was observed after 90 s. When 50  $\mu\text{l}$  of the sample was injected there was again a drop in  $\text{H}_3\text{O}^+$  signal at around 10 s after sample injection but then the signal increased after 60 s and a steady signal was

observed after 280 s. The main reason for the difference is the volume of sample injected to the HIS source which dictates the time it takes to vaporise. In addition, the fact that a long inlet tube was used between the HIS outlet and the drift tube may be problematical. The concern here is that the inlet tube was cooler than the HIS and this may have caused some condensation of water before it enters the drift tube, thus lengthening the effective injection time.

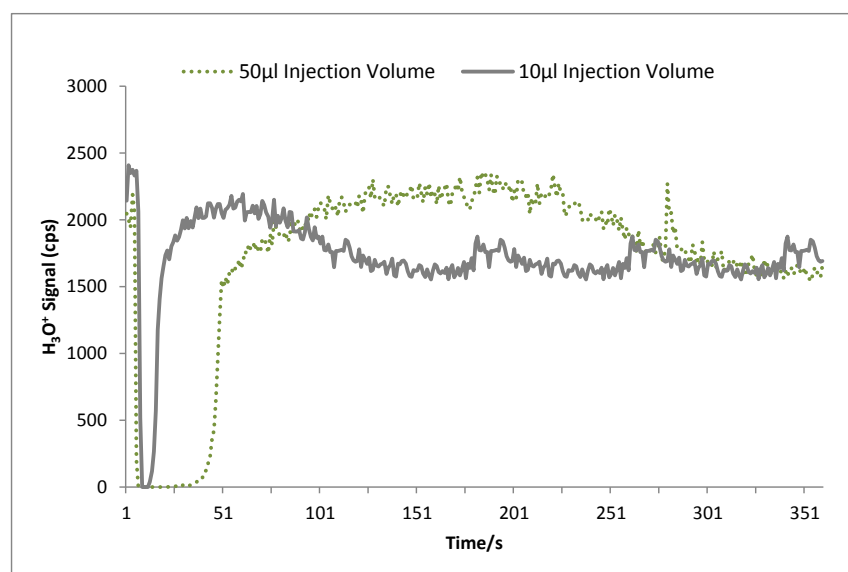


Figure 3.5 Response of the PTR-ToF-MS instrument when injecting water with the original setup at no injection, injection starts and reaching a stable signal. The time between the start of the injection and reaching a stable signal can be estimated to be about 40 seconds

Given the concern about the length of inlet line, it was decided to change the instrumental setup. Two metal rods were attached to the base-plate of the drift tube and the HIS was attached to these rods. A photograph of the setup was shown in Figure 3.3. The main advantage of this setup was that only 10 cm of Teflon tube was required to connect the HIS outlet to the drift tube inlet. To investigate the effect of water on hydronium ion with the updated setup, 1.0 µl and 10 µl of water

was injected into the HIS and data were collected for 360 s. The data generated are presented in Figure 3.6 and it was observed that for both 1.0  $\mu\text{l}$  and 10.0  $\mu\text{l}$  injection volumes, there was a drop in  $\text{H}_3\text{O}^+$  sensitivity at around 5 s after the samples were injected and after 10 s a steady signal level was achieved.

Therefore, it indicates that with shorter Teflon tube between HIS and drift tube, a steady  $\text{H}_3\text{O}^+$  signal was observed after 10 s instead of 50 s with the original set-up.

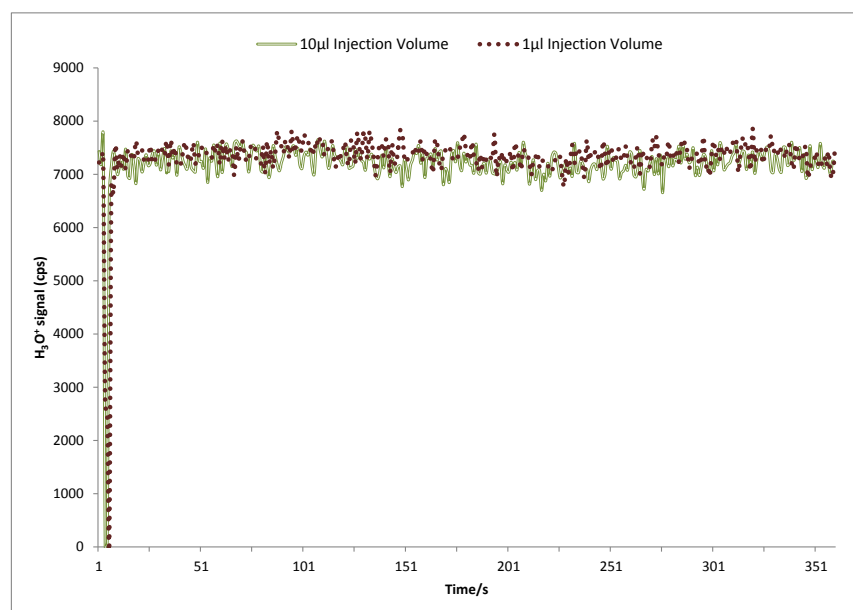


Figure 3.6 Response of the PTR-ToF-MS instrument when injecting water with new set up (shorter inlet tube). The time between start of the injection and reaching a stable signal is about 10 s.

Other liquid samples were also tested with the HIS. In experiments presented elsewhere in this thesis a liquid-liquid extraction procedure to extract and dissolve compounds was employed. Consequently, the effect of other solvents on  $\text{H}_3\text{O}^+$  signal was also monitored. Hexane was used as the organic solvent to monitor its effect. The main reason for choosing hexane was that it is not protonated by  $\text{H}_3\text{O}^+$  due to its higher proton affinity, thus simplifying the analysis.

A 10  $\mu\text{l}$  of hexane was injected into the HIS with the long inlet tube, 50  $\mu\text{l}$  of hexane was injected to the HIS with the short tube, and the results are summarised in Figure 3.6.

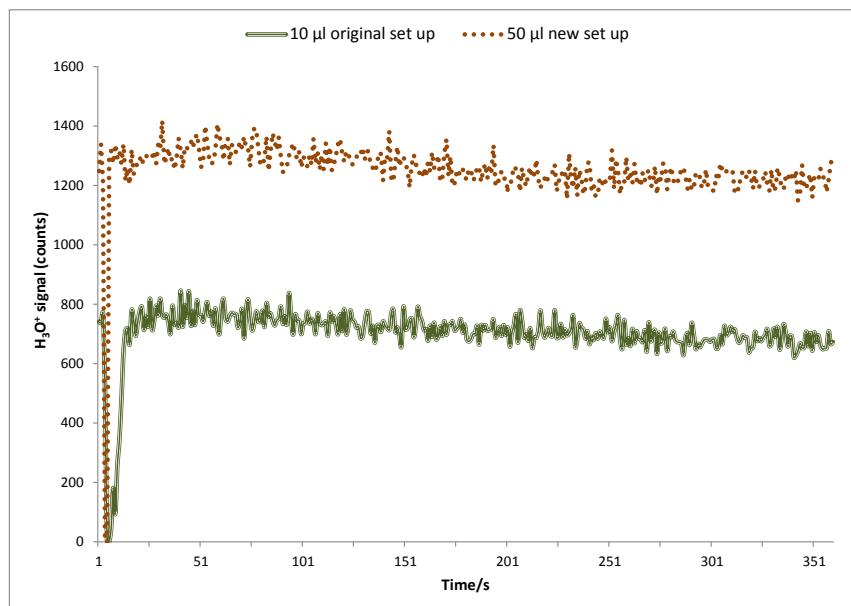


Figure 3.7 Response of the PTR-ToF-MS instrument when injecting hexane into HIS with original setup and new setup.

When 10  $\mu\text{l}$  of hexane was injected into HIS with the long inlet tube, there was a drop in  $\text{H}_3\text{O}^+$  signal at ca. 5 s and from around 20 s, the signal increased and then became stable at 50 s. When 50  $\mu\text{l}$  of hexane was injected into HIS with the short tube, a steady signal was achieved after only 10 s. Similar to the aqueous sample, with the updated setup, for the organic solvent, a stable  $\text{H}_3\text{O}^+$  was observed after 10 s instead of 50 s from the original set-up.

During the course of the experiment, it was observed that different samples behaved differently when injected into the source. For example, if water is introduced it took some time, depending on the sample volume, for it to become totally vaporised. This observation was made by visual inspection of the vaporisation process in HIS, as the source is made of glass. If the

sample consists mainly of an organic volatile solvent, then vaporisation of the sample is instantaneous.

The data shown in Figures 3.5 - 3.7 shows the benefit of using a shorter inlet tube, which delivers a stable  $\text{H}_3\text{O}^+$  signal after 10 s whereas the long inlet tube required 60 s.

### 3.4.2 Analytical tests and calibrations

After finding the ideal injection conditions and injection volume, calibration standard samples were then injected into the HIS, with updated setup. The observed peak areas for the compounds were plotted and are presented in Figure 3.8.

A large background signal at the chosen  $m/z$  was observed during the course of the study. The water sample at a different concentration and injection volume (1.0 – 100  $\mu\text{l}$ ) was used for different experiments during the course of the study. Therefore, either the un-vaporised or a concentrated sample was the reason for the contamination in the HIS.

The background-subtracted data were used for the calculations. In addition, at-least five to one signal to noise ratio was achieved in the study, therefore this contamination was not considered to have an impact on the data generated in the study.

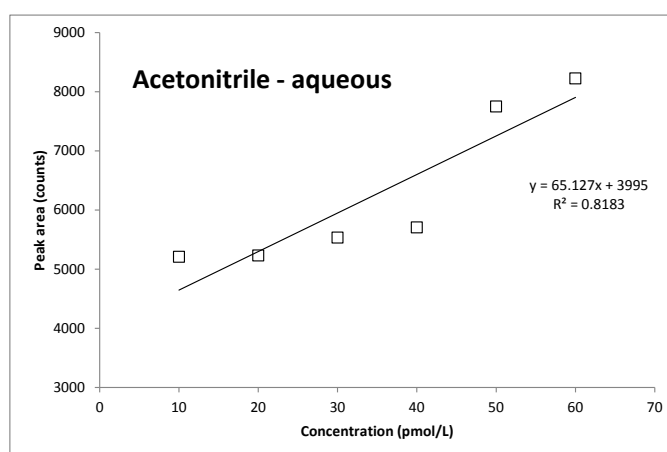


Figure 3.8 Plots of a signal for protonated methanol, acetonitrile, acetaldehyde, acetone and 2-butanone vs. concentration in water with new setup.

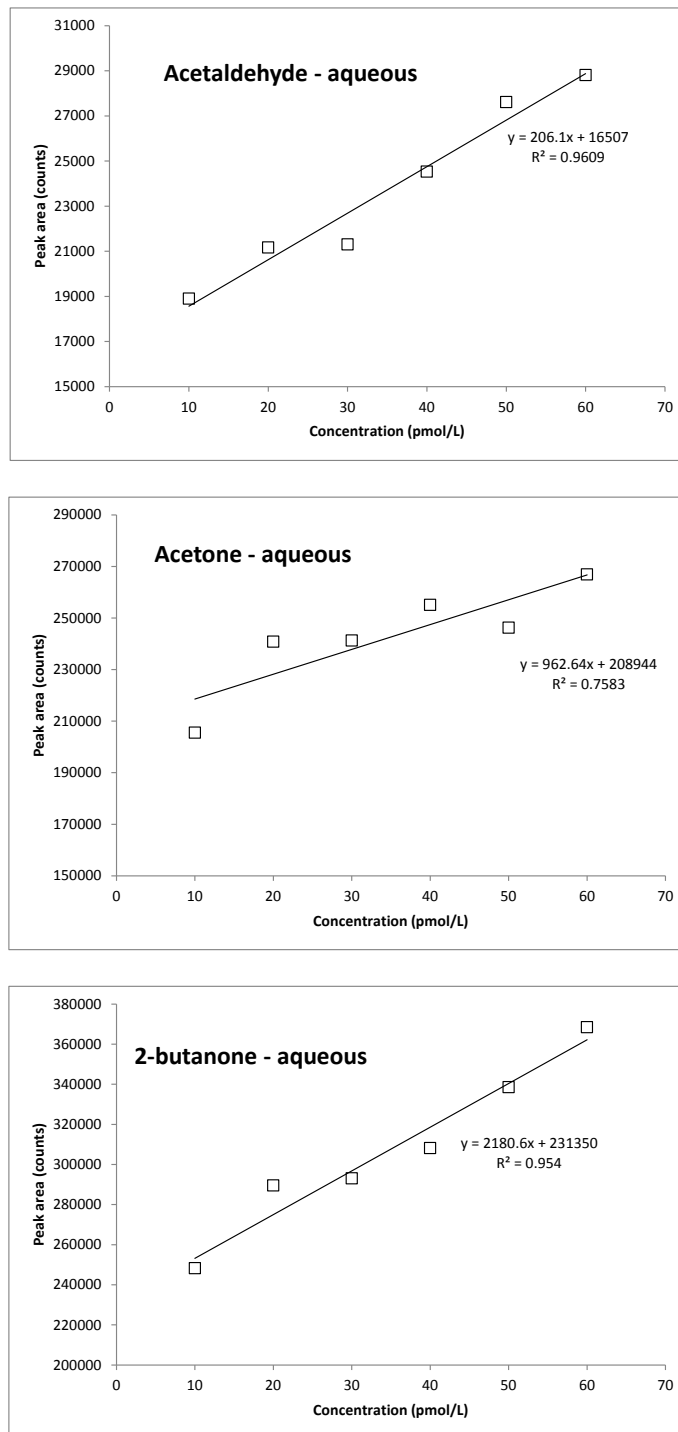


Figure 3.8 Plots of a signal for protonated methanol, acetonitrile, acetaldehyde, acetone and 2-butanone vs. concentration in water with new setup.

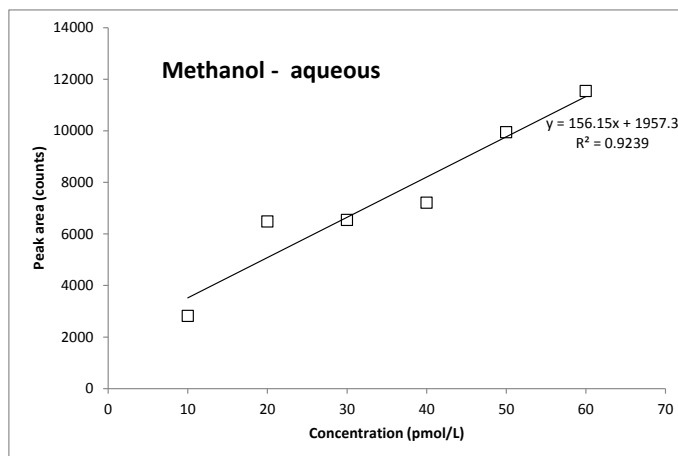


Figure 3.8 Plots of a signal for protonated methanol, acetonitrile, acetaldehyde, acetone and 2-butanone vs. concentration in water with new set up.

For the updated setup, linear response observed for all the compounds analysed in the experiment. The correlation coefficient, denoted by  $r$ , is a measure of the strength and direction of a linear response between two variables. The value of  $r$  can range between +1 and -1, with a  $r$  value of 0 indicating no linear relationship while 1 indicates a perfect linear relationship. The values between 0 and 0.3 indicate a weak linear relationship, 0.3 to 0.7 indicate a moderate linear relationship and 0.7 to 1.0 indicates a strong linear relationship. The  $r$  values observed from the calibration curves presented in Figure 3.8 were 0.81, 0.96, 0.76, 0.95 and 0.92 for acetonitrile, acetaldehyde, acetone, 2-butanone and methanol, respectively. These values indicate that a strong linear relationship was observed when aqueous standards were injected.

To calibrate the HIS for the use with a volatile organic solvent, calibration standards were also prepared in hexane. A 10  $\mu\text{l}$  of the calibration standard sample were injected into the HIS source. The observed peaks are plotted and data are presented in Figure 3.9.

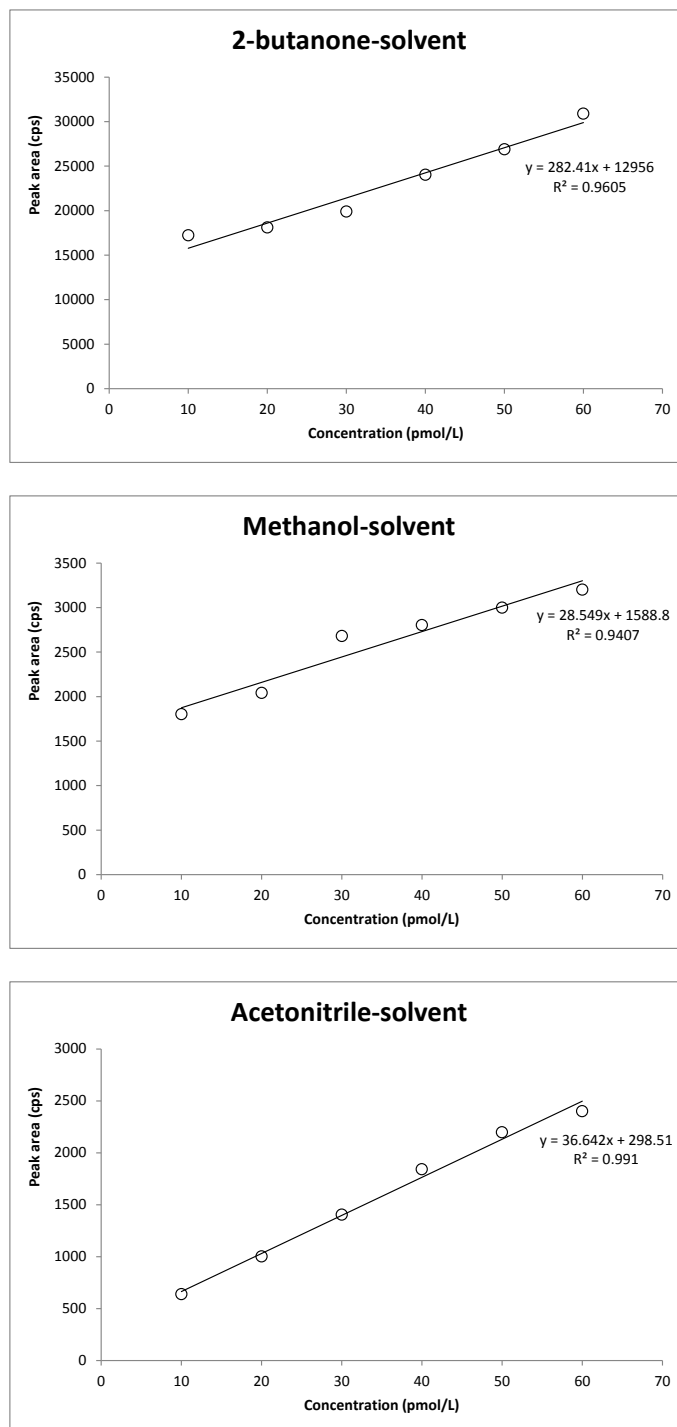


Figure 3.9 Plots of signal for protonated methanol, acetonitrile, acetaldehyde, acetone and 2-butanone versus concentration in hexane.

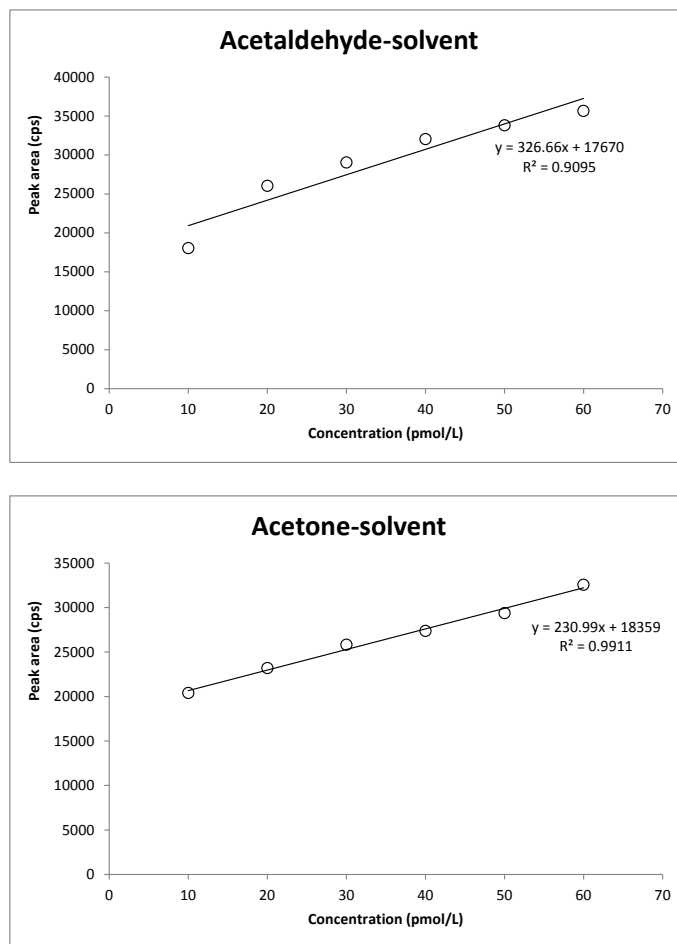


Figure 3.10 Plots of signal for protonated methanol, acetonitrile, acetaldehyde, acetone and 2-butanone versus concentration in hexane.

The  $r$  values observed from the calibration curves presented in Figure 3.9 were 0.96, 0.94, 0.99, 0.91 and 0.99 for 2-butanone, methanol, acetonitrile, acetaldehyde and acetone, respectively. As discussed earlier in this section, the  $r$  value ranging from 0.7 to 1.0 indicates a strong linear relationship. Therefore, the observed  $r$  values indicate that a strong linear relationship was observed when standards were prepared in organic solvent.

The calibration of headspace analysis was carried out by injecting the headspace above the aqueous standards. Prior to the injection, samples were thawed to room temperature and were mixed vigorously and then heated at 40°C for at least 10 minutes. As sufficient sensitivity was observed for the

compounds, a 50  $\mu\text{L}$  injection volume was used. Data observed from this experiment are presented in Figure 3.10.

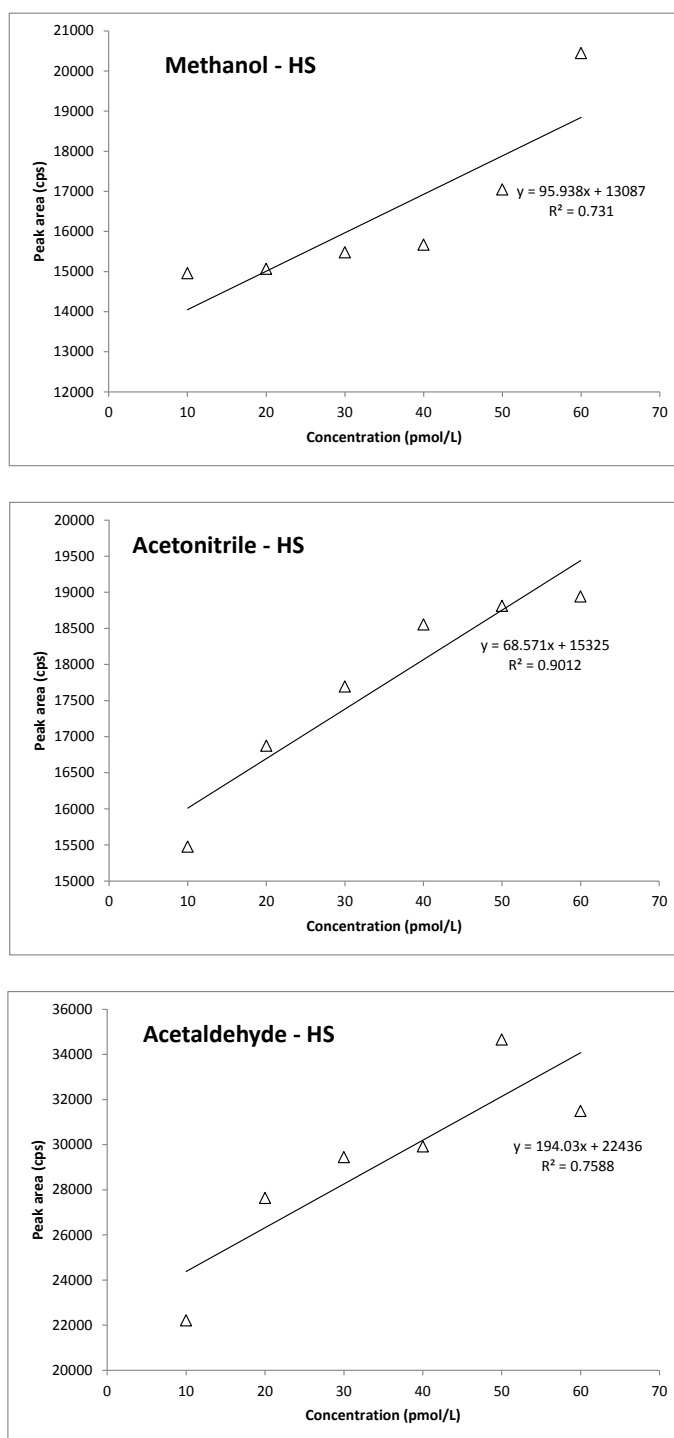


Figure 3.11 Plots of signal for protonated methanol, acetonitrile, acetaldehyde, acetone and 2-butanone vs. concentration in headspace above water standards

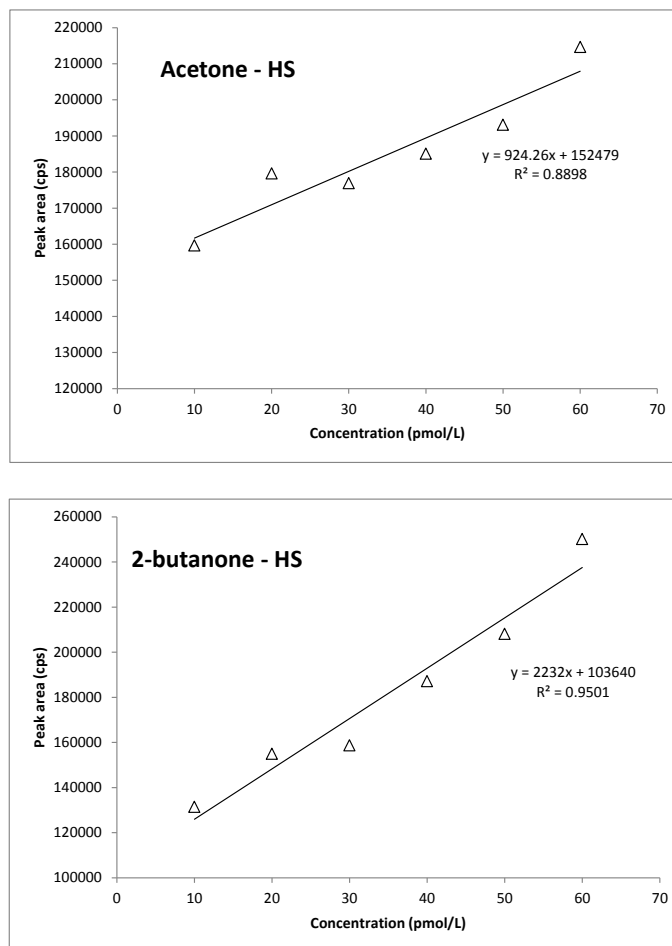


Figure 3.12 Plots of signal for protonated methanol, acetonitrile, acetaldehyde, acetone and 2-butanone vs. concentration in headspace above water standards

The  $r$  values observed from the calibration curves presented in Figure 3.10 were 0.90, 0.73, 0.95, 0.89 and 0.76 for acetonitrile, methanol, 2-butanone, acetone and acetaldehyde, respectively. As discussed earlier in this section, the  $r$  value ranging from 0.7 to 1.0 indicates a strong linear relationship. Therefore, the observed  $r$  values indicate that a strong linear relationship was observed when the headspace above the aqueous standards were analysed.

A series of experiments were carried out to evaluate the precision of the injection technique. To assess the precision, multiple injection of the same standard sample was made under what were otherwise the same operating conditions. The

precision of the injection was not only dependent on the accuracy of sample drawing of the user, but it was also dependent on the injection volume, where the needle is placed during the injection and the temperature of the HIS. These experiments also helped to reveal the optimum technique for sample injection.

The precision was calculated by using the following equation:

$$Precision = \frac{Standard\ deviation}{Mean} \times 100 \quad (3.1)$$

It was noted that a precision in the range of 7 – 20 % was observed for liquid samples while a precision of  $\leq 10\%$  was observed for the liquid headspace and solvent standard samples.

The Limit of Detection (LoD) for the different compound was also calculated. The LoD is the lowest amount of the investigated compounds in a sample that can be detected but not necessarily quantified. The limit of detection can be calculate by [17],

1). Signal-to-noise ratio method: Signal-to-noise ratio method is usually used for the calculation of LoD in separation and spectrometric method. The minimum signal/noise ratio of  $\geq 3$  is used in all the different experiments documented in this thesis.

2). Based on the calculation using the standard deviation of the response and the slope method: By using this method, the LoD can be calculated by using the following equation,

$$C_{LoD} = \frac{3s}{m} \quad (3.2)$$

Where  $s$  is the standard deviation and  $m$  is the slope of related calibration line.

Table 3.1 The limit of detection (pmol/l) for different compounds when injected in different matrix

	Methanol	Acetonitrile	Acetaldehyde	Acetone	2-butanone
Aqueous Injection	1.17	1.49	1.76	18.7	0.44
Solvent Injection	6.40	3.72	1.97	4.50	0.07
Headspace Injection	1.05	1.42	1.68	4.69	0.06

As seen in Table 3.1, in general a better LoD was observed when headspace above the liquid was analysed.

The poor LoD was observed for methanol and acetonitrile when calibration standards were prepared in solvent. The possible cause for this is that both methanol and acetonitrile have poor solubility in hexane [16]. For acetone, comparable LoD was observed for solvent and headspace analysis' but unexpectedly different LoD was observed for acetone from liquid injection. There are no analytical reasons i.e. injection error or standard preparation error as the same set of calibration solutions were used for headspace injections. Therefore, only plausible explanation for this is acetone might have suffered from the instrumental set-up, *i.e.* a high background signal for acetone might have affected the calibration, sample might not have vaporised completely or the longer data collection period was required.

Jurschik *et al.* [13] reported the LoD of pyridine, methanol and acetonitrile in the region of 100 ppt from their direct aqueous injection (DAI) technique.

To compare the LoD from HIS to DAI, the LoD values obtained from the HIS were converted to ppt by using following Equation (3.3) [18]:

$$C_{(\text{ppm})} = 10^6 \times C \times M / \rho \quad (3.3)$$

Where C is concentration *mol/l*, M is molecular weight in *g/mol* of the compound and  $\rho$  is the density of water in *kg/m<sup>3</sup>*.

The achieved LoD for different compounds prepared in water from HIS was 1 ppt when compare to 100 ppt from DAI.

Therefore, up to 100-fold increase in LoD was observed in HIS. In DAI at-least, 200-fold more aqueous sample was injected and this high injection volume might have affected the efficient vaporisation of sample therefore lower LoD compared to HIS was observed. As discussed earlier in this chapter, efficient vaporisation is critical to achieve the better sensitivity and LoD when dealing with the aqueous samples.

To confirm the results obtained from the HIS source, standards prepared in hexane were also injected into a GC-MS system. Helium was used as a carrier gas and GC oven was set to rise from 50°C to 250°C over the course of a 10 minute run. The run period was set for a shorter duration compared to the normal 45 to 60 minutes as very clean samples were injected for the analysis. Calibration plots obtained from the experiment are shown in Figure 3.11.

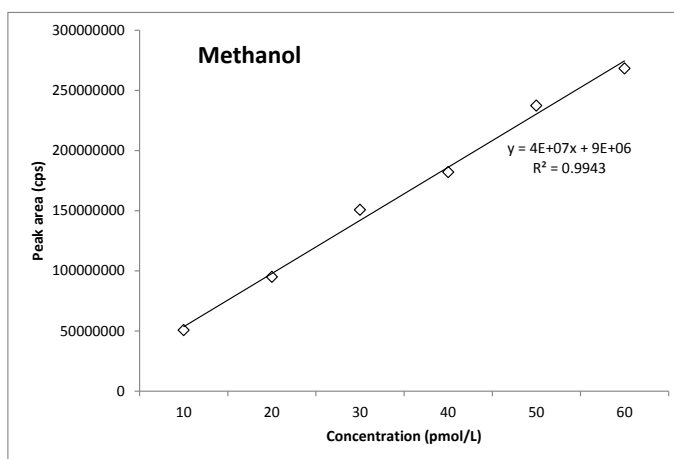


Figure 3.13 Plots of 2-butanone, acetone, acetonitrile and acetaldehyde signals as a function of concentration in hexane and analysed on GC-MS.

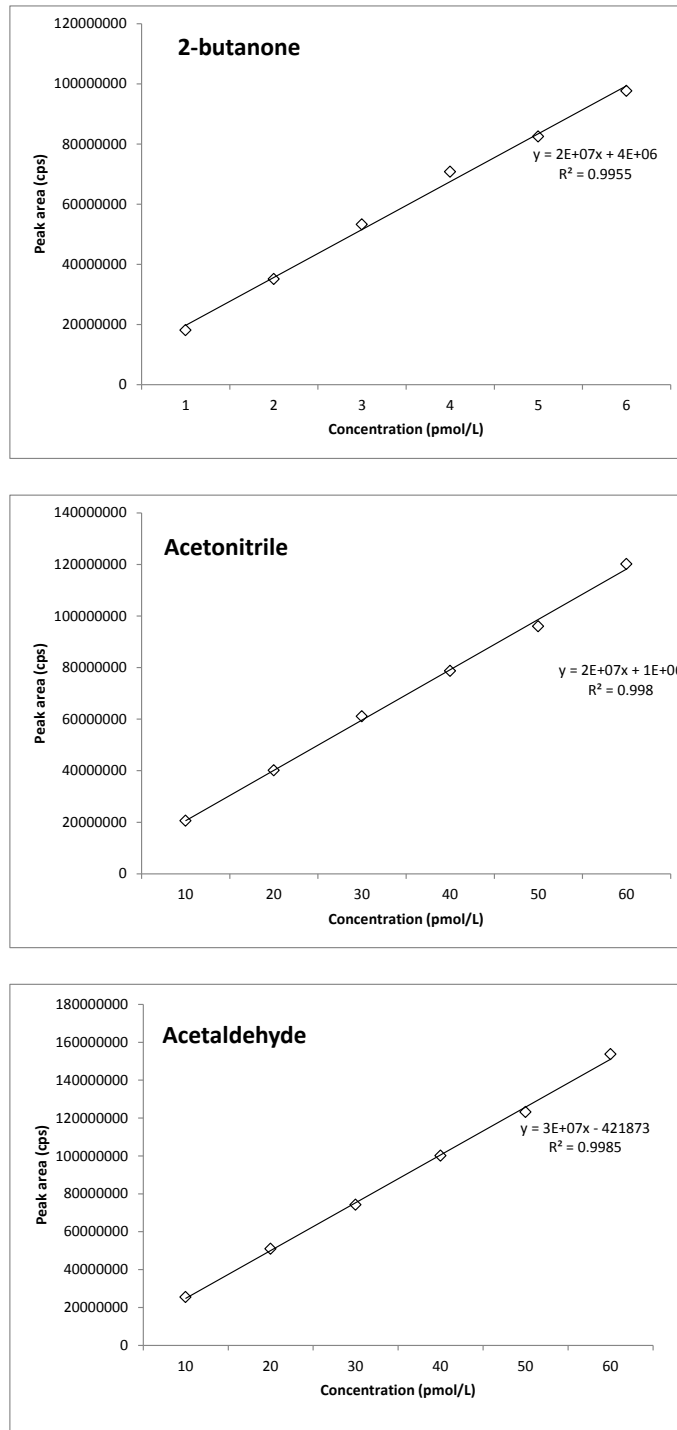


Figure 3.14 Plots of 2-butanone, acetone, acetonitrile and acetaldehyde signals as a function of concentration in hexane and analysed on GC-MS.

The observed  $r$  values from the Figure 3.11 were in the region of 0.99 for all compounds; therefore it indicates a strong linear relationship.

In the calibration curve, a slope is the indication of the sensitivity of the method, *i.e.* proportionality constant between response and concentration. Generally, the greater the slope implies to greater the sensitivity of the method.

Table 3.2 The sensitivity (pmol/l) for different compounds when injected in different matrix

	Methanol	Acetonitrile	Acetaldehyde	Acetone	2-butanone
Aqueous Injection	156	65	206	963	2181
Solvent Injection	29	36	327	234	282
Headspace Injection	96	69	194	924	2232

In general, the comparable calibration slope was observed between aqueous and headspace above aqueous standards (see Table 3.2). But the low calibration slope was observed when calibration standards were prepared in organic solvent. This low slope could not be due the poor instrumental sensitivity as acceptable sensitivity was observed for aqueous standards. The possible reasons for this could be the poor solubility of the compounds in hexane.

Jardine *et al.* [14] reported a calibration slope of  $1.58e^{-5}$  ppbv for acetone. The observed calibration slope for acetone from HIS when aqueous standard was injected was 963 pmol/l ( $5.59e^{-3}$  ppb; conversion made by using Equation 1). The observed sensitivity of the acetone was up to 100-fold higher in HIS when compared to [14]. The possible reason for the difference in sensitivity is due to the large amount of sample was used in the DSI. As discussed earlier in this chapter, efficient vaporisation is critical to achieve the better sensitivity and LoD when dealing with the aqueous samples.

The calibration slopes from the HIS were compared to the calibration slope generated by GC-MS. It was observed from the data that the calibration slopes from GC-MS was at-least 200-fold more sensitive than HIS. Jardine *et al.* [14] also reported at-

least a 150 % difference between the slope generated by using PTR-MS and GC-MS.

In the current study, the same calibration standards were used for both GC-MS and HIS-PTR-ToF-MS solution. Therefore, the observed variability in the sensitivity from the calibration curve is due to the injection inaccuracy, variability in the vaporisation of the sample and use of the chromatographic separation in GC. In GC-MS experiments, auto-sampler was used to make an injection compared to manual injection made on the HIS and also heating in the GC-MS is more controlled and uniform compare the HIS to evaporate the sample.

In summary, a better LoD and sensitivity was observed when compared to DAI and DSI. The overall sensitivity of the technique over DSI and DAI not claimed, as further work needed to analyse more compound to investigate the sensitivity of the technique over the broad range of compounds. However, this technique has provided a good base to explore the liquid analysis application for PTR-MS.

### **3.5 CONCLUSIONS**

In this chapter, a newly developed heated inlet source (HIS) was coupled with PTR-TOF-MS. The HIS source can be used not only for aqueous samples, but also for organic solvents and aqueous headspace measurements and it can be used to perform standard calibration. The different applications developed by HIS are, characterisation of whiskies, analysis and quantification of the VOCs from the headspace of human urine and analysis of semi-volatile compounds from waters and these applications are discussed in Chapters 5, 6 and 7, respectively.

The HIS system also overcomes the limitation of the currently available permeation and diffusion tubes and may provide a useful alternative to portable pre-prepared gas mixture

standards in cylinders and expensive permeation tubes.

Currently costly, low field portability permeation and diffusion tubes methods are used for the generation of low concentration VOC standards. These techniques are very costly and suffer from poor accuracy, long calibration time, low compound availability and difficulties in preparing the complex mixtures. The HIS can be used for the calibration purposes as low limit of detection is achieved for the different VOCs used in this study.

The best method for the injection of compounds is dependent on the whether it is in aqueous or solvent or in headspace. For aqueous samples, smaller injection volumes (below 10  $\mu\text{L}$ ) were found to give acceptable precision compared to organic solvent where due to the high volatility higher sample volume can be injected without compromising on the precision of the injections. In the case of the aqueous headspace, the injection volume has no limit, as much as 1000  $\mu\text{l}$  can be injected without compromising on the stability of the hydronium ion but consideration should be given on the potential contamination due to large sample injection.

Injection accuracy was also measured in this chapter, where multiple injection of aqueous, organic solvent and aqueous headspace sample was measured. For aqueous samples 100% vaporisation of the sample is very critical. In addition, the time required for the complete vaporisation and the length of the exposed Teflon tubing was noted because these parameters have an impact on the precision of the multiple injections. The higher the injection volume, the higher the injection variability was noted. For organic solvents 100% vaporisation was achieved very quickly, thus good precision was observed.

With the parameters stated above, good linearity between the concentration in the aqueous, organic solvent and aqueous headspace sample was noticed. The limit of detection (LoD) and

sensitivity of the HIS was established. It was found that LoD and sensitivity of HIS is up to 100-fold better than DSI and DAI in water.

In conclusion, an alternative technique to the direct aqueous injection (DAI) and dynamic solution injection (DSI) has been presented which is simple yet effective, cheap to make and can be a permanent part of any instrument. A key advantage is that it is very portable. The HIS source can not only be used for the calibration of the standards, whether in water or an organic solvent but it can be used for the measurement of VOCs in various liquid matrices.

### 3.6 REFERENCES

1. Jordan, A.H., S. Hanel, G. Hartungen, E. Herbig, J. Mark, L. Schottkowsky, R. Seehauser, H. Sulzer, P. Mark, T. D., An online ultra-high sensitivity Proton-transfer-reaction mass-spectrometer combined with switchable reagent ion capability *International Journal of Mass Spectrometry*, 2009. 286(1): p. 32-38.
2. Lindinger, W., R. Fall, and T. Karl, *Adv. Gas-Phase Ion Chem.*, 2001. 4: p. 1.
3. Blake, R.S., P.S. Monks, and A.M. Ellis, Proton-transfer reaction mass spectrometry. *Chemical Reviews*, 2009. 109(3): p. 861-896.
4. Hansel, A., et al., Proton transfer reaction mass spectrometry: on-line trace gas analysis at the ppb level. *International Journal of Mass Spectrometry and Ion Processes*, 1995. 149–150(0): p. 609-619.
5. Blake, R.S., Wyche, K.P., Ellis, A.E., Mons, P.S., Chemical ionization reaction time-of-flight mass spectrometry: Multi-reagent analysis for determination of trace gas composition. *International Journal of Mass Spectrometry*, 2006. 254(1–2): p. 85-93.
6. Prazeller, P., Palmer, P.T., Boscaini, E., Jobson, T., Alexander, M., Proton transfer reaction ion trap mass spectrometer. *Rapid Communications in Mass Spectrometry*, 2003. 17(14): p. 1593-1599.
7. Wyche, K.P., Blake, R.S., Willis, K.A., Monks, P.S., Ellis, A.M., Differentiation of isobaric compounds using

- chemical ionization reaction mass spectrometry. Rapid communications in mass spectrometry : RCM, 2005. 19(22): p. 3356-3362.
8. Hewitt Cn Fau - Hayward, S., A. Hayward S Fau - Tani, and T. A, - The application of proton transfer reaction-mass spectrometry (PTR-MS) to the monitoring and analysis of volatile organic compounds in the atmosphere. J Environ Monit, 2003. 5(1): p. 1-7.
  9. Lasekan, O. and S. Otto, In vivo analysis of palm wine (*Elaeis guineensis*) volatile organic compounds (VOCs) by proton transfer reaction-mass spectrometry. International Journal of Mass Spectrometry, 2009. 282(1-2): p. 45-49.
  10. Willis, K.A., Development of Chemical Ionisation Reaction Time-of-Flight Mass Spectrometry for the Analysis of Volatile Organic Compounds in Exhaled Breath. PhD Thesis, University of Leicester, 2009.
  11. Alexander, M., et al., Membrane introduction proton-transfer reaction mass spectrometry. International Journal of Mass Spectrometry, 2003. 223-224(0): p. 763-770.
  12. Boscaini, E. and M.L.P. Alexander, Peter Mark, Tilmann D., Membrane inlet proton transfer reaction mass spectrometry (MI-PTRMS) for direct measurements of VOCs in water. International Journal of Mass Spectrometry, 2004. 239(23): p. 171-177.
  13. Jurschik, S.T., A. Sulzer, P. Haidacher, S. Jordan, A. Schotchkowsky, R. Hartungen, E. Hanel, G. Seehauser, H. Mark, L. Mark, T. D. , Direct aqueous injection analysis of trace compounds in water with proton-transfer-reaction mass spectrometry (PTR-MS). International Journal of Mass Spectrometry. 289(2-3): p. 173-176.
  14. Jardine, K.J., Henderson, W.M., Huxman, T.E., Abrell, L., Dynamic Solution Injection: A new method for preparing pptv-ppbv standard atmospheres of volatile organic compounds. Atmospheric Measurement Techniques, 2010. 3(6): p. 1569-1576.
  15. Srinivasan, N., Johnso, R.C., Kasthurikrishnan, N., Wond, P., Cooks, R.G., Membrane introduction mass spectrometry. Analytica Chimica Acta, 1997. 350(3): p. 257-271.
  16. <http://www.sigmaaldrich.com/chemistry/solvents/hexane-center/miscibility-immiscibility.html>
  17. Gumustas, M, Ozkan, S, The Role of and Place of Method Validation in Drug Analysis Using Electroanalytical Technique. The Open Analytical Chemistry Journal, 2011, 5, 1-21

18. <http://www.rapidtables.com/math/number/PPM.htm#ppmw>

## **CHAPTER 4: DYNAMIC CALIBRATION OF STANDARDS SOLUTIONS USING A CAPILLARY INLET SOURCE (CIS)**

---

### **4.1 INTRODUCTION**

To extend the application of PTR-MS [1-4] for the analysis of VOCs and other volatile and semi-volatile compounds in aqueous solutions would greatly expand the scope of PTR-MS.

Some progress has been made in this regard, as detailed in the previous chapter. Different approaches, *e.g.* membrane inlet proton transfer mass spectrometry [6], direct aqueous injection analysis [5] and dynamic solution injection [7] has been developed for the measurement of the VOCs from the liquid and they are discussed in detail in Chapter 3.

A new source was designed for the introduction of liquid samples into PTR-MS instrument, a Heated Inlet Source (HIS), and this was described in detail in Chapter 3. This source was introduced to increase the injection volume over the course of the experiments and to achieve an instant 100% vaporisation of the aqueous samples. In brief, the HIS source is made of a heated cylindrical glass tube, with three inlets, one for sample injection, a second inlet for the addition of a carrier gas and the third connected to the drift tube. Although the source could be used for both aqueous and non-aqueous liquid samples, but it has a disadvantage over a higher injection volume of the aqueous samples as poor accuracy was observed when higher injection volume was used.

Different matrixes were used for the experiments, *e.g.* water, solvents and aqueous headspace. Precise data were observed for the solvents and aqueous headspace samples, but the

inconsistency were observed with aqueous samples with higher injection volume to achieve a greater sensitivity. In addition the exposed tubing between the HIS and the drift tube limited its use with higher injection volume due to possible condensation related problems. With the HIS technique aqueous samples with injection volumes of below 10.0  $\mu\text{l}$  could be dealt with satisfactorily, but with higher injection volumes, reproducibility in the analysis was lost. For the analysis of aqueous sample, to achieve higher sensitivity, higher amount of samples might be required, but it will not be possible with the HIS source.

To overcome the volume limitation with the HIS source, it was decided to design a new source where a small but continuous flow of aqueous solution can be introduced. The concept here is inspired by high-pressure liquid chromatography (HPLC). At any instant in time, a small volume of liquid is present in the capillary inlet source (CIS) source, and thus by maintaining a high temperature, vaporisation should be instant. Furthermore, the sensitivity issue is addressed by using a continuously flowing stream of analyte rather than an injected pulse.

The CIS design and set-up is inspired from the LC-MS instrument. The CIS source is a simple cylindrical tube made from stainless steel with three inlets (two for gas and one for sample) and one outlet. The CIS source is mounted on the top PTR with external heat source, and the syringe pump carried out the sample introduction. As discussed in the Chapter 3 (Section 3.1 Introduction), when compared to DSI, DAI and MIMS, no additional pumps or expensive fibres are required for the analysis. With the CIS source, sample can be injected throughout the course of the injection, which was the limiting factor with the HIS.

In this chapter, the design of the CIS is discussed in detail along with calibration data generated from the injection of aqueous test samples.

## 4.2 SOURCE DESIGN

### 4.2.1 Overview

A schematic diagram of the CIS source is presented in Figure 4.1. The basic principle of the CIS is the addition of a small but continuous flow of aqueous sample into the drift tube via a heated inlet capillary. The sample introduction into heated chamber was done via inlet capillary. The CIS was heated by the use of external heat source. The nitrogen was introduced from the top of the CIS by two inlets, was also getting heated by the external heat source. The sample is vaporised in the CIS source, and carried to the drift tube by nitrogen through sample outlet, which is connected to the drift tube. The CIS source consists of the heated chamber, two nitrogen inlet connections, one sample outlet source, sample inlet capillary and heating arrangement.

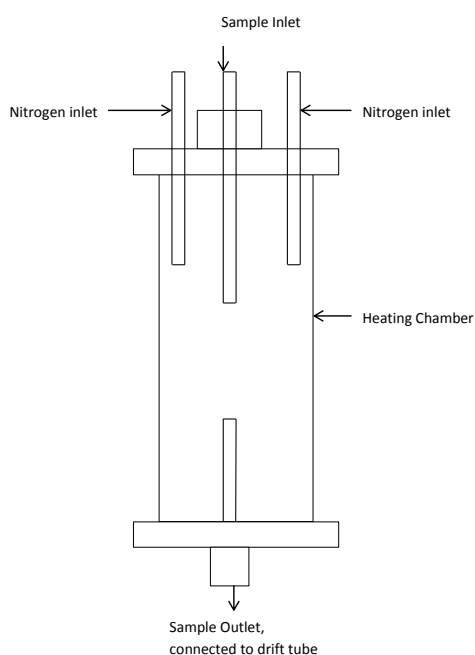


Figure 4.1 Schematic diagram of the Capillary inlet source



Figure 4.2 Complete CIS source

#### 4.2.2 Source construction

The workshop at Department of Chemistry of the University of Leicester has constructed the CIS source. It has a 15 cm long stainless steel housing with two 5-inch diameter flanges at the top and bottom.

At the top of the source, a 5 cm flange and a chamber, cover was attached to the heated chamber. Insulated PTFE was placed between the flange and cover to insulate the top part of the heated chamber. In the centre of the top flange, a sample inlet probe was attached to the screw connection. The sample inlet probe is essentially a micro capillary tube, and purchased from the AB Sciex UK Limited, Cheshire, UK (see Figure 4.3). The sample passed through the inlet capillary, which was connected to syringe pump by using PEEK tubing.



Figure 4.3 Sample inlet probe from AB Sciex UK Limited, Cheshire, UK

The nitrogen was introduced through gas inlets from both sides of the inlet probe to achieve the 100% vaporisation, to carry the vaporised sample and to maintain the pressure of the drift tube.

This design not only allowed the inlet of the nitrogen gas to the heated chamber, but due to the cross-flow of the gas stream, it also allowed the mixing of the vaporised sample and the uniform introduction of the sample to the drift tube.

Gas inlets are made of stainless tubes 5 cm long (see Figure 4.4) and go into the main 15 cm hollow tube and the top of the inlet connection has the standard 1/8" Swagelok connection. In addition, nitrogen was also pre-heated to the same temperature of the CIS. This aided in the efficient vaporisation of the sample.

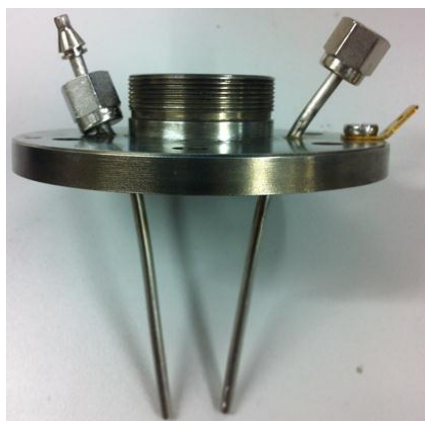


Figure 4.4 Top flange showing the sample inlet and gas inlet connections.

The bottom flange (see Figure 4.5) has a sample outlet connection, which was used to connect the CIS to the drift tube via a Swagelok connection. The connecting tube from the CIS was made of both stainless steel and Teflon. The stainless steel was required to support the weight of the CIS when housed on the drift tube. The drift tube operated at high voltage (up to 3000 V), therefore to isolate the CIS from the drift tube, a Teflon tube was placed between the CIS outlet and the drift tube inlet. The Teflon tube was not strong enough to support the weight of the CIS when

mounted vertically on the drift tube. Therefore, to support the CIS, it was placed inside the heated chamber.



Figure 4.5 Photograph of the bottom flange.

The CIS unit was oriented vertically above the drift tube so that the end of the CIS was only 5 cm from the drift tube entrance. This short distance helped to avoid any cooling of the sample as it enters into the drift tube.

#### 4.2.3 Source heating

Initially the CIS was heated with a metal jacket heater, similar to the one used in the HIS described in Chapter 3 to provide the uniform heating throughout the length of the heated chamber. A photograph of the metal jacket heater is shown in Figure 4.6. As the CIS was made of metal, the problem was encountered with electrical discharge in CIS and drift tube, and drift tube was not able to maintain its operating voltage. It quickly became obvious that metal jacket heater is not the ideal choice, even though it could maintain a constant temperature throughout the length of the source and that temperature was easy to control. Therefore, other alternatives including a ceramic heater were considered. A ceramic heater is rather expensive. In addition, a limited amount of information was found that details the operating conditions and lifetime of the ceramic heater

particularly when used under very high voltages (up to 3000 V) that are required for the University of Leicester PTR-ToF-MS instrument. The commercial ceramic heaters including the one used in modern mass spectrometer are not designed to operate under high voltages [8]; therefore, ceramic heaters were also not a viable option to heat the CIS.



Figure 4.6 A photograph of metal jacket heater

Eventually the decision was made to use an external heater for the CIS. In-house build external heater consisted of halogen lights as remote sources of heat. A similar idea used previously in the Leicester PTR-MS group for disinfecting tedlar bags (used for collecting human breath sample) by heat treatment [9] and therefore seemed a logical thing to try here.

The use of halogen lights as a source of heat is not without complications. One challenge is the precise control of the CIS temperature. Further, the exposure to very bright light was uncomfortable. Halogen lights were an ideal choice for heating Tedlar bags, as they were not attached to the instrument. Furthermore, the heating of these bags could be done in a cordoned-off area of the laboratory where no user is exposed to the bright light for any significant length of time.

Another problem with lamp heating is that it is difficult to localise the heat on the CIS alone. Indeed, there was anticipation that surrounding components such as Teflon and PEEK tubing could melt if exposed to the light for any significant length of time. It was therefore necessary not only to contain the light for efficient heating of the CIS source but also to reduce the brightness to reduce the exposure for people in the vicinity of the instrument. To overcome these problems a housing unit was built from the perforated metal plate and the inside of the unit was covered with aluminium foil to reflect the light within the housing unit. This unit was attached to the halogen light unit and CIS was placed inside the housing unit. A small fan was also attached to the back of the halogen light housing device to avoid overheating and to extend the lifetime of the light emitting diode. A photograph of the heating unit is presented in Figure 4.7.



Figure 4.7 Side view of the heating unit

To determine the heating capacity of the halogen light the CIS was placed inside the housing unit. Both external and internal temperatures were monitored with the help of a simple mercury thermometer. It was observed that after 20 – 30 minutes of heating the external temperature was in the range of 200°C while the internal temperature was close to 100°C.

As discussed earlier, to electrically isolate the CIS from the drift tube a small Teflon tube was used. Unfortunately, the Teflon

tube is not able to withstand the weight of the CIS on its own therefore additional support was required. The CIS unit was placed inside the heating unit and the perforated metal plate used in the construction of the heating unit served to support the weight of the CIS. Alas, this had the knock-on effect of disturbing the ideal settings of the CIS, where CIS was mounted vertically on the drift tube without any support, uniform heating was applied to the CIS without the bright light and samples were injected through capillary inlet tube.

Further work is required to find a better-controlled heating source that not only maintain a steady temperature, but also the ability to increase or decrease the temperature of the source when required. Currently, it is not possible to either increase or decrease the temperature in any controlled manner.

## **4.3 EXPERIMENTAL**

### **4.3.1 PTR-ToF-MS**

Chapter 2 details the PTR-ToF-MS instrument used for this study. Briefly, the conditions used were as follows. The upstream drift tube voltage was set at 2500V and the drift tube pressure was 6.0 mbar, achieved with a carrier gas (nitrogen) flow of 225 lit/min. Ion counts rates observed during the experiments were around  $1500 \text{ s}^{-1}$  for  $\text{H}_3\text{O}^+$  and  $200 \text{ s}^{-1}$  for  $\text{H}_3\text{O}^+(\text{H}_2\text{O})$ . The temperature of the drift tube was set at  $40^\circ\text{C}$ .

### **4.3.2 Gases and reagent**

Nitrogen was used as a carrier gas and was obtained from BOC (high purity grade: 99.999%). Other chemicals used for the experiments were acetone (HPLC grade Sigma, UK), acetonitrile (HPLC grade Sigma, UK), and 2-butanone (Sigma, UK) and de-ionised water (sourced in-house).

### 4.3.3 Liquid Standards

Standard aqueous solutions of the above compounds (section 4.3.2) were prepared at a concentration of 10.0, 20.0, 30.0, 40.0 and 50.0 pmol/l. Acetonitrile, acetone and 2-butanone were selected for the experiments as they are volatile, does not fragment, in liquid form and are readily soluble in water. To prepare the aqueous standards for calibration, a concentrated stock standard was prepared at 20.0 nanomol/l for each compound. A serial dilution was performed to prepare the specific calibration standards listed above. All the solutions were prepared in glass volumetric flasks and refrigerated when not in use. Hamilton gas-tight syringes were used for transferring precise quantities of the calibrants into the stock containers. All the syringes were cleaned with hexane and sonicated prior to and after the preparation of the stocks and calibration standards.

Stock solutions were prepared in a separate laboratory from that used for the PTR-ToF-MS experiments to prevent the contamination of surrounding.

### 4.3.4 Sample Injection

For sample introduction, initially an HPLC pump was employed. The main reason for the use of an HPLC pump was to maintain a steady flow of the liquid into the CIS. If HPLC pumps are to be used, a sample introduction technique was also required as an auto-sampler was not available. It was therefore decided to connect the HPLC pump directly to the CIS by using PEEK tubing, but to split the flow by using a T - piece. By doing this either a syringe pump or manual injection could be used to introduce the sample through the T-piece. This set up is very similar to that used in routine HPLC-MS work, but it was found that the HPLC pump that was available for use was not able to maintain

the steady very low flow required. If a mobile phase splitting technique was used to reduce the flow rate, the setup becomes very impractical, as there is a possibility of liquid spillage around the instrument, which is operated under a high voltage.

Therefore, this set-up is impractical for routine use. Another problem with the use of an HPLC pump was that as manual injection has to be made due to the non-availability of the auto-sampler and the continuous flow of mobile phase to the drift tube between two experiments. As discussed in the Chapter 2 of this thesis, higher amount of the water vapour in the drift tube can increase the formation of water dimer in the PTR spectra and it can complicate the data analysis.

Another factor that had an impact on the CIS was the sample injection. Two different options were available. The first option was to manually inject the sample, but by doing that the same vaporisation issues seen in the HIS source (see Chapter 3) would have appeared as the whole sample would be introduced to the drift tube as a pulse. The second option was to use a syringe pump at a very low flow rate. The only issue with the use of syringe pump was the possibility of the contamination. The main source of contamination between two injections could come from the residual sample left in the syringe and PEEK tubing. So, to minimise the contamination issues, pure water was injected after each experiment with similar duration, *i.e.* data collection time for the efficient flushing of the PEEK tubing. The requirement of the additional PEEK tube-flushing step between experiments also meant that the real-time analysis would not be possible with the CIS. After due consideration, a syringe pump was used for the sample introduction. The syringe was connected to the CIS by PEEK tubing and flow of the sample was controlled by the syringe pump. If necessary sample flow splitting was applied to get the desired flow. Samples were

typically injected at a rate of  $1.0 \mu\text{l/s}$  and the total amount of sample that entered the drift tube depended on the run time. The experimental setup for the CIS is shown in Figure 4.8.

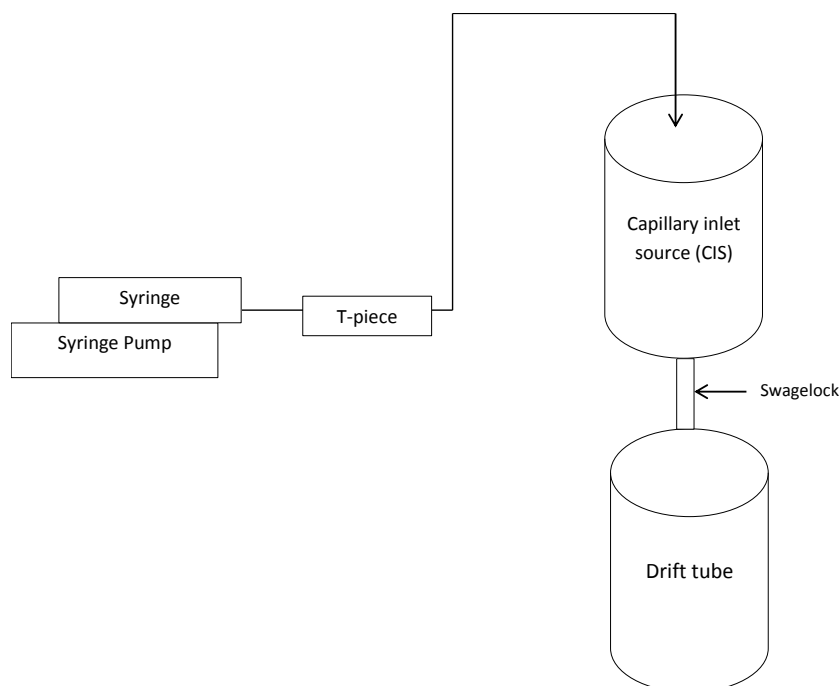


Figure 4.8 Diagram of Capillary Inlet Source system. A calibration solution in the syringe is connected to the inlet of the CIS through the T - piece

Prior to the start of experiment, background signals were acquired from 10 experiments of similar duration to those of analyte experimental cycles without introducing any sample.

## 4.4 RESULTS

### 4.4.1 Effect on Hydronium Ion

Since hydronium ion was used as the proton transfer reagent for the measurement of VOCs, it is naturally crucial that a steady  $\text{H}_3\text{O}^+$  is maintained during the course of the experiment. A small, steady flow of  $1.0 \mu\text{l/s}$  was used to ensure that 100% vaporisation is achieved throughout the experiment. To monitor this effect, aqueous sample was continuously introduced into the drift tube via CIS source. Figure 4.8 shows the finding from this experiment. To show the difference between

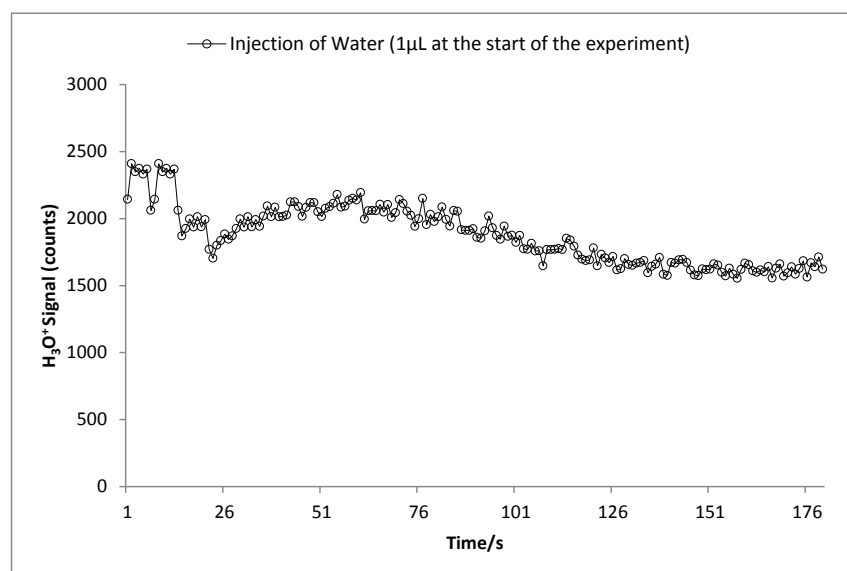


Figure 4.9 Response of the H<sub>3</sub>O<sup>+</sup> (un-normalised) when introducing the pure water sample at 1.0 µl/s flow rate for 180 s run from CIS

As seen in the above figure, a relatively steady signal of H<sub>3</sub>O<sup>+</sup> was observed during the experiment. It was noted that for the first 20 s the H<sub>3</sub>O<sup>+</sup> was jumpy but settled after 20 s. After roughly 100 s, a second decline was observed, followed by a plateau. A similar trend was observed in the HIS when 10 µl of water sample was injected (see Chapter 3).

The main reason for this drop in H<sub>3</sub>O<sup>+</sup> signal after 100 s and before it reaches a plateau could be due to the settling down effect because of the heating or due to the accuracy of the sample flow as the very small flow rate was used for the experiment. Jurschik *et al.* [5] reported a similar pattern in their publication when they continuously injected aqueous sample into their PTR-MS instrument by using a syringe pump.

During the calibration stage of the experiment no effect of drop in H<sub>3</sub>O<sup>+</sup> signal after 100 s was observed. The main reason for this is that the data in the calibration experiments were collected for 100 s and therefore the modest effect of any changes in the H<sub>3</sub>O<sup>+</sup> level were average out.

#### 4.4.2 Calibration of Different VOCs

After establishing the ideal experimental condition, as discussed in Section 3, some water sample containing VOCs were injected. Data generated from the run are normalised.

As discussed in Chapter 3, a large background signal at the chosen  $m/z$  was also observed during the course of the study. The water sample at a different concentration and at a different flow rate was used for different experiments. Therefore, either the un-vaporised or a concentrated sample was the reason for the contamination in the CIS.

As a standard practice, throughout the different experiments performed for this thesis, background noise of the PTR-MS instruments was subtracted from the data. Calibration curve for 2-butanone, acetonitrile and acetone is presented in Figure 4.10, 4.11 and 4.12, respectively.

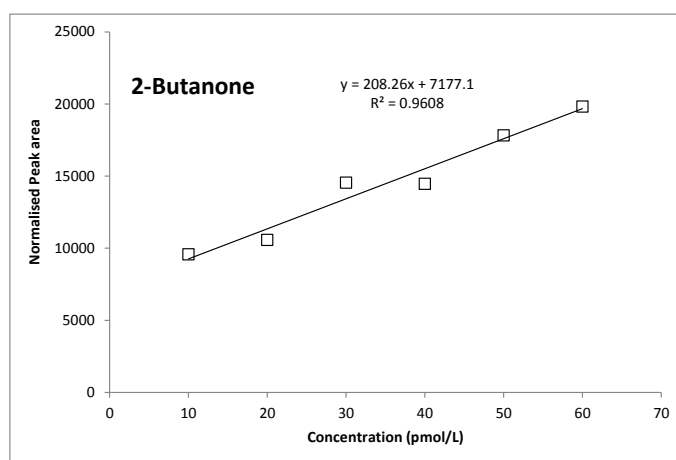


Figure 4.10 Calibration curve for 2-butanone in water over the concentration range of 10 to 60 pm /l

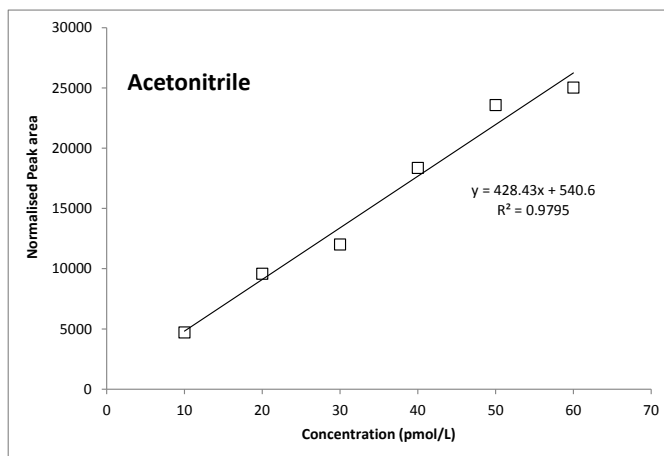


Figure 4.11 Calibration curve for acetonitrile in water over the concentration range of 10 to 60 pm/l

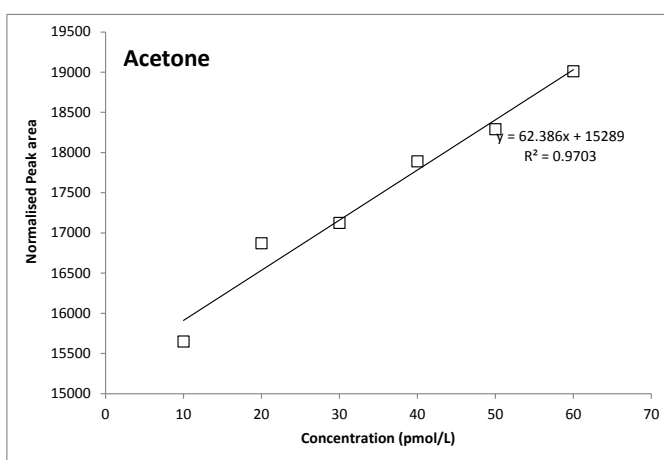


Figure 4.12 Calibration curve for acetone in water over the concentration range of 10 to 60 pm/l

The correlation coefficient, denoted by  $r$  is a measure of the strength and direction of a linear response between two variables. The value of  $r$  can range between +1 and -1, with an  $r$  value of 0 indicating no linear relationship while 1 indicates a perfect linear relationship. The values between 0 and 0.3 indicate a weak linear relationship, 0.3 to 0.7 indicate a moderate linear relationship and 0.7 to 1.0 indicates a strong linear relationship. The correlation coefficient for 2-butanone is 0.9608, for acetonitrile is 0.9795 and for acetone is 0.9703. This correlation coefficient values indicates a strong linear relationship observed from the data generated by using the CIS.

In the calibration curve, a slope is the indication of the sensitivity of the method, *i.e.* proportionality constant between response and concentration. Generally, the greater the slope implies greater the sensitivity of the method.

Table 4.1 The sensitivity (pmol/l) for different compounds when injected in different matrices

	Acetonitrile	Acetone	2-butanone
CIS source	428.4	62.0	208
HIS (1 $\mu$ l water injection)*	65.1	962.6	326

\*Data taken from the experiments performed for Chapter 3.

The sensitivity of the acetonitrile generated by CIS was greater than the sensitivity achieved by HIS. No major change in the sensitivity was observed for 2-butanone. The major change was for acetone, where sensitivity was at-least 10-fold lower in CIS. This was an unexpected observation as it was thought that with the high injection volume, high sensitivity would be observed. There were no analytical reasons for the poor sensitivity of acetone *i.e.* preparation error or low instrumental sensitivity for the compounds as acceptable sensitivity was observed for the HIS. The possible reason for the poor sensitivity for acetone could be due to the CIS operational conditions as the employed conditions might not be suitable for acetone *e.g.* temperature, a sample flow rate, or a high background signal for acetone affected the calibration.

The observed slopes for acetone, 2-butanone and acetonitrile were also compared with the slope generated by GC-MS (see Chapter 3, Figure 3.11). It was noted that the observed slope in this study was at-least 200% lower when compared to the slopes generated by GC-MS. The main reason for the major difference in sensitivity is possibly due to the sophistication of GC-MS instruments in regards to controlled heating for the sample

vaporisation, accurate and precision sampling with the use auto-sampler and chromatographic separation of the compound are the possible reason for the difference in sensitivity from GC-MS to the current technique.

Table 4.2 The limit of detection (pmol/l) for different compounds when injected in different matrices

	Acetonitrile	Acetone	2-butanone
CIS source	0.35	69.8	0.69
HIS source (1 $\mu$ l water injection)*	1.49	18.7	0.44

\*Data taken from the experiments performed for Chapter 3.

The theoretical limit of detection (LoD) was calculated for compound as per the description stated in section 3.4 of Chapter 3. Table 4.2 details the LoD data for compounds analysed by the CIS. Observed LoD was poor for acetone in CIS source when compared to HIS source due to poor sensitivity for the acetone as previously discussed. Comparable LoD was observed for 2-butanone, while a slight improvement on the LoD was observed for acetonitrile. The LoD observed in this study was in the region of 1-10 ppt, which is better than the LoD of 100 ppt reported by Jurschik *et al.* [5].

In summary, once the initial instrumental setup was completed, performing the experiments on the CIS is quick. Even-though there is a possibility to achieve a low LoD with the CIS when compared to the HIS, further work is required to optimise the CIS operational conditions. The experimental set up is relatively easy and quick when compared to the experimental setup employed by Jurschik *et al.* [5]. In the current experiments, data were generated from small flow rate of the water sample, further work is required to investigate the effect of high flow rate, *i.e.* 10-50  $\mu$ l/s and also to different matrix type for example, different solvents. Further development in the design is also required to achieve uniform, controllable heating. In

addition, the additional support to mount the CIS source on the top of the drift tube without any support will make the whole setup more practical.

## 4.5 CONCLUSION

In this chapter, a new inlet design, known as the capillary inlet source (CIS), for injecting liquid analytes into a PTR-MS system was described. The CIS source developed to overcome some of the limitations of the HIS source, which detailed in the previous chapter. The calibration of CIS source was completed with good linear response over the chosen calibration range (10 to 60 pmol/l). The CIS source can be used for the determination of volatile and semi-volatile compounds from aqueous samples, particularly when large sample volume is required to be injected.

Even though, comparable calibration lines were observed at flow of 1.0  $\mu\text{L}$  per second, there is a reservation that with higher flow rate, 100% vaporisation might not be achievable due to a limited heating capacity of the halogen lights. In addition, there is a higher risk of source contamination with high flow rate between two samples. At the small flow rate it is assumed that all the vaporised samples from the CIS has been transferred to the drift tube but if samples are not vaporised efficiently either due to high sample volume or insufficient heating than same cannot be assumed. During the course of the experiments, only three VOCs were used and no contamination issues were found. A further investigation is required to monitor any possible CIS contamination issues due to the deposition inside the source.

The CIS source attached to the drift tube via a Swagelok fitting, it opens up the opportunity to use multiple add-on techniques, *e.g.* heated inlet source (HIS), capillary inlet source (CIS) or atmospheric pressure chemical ionisation (APCI) source with the

University of Leicester PTR-TOF-MS. With this new set-up, even though, it is possible to interchange different add-on, but it is not practical due to hardware limitation. For example, if HIS was used to inject headspace sample, than it was not possible to switch to CIS for aqueous samples within the matter of minutes. The main reason for this was that the instruments struggles to maintain the drift tube pressure. Also, there was a chance that if the operator is not aware of the instrument operating procedures, charging issues can occur in the drift tube due to the higher moisture presence.

The sensitivity and limit of detection (LoD) for the compound used in this study were compared with HIS and literature. The sensitivity and LoD was improved for acetonitrile and was comparable for 2-butanone, but it was poor for acetone. The sensitivity and LoD data were up to 100-fold greater for a selected compounds in water when compared to the literature [5, 7]. Even-though better sensitivity and LoD was observed in CIS but it cannot be claimed that the CIS offers the better sensitivity and LoD to dynamic solution injection (DSI) and direct aqueous injection (DAI) technique, as further experiments are required to establish the sensitivity and LoD over a broad range of compounds.

In conclusion, the new CIS source was designed to overcome some of the limitations of the HIS. Additionally, three VOCs were calibrated on the CIS source and produced comparable data. However, as discussed above, even though new source promised to be an ideal design for the measurements of the volatile and semi-volatile compounds from aqueous sample, for its routine use further work is required to solve the points discussed in this chapter.

---

## 4.6 REFERENCES

1. Blake, R.S., P.S. Monks, and A.M. Ellis, Proton-transfer reaction mass spectrometry. *Chemical Reviews*, 2009. 109(3): p. 861-896.
2. De Gouw, J. and C. Warneke, Measurements of volatile organic compounds in the earth's atmosphere using proton-transfer-reaction mass spectrometry. *Mass Spectrometry Reviews*, 2007. 26(2): p. 223-257.
3. Blake, R.S., Monitoring tropospheric composition using time of flight chemical ionisation mass spectrometric techniques. Thesis: University of Leicester, 2005.
4. Hansel, A., Jordan, A., Holzinger, R., Prazeller, P., Vogel, W., Lindinger, W., Proton transfer reaction mass spectrometry: on-line trace gas analysis at the ppb level. *International Journal of Mass Spectrometry and Ion Processes*, 1995. 149–150(0): p. 609-619.
5. Jurschik, S.T., A. Sulzer, P. Haidacher, S. Jordan, A. Schotchkowsky, R. Hartungen, E. Hanel, G. Seehauser, H. Mark, L. Mark, T. D. , Direct aqueous injection analysis of trace compounds in water with proton-transfer-reaction mass spectrometry (PTR-MS). *International Journal of Mass Spectrometry*. 289(2-3): p. 173-176.
6. Boscaini, E.A., Michael L.; Prazeller, Peter; Mark, Tilmann D., Membrane inlet proton transfer reaction mass spectrometry (MI-PTRMS) for direct measurements of VOCs in water. *International Journal of Mass Spectrometry*, 2004. 239(2-3): p. 171-177.
7. Jardine, K.J., Henderson, W.M., Huxman, T.E., Abrell, L., Dynamic Solution Injection: A new method for preparing pptv-ppbv standard atmospheres of volatile organic compounds. *Atmospheric Measurement Techniques*, 2010. 3(6): p. 1569-1576.

## **CHAPTER 5: CHARACTERISATION OF WHISKIES USING PTR-TOF-MS**

---

### **5.1 INTRODUCTION**

There is an increasing demand for rapid, low cost analysis of volatile organic compounds (VOCs) for the application in food science and technology. The main motivation is to use the VOCs emitted into the gas phase to determine the quality, origin, flavour [1] or any adulteration [2, 3] of the food item [4].

The established techniques are in use for the analysis of VOCs from the whiskey, and they mainly use the gas chromatography (GC) with different detectors [5-7]. These techniques can be very selective and reliable. For most of the established technique, to measure the VOCs, which are present at very low level, requires sample pre-treatment such as sample clean up or pre-concentration to detect the VOCs. A large number of publications are available for the direct measurement of different volatile and non-volatile compounds from the whisky [8].

The sensitivity and speed of PTR-MS measurements makes it possible to analyse a far higher number of samples in a much shorter time than more established techniques such as GC-MS. In fact, the time required to characterise a single sample can be reduced by a factor of about one hundred with the use of PTR-MS in place of GC-MS

PTR-MS offers an alternative to widely used techniques such as GC-MS. It has a high sensitivity, and thus requires no pre-concentration, and shows minimal fragmentation of product ion [9] compared to SIFT-MS. This in turn allows for the fast analysis

of the samples, which can be critical during the food manufacturing and the flavour analysis process.

Several factors can affect the volatile composition of the food item, including the geographical location and the effect of the manufacturing process. For these reasons the profiles of emitted VOCs was used to distinguish food with different geographical origins or with different manufacturing processes. Examples where this has been applied include cheese, butter, olive oil and wines [10-13].

An area where volatile analysis may provide beneficial information is for alcoholic beverages, since the flavour of many of these drinks are linked to the characteristic 'smell' provided by the drink. A good example is whisky, which is a type of distilled alcoholic beverage made from fermented grain [14]. Different grains are used for the different varieties, including barley, malted barley, rye, wheat and corn. The whisky may be stored in the different kinds of cask for ageing before becoming the finished product. The different ingredients, different fermentation process, storage vessels and durations lead to the characteristic flavours of different whiskies [15-17].

Whisky and other distilled beverages such as cognac and rum are complex beverages containing a vast range of flavouring compounds [18]. The flavouring chemicals include carbonyl compounds, alcohols, carboxylic acids, esters, nitrogen- and sulphur-containing compounds, tannins, polyphenolic compounds, terpenes, heterocyclic compounds and esters of fatty acids [14, 19, 20].

For alcoholic beverages such as whisky, congeners are the substances produced during the fermentation process. Congeners are responsible for most of the taste and aroma of the distilled beverages, and contribute to the taste of non-distilled drinks. Different compounds such as ketones,

aldehydes, alcohols, esters and fatty acids are the main constituents of the congeners [15].

Various analytical methods using GC-MS as a detector is developed, using different extraction methods such as solvent extraction, simultaneous distillation/extraction, purge and trap, and SPME to measure flavour compounds [4-6, 8]. As discussed earlier in this section, all of these published methods require a lengthy sample pre-treatment and long analysis time.

Recently Mignani *et al.* [21] published work, which identifies the region of origin of single malt whiskies by using optical spectroscopy together with pattern recognition. Optical spectroscopy was used innovatively as a rapid and non-destructive tool for differentiating distinctive single-malt Scotch whiskies with respect to commercial-grade blend and classifying them according to the region of production. In their experiments, absorption and fluorescence spectroscopy was carried out without any sample treatment or handling. In a different study, Demyttenarere *et al.* analysed the volatiles from malt whisky by Solid Phase Micro Extraction (SPME) and stir bar sorptive extraction [22]. In this technique, both SPME and stir bar sorptive (SBSE) [23] were used as an extraction technique, and GC has a detection technique to analyse the composition of the volatiles in the whisky. They identified 40 different VOC from the whisky samples. Some literature material is available for the characterisation of whisky and other alcoholic beverages by using solid-phase micro-extraction (SPME) with GC-MS [24-27]. Fitzgerald *et al.* characterised whiskies using SPME with GC-MS [24]. Rocha *et al.*, Lopez *et al.* and Campo *et al.* used SPME with GC-MS to analyse the volatile compounds from wine. In all of these studies, the focus was to establish the method for the detection of the different VOCs and this was done by selecting ideal coating for SPME fibre, extraction time and effect of pH. It

was observed from these studies that even though they were able to identify different VOCs from the whisky samples, they also required the extensive pre-treatment.

The aim of this study is to characterise the different whisky samples and to identify different VOCs. The whisky samples have at least 40% alcohol content. The analysis of alcoholic beverages is challenging because of the complexity of chemical ionisation in the presence of large amounts of ethanol. Ethanol, like other alcohol and aldehydes, fragments when ionized under standard PTR-MS operating conditions. More importantly, it also competes with water for protons, which complicates the chemical ionisation process [28-30].

To date, the only work using PTR-MS to measure alcohol volatiles was by Boscaini *et al.* [10], who investigated a few varieties of wine. In their work analysis of VOCs was performed by flushing the wine headspace with ethanol-saturated nitrogen. Boscaini *et al.* [10] reported a characterisation of the two varieties of red wine and two varieties of white wine, but they did not make any effort to identify the key VOCs present in the wine headspace.

In the current study headspace injection and direct injection of whisky samples was used as an injection technique with the heated inlet source (HIS). It is shown that characterisation of whisky volatiles can be performed using PTR-MS.

## **5.2 EXPERIMENTAL**

### **5.2.1 Experimental set-up**

Experiments for the characterisation of whisky were performed by direct injection and headspace analysis on the Leicester PTR-ToF-MS instrument.

The Leicester PTR-ToF-MS instrument is a custom-built instrument. The heated inlet source (HIS) was used as an add-on to the instrumental set-up for sample injection. Details about the Leicester PTR-ToF-MS and the HIS source are presented in Chapters 2 and 3, respectively.

Typical drift tube condition in both the Leicester and Nottingham instruments were a pressure of 1.5 mbar and a drift tube temperature 40°C.

At least 30 blank injections were made at the start and end of the experiments for background measurements. An injection volume of 10 µl was used for the direct injection and 1000 µl was used for the headspace analysis. A Hamilton gas tight syringe was used for the injection. The HIS was set at 100°C for the study.

### 5.2.2 Whisky and other reagent used for the experiments

Different samples used in this study were,

1. Glenfiddich, 15 year old single malt matured in three types of oak cask (40% alcohol)
2. Glenturret 10 year old single malt (40% alcohol)
3. WM Morrison single malt whisky blend (40% alcohol)
4. Jack Daniels, a Tennessee whisky made from corn (40% alcohol)
5. Chivas Regal, blended single malt (40% alcohol)
6. Hennessy, a cognac is a variety of brandy made from grape (40% alcohol)

The whisky samples were purchased from the local supermarket. During the course of the experiment, whisky samples were identified by using the first two letters of the brand name. For example, for Glenturret as GL, Glenfiddich as GF, Jack Daniels as JD, WM Morrison as WM. One bottle of each type and five replicates of each technique were analysed for the

experiments. The whisky samples were stored at room temperature in their original container when not used and samples were taken for analysis at the same temperature to avoid any temperature related anomalies in the results.

Other reagents used during the course of the experiments were de-ionised water (in-house, University of Leicester) and ethanol (Departmental issued, University of Leicester).

### 5.2.3 Sample preparation

Ethanol ( $776 \text{ kJ mol}^{-1}$ ) has a higher proton affinity compared to water ( $691 \text{ kJ mol}^{-1}$ ) and therefore in the analysis of the VOC content of an analyte containing a high percentage of ethanol, special consideration should be given to the presence of the protonated ethanol and its cluster ions and its effects on the proton transfer process. In the current experiments, a fixed volume of sample was injected for a particular run. Therefore, during the early stage of the run, protonated ethanol and its cluster ions were in higher concentration than hydronium ion but later in the run, the hydronium ions were dominant. This behaviour could cause the varied effect on the spectra if ethanol levels in the samples varies for any practical reasons or otherwise.

All of the whisky samples have an alcohol (ethanol) level of 40%. Any attempt to remove the alcohol prior to PTR-MS analysis could have a detrimental effect on other VOCs present in the liquid. An alternative to removing the ethanol from the samples was to dilute the samples to a level where the percentage of ethanol becomes relatively small, but of course the main disadvantage of doing this is that all other VOCs will be diluted simultaneously, which will affect the detection sensitivity. Yet another approach is to increase the ethanol content to a level where only protonated ethanol is available during the

experiment for the proton transfer, avoiding the possibility of a dual protonation mechanism. This approach was used in this chapter. This approach had a possible disadvantage that any compounds with their proton affinity lower than ethanol, would not get protonated. But, as discussed in section 5.3, high amount of residual moisture was observed in the drift tube, which resulted in the presence of the hydronium ion, therefore protonation would have occurred by hydronium or protonated ethanol.

### 5.2.4 Ethanol standard solutions

To measure the impact on the concentration of hydronium ion in the presence of the ethanol at various levels, standard solutions of ethanol at 5%, 10%, 50% and 100% concentration (by volume) were prepared in distilled water.

The direct injection and standard solution headspace analysis of the samples was performed for five replicates using both techniques at the above stated levels.

#### 5.2.4.1 Direct injection and headspace

For direct injection, different dilution schemes were investigated by adding different volumes of absolute ethanol to 1 mL of whisky. It was observed that with a lower dilution factor, *e.g.* two-fold, the sample was taking considerably longer to evaporate in the HIS source, whereas with high dilution factor such as five-fold, the sensitivity of the VOC was affected. Three-fold dilution provided a satisfactory compromise between vaporisation time for the sample and the observed sensitivity of the VOC detection. Samples were prepared in 10 mL screw cap glass vials by adding 1 mL of whisky sample by pipette using a 1000  $\mu$ L Gilson pippetman classic. 3 mL of absolute ethanol was added to the sample by using a similar pipette. Samples were thoroughly mixed by inversion for at least 1 minute prior to

sample injection. 10  $\mu\text{L}$  of the sample was injected into the HIS source for analysis.

For headspace analysis, samples were prepared as stated above and a 1 mL aliquot was pipetted into a gas-tight GC vial. The samples were then placed on the hot plate set at 30°C for 5 minutes and 1000  $\mu\text{L}$  of headspace was immediately injected into the HIS source for the analysis.

### 5.2.5 Data collection and analysis

The mass spectrometric data were collected over the range of  $m/z$  0 – 250 for 100 seconds per run. The data were then processed using Grams-AI software. Mean normalised, background subtracted data were used for the subsequent data analysis and data analysis was performed by using Microsoft Excel and Matlab (2007 a) with PCA toolbox (Version 6).

## 5.3 RESULTS AND DISCUSSION

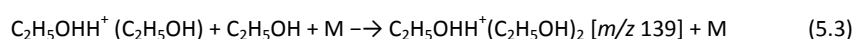
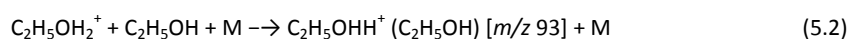
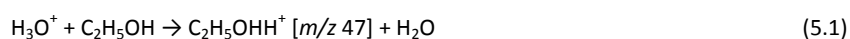
In the following subsections the ion chemistry and the effect of ethanol on hydronium is discussed first, in section 5.3.1. The various VOCs observed during the course of the study are then identified in section 5.3.2. The direct injection and headspace flushing technique is discussed in Section 5.3.3, and the discrimination of different whisky samples is discussed in Section 5.3.4.

### 5.3.1 Ion chemistry and effect of ethanol on hydronium

In PTR-MS, the ionisation process is dominated by proton transfer reactions, usually from  $\text{H}_3\text{O}^+$ , and secondary ion-molecule reactions are assumed negligible. In using PTR-MS for the quantification of VOCs by pseudo-first order kinetics, we assume that the  $\text{H}_3\text{O}^+$  primary ion signal is not depleted by reactions with analyte molecules. Both premises should be fulfilled for successful compound identification and

quantification using PTR-MS. For samples with high ethanol content, these conditions are not fulfilled for reasons mentioned earlier and discussed in more detail below.

When ethanol enters the PTR-MS instrument in large quantity, the  $\text{H}_3\text{O}^+$  primary ions are efficiently converted into protonated ethanol ions and protonated ethanol cluster ions, as shown below:



In the above equations, “M” is a third body collision partner. Dehydration of the product ions can also occur and produces  $\text{C}_2\text{H}_5^+$  [ $m/z$  29],  $\text{C}_2\text{H}_5^+(\text{C}_2\text{H}_5\text{OH})$  [ $m/z$  75] and  $\text{C}_2\text{H}_5^+(\text{C}_2\text{H}_5\text{OH})_2$  [ $m/z$  121] ions, respectively [31]. Reactions of organic molecules M (*e.g.* ethanol) with  $\text{H}_3\text{O}^+$  ions are dominated by exothermic proton transfer reactions to produce  $\text{MH}^+$  ions (*e.g.*  $\text{C}_2\text{H}_5\text{OH}_2^+$ ), which can also react with the water molecules present to form hydrated protonated ethanol ions.

Dryahina *et al.* [32] discussed the reactions of  $\text{H}_3\text{O}^+$  and its clusters with ethanol. At high concentrations of water, the  $\text{H}_3\text{O}^+$  ions are rapidly hydrated to  $\text{H}_3\text{O}^+(\text{H}_2\text{O})_{1,2,3}$  ions. The latter can also be produced in the reactions of the hydrated  $\text{H}_3\text{O}^+$  ions with M. Then sequential reactions that involve ligand switching of  $\text{H}_2\text{O}$  molecules by  $\text{C}_2\text{H}_5\text{OH}$  molecules form protonated ethanol cluster ions.

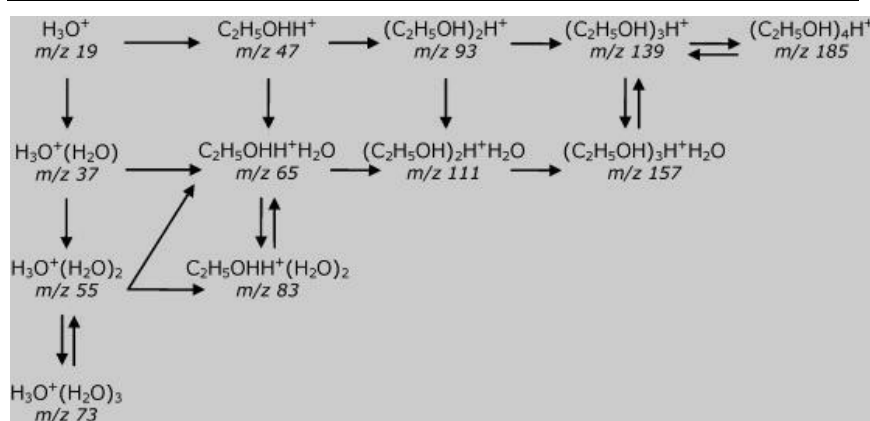


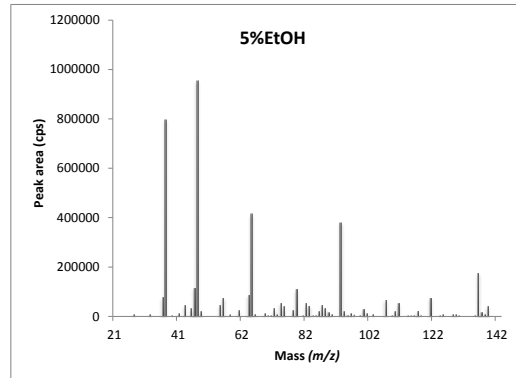
Figure 5.1 The full scheme of the ion chemistry reaction system of  $\text{H}_3\text{O}^+$  with ethanol and water vapour

In Figure 5.1 the formation of  $\text{H}_3\text{O}^+(\text{H}_2\text{O})_{1,2,3}$  ions and the  $\text{C}_2\text{H}_5\text{OH}_2+(\text{C}_2\text{H}_5\text{OH})_{1,2,3}$  ions is shown in the vertical and horizontal directions, respectively, and production of the mixed clusters is possible by alternative routes, as indicated. All ions from the  $\text{H}_3\text{O}^+(\text{H}_2\text{O})_{1,2,3}$  group are efficiently removed by their reactions with ethanol molecules. The double arrows indicate the possibility of reverse reaction at the temperature of the carrier gas. Thus, the concentrations of each pair of ions connected by double arrows can approach ion–molecule kinetic equilibrium.

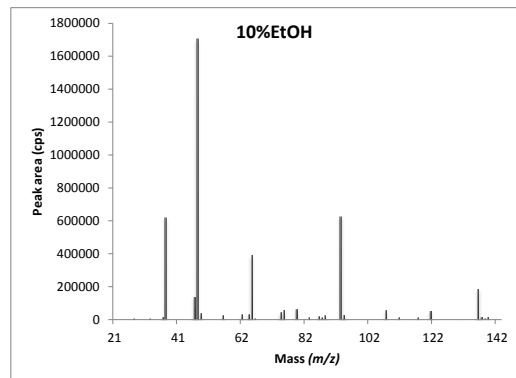
For the Leicester PTR-TOF-MS, standard solutions with different percentages of alcohol were prepared in water and 10  $\mu\text{L}$  of individual standards were injected into the HIS source to investigate the influence of ethanol on product ion distribution. As a part of the routine instrumental setup for the Leicester PTR-TOF-MS, a bubbler was used for the introduction of the water vapour for the production of hydronium ions. However, during this part of the investigation, the bubbler was not used, as the residual water present in the drift tube and water present in the standard solution was enough to provide the constant sensitivity mass-spectrum for hydronium during the experiment. Figure 5.2 shows the mass spectra obtained when injecting the

standard solution to the drift tube at (a) a 5% ethanol/water solution (b) a 10% ethanol/water solution (c) a 50% ethanol/water solution, and (c) absolute ethanol.

(a)



(b)



(c)

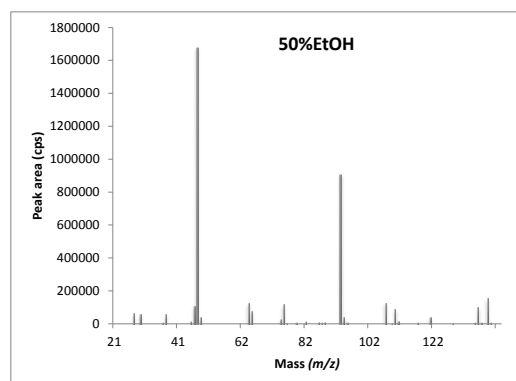


Figure 5.2 PTR-MS mass spectra for ethanol/water solution (a) 5%, (b) 10%, (c) 50% and (d) 100%.

(d)

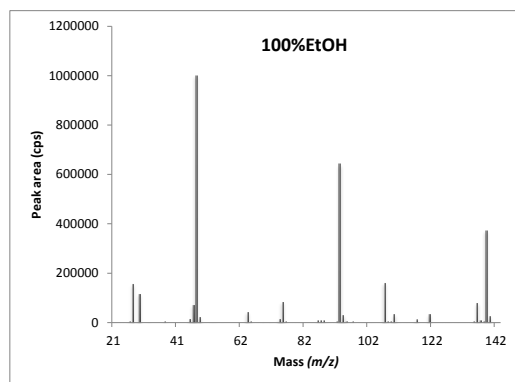


Figure 5.2 PTR-MS mass spectra for ethanol/water solution (a) 5%, (b) 10%, (c) 50% and (d) 100%.

As expected, the quantity of ethanol cluster ions increases with the increase in the ethanol content. As seen in the graphs, the most intense ions are at  $m/z$  47. Other intense peaks observed are  $m/z$  93 and  $m/z$  139 and they can be assigned to the cluster of ethanol. However, in all cases, a strong peak for  $\text{H}_3\text{O}^+$  at  $m/z$  19 is still present, meaning that we have a mixed proton transfer reagent scenario due to the moisture in the instrument and the liquid samples used for the analysis. The chemical ionisation scheme for the detection of the VOCs may therefore involve all of the following process:

- Proton transfer from  $\text{H}_3\text{O}^+$
- Proton transfer from the protonated ethanol [33]
- Ligand switching reaction from protonated ethanol clusters

To investigate the differences in the intensities of the protonated ethanol and hydronium contribution, 100  $\mu\text{L}$  of absolute ethanol was injected into the HIS source and 100 scans of 1 second duration were collected. Figure 5.3 shows a plot of signal level for  $m/z$  of 19 ( $\text{H}_3\text{O}^+$ ), 49, 93 and 139 (ethanol and its fragments) as a function of scan number (essentially time).

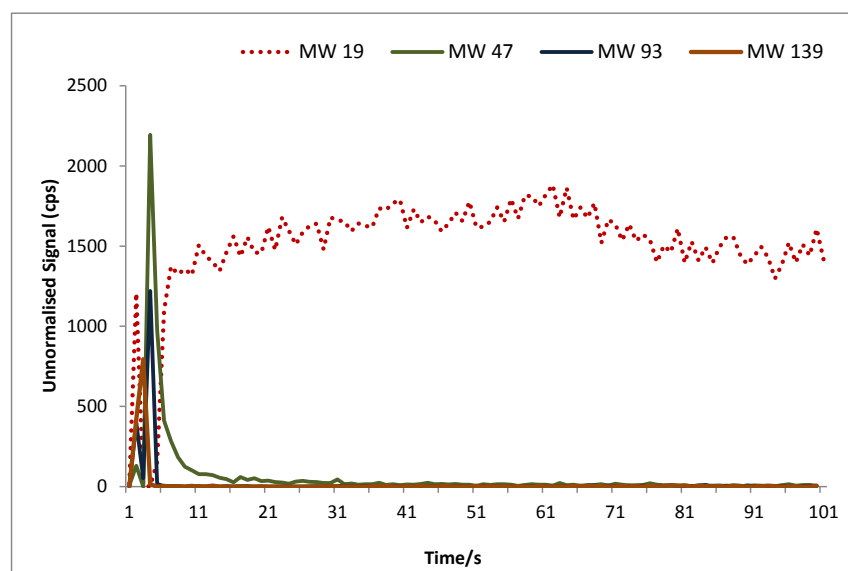


Figure 5.3 Injection was made in the absence of the water vapour. MW 19 was observed due the residual moisture in the drift tube. After injecting the ethanol, stable  $\text{H}_3\text{O}^+$  was observed after 10 s where no stable signal was observed for ethanol and its fragments at MW 47, 93 and 139

It was observed from the graph that, for the first 10 s, no  $\text{H}_3\text{O}^+$  was present, followed by a large spike in the signal for protonated ethanol and its fragment ions. However, after this initial spike, the signal depleted quickly away and a steady signal for  $\text{H}_3\text{O}^+$  was observed.

In this experiment, 100  $\mu\text{L}$  of ethanol was added to the HIS source at the start of the run. As discussed earlier in this chapter, ethanol and its cluster ions were immediately protonated, and if ethanol was supplied continuously, the intensity of the protonate ethanol and its cluster ions would have remained steady. In this experiment, instead, as only a small amount of ethanol was injected at the start of the run, peaks for protonated ethanol and its cluster ions were depleted after about 10 s. Therefore, during the course of the run, protonated ethanol or  $\text{H}_3\text{O}^+$  was always available for the proton transfer reaction. Therefore, this phenomenon had no impact on the experiment.

### 5.3.2 Analyte Identification

During the experiment, it was observed that dilution of whisky sample with ethanol had an impact on the mass profile of the sample, particularly in regards to the intensity of certain volatile compounds. For analyte identification purposes, peaks observed from whisky samples (diluted with ethanol and without dilution) were considered. Typical examples shown in Figure 5.4.

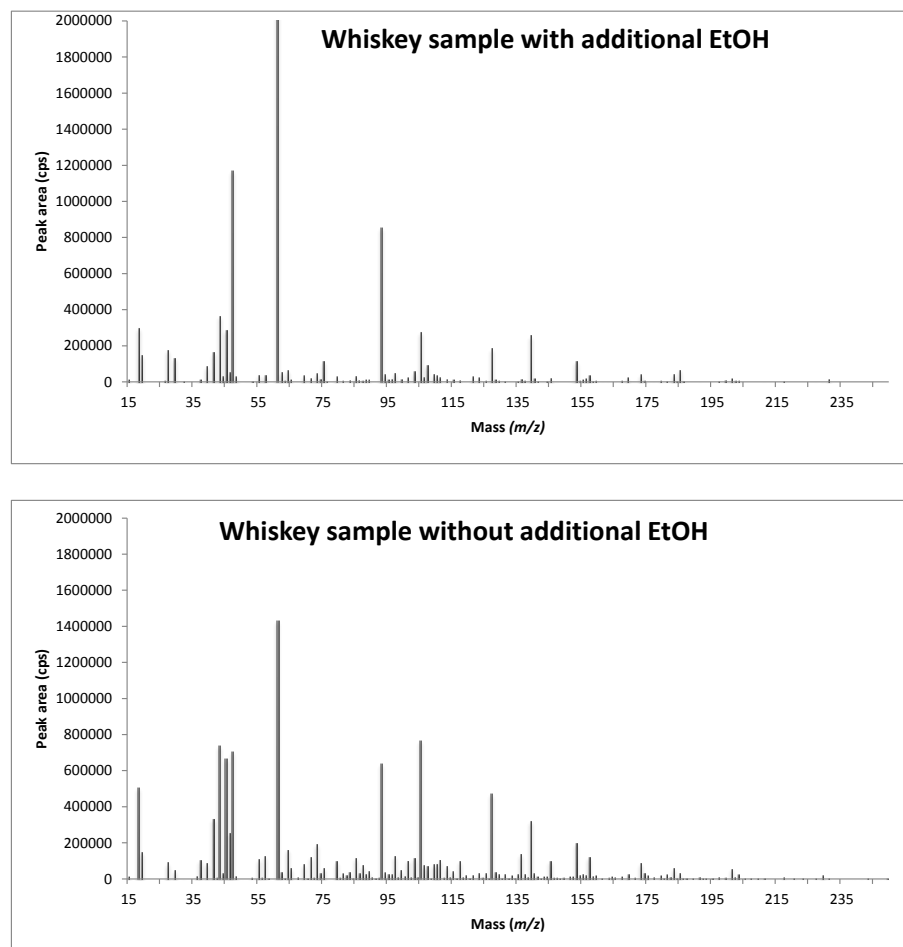


Figure 5.4 Typical mass spectrum from the direct injection of whisky samples with and without the addition of the ethanol (Dominant  $\text{H}_3\text{O}^+$  signal at  $m/z$  19 was removed from the graph for better representation of other VOCs)

Even though the PTR-MS technique does not provide the absolute identification of compounds, literature can assist the tentative assignment of many signals [14, 18, 20, 24, 34-39]. The publication on alcohol drinking by the International Agency for

Research on Cancer [40] was also used for the guidance for the volatile identification purposes.

Acetaldehyde ( $C_2H_4O$ , molecular mass = 44.1 Da) also known as ethanal is an organic volatile compound. It is one of the most important aldehydes, occurring widely in nature. Acetaldehyde occurs naturally in coffee, bread, and ripe fruits. Acetaldehyde is also produced by oxidation of ethylene and is popularly believed to be a cause of hangover from alcohol consumption [47].

MacNamara *et al.* [20] also identified the acetaldehyde from the headspace of the whisky, which were un-aged, three and six years old. The analysis was performed by using two-dimensional gas chromatography. They have reported that with ageing, the concentration of acetaldehyde increased from 36 mg/l at 0 years to 99 mg/l at 6 years. The whisky samples used in this work are at-least ten years old, so the observed peak at  $m/z$  45 could be due to acetaldehyde.

Acetone ( $C_3H_6O$ , molecular mass = 58 Da) also known as propanone is an organic volatile compound. MacNamara *et al.* [20] identified the acetone as a one of the major volatile compounds from the headspace of whisky. Nykanen and Suomalainen *et al.* [41] reported the acetone levels in the range of 03 – 10 mg/l from the headspace of the whisky samples. Therefore, the observed peak at  $m/z$  59 could be due to acetone.

Acetic acid ( $C_2H_4O_2$ , molecular mass = 60 Da) also known as ethanoic acid is the simplest volatile carboxylic acid. Alcohols, in the case of whisky the ethanol, converted in large parts to the corresponding carboxylic acid (acetic acid in the case of ethanol) in the presence of atmospheric oxygen. Beside this possibility of oxidative production of acetic acid, fermentation and decay processes of sugar can produce it by microorganisms.

Lallinykanen *et al.* [42] applied gas chromatography to eight

different types of whisky to determine the relative proportions of volatile fatty acids. They have reported that acetic acid represents 40 – 95% of the total amount of volatile acids in the whisky. The whisky samples used in the study contained at-least 40% ethanol; therefore, the observed mass spectrum at  $m/z$  61 could be due to acetic acid.

Methyl acetate ( $C_3H_6O_2$ , molecular mass = 74 Da) also known as acetic acid methyl ester, is a carboxylate ester. Fitzgerald *et al.* [24] identified the methyl acetate as one of the congener compounds from whisky by using solid phase micro extraction (SPME) as an extraction technique and GC-MS as a detection technique. Distilled alcoholic spirits such as whisky are characterised by the presence of congeners, which arise during the fermentation, distillation and storage process. These compounds are fusel alcohols, fatty acids and esters, which are called organoleptic substances and can be present in relatively large amounts, up to 3 g/l [24]. They have reported < 12 mg/l concentration of methyl acetate in Scotch whisky.

MacNamara *et al.* [20] identified the methyl acetate as one of the major compounds in the volatile fraction. The Scotch whiskeys were used in this study; therefore, observed mass spectrum at  $m/z$  75 could be due to methyl acetate.

Ethyl acetate ( $C_4H_8O_2$ , molecular mass = 88 Da) also known as ethyl ethanoate is a volatile organic compound. Fitzgerald *et al.* [24] identified the ethyl acetate as one of the congeners compounds from the whisky by using solid phase micro extraction (SPME) as an extraction technique and GC-MS as a detection technique. It was also discussed in [40] that ethyl acetate is quantitatively the most important component of the ester fraction, usually accounting for over 50% of the total ester fraction. Fitzgerald *et al.* [24] reported the concentration of ethyl acetate from the Scotch whisky in the region of 110 mg/l.

MacNamara *et al.* [20] measured the ethyl acetate from the whisky aged at 0, 3 and 6 years and the reported concentrations of ethyl acetate was 148, 411 and 523 mg/l. They have shown that the amount of ethyl acetate increases with the ageing of the whisky. The whisky samples used in the study were aged for at-least 10 years, therefore the observed mass spectrum at  $m/z$  89 could be due to ethyl acetate.

Decanoic acid ( $C_{10}H_{20}O_2$ , molecular mass = 172 Da) also called capric acid, is a saturated fatty acid. The decanoic acid is the second largest acid component in distilled beverages after acetic acid [40]. It is used in organic synthesis and industrially in the manufacture of perfumes, lubricants, greases, rubber, dyes, plastics, food additives and pharmaceuticals. Camara *et al.* [43] determined the volatile compounds present in the commercial whisky samples by using a dynamic headspace SPME and gas chromatography coupled to ion trap mass spectrometry. They identified the decanoic acid in their experiment.

MacNamara *et al.* [44] analysed the decanoic acid by using rapid gas chromatography analysis. They used the direct injection technique for the measurement and reported the average concentration of 3.90 ng/ $\mu$ l. The peak observed at  $m/z$  173 could be due to decanoic acid.

Octanoic acid ( $C_8H_{16}O_2$ , molecular mass = 144 Da) also called caprylic acid, is a saturated fatty acid. Caprylic acid is an antimicrobial pesticide used as a food contact surface sanitizer in commercial food handling establishments on dairy equipment, food-processing equipment, breweries, wineries, and beverage processing plants. Octanoic acid is the third largest aliphatic acid after acetic acid and decanoic acid in whisky [40]. Camara *et al.* [43] identified the octanoic acid in their experiment detailed in the paragraph above. MacNamara *et al.* [44] analysed octanoic acid by using rapid GC analysis.

They reported the average concentration of 3.17 ng/ $\mu$ l. The peak observed at  $m/z$  145 could be due to decanoic acid.

### 5.3.3 Precision of the measurement of ethanol from Whisky samples

The precision of the measurement of ethanol from the whisky samples used in this study was determined. The determination was done by analysing all five types of whisky samples in triplicate and mean data (mass spectrum data counts) were used for calculations. Ethanol was used for the determination of precision, as it is the most formidable VOCs in whisky sample.

The calculation for precision was performed using following equation.

$$Precision = \frac{Standard\ deviation}{Mean} \times 100 \quad (5.4)$$

Table 5.1 contains the precision data generated from five whisky samples.

Table 5.1 The precision data for ethanol from five whisky samples.

Whisky	Ethanol
GT-HS	438259
GF-HS	487973
WM-HS	423494
JD-HS	403415
CR-HS	348072
Mean (peak area in cps)	420242
Standard deviation (n-1)	51025
Precision (5)	12

The observed precision for the measurement of ethanol from whisky samples was 12.0%.

During the course of the experiments, sample introduction to the HIS source was performed by the use of manual injection. Therefore, the observed precision from multiple injections was deemed satisfactory.

#### 5.3.4 Whisky Discrimination

Whisky discrimination was performed by plotting the graphs of different VOCs from different brands of whiskeys.

No published work is available which characterises the same whisky samples that have been used in the experiments detailed in this chapter. But the different Scotch whiskies were characterised by Mignani *et al.* Mignani *et al.* characterised the production region of single-malt Scotch whiskies by using optical spectroscopy and pattern recognition techniques. In their work, absorption and fluorescence spectroscopies were carried out without any sample pre-treatment or handling and the data were processed by means of multivariate analysis [21]. A good separation of whiskies from the highland, island and blends were reported in [21].

Camara *et al.* evaluated the volatile constituents of Scotch whisky by using SPME as an extraction technique and gas chromatography coupled with ion trap mass spectrometry for analysis. In their work, they adjusted the alcohol content to 13% (v/v). The majority of their work was concentrated on developing the ideal SPME condition, but they also identified seven volatile compounds from three Scotch whiskies [37].

Fitzgerald *et al.* characterised whiskies by using SPME with GC-MS. One of the major differences from the work by Camara *et al.* was that the alcohol content of whisky was not adjusted [24] and the second difference was different detection techniques were used.

Figure 5.5 displays abundances of ions, which showed significant differences between various whisky varieties. A characteristic pattern for each variety is observed. This difference in the ions also confirms that different whiskey types have the different levels of VOCs.

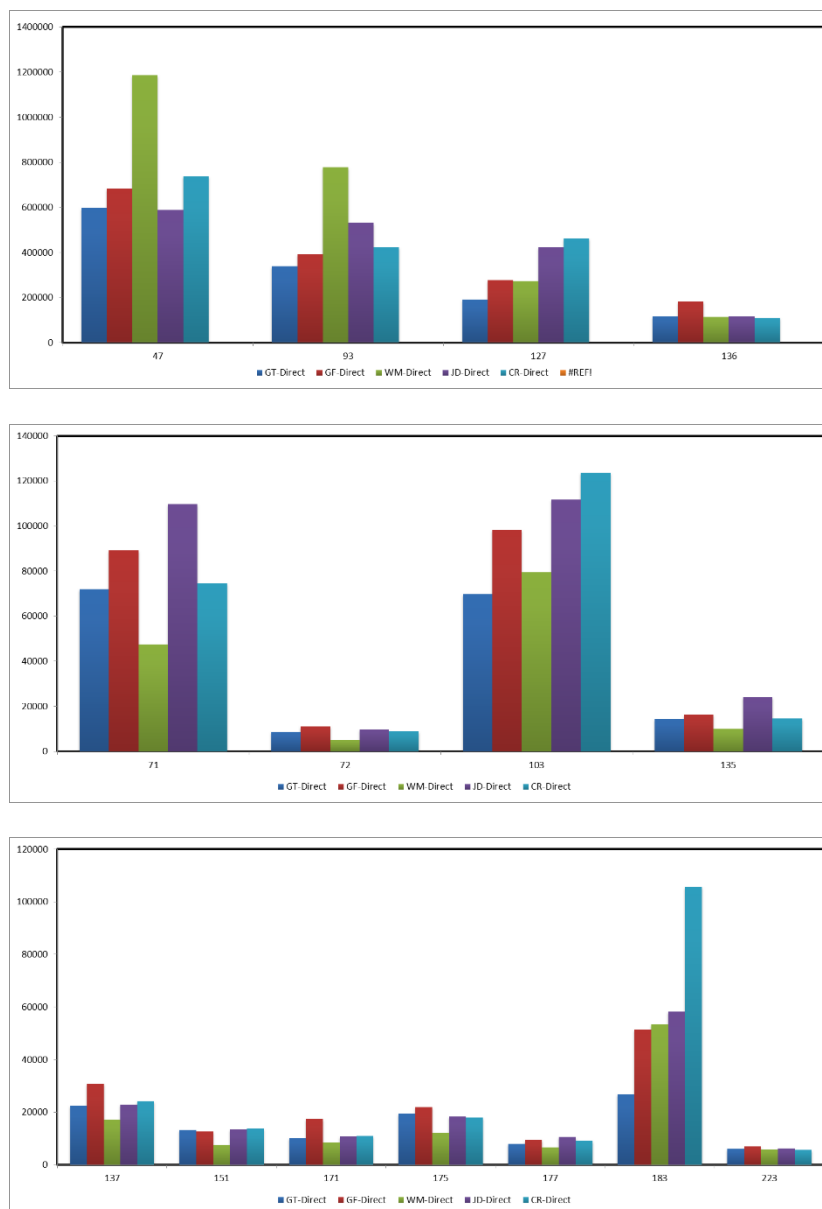


Figure 5.5 Abundances of ions with significant differences between whisky varieties.

Garcia *et al.* [45] characterised the Scotch whisky by using electrospray ionisation-fourier transform mass spectrometry (ESI FT-ICR MS). They employed a direct mass spectrometry analysis to characterise the whisky samples and to screen for

adulteration and counterfeiting. They have shown the clear separation of the Scotch whisky in the PCA data.

Moller *et al.* [46] characterised the Scotch, American and counterfeit whisky samples by using electrospray ionisation mass spectrometry fingerprinting. They have employed a direct injection technique for the experiment by adding formic acid to the whisky samples for positive mode (ESI(+)) analysis and ammonium hydroxide for negative mode analysis (ESI (-)). They have shown the differences in the mass spectrum between different whisky samples, similar differences is also shown in the samples used in this study in Figure 5.7. They also successfully characterise the different whisky sample used in their work by PCA analysis

Successful characterisation of different whisky samples as shown in [45] and [46] is also observed in this study. The total experiment time for [45] and [46] is not detailed therefore, experiment duration is not comparable. The main difference from the current study to [45] and [46] is that the whole profile of mass spectrum is used in this study for the characterisation purposes instead of selected mass channels for the pre-determined compounds observed in the whiskies compared. In addition, as selected mass channels are used in [45] and [46]; additional experiments are required to identify the different compounds in the whisky and to establish the mass channels for the compounds. These procedures are time consuming and restrict the characterisation based on only a few compounds instead of the full mass profile. Therefore, the technique discussed in this chapter has an advantage over the [45] and [46] techniques, as not only it is possible to characterise the whisky samples based on complete mass profile but also no additional experiments are required.

In all of the above referenced work except for Mignani *et al.* [21], Garcia *et al.* [45] and Moller *et al.* [46] required long sample preparation and run time. Work published by Camara *et al.* [37] and Fitzgerald *et al.* [24] was also concentrated on developing the ideal SPME condition for the optimum sensitivity. Headspace flushing technique described by Boscaini *et al.* [10] required the high amount of ethanol and complicated experimental set up. In this chapter, an alternative technique, heated inlet source (HIS) was used to successfully characterise the whisky samples and the effect of additional ethanol on the volatile profile of the whisky samples. No sample pre-treatment was required for this technique, also the set up was very quick and required less sample, solvent and other materials.

## 5.4 CONCLUSION

Mass spectral “fingerprints” were made using PTR-MS for five different single malt whiskies made from either wheat or corn. To characterise the whisky samples, direct injection of whisky or its headspace, either diluted with ethanol or without any dilution was employed.

In direct injection of either the whisky sample or its headspace, performed on Leicester PTR-TOF-MS, the impact of ethanol on hydronium was first assessed by injection of different percentages of ethanol in water. It was observed that even though the levels of ethanol and its fragments and cluster ions increased with increased percentage of ethanol in water, a consistent hydronium signal was observed in all the experiments; even supply of water vapour was stopped for the production hydronium ion. This was due to the high amount of residual moisture in the drift tube of the PTR source.

As discussed in Chapter 3, in the heated inlet source (HIS), the nature of the sample has an impact on the sensitivity of the

analyte, *i.e.* the quicker the sample is vaporised, the better the sensitivity. Whisky is an alcoholic beverage with normal alcohol content at 40%. To achieve a better vaporisation without compromising on the limit of detection, whisky samples were diluted with ethanol during this study. After considering the data, it was decided to dilute one part of the whisky sample with three parts of ethanol for experiments where ethanol was not measured as a volatile constituent of the whisky. A consistent signal for the hydronium was observed in all experiments. When 100% ethanol was injected to monitor the  $\text{H}_3\text{O}^+$ , it was observed that there was a drop in the  $\text{H}_3\text{O}^+$  for the first 10-15 s and ethanol signal was dominant. After the initial time, ethanol gets depleted and steady the  $\text{H}_3\text{O}^+$  signal was observed. This was due to the fact that only the fixed amount of ethanol was injected at a time compared to continuous feeding of ethanol, even in the latter case,  $\text{H}_3\text{O}^+$  was monitored.

In total five different brands and blend of whisky was used in this chapter. A cognac was also used as an additional validation tool to monitor the VOC profile and characterisation characteristics with other whisky samples. During the course of the experiments, analysis was performed by injecting the headspace and direct injection of whisky sample undiluted and diluted with ethanol. In all techniques, good separation between different brands was observed. It was also observed that a cognac, used in the experiments has a different VOC profile to the whisky samples and it was not characterised in the same groups as the whisky samples.

Clear differences were observed in the measurement of the VOC profiles for direct injection when compared with headspace analysis.

A new method to measure VOC profile of whisky has been developed and effect of the ethanol on hydronium was

investigated in detail. Characteristic mass spectral fingerprints of different whisky varieties have been obtained. In this chapter, characterisation of the whisky VOCs was performed across all measured VOCs, not only the few selected compounds. The new direct injection technique is quick compared to headspace flushing technique developed by Boscaini *et al.*, it also requires less sample volume and this technique does not require using expensive SPME files nor does it require any additional sample preparation time.

Possible future applications for the technique include quality control and production monitoring. The ideal extension of this chapter should be to characterise the VOC profiles from single malt whisky from different parts of Scotland. A similar approach is applicable for perfumes, brandy, rum or similar type of matrixes.

## 5.5 REFERENCES:

1. Maarse, H., Volatile compounds in food and beverages. 1991, New York: Marcel Dekker.
2. McIntyre, A.C., Bilyk, M.L., Nordon, A., Colquhoun, G., Littlejoh, D., Detection of counterfeit Scotch whisky samples using mid-infrared spectrometry with an attenuated total reflectance probe incorporating polycrystalline silver halide fibres. *Analytica Chimica Acta*, 2011. 690(2): p. 228-233.
3. Meier-Augenstein, W., H.F. Kemp, and S.M.L. Hardie, Detection of counterfeit scotch whisky by 2H and 18O stable isotope analysis. *Food Chemistry*, 2012. 133(3): p. 1070-1074.
4. Pérès, C., Begnaud, F., Eveleigh, L., Berdague, J.-L., Fast characterization of foodstuff by headspace mass spectrometry (HS-MS). *TrAC Trends in Analytical Chemistry*, 2003. 22(11): p. 858-866.
5. Ashraf, N., Linforth, R.S.T., Bealin-Kelly, F., Smart, K., Taylor, A.J., Rapid analysis of selected beer volatiles by atmospheric pressure chemical ionisation-mass spectrometry. *International Journal of Mass Spectrometry*, 2010. 294(1): p. 47-53.

6. Bonino, M., Schellino, R., Rizzi, C., Aigotti, R., Delfini, C., Baiocchi, C., Aroma compounds of an Italian wine (Ruché) by HS–SPME analysis coupled with GC–ITMS. *Food Chemistry*, 2003. 80(1): p. 125-133.
7. Lasekan, O. and S. Otto, In vivo analysis of palm wine (*Elaeis guineensis*) volatile organic compounds (VOCs) by proton transfer reaction-mass spectrometry. *International Journal of Mass Spectrometry*, 2009. 282(1–2): p. 45-49.
8. Jublot, L., R.S.T. Linforth, and A.J. Taylor, Direct atmospheric pressure chemical ionisation ion trap mass spectrometry for aroma analysis: Speed, sensitivity and resolution of isobaric compounds. *International Journal of Mass Spectrometry*, 2005. 243(3): p. 269-277.
9. Blake, R.S., P.S. Monks, and A.M. Ellis, Proton-Transfer Reaction Mass Spectrometry. *Chemical Reviews*, 2009. 109(3): p. 861-896.
10. Boscaini, E., Mikoviny, T., Wisthaler, A., Hartungen, E.V., Mark, T.D., Characterization of wine with PTR-MS. *International Journal of Mass Spectrometry*, 2004. 239(2–3): p. 215-219.
11. Araghipour, N., et al., Geographical origin classification of olive oils by PTR-MS. *Food Chemistry*, 2008. 108(1): p. 374-383.
12. Biasioli, F., Gasperi, F., Yeretjian, C., Mark, T.D., PTR-MS monitoring of VOCs and BVOCs in food science and technology. *TrAC Trends in Analytical Chemistry*, 2011. 30(7): p. 968-977.
13. Raseetha, S., Heenan, S.P., Oey, I., Burritt, D.J., Hamid, N., A new strategy to assess the quality of broccoli (*Brassica oleracea* L. italica) based on enzymatic changes and volatile mass ion profile using Proton Transfer Reaction Mass Spectrometry (PTR-MS). *Innovative Food Science & Emerging Technologies*, 2011. 12(2): p. 197-205.
14. Hans-Dieter Belitz (Author) , W.G.A., Peter Schieberle (Author), *Food Chemistry*. Springer-Verlag. 2004: Springer-Verlag. 1070.
15. Piggott, J.R., J.M. Conner, and A. Paterson, Flavour development in whisky maturation, in *Developments in Food Science*, C. George, Editor. 1995, Elsevier. p. 1731-1751.
16. Lee, K.Y.M., Paterson, A., Piggott, J.R., Richardson, G.D., Perception of whisky flavour reference compounds by Scottish distillers. *Journal of the Institute of Brewing*, 2000. 106(4): p. 203-208.

17. Guy, C., J.R. Piggott, and S. Marie, Consumer profiling of Scotch whisky. *Food Quality and Preference*, 1989. 1(2): p. 69-73.
18. Williams, A.A. and O.G. Tucknott, The volatile components of Scotch whisky. *Journal of the Science of Food and Agriculture*, 1972. 23(1): p. 1-7.
19. Goss, K.A., R. Alharethi, and M. Laposata, Fatty Acid Ethyl Ester Synthesis in the Preparation of Scotch Whiskey. *Alcohol*, 1999. 17(3): p. 241-245.
20. MacNamara, K.v.W., C. J. Augustyn, O. P. Rapp, A., Flavour Components of Whiskey. II. Ageing Changes in the High-Volatility Fraction. *SOUTH AFRICAN JOURNAL FOR ENOLOGY AND*, 2001. 22(Part 2): p. 75-81.
21. Mignani, A.G., Ciaccheri, L., Gordillo, B., Mencaglia, A.A., Gonzalez-Miret, M.L., Heredia, F.J., Culshaw, B., Identifying the production region of single-malt Scotch whiskies using optical spectroscopy and pattern recognition techniques. *Sensors and Actuators B: Chemical*, 10.1016/j.snb.2012.05.011.
22. Demyttenaere, J.C.R., et al., Analysis of volatiles of malt whisky by solid-phase microextraction and stir bar sorptive extraction. *Journal of Chromatography A*, 2003. 985(1–2): p. 221-232.
23. Baltussen, E., Sandra, P., David, F., Cramers, C., Stir bar sorptive extraction (SBSE), a novel extraction technique for aqueous samples: Theory and principles. *Journal of Microcolumn Separations*, 1999. 11(10): p. 737-747.
24. Fitzgerald, G., James, K.J., MacNamara, K., Stack, M.A., Characterisation of whiskeys using solid-phase microextraction with gas chromatography–mass spectrometry. *Journal of Chromatography A*, 2000. 896(1–2): p. 351-359.
25. Campo, E., J. Cacho, and V. Ferreira, Solid phase extraction, multidimensional gas chromatography mass spectrometry determination of four novel aroma powerful ethyl esters: Assessment of their occurrence and importance in wine and other alcoholic beverages. *Journal of Chromatography A*, 2007. 1140(1–2): p. 180-188.
26. López, R., Aznar, M., Cacho, J., Ferreira, V., Determination of minor and trace volatile compounds in wine by solid-phase extraction and gas chromatography with mass spectrometric detection. *Journal of Chromatography A*, 2002. 966(1–2): p. 167-177.
27. Rocha, S.M., Coutinho, P., Barros, A., Delgadillo, I., Coimbra, M.A. , Rapid tool for distinction of wines based

- on the global volatile signature. *Journal of Chromatography A*, 2006. 1114(2): p. 188-197.
28. Buhr, K., S. van Ruth, and C. Delahunty, Analysis of volatile flavour compounds by Proton Transfer Reaction-Mass Spectrometry: fragmentation patterns and discrimination between isobaric and isomeric compounds. *International Journal of Mass Spectrometry*, 2002. 221(1): p. 1-7.
  29. Aprea, E., Biasioli, F., Mark, T.D., Gasperi, F., PTR-MS study of esters in water and water/ethanol solutions: Fragmentation patterns and partition coefficients. *International Journal of Mass Spectrometry*, 2007. 262(1–2): p. 114-121.
  30. Inomata, S. and H. Tanimoto, A deuterium-labeling study on the reproduction of hydronium ions in the PTR-MS detection of ethanol. *International Journal of Mass Spectrometry*, 2009. 285(1–2): p. 95-99.
  31. Wang Yong, F. and C. Lifshitz, The reactivity of neat and mixed proton-bound ethanol clusters. *International Journal of Mass Spectrometry and Ion Processes*, 1995. 149–150(0): p. 13-25.
  32. Dryahina, K., Pehal, F., Smith, D., Spanel, P., Quantification of methylamine in the headspace of ethanol of agricultural origin by selected ion flow tube mass spectrometry. *International Journal of Mass Spectrometry*, 2009. 286(1): p. 1-6.
  33. Dhooghe, F., et al., FA-SIFT study of reactions of protonated water and ethanol clusters with  $\alpha$ -pinene and linalool in view of their selective detection by CIMS. *International Journal of Mass Spectrometry*, 2010. 290(2–3): p. 106-112.
  34. Vichi, S., Santini, C., Natali, N., Riponi, C., Lopez-Tamames, E., Buxaderas, S., Volatile and semi-volatile components of oak wood chips analysed by Accelerated Solvent Extraction (ASE) coupled to gas chromatography–mass spectrometry (GC–MS). *Food Chemistry*, 2007. 102(4): p. 1260-1269.
  35. Reid, K.J.G., J.S. Swan, and C.S. Gutteridge, Assessment of Scotch whisky quality by pyrolysis—mass spectrometry and the subsequent correlation of quality with the oak wood cask. *Journal of Analytical and Applied Pyrolysis*, 1993. 25(0): p. 49-62.
  36. S.-Q. Liu, R.H., V.L. Crow, Esters and their biosynthesis in fermented dairy products: a review. *International Dairy Journal*, 2004(14): p. 923-945.
  37. Câmara, J.S., Marques, J.C.; Perestrelo, R.M.; Rodrigues, F.; Oliveira, L.; Andrade, P, Caldeira.M and M. Caldeira,

- Evaluation of volatile constituents profile in Scotch whisky by SPME/GC-ITMS. IUFoST World Congress, 2006.
38. Poisson, L. and P. Schieberle, Characterization of the Most Odor-Active Compounds in an American Bourbon Whisky by Application of the Aroma Extract Dilution Analysis. *Journal of Agricultural and Food Chemistry*, 2008. 56(14): p. 5813-5819.
  39. Kahn, J.H., et al., Whiskey Composition: Identification of Additional Components by Gas Chromatography-Mass Spectrometry. *Journal of Food Science*, 1969. 34(6): p. 587-591.
  40. Organisation, W.H., IARC Monographs on the evaluation of the carcinogenic risks to human; alcohol drinking. 1988. 44.
  41. Nykänen, L. and H. Suomalainen, Aroma of beer, wine, and distilled alcoholic beverages. 1983, Dordrecht, pp 1-413.
  42. Nykänen, L., E. Puputti, and H. Suomalainen, Volatile Fatty Acids in Some Brands of Whisky, Cognac and Rum. *Journal of Food Science*, 1968. 33(1): p. 88-92.
  43. Câmara, J.S., Marques, J.C., Perestrelo, R.M., Rodrigues, F., Oliverira, L., Andrade, P., Caldeira, M., Comparative study of the whisky aroma profile based on headspace solid phase microextraction using different fibre coatings. *Journal of Chromatography A*, 2007. 1150(1-2): p. 198-207.
  44. MacNamara, K., M. Lee, and A. Robbat Jr, Rapid gas chromatographic analysis of less abundant compounds in distilled spirits by direct injection with ethanol-water venting and mass spectrometric data deconvolution. *Journal of Chromatography A*, 2010. 1217(1): p. 136-142.
  45. Caldeira, M., Rodrigues, F., Perestrelo, R., Marques, J.C., Câmara, J.S., Comparison of two extraction methods for evaluation of volatile constituents patterns in commercial whiskeys: Elucidation of the main odour-active compounds. *Talanta*, 2007. 74(1): p. 78-90.
  46. Moller, J.K.S., R.R. Catharino, and M.N. Eberlin, Electrospray ionization mass spectrometry fingerprinting of whisky: immediate proof of origin and authenticity. *Analyst*, 2005. 130(6): p. 890-897.

## **CHAPTER 6: HEADSPACE AND DIRECT ANALYSIS OF URINE BY HIS-PTR-TOF-MS**

---

### **6.1 INTRODUCTION**

Urinalysis is the oldest known clinical laboratory test. Even before the physicians were performing bloodletting, they knew the value of examining the patient's urine. Urine contaminated with bacteria has a typically pungent smell, whilst the presence of ketones causes a sweet and fruity smell. Dark yellow urine is often indicative of dehydration. Dark orange to brown urine can be a symptom of jaundice [1].

A healthy adult produces between 750 and 2500 mL of urine in a 24-hour period, at an average rate of ~50 mL/hour. The urine production is dependent on the fluid intake, temperature and other fluid losses such as perspiration, diarrhoea and vomiting. Urine is a complex mixture of water, electrolytes, organic acids, nitrogen-containing compounds, hormones, enzymes and proteins. Normal urine is usually clear or transparent.

Urine is used for a wealth of biochemical tests including 5-hydroxyindoleacetic acid (5-HIAA for carcinoid tumours), urinary porphyrins and  $\beta$  human chorionic gonadotrophin ( $\beta$ -HCG and pregnancy tests). Urine is an ideal medium for non-invasive investigation of metabolic processes occurring in the body [2]. The samples are quick, painless and easy to collect [3].

The detection of organic molecules has clear diagnostic value in medicine. Various analytical procedures are established to detect the VOCs in breath samples and the headspace above a liquid in a sealed container. Each of these procedures are faced with numerous practical problems involved in sampling and separating organic volatiles from biological samples, low

concentrations, and the amount of water in air or headspace [4, 5]. Several different measurement techniques are available to measure the VOCs. Gas chromatography with or without mass spectrometry (GC or GC-MS) is the commonly used analytical method. These techniques are based on the separation of compounds between a liquid and gas phase along a column. Because of these, they are used for the qualitative and quantitative analysis of a large number of compounds because of its high sensitivity, reproducibility and resolution. In general, GC-MS is used to analyse non-polar compounds soluble in non-polar solvents such as hexane, ethyl acetate and acetone.

The levels of VOCs in urine vary depending on the environment, exposure to particular pollutants, food/drink intake, illness or metabolism but in general they are typically present at levels of  $< \mu\text{g L}^{-1}$  [6]. Analysis of VOCs at such a low level by direct analysis is difficult, as they are near or below the limits of detection of GC and GC-MS. Most methods therefore require a clean-up procedure by using either a solid phase extraction (SPE), liquid-liquid extraction (LLE) or solid phase micro-extraction (SPME). These clean-up procedures are followed by a pre-concentration of the specimen by evaporating the extraction solvent and bringing the compound to a small quantity of solution. Therefore, these techniques become cumbersome and time consuming. High performance liquid chromatography (HPLC) with or without mass spectrometry is another technique used for the analysis of VOCs from liquid *e.g.* water, urine or solid *e.g.* soil, pharmaceutical products. This technique also faces limitations *i.e.* requirement of pre-concentration of compounds, clean-up, similar to GC-MS.

Ghoos *et al.* [7] screened the volatile compounds emitted from urine and faeces by means of an off-line closed-loop trapping system and high-resolution gas chromatography-ion trap

detection. Ghooos *et al.* [7] have identified 140 compounds from urine and faeces. Wahl *et al.* [2] developed a method to determine the volatile organic compounds in human urine by headspace gas chromatography-mass spectrometry. A multipurpose sampler was designed for liquid, gaseous and a headspace sample was used for the GC-MS analysis. The VOC profile in human urine was determined and 34 components were identified. Fustinoni *et al.* [8] used SPME with GC-MS for the measurement of the benzene, toluene, ethylbenzene and xylene (BTEX) in the urine of people exposed to these airborne pollutants present in the living environment. It was shown in these publications that GC-MS was successfully used not only for measuring the VOCs from the urine but also for identifying different compounds. One thing common in all these publications was that complicated analysis and instrumental setup was required, so that direct real time analysis was not possible.

Spanel *et al.* [9, 10] successfully applied SIFT-MS to the measurement of different VOCs from urine headspace. To maintain a pH, appropriate amount of HCL or NaOH was added to a 10-mL portion of urine in a glass bottle. Section 6.3 details the effect of pH on different VOCs. The bottles were then heated to 40°C. The headspace from each sample was injected into the SIFT-MS instrument. The SIFT-MS instruments produce real-time analysis but suffer from poor sensitivity compared to PTR-MS. To counteract this, a large sample volume was used.

There is a significant and growing body of literature describing measurements of the VOCs contained within human breath using PTR-MS [11]. However, there is little published work on the measurement of VOCs in the headspace of urine by using PTR-MS. Pinggera *et al.* [12] published the measurement of urinary acetonitrile concentration by PTR-MS and showed that it

correlates with recent smoking behaviour. In their study, urine samples were diluted 1:2 with distilled water and heated to 37°C. The Teflon tube used for the collection of volatile organic compounds for the analysis [13].

In the current chapter, different ketones, aldehydes, alcohols, were quantified from the headspace of urine samples from five volunteers using PTR-MS. The effects of adding salt and changing the pH on the emission of VOCs was examined in this study.

## **6.2 EXPERIMENTAL**

### **6.2.1 Experimental set-up**

Experiments for the urine analysis were performed using the Leicester PTR-ToF-MS instrument, which was described in Chapter 2. The heated inlet source (HIS), described in Chapter 3, was used for the direct injection of urine sample and also for the injection of the headspace above the urine.

Typical drift tube conditions for these experiments used a pressure of 6 mbar and a drift tube temperature of 40 °C.

An injection volume of 10 µL was used for the direct injection technique. An injection volume of 1000 µL was used for the headspace analysis. At least 30 blank injections were made at the start and end of the experiments for background measurement. Additional checks were done for contamination of instruments prior to and after the experiments.

### **6.2.2 Sample collection, storage and reagents**

Urine samples were collected from three healthy male and two healthy female volunteers, who were on a mixed diet.

To keep the volunteer ID anonymous, numbers instead of personal information is used in the data tables. The samples

were collected into 20 mL sterile glass containers. Samples were analysed fresh where possible, but otherwise were stored in a refrigerator and analysed within 24 hours of the sample collection.

As a part of the sample collection procedure, each volunteer was requested to record information on the sample collection vial and to cover the cap with parafilm to avoid the loss of the VOCs prior to measurement.

Volunteers provide the following information:

- Unique ID to identify sample (volunteer's initials)
- Recent food/drink consumption (within 2 hours of analysis)
- Smoking status: current and duration from the last cigarette

Analytical grade chemicals, sodium hydroxide (Thermo Fisher), hydro-chloric acid (Thermo Fisher), sodium chloride (Thermo Fisher), acetone (Sigma Aldrich) and formaldehyde (Sigma Aldrich) were used in the experiments. Deionised water was obtained from the Stores in the Leicester Chemistry Department store.

### 6.2.3 Sample preparation

The main aim of the experiment was not only to determine and measure the different VOCs from the urine either by direct injection or by headspace analysis, but also to observe the effect of salt and pH on the sensitivity and recovery of the VOCs.

To measure the impact of salt, and pH on the recovery of the VOCs from the urine sample, four different sample preparation techniques were used.

1. No pH adjustment (pH 5.0 to 7.0) and no salt addition.  
1 mL of urine placed in 2 mL screw capped GC-vial

2. No pH adjustment (pH 5.0 to 7.0) with salt addition.  
1 mL of urine was placed in a 2 mL screw capped GC-vial and 1 g of sodium chloride was added.
3. Acidic conditions (pH 1.0 to 2).  
1 mL of urine was placed in a 2 mL screw capped GC-vial and 20  $\mu$ L of 1M HCL was added.
4. Alkaline conditions (pH 12-14).  
1 mL of urine was placed in 2 mL screw capped GC-vial and 20  $\mu$ L of 1M NaOH was added.

All the vials were capped as soon as preparation was completed and mixed vigorously for at least 2 minutes prior to either placing the sample on a hot plate for headspace injection or making direct injection.

For the measurement of the acetonitrile and other smoking related compounds, urine samples from the one person out of the five volunteers who was a smoker, was collected within half an hour of smoking to ensure that acetonitrile and other smoking related compounds were absorbed in the blood stream.

To minimise contamination, volunteers were requested to wash their hands prior to sample collection.

#### 6.2.4 Headspace and direct injections

For headspace analysis, samples were prepared as per Section 6.2.3. Samples were placed on the hot plate set at 40°C for at least 10 minutes. After that time, 1000  $\mu$ L of headspace was injected into the HIS source.

For direct injection analysis, samples were prepared as per Section 6.2.3 and were mixed vigorously. A quantity of  $\leq 20$   $\mu$ L was injected directly into the HIS source, which was set at 100 °C, allowing 100% vaporisation of the urine sample.

### 6.2.5 Calculations

The VOC concentration was calculated from the peak area in the sample vs concentration of the spiked calibration standards concentration regression equation, with no weighting factor.

$$Y = m \cdot X + b \quad (6.1)$$

$$X = (Y - b) / m \quad (6.2)$$

Where, Y = peak area of VOC, m = slope of the calibration curve, x = concentration of VOC and b = y-axis intercept of the calibration curve. Therefore, the concentration of unknown sample was calculated by using equation 2.

## 6.3 RESULTS AND DISCUSSION

### 6.3.1 Comparison of VOC profiles from direct injection and headspace analysis

In order to compare the VOC profiles from direct injection and headspace analysis, a urine sample from one volunteer was used. 1 mL of urine sample was transferred into two screw capped GC-vials, with one vial labelled for direct injection, the second for headspace analysis. In both vials, 1 g of sodium chloride was added and the pH of the sample was not adjusted for these experiments. 10 µL from the direct injection vial was injected into the HIS source. A headspace sample was placed on the hotplate, set at 40°C, for at-least 10 minutes and 1000 µL of the headspace above the urine sample was injected in to the HIS source.

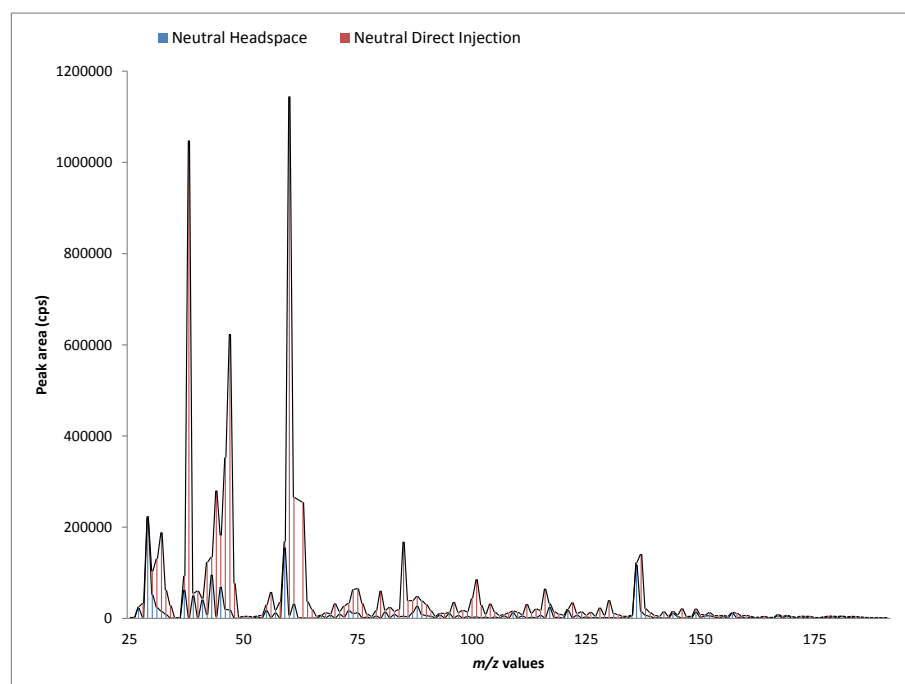


Figure 6.1 Full scan mass spectrum observed from the direct injection of urine and urine headspace from the urine sample collected from the one volunteer

Full mass spectral scans for the headspace and direct injection samples are shown in Figure 6.1. The region below  $m/z$  25 has been removed because this region is dominated by signals from  $\text{H}_3\text{O}^+$  and  $\text{NH}_4^+$ . A discussion of specific VOCs observed is given in later sections. It was found during the experiments that even though the same VOCs were observed for both direct and headspace injection, the sensitivities for detection of these VOCs varied. These differences in the sensitivity are summarised in Figure 6.2. For the majority of the compounds, greater sensitivity was observed with direct injection compared with the headspace analysis. The main reason for this is simply that the quantity of compounds injected from the headspace is lower than that for the directly injected aqueous samples.

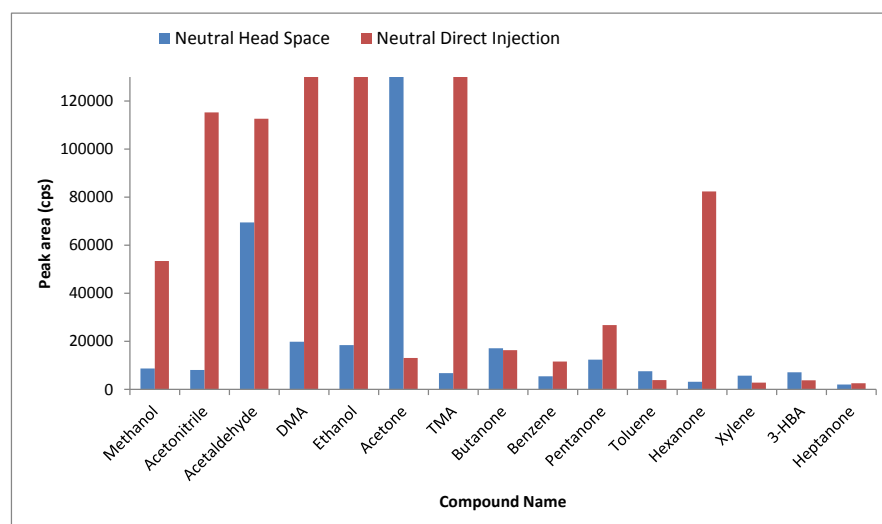


Figure 6.2 Difference from direct injection to headspace injection on major VOCs

Even though better sensitivity was achieved with the direct injection technique, it has its drawbacks in regards to contamination and other instrument related issues. Urine is a complex mixture of salts, protein, peptides and other biological and chemical compounds. During the course of the experiments, it was observed that when urine samples were injected directly, salt residues were observed inside the HIS source. The orifice between drift tube and the ToF-MS was covered with dry residue during the experiments. As a size of the orifice is small (200 microns diameter), deposition could be the reason for the blockage. The headspace analysis on the other hand suffers from the low sensitivity compared to the direct injection but the contamination related issues do not affect it.

As seen in Figure 6.2, generally, a higher sensitivity was observed for the majority of VOCs with direct injection of urine sample compare to urine headspace. In general, sensitivity of the compounds in direct injection technique was 1 to 30 fold greater than the headspace analysis, depending on the compound. For example, the sensitivity of ethanol was at least 30 fold and trimethylamine was at least 20 fold higher for the

direct injection technique. Acetone bucks the trend by actually showing sensitivity at least 10 fold higher in the headspace analysis when compared to the direct injection technique.

### 6.3.2 Influence of salt, acid and base

The effect of salt and pH on VOC detection was investigated. In general, the addition of salts led to an increase of the extraction yield *i.e.* sensitivity because of the salting-out effect. Salting increases the ionic strength of the aqueous solution and, in this way, can decrease the solubility of an organic analyte, thus partitioning the volatile compounds from the aqueous solution and into the headspace [2, 3]. The effect on the sensitivity with the amount of salt added is compound specific. Yang *et al.* [4] developed an application of solid-phase micro-extraction (SPME) in flavour analysis for 25 common flavour components by using gas chromatography as detection technique. They have reported four different types of behaviour of the volatile component with different amounts of salt in their experiments. They have concluded that,

- a) Sensitivity increases with increasing salt concentration (ethyl butyrate, *cis*-3-hexenol, benzaldehyde, linalool, phenylethyl alcohol, cinnamic aldehyde,  $\gamma$ -decalactone, heliotropin, and triethyl citrate)
- b) Sensitivity increases initially and then levels off at higher salt concentration (*cis*-3-hexenyl acetate, ethyl acetate, and geranial)
- c) Sensitivity increases initially and then decreases with increasing salt concentration (ethyl hexanoate, hexanoic acid, and triacetin)
- d) Sensitivity decreases with higher salt concentration (limonene, anethole, and  $\beta$ -ionone)

As per the discussion in Section 6.3.1 regarding the contamination, blockage issues with direct injection of urine, only headspace analysis was used for the rest of the experiments and data from the headspace analysis is discussed in Section 6.3.2 - 6.3.11.

A urine sample from one volunteer was split between two different glass containers. In one container, salt was added and in the second container, the sample was as received. Headspace analysis from both samples was performed and measurements obtained are shown in Figure 6.3.

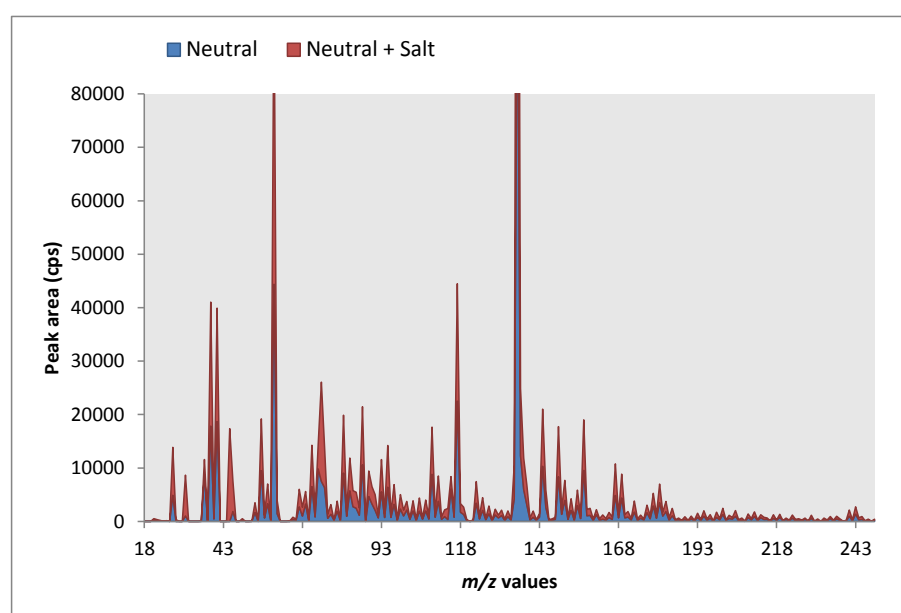


Figure 6.3 Effect of salt in urine on the VOCs emitted

The mass spectrum from the sample with no salt added is plotted in blue and that for added salt shown in red. The sensitivity for most of the compounds was greater when salt was added to the sample than when it was not.

Mirhosseini *et al.* has also reported a similar increase in the concentration of different VOCs e.g.  $\alpha$ -pinene, ethyl butyrate, hexanal, 3-carene, octanal, decanal, linalool and neral when measuring from orange beverage emulsion by using HS-SPME as an extraction technique and GC-FID as a detection technique

[15]. After this observation, salt was added to all the further experiments described in this chapter.

A change in the pH of the samples also has an effect on the sensitivity of the analytical method. The effect of pH is somewhat similar to ionic strength. Polar analytes were affected more greatly by pH than nonpolar analytes. As expected, acetic acid with the lower pH is best extracted under acidic conditions, and isopropylamine and propionitrile with higher pH are best extracted under basic conditions [17]. For nitrogen containing compounds, such as ammonia, higher sensitivity was observed under basic condition (pH range 10 – 12) as illustrated in Figure 6.4. Acids and sulphur containing compounds are more sensitive under acidic conditions. For acetonitrile, a higher sensitivity was observed under neutral pH compared to acidic or basic pH as seen in Figure 6.10. For acetone, higher sensitivity was observed at both acidic (pH range 2-3) and neutral pH compare to basic pH as seen in Figure 6.6.

### 6.3.3 VOC characterisation

The headspace of urine samples from the healthy individuals were analysed as detailed in the Section 2 of this chapter. Identification of specific VOCs is only attempted for those with molecular weights below 150 amu. In addition, VOC profiles can also be affected by diet and this complicates the characterisation, particularly of higher molecular weight compounds. High molecular weight compounds characterisation requires special confirmatory analysis e.g. by use of NMR and this is beyond the scope of the present work.

Ammonia, formaldehyde, propanol, methanol, acetonitrile, acetaldehyde, dimethylamine (DMA), trimethylamine (TMA), acetone, butanone, pentanone, hexanone, heptanoe benzene, toluene and phenol were identified and quantified in this

chapter. The identification and quantification is discussed in detail in sections 6.3.4 to 6.3.10.

3- Hydroxybutyric acid (3-HBA,  $C_4H_8O_3$ , molecular mass = 104.1 Da) was also identified in the experiments. 3-HBA is a part of the ketone body, which is important in the diagnosis of ketoacidosis. Ketone body is discussed in detail in Section 3.5. The 3-HBA readily reacts with  $H_3O^+$  to produce a protonated ion at  $m/z$  105 [18].

Acetic acid ( $C_2H_4O_2$ , molecular mass = 60 Da) and hexanoic acid ( $C_6H_{12}O_2$ , molecular mass = 116 Da) were also observed in the headspace of urine. Both acetic acid and hexanoic acid readily react with  $H_3O^+$  to produce protonated ion at  $m/z$  61 and  $m/z$  117, respectively [19]. Kumar *et al.* analysed the gastric content of healthy subjects and patients with gastro-esophageal cancer by using SIFT-MS [20]. They reported significantly higher quantities of acetic acid and hexanoic acid in the cancer patients when compared to healthy subjects.

Haung *et al.* have subsequently analysed the headspace of urine samples from patients with gastro-esophageal illness. The samples were analysed alongside with healthy subject by using SIFT-MS [21]. Haung *et al.* have reported the similar trend in the concentration of acetic acid and hexanoic acid as reported by Kumar *et al.* Kumar *et al.* and Haung *et al.* indicated it in their paper that healthy individuals also have acetic acid and hexanoic acid in range of 18 – 25 ppbv. Therefore, peaks observed at  $m/z$  61 and  $m/z$  117 could be for the acetic acid and hexanoic acid.

Isoprene ( $C_5H_8$ , molecular mass = 68 Da) reacts with  $H_3O^+$  ions to form the protonated parent ion at  $m/z$  69 [22]. Isoprene presence in the human tissue is of endogenous origin; however, its metabolic pathway is still uncertain. It is commonly accepted that isoprene is a by-product of cholesterol biosynthesis [23].

A peak at  $m/z$  89 was seen in all urine headspace samples. Potential compounds with molecular masses of 88 Da include butyric acid and ethyl acetate. Ethyl acetate is a constituent of natural aromas and ubiquitous in fruit, vegetables, beverages (beer, coffee, tea) [24] and cheese. Thus, the peak observed at  $m/z$  89 could be from ethyl acetate on the basis of dietary exposure. In addition, the sensitivity of the  $m/z$  89 was higher in the headspace urine sample of a smoker compared to four non-smoker volunteers. In April 1994, The United States Department of Health and Human Services has published the list of additives in cigarettes. Ethyl acetate is present in that list [25]. Thus, although not proven here, ethyl acetate is a good candidate for the peak at  $m/z$  89.

A peak at  $m/z$  113 was seen in all headspace samples, with the largest signal occurring under acidic conditions. One compound with a molecular mass of 112 is sorbic acid, a common food preservative. The human intake of sorbic acid is estimated to range from 0.01 to 1.1 mg/kg/day, and the urinary excretion of sorbic acid is in the range of 0.12 to 1.03  $\mu\text{g}/\text{kg}$  per day [26]. All volunteers in the present study were on a varied diet with regular intake of sorbic acid and thus the peak at  $m/z$  113 could derive from sorbic acid.

#### 6.3.4 Precision and bias

The precision of the measurement of VOCs from the urine samples was determined by analysing six aliquot of the same urine sample. The un-normalised mass spectrum data are used to determine the precision.

The precision was calculated by using following equation.

$$\textit{Precision} = \frac{\textit{Standard deviation}}{\textit{Mean}} \times 100 \quad (6.3)$$

Table 6.1 contains the precision data generated from six injection of same sample.

Table 6.1 The precision of the measurement for the VOCs

Number	Ammonia	Formaldehyde	Acetonitrile	Acetaldehyde	Acetone
1	64391	927	323	14103	6442
2	83976	609	300	11967	7023
3	81147	805	395	12436	5369
4	88586	882	276	12036	6988
5	94571	848	269	8980	5111
6	83778	922	359	10102	5658
Mean (peak area in cps)	82742	832	320	11604	6099
Standard deviation	10159	119	49	1811	832
Precision (%)	12.3	14.3	15.4	15.6	13.7

The observed precision for the VOCs (different aldehyde and ketones and ammonia) are presented in Table 6.1 was in region of 12.3% to 15.6%.

During the course of the experiments, sample introduction to the HIS was done by manual injection. Therefore, the observed precision from multiple injections was deemed satisfactory.

The bias of the measurement was calculated by making the multiple injection (n=4) of acetone and acetonitrile working solution.

The calculation for bias was performed using following equation.

$$Bias = \frac{Mean}{Nominal\ concentration} \times 100 - 100 \quad (6.4)$$

Table 6.2 contains the data for bias generated by injection the standard prepared 30 nmol/l

Table 6.2 The bias of the measurement

Number	Acetonitrile	Acetone
	30 nmol/L	30 nmol/L
1	27.9	25.4
2	17.6*	23.9
3	34.3	13.0*
4	30.4	27.1
Mean (nmol/l)	27.5 (30.9)	22.4 (25.5)
Standard deviation (n-1)	7.14 (3.22)	6.37 (1.63)
Precision (%)	25.9 (10.4)	53.1 (6.4)
Bias (%)	-8.2 (2.8)	-25.4 (-15.0)

\*Data in bracket excludes the outlier

The low bias was observed for both acetonitrile and acetone. Following the close inspection of the data, it was noted that at least one concentration value was abnormally lower for both acetonitrile and acetone. The possible reasons for this low result could be the injection error.

For acetonitrile, bias and precision when including the outlier is -8.2% and 25.9%. When outlier is excluded from the calculation, the observed bias is 2.8% and precision is 10.4%.

For acetone, bias and precision when including the outlier is -25.4% and 53.1%. When outlier is excluded from the calculation, the observed bias is -15.0% and precision is 6.4%

Acceptable precision was observed for both acetone and acetonitrile. Acceptable bias was observed for acetonitrile but for acetone, low bias was observed. As documented in Chapter 3, a high residual contamination was noted in HIS. This contamination had an impact on calibration and could be the possible reason for low bias.

### 6.3.5 Ammonia

Ammonia is considered a normal constituent of all body fluids, resulting from the metabolism of amino acids [27]. The most common source of ammonia in urine is through eating various food that have high concentrations of nitrogen e.g. protein, meats, eggs and a few vegetables like asparagus. Exhaled ammonia is thought to mostly originate from the oral cavity [28], with the systemic ammonia concentration found to be ca. 100 ppbv in healthy subjects [29]. Ammonia is normally converted to urea by the liver, which is subsequently transferred into the kidneys and is excreted in urine. Ammonia levels can rise when liver function is impaired [30] and elevated ammonia concentrations have been observed in conditions such as cirrhosis and end-stage renal failure. *H. pylori* bacteria produce urea enzymes that break urea into ammonia and carbon dioxide, and the elevation of these products can be used to make a positive diagnosis of infection [31, 32].

Ammonia (proton affinity: 854 kJ mol<sup>-1</sup>) is one of the inorganic molecules with a higher proton affinity than water (proton affinity: 691 kJ mol<sup>-1</sup>) and this is the reason why ammonia is detectable in PTR-MS using H<sub>3</sub>O<sup>+</sup>.

Some clustering of the product NH<sub>4</sub><sup>+</sup> ions occurs in three body association reactions with the relatively large concentration of water molecules that are inevitably introduced from a urine sample. This results in small fractions of NH<sub>4</sub><sup>+</sup> (H<sub>2</sub>O)<sub>1,2</sub> ions at *m/z* 36 and *m/z* 54.

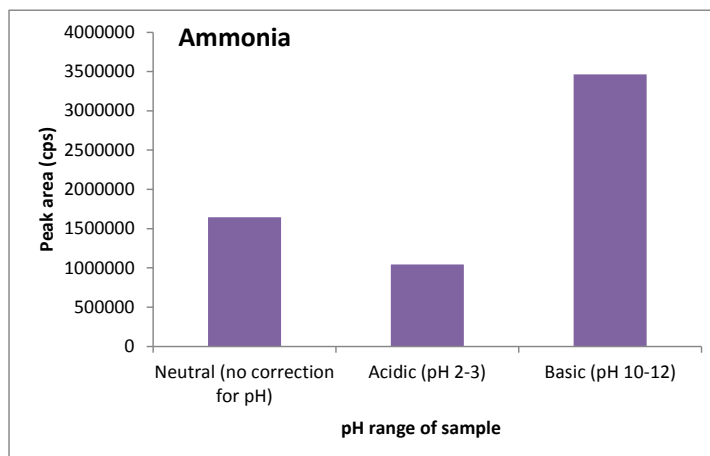


Figure 6.4 A presentation of level of ammonia at three different pH levels from the headspace analysis of the urine sample from one volunteer

During the course of the experiments, to achieve the maximum sensitivity, the effect of pH was also examined. As seen in Figure 6.4 maximum sensitivity was observed at a basic pH compared to acidic or neutral pH, and thus basic pH was maintained during the experiments when quantification of ammonia was performed.

Ammonia from the urine samples from the five healthy volunteers were measured during the course of the experiment.

Table 6.3 Concentration of ammonia in nmol/Litre from the urine of five healthy volunteers

Volunteer	Amount of ammonia
1	783
2	1107
3	1172
4	647
5	680

Table 6.3 contains the data generated from the experiment. A large concentration of ammonia was found in all individuals. The ammonia concentration obtained from the headspace analysis experiments fell in the range from 647 nmol/Litre to

1172 nmol/Litre. Diskin *et al.* measured the ammonia and acetone in urine headspace and breath during ovulation quantified by SIFT-MS.

The concentration of ammonia from the headspace of urine observed in this chapter were lower compare to the urine headspace concentration data reported by Diskin *et al.* [33]. The reported headspace concentration of ammonia from urine headspace was in the range of 34 – 1966  $\mu\text{mol/l}$  (34000 – 1966000 nmol/l) [33]. One of the possible reasons for this difference is Diskin *et al.* used 10 mL of sample compared to 1 mL of sample used in this chapter. In addition, all the healthy volunteers recruited in the Diskin *et al.* study were going through their ovulation cycle and that could have influenced the higher concentration of ammonia.

### 6.3.6 Ketones

This section describes the finding from experiments carried out to measure the levels of acetone, pentanone, butanone, heptanone and hexanone from urine samples from five healthy volunteers.

Ketones are present in the blood stream of all humans and linked to dextrose metabolism, to be a product of lipolysis and to be elevated by ketoacidosis [34]. Ketones also appears in the exhaled breath of healthy people at relatively low concentration [35] and in urine [9].

The details of the biochemical routes to acetone production are well-understood [36]. Acetone is formed from the decarboxylation of acetoacetic acid [37]. Acetone levels are elevated during fasting or starvation when carbohydrates are scarce and the breakdown of fatty acids provides a source of energy, and during high fat, low carbohydrate diets [38, 39]. Acetone can also be formed from the enzymatic ingestion and

conversion of propan-2-ol. Ketone bodies are three water-soluble compounds that are produced as a by-product when fatty acids are broken down for energy in liver. The three endogenous ketone bodies are acetone, acetoacetic acid and beta-hydroxyacid, although acetoacetic acid and beta-hydroxybutric acid is not technically a ketone but a carboxylic acid. Ketone bodies are present in the healthy human, but elevated levels are associated with liver disease [40, 41] and congestive heart failure [42].

All ketones readily react with  $\text{H}_3\text{O}^+$  as illustrated for acetone in reaction 1.

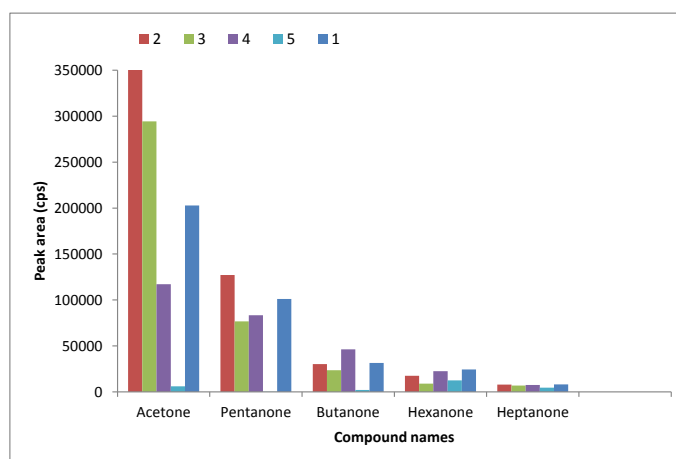


Figure 6.5 Levels of ketones from urine headspace from five healthy volunteer

The relative quantities of ketones determined from a headspace analysis of neutral pH urine are presented in Figure 6.5. Acetone is clearly the most abundant of the ketones in all individuals except for volunteer 5, with progressive decline in abundance as the chain length increased. Wang *et al.* analysed the different ketones in the urine headspace using SIFT-MS and have reported acetone levels at 600 to 800 ppb while other ketones, *e.g.* pentanone, hexanone and heptanone are present in the

urine headspace at much lower levels, typically at 20-80 ppb [18].

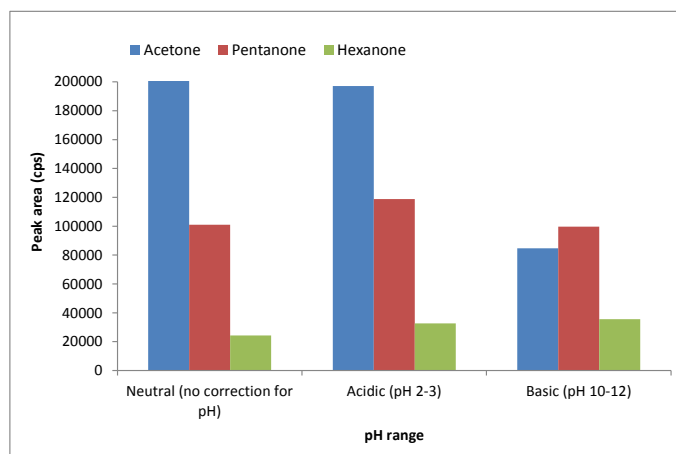


Figure 6.6 A presentation of level of acetone, pentanone acid and heptanone at three different pH levels from the headspace analysis of the urine sample from one volunteer

Figure 6.6 shows how the ketone levels vary with pH. Acetone was already discussed in this sense in section 6.3.2, where it was observed that the sensitivity to acetone detection was the lowest for basic conditions. For these heavier ketones, the effect of pH on the detection is negligible. Smith *et al.* [9], who analysed the urine headspace from two individuals, also reported a similar pattern. They reported that concentration of acetone and other ketones in the headspace do not change significantly as the pH changes [9].

Table 6.4 contains the data for acetone, butanone, pentanone, hexanone and heptanone from a urine samples from the five healthy volunteers.

Table 6.4 Concentration of ketones in nmol/Litre from the headspace analysis of urine from five healthy volunteers

Volunteer	Acetone	Butanone	Pentanone	Hexanone	Heptanone

Volunteer	Acetone	Butanone	Pentanone	Hexanone	Heptanone
1	1250	226	639	240	311
2	2150	209	798	225	539
3	1780	167	486	164	768
4	705	299	538	301	170
5	505	1.2	0.63	142	57.0

The urine headspace concentration of ketone distribution displayed a median concentration of 1250 nmol/L for acetone, 167 nmol/L for butanone, 486 nmol/L for pentanone, 164 nmol/L for hexanone and 170 nmol/L for heptanone. Pysaneko *et al.* [43] has determined the acetone, butanone, pentanone, hexanone and heptanone levels in the headspace of urine solution and headspace by SIFT-MS. In their study the ketones in the urine of three healthy volunteers, were measured using acidified urine at 37°C. The reported range of acetone, butanone, pentanone, hexanone and heptanone was 6000 - 14000, 50 - 160, 60 - 140, 10 and 20 - 80 nmol/L. They have discussed that acidification of the urine does not greatly change the partition of the ketones into the headspace phase, but it released the ketone molecules from their binding to other constituents of urine (*e.g.* proteins), thus increasing the headspace levels. Wang *et al.* measured the urine acetone in “normal people” and in exposed workers. The samples from exposed workers were taken 16 h after the end of the work-shift. In total samples from 89 non-occupationally exposed subjects and three groups of workers exposed to acetone or isopropanol were collected and analysed by using headspace and detection was performed by using GC-MS [44]. The reported concentration of acetone was ~1550 nmol/l (842 µg/L) in urine from non-exposed subjects and ~3500 nmol/l (2206 µg/L) in exposed subjects. Haung *et al.* has quantified the acetone from the headspace of urine sample by using SIFT-MS [53]. They have

reported a median concentration of 2280 nmol/L (1326 ppbv) from cancer patient, 1520 nmol/L (882 ppbv) from positive control and 456 nmol/L (265 ppbv) from the healthy controls. Delgado *et al.* used ion mobility spectroscopy with an ultraviolet ionisation as a vanguard screening system for the detection acetone in urine as a biomarker [45]. They have reported the concentration of acetone in a region of 465 nmol/l ( $27 \pm 3$  mg/L, converted by using:  $\text{weight (g)}/\text{molecular weight (g)} = \text{mmol/L} * 1000 = \mu\text{mol/L}$ ).

The observed concentration of ketones found in the current study is lower than the reported concentration by Pysaneko *et al.*, although the overall profile of concentration of different ketones from the urine headspace was comparable. The level of acetone in urine varies from individual to individual and a number of different factors could influence it, *e.g.* the time at which the sample is collected. Urine samples collected in the morning, before, or after a meal can influence on the level of acetone. Observed urine acetone concentration data in the current study are typical of those obtained in the blood and urine obtained in other studies [46, 47].

### 6.3.7 Aldehydes

The C<sub>1</sub>-C<sub>10</sub> aldehydes have been detected in the breath and blood streams of healthy subjects, of which acetaldehyde is the most commonly reported [27, 28, and 48]. Acetaldehyde is the first metabolite of the enzymatic oxidation ethanol [49] and a relatively low concentration was produced by oxidation of endogenous ethanol [34]. As ethanol concentrations are elevated after the consumption of alcoholic drinks, acetaldehyde concentrations are similarly increased. The simplest aldehyde, formaldehyde, has been measured in low concentration in healthy individuals [28].

Aldehydes are also formed by free-radical-induced reactions with cellular lipids. The presence of aldehydes with low molecular weight is considered a cancer marker [10, 11, 50, 51], and as evidence that free-radical mediated reactions have taken place recently [52]. An increase in aldehyde concentration implies greater oxidative stress. High levels of aldehydes such as formaldehyde, hexanal, acetaldehyde, heptanal have been found in the blood of cancer patients and these aldehydes were regarded as biomarkers of cancer [53-55].

The protonation of aldehyde (formaldehyde) by  $\text{H}_3\text{O}^+$  proceeds by the reaction (2).



In the present experiment, also seen in the experiments discussed in Chapter 5, residual moisture was observed in the drift tube. The level of residual moisture in drift tube exceeds the level of aldehydes, and it resulted in the presence of monomer and dimer for aldehydes in the data. The formation of water clusters is association reactions and these reactions are not stable at the drift tube temperature, therefore they are not reliable to use for the quantification purpose.

Peak area of the different aldehydes observed and quantified during the experiments is presented in Figure 6.7.

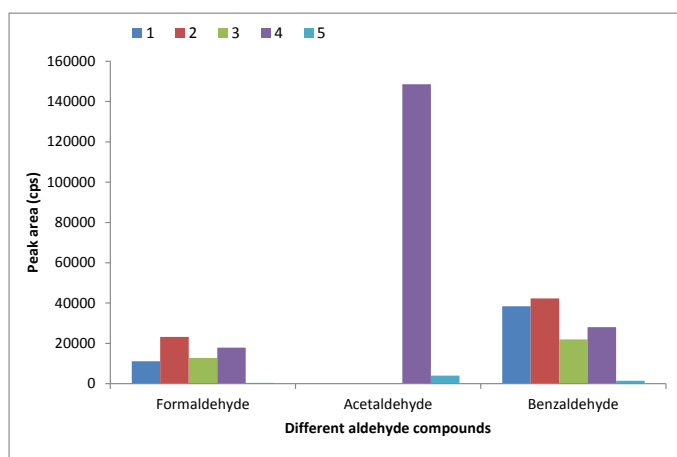


Figure 6.7 Aldehyde levels measured for five volunteers

The relative quantities of aldehydes from a headspace analysis of acidic pH urine are presented in Figure 6.8. Acetaldehyde was only observed in two out of five volunteers.

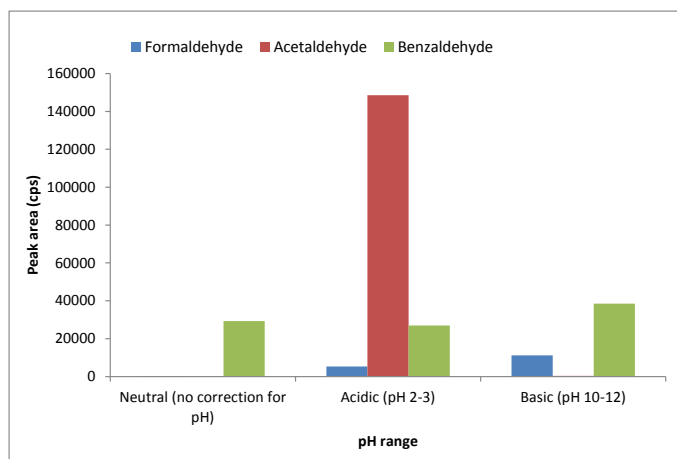


Figure 6.8 A presentation of level of different aldehydes at three different pH levels from the headspace analysis of the urine sample from one volunteer

Figure 6.8 shows how the aldehyde levels vary with pH. It was observed that relatively high sensitivity was observed for acetaldehyde under acidic condition whereas sensitivity of formaldehyde and benzaldehyde was similar at both acidic and basic pH.

The quantification of formaldehyde and acetaldehyde was performed from the headspace of basic urine samples. The quantification of benzaldehyde was performed from the headspace of acidic urine samples. The concentration data are presented in Table 6.5.

Table 6.5 Concentration of aldehydes in nmol/l from the headspace analysis of urine from five healthy volunteers

Volunteer	Formaldehyde	Acetaldehyde	Benzaldehyde
1	14.1	0.0	74.9
2	40.9	0.0	83.5

---

Volunteer	Formaldehyde	Acetaldehyde	Benzaldehyde
3	17.8	0.0	38.3
4	29.0	320.3	51.7
5	0.0	0.0	0.0

Spanel *et al.* [10] reported the mean concentration of formaldehyde from the headspace of urine by using selected ion flow tube mass spectrometry (SIFT-MS). The reported mean concentration was 366 nmol/l (11.0 µg/mL) from healthy individuals, 832 nmol/l (25.0 µg/mL) from a prostate cancer patient and 2830 nmol/l from the bladder cancer patient. In the current chapter, observed concentrations of formaldehyde from the urine headspace sample was in the range of 14.1 - 40.9 nmol/L (0.423 – 1.23 ppb; converted by using  $C_{(\text{ppm})} = 10^6 \times C_{(\text{mol/l})} \times M_{(\text{g/mol})} / \rho_{(\text{mg/k3})}$ ). The observed concentration of formaldehyde was lower in the current study compared to the concentration of the formaldehyde from the healthy volunteer reported by Spanel *et al.* [10].

In the current experiment, quantifiable acetaldehyde was observed from one individual out of five volunteers. In particular, the sample that produced detectable acetaldehyde was from the individual with a smoking habit. Acetaldehyde is a major component of tobacco smoke and the level of acetaldehyde in smokers is around 10 times higher when compared to non-smokers as described by Talhout *et al.* [56]. In the current chapter, the observed concentration of acetaldehyde from one volunteer with an occasional smoking habit was 320.3 nmol/l (14.1 ppb). Haung *et al.* quantified the acetaldehyde from the headspace of urine samples by using SIFT-MS [21]. They have reported the median concentration of 3178 nmol/l (140 ppbv) from cancer patients, 2088 nmol/l

(92 ppbv) from positive controls and 1316 nmol/l (58 ppbv) from the healthy controls.

The observed concentration of formaldehyde was lower in this study compared to the data published by Spanel *et al.* [10]. Acetaldehyde was only quantified from one volunteer in this study and observed concentration was lower than the concentration data reported by Haung *et al.* [21]. Number of factors for example diet, alcohol consumption and smoking could influence the level of aldehyde in the individual. The observed low concentration of acetaldehyde could be influenced by the occasional smoking habit of the volunteer. It was also observed that a high amount of moisture was present in the drift tube during the course of the experiment due to the water content of urine. The high moisture content has an impact on the protonation and water cluster ions were observed. These observations could also have influenced the low concentration of formaldehyde observed in this study.

### 6.3.8 Acetonitrile

Identification of a volatile marker for smoking has been of considerable interest for many years. In the last 20 years, cigarette smoking has been shown to be strongly associated with the development of bladder cancer and lung cancer [11, 57], as well as heart attacks. Acetonitrile is used as the lead volatile marker for smoking [58].

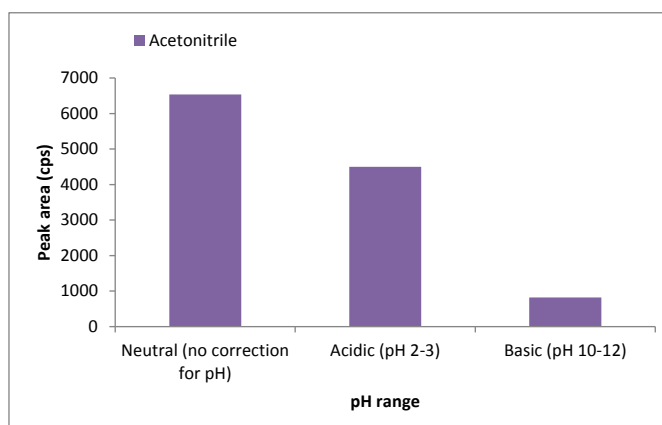


Figure 6.9 A presentation of level of acetonitrile at three different pH levels from the headspace analysis of the urine sample from one volunteer.

Figure 6.9 shows how acetonitrile levels vary with pH. It was observed that at neutral and acidic pH, acetonitrile was detected with higher sensitivity compared to basic pH conditions.

Out of five healthy individuals, one individual was a smoker and volunteered to smoke prior to the urine sample collection. The observed concentration of acetonitrile is presented in Table 6.6.

Table 6.6 Concentration of acetonitrile in nmol/Litre from the headspace analysis of urine from five healthy volunteers

Volunteer	Acetonitrile
1	15000
2	18000
3	28000
4	90000
5	10000

A high concentration for acetonitrile was observed for the individual who is an occasional smoker (Volunteer: 4) compared to the non-smokers. Except for the smoker, the acetonitrile concentration was in range of 10.0 – 28.0 nmol/litre (0.410 – 1.15 ppb). For the smoker, who is an occasional smoker, the acetonitrile concentration was 90.0 nmol/Litre (4.0 ppb).

S M Abbott *et al.* [59] measured the headspace acetonitrile from urine samples by using SIFT-MS. They have reported mean acetonitrile concentration of 1534 nmol/l (63.0 ppb) for smokers and 73 nmol/l (3.0 ppb) for non-smokers. In the same publication, breath acetonitrile for smokers was reported at 1681 nmol/l (69.0 ppb) and for non-smokers at 49 nmol/l (2.0 ppb). Pinggera *et al.* [12] reported the level of 91 nmol/l

(3.74 ppbv) for non-smokers and 682 nmol/l (28 ppbv) for smokers from the urine headspace using PTR-MS. The acetonitrile concentration from the non-smokers is comparable to the data reported by Pinggera *et al.* and S M Abbott *et al.* Observed level of acetonitrile was low in the smokers. The main reason for the low observed concentration could be due to the fact that volunteer MAP was an occasional smoker while regular smokers were recruited in the study discussed by Pinggera *et al.* and S M Abbott *et al.*

### 6.3.9 Dimethyl amine and Trimethyl amine

The short-chain aliphatic amines, like dimethyl amine (DMA) and trimethyl amine (TMA), are constituents of human urine. DMA was a possible neurotoxin in uremic patients [60]. TMA is associated with the fish odour syndrome. They are present in the diet (in marine fish) and originate from the enterobacterial metabolism of precursors such as food derived carnitine and choline [61].

Both DMA and TMA readily react with  $\text{H}_3\text{O}^+$  and produces protonated DMA and TMA.

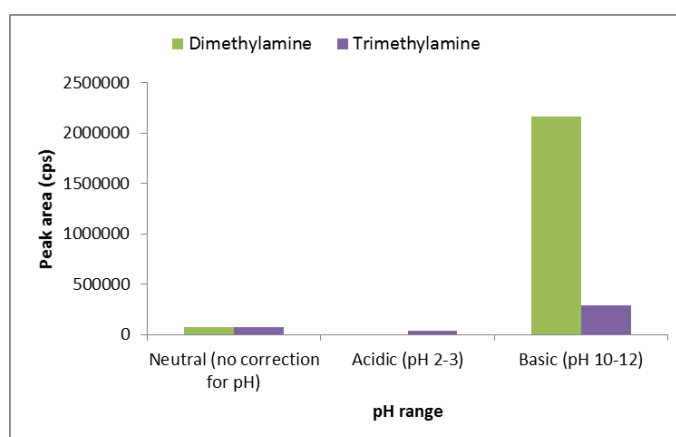


Figure 6.10 A presentation of level of DMA and TMA at three different pH levels from the headspace analysis of the urine sample from one volunteer.

Figure 6.10 shows how the DMA and TMA levels vary with pH. Both DMA and TMA were more sensitive to detection under basic pH conditions. Table 6.7 contains the concentration data for DMA and TMA.

Table 6.7 Concentration of DMA and TMA in nmol/Litre from the headspace analysis of urine from five healthy volunteers

Volunteer	Dimethylamine	Trimethylamine
1	4817	638
2	11274	1917
3	5126	933
4	1439	194
5	13	28

The urine headspace concentrations of DMA and TMA was in the range of 13 – 11274 nmol/L (0.000585 – 0.507 mg); and 28 – 1917 nmol/L (1.66 – 0.113 mg) respectively. Zhang *et al.* [61] measured the DMA and TMA in human urine headspace using GC. They have reported the concentration of DMA from healthy volunteers in the range of 180000 – 600000 nmol/l (8.4 – 27.2 mg per day) while that of TMA was 3380 – 45000 nmol/l (0.2 – 2.7 mg). Wahl *et al.* analysed the TMA in human urine by using headspace GC-MS [62]. They reported the absolute concentration of TMA of 25000 nmol/l (1.5 µg/mL) in human urine.

DMA exists in foods at µg/g (ppm) levels [26-28] although higher concentrations are found in fish [27, 29, 30], particularly after freezing [31]. The major dietary source is via the demethylation of TMA produced by the action of gut microflora. As levels of DMA in urine is dependant to dietary intake or by a different mechanism in human body, the levels varied from individual to individual.

TMA readily oxidised to trimethylamine-N-oxide (TMAO) by a flavin containing monooxygenase in the liver. Healthy young volunteers reported to excrete about 1 mg of TMA and 40 mg of TMAO per day in urine under normal dietary intake. The majority of individuals excrete more than 90% of TMA in the form of TMAO [63]. Wahl *et al.* measured the total TMA (TMA+TMAO) in their study, whereas in the current study only TMA was measured, as TMAO was not identified in the PTR-MS. As 90% of TMA gets converted into TMAO [63] and only TMA is quantified in this study, this could be the possible reason for the low observed concentration for TMA.

### 6.3.10 Benzene and toluene

Benzene and toluene are important industrial chemicals used worldwide as feedstock for plastic, as well as for solvents [64]. Recently they have acquired great relevance as pollutants of the outdoor and indoor human environment. Sources of these pollutants include traffic and smoking.

The lungs readily absorb these organic compounds on inhalation. Significant absorption may also occur through skin, whenever these solvents are in contact with it. Part of the benzene and toluene is eliminated unchanged in urine, but most of it is metabolized in the liver and excreted in the form of its metabolites [65].

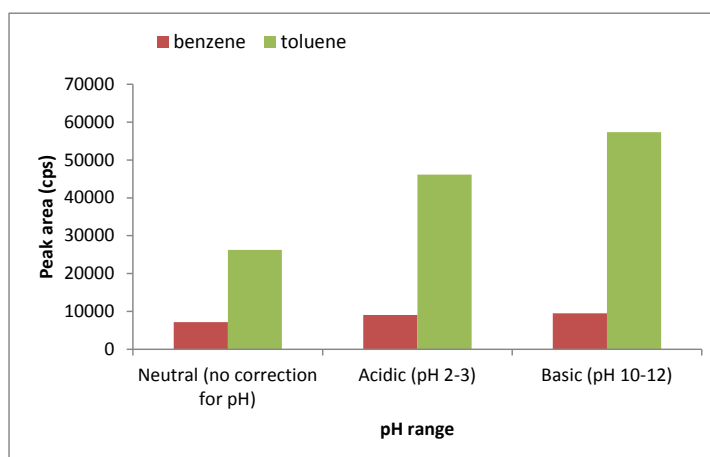


Figure 6.11 A presentation of level of benzene and toluene at three different pH levels from the headspace analysis of the urine sample from one volunteer.

Figure 6.11 shows how the benzene and toluene levels detected by headspace PTR-MS in urine vary with pH condition. Both benzene and toluene were more sensitive under basic pH conditions. Table 6.8 contains the concentration data for benzene and toluene.

Table 6.8 Concentration of Benzene and Toluene in nmol/Litre from the headspace analysis of urine from five healthy volunteers

Volunteer	Benzene	Toluene
1	1.9	149.2
2	8.4	149.0
3	2.3	87.0
4	6.0	110.7

The Observed concentration of benzene from volunteers was in the range of 2.3 - 8.4 nmol/Litre (0.179 – 0.655 ppb), while for toluene, it was 87.0 to 149.2 nmol/Litre (5.24 – 13.7 ppb).

Kramer Alkalde *et al.* [65] reported the benzene concentration in the range of 17 – 2000 nmol/l (1.37 to 162.5 ppb) for benzene and 23 – 1888 nmol/l (2.10 to 174.3 ppb) for toluene from the urine headspace by using SPME as extraction method and GC-MS as detection technique. By using similar matrix, extraction and detection technique S Fustinoni *et al.* [8] reported the benzene concentration of 1500 nmol/l (123 ng/Litre) and toluene concentration of 2300 nmol/l (215 ng/Litre).

The observed concentration data generated in this study are in agreement with the data reported in [65]. The observed concentration from this study was lower when compared to the data reported by S Fustinoni *et al.* [8]. The main reason for the

lower concentration of the data could be that data generated in [8] was from the urine samples collected from the subjects who were exposed to these airborne pollutants.

### 6.3.11 Alcohols

The use of alcoholic beverages is probably the most ancient and widespread social habit. Alcohol is the most used psychoactive substance in the world because it is licit, easily obtained and cheap. In forensic toxicology analysis, determination of alcohol concentration is more frequent. Natural metabolism also produces the alcohol [66, 67]. Alcohol readily reacts with hydronium ions. It can also produce the fragments ions when it reacts with the hydronium ion. Chapter 5 of this thesis details the chemistry of alcohol with  $H_3O^+$ .

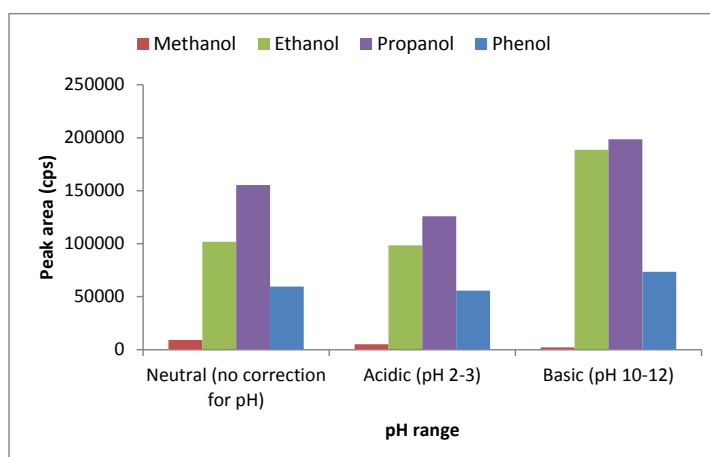


Figure 6.12 Level of methanol, ethanol, propanol and phenol at three different pH values from the headspace pH analysis of the urine sample from one volunteer.

Figure 6.12 shows how the methanol, ethanol, propanol and phenol levels vary with pH condition. Both ethanol and propanol gave higher sensitivity at basic pH, whereas methanol and phenol gave slightly higher sensitivity at neutral pH condition. Table 6.9 contains the concentration data for methanol, ethanol, propanol and phenol.

Table 6.9 Concentration of Methanol, Ethanol and Propanol in nmol/Litre from the headspace analysis of urine from five healthy volunteers

Volunteer	Methanol	Ethanol	Propanol	Phenol
1	34.7	1317.1	1386.1	514.1
2	25.7	1884.7	1602.9	616.9
3	64.7	981.7	55.1	343.8
4	26.3	839.7	2210.4	469.5
5	23.7	149.2	17.0	23.4

The concentration of methanol ranged from 23.7 - 64.7 nmol/L (0.000759 – 0.00207 mg), while those of ethanol and propanol were 149.2 - 1884.7 nmol/L (0.00687 – 0.0868 mg) and 17.0 - 2210.4 nmol/L (0.00104 – 0.135 mg), respectively. It was also observed that propanol levels were higher in a volunteer with an occasional smoking habit (volunteer: 4) compared to the other non-smoker individuals.

Correa *et al.* reported the urine ethanol level in ten healthy volunteers after a single dose of whisky (0.68 g ethanol per kilogram of body weight) in the range of 0.00 g/l at 0hr to 800000 nmol/l (0.04 g/l) at 7 hr peaking at 27000000 nmol/l (1.28 g/l) at 2 hr. The analysis was performed by using headspace gas chromatography with capillary column [68].

Liebich *et al.* have quantified the endogenous aliphatic alcohols in serum and urine by using GC. They have reported the ethanol concentration of 156 nmol/l (7.2 mg) per 24 hours from healthy volunteers and propanol concentration of 4 nmol/l (0.24 mg) per 24 hour [69]. The observed concentration of propanol from this study is comparable to the data reported by Liebich *et al.* The concentration of ethanol obtained in this study was lower than the concentration reported by Correa *et al.* In Correa *et al.* study, subjected consumed the alcohol prior to experiment and that would be reason for the high concentration of the ethanol observed in their study.

In the current experiments, levels of phenol were in the range of 23.4 - 616.9 nmol/L (2.2 – 58.1 ng/mL, conversion made by using: concentration in nmol/L X MW (g/mol)/1000mL).

Crespin *et al.* determined the free and conjugated phenol compounds in human urine by using SPME and GCMS. They have reported a phenol levels in human urine in range of 28 – 5600 nmol/l (2.7 ng/mL to 530 ng/mL) [5]. Huang *et al.* measured the headspace of urine samples from cancer cohort, positive control and healthy control and analysed them by SIFT-MS. They have reported the median 127 nmol/l (12 ppbv) of phenol cancer cohort, 150 nmol/l (14 ppbv) in positive control and 360 nmol/l (34 ppbv) in healthy control [21]. The observed concentration of phenol from the healthy volunteers in this study was comparable to do the data reported by Crespin *et al.*

#### **6.4 URINE HEADSPACE ANALYSIS VS. BREATH ANALYSIS**

Both urine and breath VOC analysis are useful for the measurement of the VOCs for metabolic identification or for the early detection of the disease. In medicine, for the measurement of VOCs, urine is extensively used. The main advantages associated with breath and urine compared to blood, as they are non-invasive and painless to extract. Collection of urine sample is possible from the toddlers.

Urine is a very complex mixture of water, electrolytes, hormones, protein and enzymes. Urine is considered as a “dirty” matrix. On the other hand, breath consists of air with a large quantity of moisture and inert gases and is a relatively clean matrix compared to urine. This has an advantage when measuring VOCs in small quantities as any mass spectrometry signals or a signal from any measurement technique will be free from the background noise.

Sample collection, transport and duration between collection and analysis is an important factor in medicine. Conventionally, breath samples for VOC analysis is collected in large volumes into containers free from contamination. Such samples then need to be concentrated, which usually involves passing the samples through a trap that captures the compounds of interest. This may be chemical interaction, resin adsorption or cryogenic distillation. The concentrated samples must then be transferred to the assay instrument. Currently, tedlar bags are widely used for the sample collection, in which subjects can blow the breath straight into the tedlar bag. After the collection, bags can be transferred to the laboratory. It is vitally important that at each stage of sample preparation and transfer that there is a minimal loss of the volatiles presents and no introduction of contamination to the samples.

Sample collection and transport for the urine is easier than breath. For the urine sample collection, subjects have to urinate in an airtight and contaminant free container. The sample container than placed either in the freezer or in the fridge for storage prior to analysis. VOCs are stable in urine for at least one week and probably longer when stored at -20°C or lower [70]. The size of the container and volume of sample handling is smaller with urine sample compared to breath samples thus sample handling is relatively easier with urine compared to breath.

### **6.5 CONCLUSION**

This small study focused on the measurement of the VOCs from the headspace of urine from five healthy individuals. The purpose of this study was to establish the method for the determination and quantification of the VOCs from urine to see if this has any potential in future clinical studies alongside the

breath analysis. The results in this study demonstrate that the combination of a use of heated inlet source (HIS) with PTR-ToF-MS is a sensitive method for simultaneous detection and quantification of several VOCs present in the headspace of urine. When the problems with direct injection technique as discussed in the following paragraph are resolved and with the use of capillary inlet source (CIS) discussed in Chapter 4, higher sensitivity than the one observed in this chapter is achievable.

Direct comparison of the VOC profiles from urine samples and the effect of salt and pH were investigated during the experiments. The direct injection yielded higher sensitivity compared to the headspace injection. The direct injection has the big disadvantage of contamination and instrument malfunction due to the nature of the matrix. Addition of salt also increased the detection sensitivity of the VOCs from the headspace of urine. Changes in the pH have different effects on the VOC detection sensitivity depending on the type of VOC. For example, amines gave better sensitivity under high pH conditions whereas for acetone was more sensitive under acidic condition.

In urine headspace analysis, quantification of five different ketones, namely acetone, pentanone, butanone, hexanone and heptone was achieved. The level of acetones was higher in all individuals compared to the other quantified ketones. This concentration profile was comparable to the ketone data from urine headspace analysis from previously published work.

The measurement of ammonia via standard methods (GC/HPLC) is notoriously difficult due to its high solubility in water. The HIS-PTR-ToF-MS technique is ideal for the measurement of ammonia from the aqueous samples.

Acetaldehyde, propanol and acetonitrile were quantified from the headspace of urine samples. It was observed that the

concentration of these VOCs were higher in the volunteer who was an occasional smoker compared to the four other volunteers.

Ethanol was also quantified from the headspace of urine samples. Ethanol production is endogenous as well as exogenous. The endogenous source is metabolism while exogenous source is alcoholic drinks. The observed level of ethanol from the five volunteers was slightly higher than reported data. The high concentration of ethanol was possibly due to varied diet.

To conclude, the VOCs positively identified from the headspace of urine samples using HIS-PTR-ToF-MS include ammonia, methanol, ethanol, propanol, acetonitrile, acetone, pentanone, butanone, hexanone, heptanone, formaldehyde, acetaldehyde, benzene, toluene and xylene. The current technique has an advantage over traditional techniques such as GC-MS because of the far shorter run time using PTR-MS. Furthermore, no sample pre-treatment or pre-concentration is required for PTR-MS. However, urine samples cannot be injected directly due to the reasons discussed in section 3.1. Thus, the PTR-MS approach described here is not suitable when higher sensitivity is required. Further work is required to develop a new way to inject the urine sample directly to the HIS without instrument malfunction. It is hoped that this method might be used in future for clinical studies to measure the VOCs from the patients suffering from cancer, or to identify alcohol abuse.

## 6.6 REFERENCES:

1. Shirasu, M. and K. Touhara, The scent of disease: volatile organic compounds of the human body related to disease and disorder. *Journal of Biochemistry*, 2011. 150(3): p. 257-266.
2. Hans Günther Wahla, A.H., Dieter Luft, Hartmut M. Liebich, *Analysis of volatile organic compounds in human*

- urine by headspace gas chromatography–mass spectrometry with a multipurpose sampler. *Journal of Chromatography A*, 1999. 847: p. 117-125.
3. Albert Zlatkis, R.S.B., and Colin F. Poole, *The Role of Organic Volatile Profiles in Clinical Diagnosis*. *CLIN. CHEM.*, 1981. 27/6: p. 789-797.
  4. Kusano, M., E. Mendez, and K.G. Furton, Comparison of the Volatile Organic Compounds from Different Biological Specimens for Profiling Potential\*. *Journal of Forensic Sciences*, 2012: p. no-no.
  5. Crespín, M.A., M. Gallego, and M. Valcarcel, Solid-phase extraction method for the determination of free and conjugated phenol compounds in human urine. *Journal of Chromatography B*, 2002. 773(2): p. 89-96.
  6. Su, F.-C., B. Mukherjee, and S. Batterman, Trends of VOC exposures among a nationally representative sample: Analysis of the NHANES 1988 through 2004 data sets. *Atmospheric Environment*, 2011. 45(28): p. 4858-4867.
  7. Ghoo, Y., Claus, D., Beypens, B., Hiele, M., Maes, B., Rutgeerts, P., Screening method for the determination of volatiles in biomedical samples by means of an off-line closed-loop trapping system and high-resolution gas chromatography-ion trap detection. *Journal of Chromatography A*, 1994. 665(2): p. 333-345.
  8. Fustinoni, S.G., Rosario; Pulvirenti, Salvatore; Buratti, Marina; Colombi, Antonio, Headspace solid-phase microextraction for the determination of benzene, toluene, ethylbenzene and xylenes in urine. *Journal of Chromatography B: Biomedical Sciences and Applications*, 1999. 723(1–2): p. 105-115.
  9. Smith, D., Španěl, P., Holland, T.A., Al Singari, W., Elder, J.B., Selected ion flow tube mass spectrometry of urine headspace. *Rapid Communications in Mass Spectrometry*, 1999. 13(8): p. 724-729.
  10. Španěl, P., Smith, D., Holland, T.A., Singary, W.A., Elder, J.B., Analysis of formaldehyde in the headspace of urine from bladder and prostate cancer patients using selected ion flow tube mass spectrometry. *Rapid Communications in Mass Spectrometry*, 1999. 13(14): p. 1354-1359.
  11. Wehinger, A., Schmid, A., Mechtcheriakov, S., Ledochowski, M., Grabmer, C., Gastl, G.A., Amann, A., Lung cancer detection by proton transfer reaction mass-spectrometric analysis of human breath gas. *International Journal of Mass Spectrometry*, 2007. 265(1): p. 49-59.

12. Germar-michael pinggera, p.l., florian bodogri, ralf herwig, gabriele steckel-berger, georg bartsch and josef rieder, Urinary acetonitrile concentrations correlate with recent smoking behaviour. *BJU International*, 2004. 95: p. 306-309.
13. Rieder J Fau - Prazeller, P., et al., - Online monitoring of air quality at the postanesthetic care unit by proton-transfer-reaction mass spectrometry. *Anesth Analg*, 2001. 92(2): p. 389-92.
14. Peppard, X.Y.a.T., Solid-Phase Microextraction for Flavor Analysis. *J. Agric. Food Chem*, 1994. 42: p. 1925-1930.
15. Mirhosseini, H., Salmah, Y., Nazimah, S.A.H., Tan, C.P., Solid-phase microextraction for headspace analysis of key volatile compounds in orange beverage emulsion. *Food Chemistry*, 2007. 105(4): p. 1659-1670.
16. Yang, X. and T. Peppard, Solid-Phase Microextraction for Flavor Analysis. *Journal of Agricultural and Food Chemistry*, 1994. 42(9): p. 1925-1930.
17. Shirey, R.E., Optimization of Extraction Conditions for Low-Molecular-Weight Analytes Using Solid-Phase Microextraction. *Journal of Chromatographic Science*, 2000. 38(3): p. 109-116.
18. Wang, T., P. Španěl, and D. Smith, Selected ion flow tube mass spectrometry of 3-hydroxybutyric acid, acetone and other ketones in the headspace of aqueous solution and urine. *International Journal of Mass Spectrometry*, 2008. 272(1): p. 78-85.
19. Allardyce, R.A.L., Vaughan S.; Hill, Alex L.; Murdoch, David R., Detection of volatile metabolites produced by bacterial growth in blood culture media by selected ion flow tube mass spectrometry (SIFT-MS). *Journal of Microbiological Methods*, 2006. 65(2): p. 361-365.
20. Kumar, S., Huang, J., Cushnir, J.R., Spanel, P., Smith, D., Hanna, G.B., Selected Ion Flow Tube-MS Analysis of Headspace Vapor from Gastric Content for the Diagnosis of Gastro-Esophageal Cancer. *Analytical Chemistry*, 2012. 84(21): p. 9550-9557.
21. Huang, J., Kumar, S., Abbassi-Ghadi, N., Spanel, P., Smith, D., Hanna, G.B., Selected Ion Flow Tube Mass Spectrometry Analysis of Volatile Metabolites in Urine Headspace for the Profiling of Gastro-Esophageal Cancer. *Analytical Chemistry*, 2013.
22. Abbott, M.S., The development and application of SIFT-MS to explore the trace gases in urine and breath and thier

- 
- association with malignancy. PhD Thesis, Keele University, 2008.
23. Willis, K.A., Development of Chemical Ionisation Reaction Time-of-Flight Mass Spectrometry for the Analysis of Volatile Organic Compounds in Exhaled Breath. PhD Thesis, University of Leicester, 2009.
  24. [//www.ico.org/decaffeination.asp](http://www.ico.org/decaffeination.asp).
  25. [//en.wikipedia.org/wiki/List\\_of\\_additives\\_in\\_cigarettes](http://en.wikipedia.org/wiki/List_of_additives_in_cigarettes).
  26. Renner, T., M. Baer-Koetzle, and G. Scherer, Determination of sorbic acid in urine by gas chromatography–mass spectrometry. *Journal of Chromatography A*, 1999. 847(1–2): p. 127-133.
  27. Claire Turner, P.Š.e.a.D.S., A longitudinal study of ammonia, acetone and propanol in the exhaled breath of 30 subjects using selected ion flow tube mass spectrometry, SIFT-MS. INSTITUTE OF PHYSICS PUBLISHING, 2006. *Physiol. Meas.* (27 (2006)): p. 321–337.
  28. Tianshu, T.W., Andriy, A.P., Kseniya, K.D., Patrik, P.S., David, D.S., Analysis of breath, exhaled via the mouth and nose, and the air in the oral cavity. *J Breath Res*, 2008. 2(3): p. 037013-037013.
  29. Smith, D., Wang, T., Pysanenko, A., Spanel, P., A selected ion flow tube mass spectrometry study of ammonia in mouth- and nose-exhaled breath and in the oral cavity. *Rapid Communications in Mass Spectrometry*, 2008. 22(6): p. 783-789.
  30. Barsotti, R.J., Measurement of ammonia in blood. *The Journal of Pediatrics*, 2001. 138(1, Supplement): p. S11-S20.
  31. Narasimhan, L.R., W. Goodman, and C.K.N. Patel, Correlation of breath ammonia with blood urea nitrogen and creatinine during hemodialysis. *Proceedings of the National Academy of Sciences*, 2001. 98(8): p. 4617-4621.
  32. Kearney Dj Fau - Hubbard, T., D. Hubbard T Fau - Putnam, and P. D, - Breath ammonia measurement in *Helicobacter pylori* infection. *Dig Dis Sci*, 2002. 47(11): p. 2523-30.
  33. Diskin Am Fau - Spanel, P., D. Spanel P Fau - Smith, and S. D, - Increase of acetone and ammonia in urine headspace and breath during ovulation quantified using selected ion flow tube mass spectrometry. *Physiol Meas*, 2003. 24(1): p. 191-9.
  34. Miekisch W Fau - Schubert, J.K., G.F.E. Schubert Jk Fau - Noeldge-Schomburg, and N.-S. GF, - Diagnostic potential of
-

- breath analysis--focus on volatile organic compounds. *Clin Chim Acta*, 2004. 347(1-2): p. 25-39.
35. Turner, C., P. Španěl, and D. Smith, A longitudinal study of ammonia, acetone and propanol in the exhaled breath of 30 subjects using selected ion flow tube mass spectrometry, SIFT-MS. *Physiological Measurement*, 2006. 27(4): p. 321-337.
  36. Taboulet P Fau - Haas, L., et al., - Urinary acetoacetate or capillary beta-hydroxybutyrate for the diagnosis of ketoacidosis in the Emergency Department setting. *Eur J Emerg Med*, 2004. 11(5): p. 251-8.
  37. Manolis, A., The diagnostic potential of breath analysis. *Clin Chem.*, 1983. 29(1): p. 5-15.
  38. Kalapos, M.P., On the mammalian acetone metabolism: from chemistry to clinical implications. *Biochimica et Biophysica Acta (BBA) - General Subjects*, 2003. 1621(2): p. 122-139.
  39. Ueta I Fau - Saito, Y., et al., - Breath acetone analysis with miniaturized sample preparation device: in-needle preconcentration and subsequent determination by gas chromatography-mass spectroscopy. *J Chromatogr B Analyt Technol Biomed Life Sci*, 2009. 877(24): p. 2551-6.
  40. Van den Velde, S., Nevens, F., Van hee, P., van Steenberghe, D., Quirynen, M., GC-MS analysis of breath odor compounds in liver patients. *Journal of Chromatography B*, 2008. 875(2): p. 344-348.
  41. Solga, S.F., Alkhuraishe, A., Cope, K., Tabesh, A., Clark, J.M., Torbenson, M., Schwartz, P., Magnuson, T., Diehl, A.M., Risby, T.H., Breath biomarkers and non-alcoholic fatty liver disease: Preliminary observations. *Biomarkers*, 2006. 11(2): p. 174-183.
  42. Kupari, M., Lommi, J., Ventila, M., Karjalainen, U., Breath acetone in congestive heart failure. *The American journal of cardiology*, 1995. 76(14): p. 1076-1078.
  43. Pysanenko, A., Wang, T., Spanel, P., Smith, D., Acetone, butanone, pentanone, hexaneone and heptanone in the headspace of aqueous solution and urine studied by selected ion flow tube mass spectrometry. *Rapid Communications in Mass Spectrometry*, 2009. 23(8): p. 1097-1104.
  44. Wang, G.M., Graziano;Perbellini, Luigi;Raineri, Emanuele;Brugnone, Francesco, Blood acetone concentration in "normal people" and in exposed workers 16 h after the end of the workshift. *International Archives*

- of Occupational and Environmental Health, 1994. 65(5): p. 285-289.
45. Garrido-Delgado, R., Arce, L., Perez-Marin, C.C., Valcarcel, M., Use of ion mobility spectroscopy with an ultraviolet ionization source as a vanguard screening system for the detection and determination of acetone in urine as a biomarker for cow and human diseases. *Talanta*, 2009. 78(3): p. 863-868.
  46. Li, N., Deng, C., Yao, N., Shen, X., Zhang, X., Determination of acetone, hexanal and heptanal in blood samples by derivatization with pentafluorobenzyl hydroxylamine followed by headspace single-drop microextraction and gas chromatography–mass spectrometry. *Analytica Chimica Acta*, 2005. 540(2): p. 317-323.
  47. Wang G Fau - Maranelli, G., et al., - Blood acetone concentration in "normal people" and in exposed workers 16 h after the end of the workshift. *Int Arch Occup Environ Health*, 1994. 65(5): p. 285-9.
  48. Dannecker Jr, J.R., E.G. Shaskan, and M. Phillips, A new highly sensitive assay for breath acetaldehyde: Detection of endogenous levels in humans. *Analytical Biochemistry*, 1981. 114(1): p. 1-7.
  49. Swift, R., Direct measurement of alcohol and its metabolites. *Addiction*, 2003. 98: p. 73-80.
  50. Deng, C., N. Li, and X. Zhang, Development of headspace solid-phase microextraction with on-fiber derivatization for determination of hexanal and heptanal in human blood. *Journal of Chromatography B*, 2004. 813(1–2): p. 47-52.
  51. Smith, D., et al., Quantification of acetaldehyde released by lung cancer cells in vitro using selected ion flow tube mass spectrometry. *Rapid Communications in Mass Spectrometry*, 2003. 17(8): p. 845-850.
  52. Halliwell, B., Free radicals, antioxidants, and human disease: curiosity, cause, or consequence? *The Lancet*, 1994. 344(8924): p. 721-724.
  53. Yazdanpanah, M., Luo, X., Lau, R., Greenberg, M., Fisher, L.J., Lehotay, D.C., Cytotoxic Aldehydes as Possible Markers for Childhood Cancer. *Free Radical Biology and Medicine*, 1997. 23(6): p. 870-878.
  54. Kato, S., et al., Chemical Ionization Mass Spectrometric Determination of Acrolein in Human Breast Cancer Cells. *Analytical Biochemistry*, 2002. 305(2): p. 251-259.

55. Kato, S., et al., Formaldehyde in human cancer cells: Detection by preconcentration-chemical ionization mass spectrometry. *Analytical Chemistry*, 2001. 73(13): p. 2992-2997.
56. Talhout, R., A. Opperhuizen, and J.G.C. van Amsterdam, Role of acetaldehyde in tobacco smoke addiction. *European Neuropsychopharmacology*, 2007. 17(10): p. 627-636.
57. Buszewski, B., Keszy, M., Ligor, T., Amann, A., Human exhaled air analytics: biomarkers of diseases. *Biomedical Chromatography*, 2007. 21(6): p. 553-566.
58. Prazeller, P., Karl, T., Jordan, A., Holzinger, R., Hansel, A., Lindinger, W., Quantification of passive smoking using proton-transfer-reaction mass spectrometry. *International Journal of Mass Spectrometry*, 1998. 178(3): p. L1-L4.
59. Abbott, S.M., Elder, J.B., Spanel, P., Smit, D., Quantification of acetonitrile in exhaled breath and urinary headspace using selected ion flow tube mass spectrometry. *International Journal of Mass Spectrometry*, 2003. 228(2-3): p. 655-665.
60. Zhang, A.Q., S.C. Mitchell, and R.L. Smith, Dimethylamine in human urine. *Clinica Chimica Acta*, 1995. 233(1-2): p. 81-88.
61. A. Q. Zhang, S.C.M., R. Ayesha and R. L. Smith, Determination of trimethylamine and related aliphatic amines in human urine by headspace gas chromatography. *Journal of Chromatography* 1992. 584: p. 141-145.
62. Wahl, H.G., Hoffmann, A., Luft, D., Liebich, H.M., Analysis of volatile organic compounds in human urine by headspace gas chromatography-mass spectrometry with a multipurpose sampler. *Journal of Chromatography A*, 1999. 847(1-2): p. 117-125.
63. Al-Waiz M Fau - Ayesha, R., et al., - A genetic polymorphism of the N-oxidation of trimethylamine in humans. *Clin Pharmacol Ther*, 1987. 42(5): p. 588-94.
64. Kuráň, P. and L. Soják, Environmental analysis of volatile organic compounds in water and sediment by gas chromatography. *Journal of Chromatography A*, 1996. 733(1-2): p. 119-141.
65. Krämer Alkalde, T., et al., Quantitative analysis of benzene, toluene, and xylenes in urine by means of headspace solid-phase microextraction. *Journal of Chromatography A*, 2004. 1027(1-2): p. 37-40.

66. ENDOGENOUS ALCOHOL. *Nutrition Reviews*, 1963. 21(11): p. 324-326.
67. Phillips, M., J. Greenberg, and V. Martinez, Endogenous breath ethanol concentrations in abstinent alcohol abusers and normals. *Alcohol*, 1988. 5(3): p. 263-265.
68. Corrêa, C.L. and R.C. Pedroso, Headspace gas chromatography with capillary column for urine alcohol determination. *Journal of Chromatography B: Biomedical Sciences and Applications*, 1997. 704(1–2): p. 365-368.
69. Liebich, H.M., H.J. Buelow, and R. Kallmayer, Quantification of endogenous aliphatic alcohols in serum and urine. *Journal of Chromatography A*, 1982. 239(0): p. 343-349.
70. Alwis, K.U., et al., Simultaneous analysis of 28 urinary VOC metabolites using ultra high performance liquid chromatography coupled with electrospray ionization tandem mass spectrometry (UPLC-ESI/MSMS). *Analytica Chimica Acta*, (0).

## **CHAPTER 7: DETECTION AND ANALYSIS OF SEMI- VOLATILE COMPOUNDS FROM WATER BY HIS-PTR-TOF-MS**

---

### **7.1 INTRODUCTION**

Proton transfer reaction mass spectrometry (PTR-MS) is a well-established technique for the measurement of trace volatile organic compounds (VOCs) in gases [1, 2] and has many applications [3-7]. No publications are found that have attempted an analysis of the semi volatile compounds. In the current study, an attempt is made on a proof-of-principle basis for the analysis of semi- volatile compounds. Different compounds were considered for the experiments were generic medicines for example paracetamol, ibuprofen and aspirin and pesticides. No ideal compound for the analysis was found from the generic medicine thus semi-volatile pesticides compounds were selected for the study.

A pesticide is generally a chemical or biological agent that through its effect deters, incapacitates, kills or discourages pests [8]. Target pests can include insects, plant pathogens, weeds, molluscs, birds, mammals and microbes that destroy property, cause nuisance, and spread disease. Pesticides are categorised into four main types: herbicides, fungicides, insecticides and bactericides [9, 10]. Many pesticides can also be grouped into chemical families. Prominent insecticide families include organochlorines, organophosphates, and carbamates. Organochlorine pesticides toxicity varies from pesticide to pesticide but their use is being slowly phased out due to their persistence and potential to bio-accumulate. Organophosphates

and carbamates have largely replaced organochlorines in pesticide industry.

This chapter focuses on organophosphates pesticides, which are extensively used for agricultural purposes. There are some 200 different organophosphates pesticides available in the marketplace. Unfortunately, organophosphates pesticides have been found in ground waters, surface waters and drinking waters in varying concentration, and therefore there is an increasing environmental concern about the quantities of these compounds [11] and the effect this could have on human health [9].

Existing methods for analysing organophosphates in water are dominated by chromatographic techniques. Prior to the instrumental analysis of environmental samples, extensive sample extraction and pre-concentration is often required. The most difficult and time-consuming step is extraction of the target analyte from the matrix [12]. Several methods have been developed to accomplish this often difficult task, including liquid-liquid extraction (LLE) [13], solid-phase extraction, supercritical fluid extraction (SFE) [14] and solid-phase micro-extraction (SPME) [15] with the use of GC-MS, GC-MS/MS [16, 17], LC-MS or LC-MS/MS [18] for identification and detection. All of these procedures are inherently time-consuming and tedious. The solid phase extraction (SPE) and SPME approaches have increased in popularity as an alternative to LLE as they avoid a few of the disadvantages of the LLE procedure, particularly the large use of solvent. Both SPE and SPME produce a clean mass spectrum by removing the unwanted matrix related compounds. However, the price of consumables, like the SPE cartridge or SPME fibre, is quite high and the extraction process can be time-consuming.

Pareja *et al.* [19] and Diaz *et al.* [20] developed the direct injection techniques to detect and analyse different pesticides from water samples. Pareja *et al.* have directly injected paddy field water sample into a liquid chromatography-quadrupole-linear ion trap-mass spectrometer (QpLIT). The list of target analytes in their experiments included organophosphates, phenylureas, sulfonylureas, carbamates, conazoles, imidazolinones as well as compounds widely used in different rice-growing countries. Diaz *et al.* has injected samples into the liquid chromatography system and employed a reversed phase separation. Detection was done by electrospray ionisation MS/MS [20].

As discussed earlier in the section, for the analysis of pesticides by using routine method, it requires a complicated instrumental setup, extensive and expensive extraction method and it takes long time for analysis. Direct injection technique developed by Pareja *et al.* and Diaz *et al.* requires the extensive chromatographic separation and a long analysis time. In addition, the detection techniques used in the published method is limited to the fix mass-channel for a particular pesticides thus it requires the harsh ionisation *i.e.* breaking up the parent molecule in the detector to detect the daughter ion. PTR-MS, on the other hand provides the softer ionisation thus parent molecules is not fragmented and Time-of-Flight mass spectrometer allow for the full scan analysis.

In this chapter, a trial study is reported on the use of PTR-MS for the quick detection and determination of pesticides from water. For the detection and determination of pesticides in water, the heated inlet source (HIS) described in Chapter 3 was employed for the introduction of water samples into the PTR-MS instrument. Two sample preparation techniques were used: the

first used direct sample injection and the second technique was liquid-liquid extraction method. The simple liquid-liquid extraction technique is employed to achieve the higher sensitivity of the pesticides. For the first technique, water samples were injected directly into the mass spectrometer while in the second technique, pesticides were extracted from the water samples by the use of a hexane/toluene mixture and a portion of the solvent mixture was injected for the analysis.

## **7.2 EXPERIMENTAL**

### **7.2.1 Instrumental set-up**

Experiments for the pesticide analysis were performed using the Leicester PTR-ToF-MS instrument, which was described in Chapter 2. A heated inlet source (HIS) was used as an add-on to the instrument for liquid sample injection. The HIS source was described in detail in Chapter 3.

Typical drift tube conditions were as follows: pressure 1.5 mbar and drift tube temperature 40°C.

At least 10 blank injections were made at the start and end of the experiments for background measurement to assess the contamination prior to and after the experiments. For the direct injection and liquid-liquid extraction, 10 -50 µL of sample was injected by using a gas tight Hamilton syringe. This liquid sample was injected into the HIS source which was set at ca. 100°C. The scan time for each experiment was 10 minutes.

### **7.2.2 Sample Preparation**

#### **7.2.2.1 Reference material and reagent**

Nine organophosphates pesticides were selected for the experiments. One of the selection criteria for the pesticides was their wider use in the UK and the rest of the world [10, 22].

Other practical selection criteria were their physical properties, and most attention was given to the physical state of the pesticides, *i.e.* solid or liquid, vapour pressure and molecular weight. As expected, the pesticides in the liquid form had a higher vapour pressure when compare to the pesticides in powder form, as seen in Table 7.1. The decrease in vapour pressure due to presence of non-volatile solute in a solution does not depend on the nature of solute but on the quantity of solute. Therefore, vapour pressure is the pressure exerted by a vapour in thermodynamic equilibrium with its condensed phases (solid or liquid) at a given temperature in a closed system. The equilibrium vapour pressure is an indication of a liquid's evaporation rate. It relates to the tendency of particles to escape from the liquid (or a solid). Thus, it implies that for a compound with a higher vapour pressure, higher sensitivity can be achieved in PTR-MS, as more compounds will be available for the proton transfer reaction.

Pesticides used in the study were purchased from the Sigma Aldrich UK. They were of analytical grade and their purity was >99% in every case.

Table 7.1 Physical property of the pesticides

Pesticides	Relative molecular mass	Formula	Appearance	Vapour pressure at 25°C (mPa)
Parathion	291.3	C <sub>10</sub> H <sub>14</sub> NO <sub>5</sub> PS	Pale yellow liquid	5.00
Methyl parathion	263.2	C <sub>8</sub> H <sub>10</sub> NO <sub>5</sub> PS	Light to tan dark liquid	0.20
Pirimiphos-methyl	305.3	C <sub>11</sub> H <sub>20</sub> N <sub>3</sub> O <sub>3</sub> PS	Straw-coloured liquid	2.00 x 10 <sup>-3</sup>
Phorate	260.4	C <sub>7</sub> H <sub>17</sub> O <sub>2</sub> PS <sub>3</sub>	Pale yellow liquid	85.00
Diazinon	304.4	C <sub>12</sub> H <sub>21</sub> N <sub>2</sub> O <sub>3</sub> PS	Colourless liquid	11.97
Fenthion	278.3	C <sub>10</sub> H <sub>15</sub> O <sub>3</sub> PS <sub>2</sub>	Colourless, almost odourless liquid; 95-98% pure fenthion is a brown oily liquid with a weak garlic odour	0.37

## Chapter 7

Pesticides	Relative molecular mass	Formula	Appearance	Vapour pressure at 25°C (mPa)
Triazophos	313.3	C <sub>12</sub> H <sub>16</sub> N <sub>3</sub> O <sub>3</sub> PS	Yellowish liquid	1.33
Atrazine	215.7	C <sub>8</sub> H <sub>14</sub> ClN <sub>5</sub>	Crystalline powder	0.039
Ethion	385.0	C <sub>9</sub> H <sub>22</sub> O <sub>4</sub> P <sub>2</sub> S <sub>4</sub>	Colourless to amber liquid	0.20

Vapour pressure information was gathered from University of Hertfordshire PPDB database [21]

Stock and working solutions were prepared by accurately weighing the required amount of pesticides reference standard in a screw top glass vial and the adding required volume to hexane or acetone to get 10.0 µg/ml of stock. The stock solution was used for compound identification and was subsequently used to prepare the working solution for calibration plots.

Other reagents used during the course of the experiments were de-ionised water (in-house, University of Leicester), hexane and toluene (Fisher, UK) and sodium chloride (Sigma Aldrich, UK).

### 7.2.2.2 Liquid-liquid extraction and direct water injection.

Direct sample injection was performed as an attempt to rapidly quantify pesticide levels in water. In the techniques, no pre-treatment was applied to the sample, *i.e.* no sample clean up to remove impurities by using different extraction techniques such as LLE, SPE or SPE, or pre-concentration for the compound of interest was employed.

The second technique employed liquid-liquid extraction. For this technique, 1 ml of water was spiked with 10 µL of working solution and 1 g of salt was added. This mixture was agitated for at-least two minutes and then 400 µl of extraction solvent (hexane/toluene mixture) was added to the samples. The spiked water and solvent mixture was mixed for at least 8 – 10 minutes

at 30°C for optimum compound recovery [22] and a 10 – 50 µL aliquot from the organic layer was injected into the mass spectrometer for analysis.

### **7.3 RESULTS AND DISCUSSION**

The organophosphate pesticides selected for the experiments were extracted from the calibration samples prepared in water by using liquid-liquid extraction. For diazinone, methyl-parathion and parathion, calibration curves were constructed from four calibration standards with lower limit of quantification at 2.00 µg/mL. For fenthion and triazophos, calibration curves were constructed from five calibration standards with lower limit of quantification at 1.00 µg/mL. No formal quantification of the pesticides from the water samples has been performed during this chapter as it was out of scope for this chapter.

In the next section, the reasoning behind the choice of extraction solvent is given and its effect on the hydronium ion is discussed. In section 7.3.2 direct injection and liquid injection, techniques are discussed. The pesticides identification and limit of detection is discussed in section 7.3.3 and 7.3.4, respectively. From section 7.3.5 to 7.2.10, different pesticides selected for the experiment are discussed.

#### **7.3.1 Extraction solvent and effect of sample on Hydronium**

The main aim of the experiment was to quantify pesticides in water at the lowest possible detection levels. This was done by two different methods, as described in section 7.2.3. In both methods water or an organic solvent is injected to the HIS and both have an impact on the hydronium ion level.

The effect of direct injection of water samples and hexane into the HIS source has been discussed in Chapter 3, and thus it will

be not be discussed in detail in this chapter. However, this has an obvious effect of this is on the level of  $\text{H}_3\text{O}^+$  and its clusters with water molecules. Very briefly, after injecting 10  $\mu\text{l}$  of water, the hydronium signal initially drops and it takes about 10 seconds to return to a stable level. The time required for  $\text{H}_3\text{O}^+$  to become steady again depended on the HIS setup. It is discussed in Chapter 3 that when HIS was placed on rode, next to the drift tube with only 10 cm of expose Teflon tube, a steady signal of  $\text{H}_3\text{O}^+$  was observed within 10 seconds after the injection. When HIS was placed on the base plate of HIS with 100 cm of exposed Teflon tube, it required at-least 50 seconds to achieve stable  $\text{H}_3\text{O}^+$  signal. The quantity of sample injected also had an impact on the  $\text{H}_3\text{O}^+$ , and precision of the data. The quantity of sample injected also had an impact on the  $\text{H}_3\text{O}^+$ . In general, the higher the sample volume longer for the  $\text{H}_3\text{O}^+$  signal to return to its original level.

For liquid-liquid extraction, to achieve a good extraction recovery from the aqueous analyte sample it was important to choose a solvent that is not miscible with water and offers a good solubility for the pesticides. It is also very important that the choice of solvent does not affect data interpretation *i.e.* by producing strong interfering peaks in the mass spectrum and/or by forming the adduct with the ions from the pesticides.

Ethanol, methanol and other alcoholic reagents were not considered due to their miscibility with water and the poor solubility of pesticides in these solvents. Most of the pesticides are soluble in acetone, but due to its miscibility with water, it was not considered for the experiments. Ethyl acetate and dichloromethane offer good solubility for the pesticides but they are partially miscible with water and they can complicate the mass spectrum by forming multiple fragment ions on

protonation. Hexane and toluene were the preferred solvents in the current work. As well as not being miscible with water and showing good solubility for most pesticides, hexane possesses a lower proton affinity than water and therefore does not contribute to the mass spectrum. Toluene is slightly less favourable in that it has a higher proton affinity than water but it shows no fragmentation in its mass spectrum on proton transfer, nor does it produce any adducts with pesticide ions.

To achieve good extraction recovery toluene was also used with hexane. Jia *et al.* [23] employed the vortex-assisted liquid-liquid micro-extraction to extract pesticides from an aqueous solution. In their work, they compared the extraction capability of toluene, *n*-hexane and cyclohexane and reported that toluene has a higher extraction capability than *n*-hexane and cyclohexane. So, to improve the extraction efficiency and avoid some of the disadvantage of solvent protonation (in case of toluene), it was decided to use a mixture of hexane and toluene with the toluene percentage at a lower level. For every five fold of hexane, one fold of toluene (5/1, v/v) was used for the mixture. This has provided an ideal mixture as pesticides were soluble in this mixture and protonated toluene mass spectrum was not dominating the mass spectra.

To determine the effect of solvent on the  $\text{H}_3\text{O}^+$  abundance, 10.0  $\mu\text{L}$  of hexane/toluene (5/1, v/v) was injected into the HIS source and data were collected for 600 s. PTR-MS data obtained from this experiment are presented in Figure 7.1.

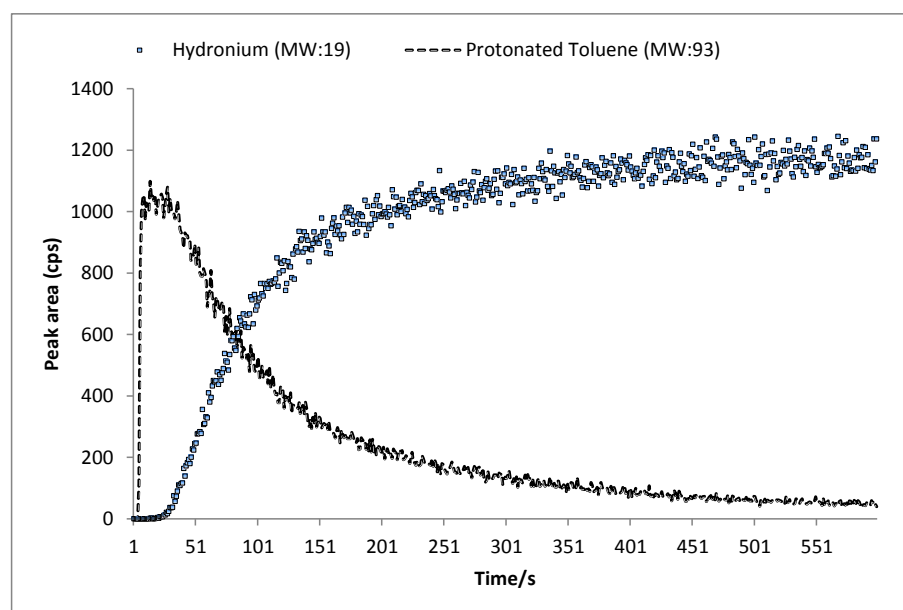


Figure 7.1 Response of the PTR-ToF-MS instrument when 10.0  $\mu\text{L}$  of hexane/toluene (5/1, v/v) was injected.

When sample was injected, the  $\text{H}_3\text{O}^+$  signal dropped almost to zero and it took about 20 s before the hydronium ion signal started to increase again. After about 200 s the  $\text{H}_3\text{O}^+$  signal stabilised. Turning now to the protonated toluene, as soon as the mixture was injected a strong signal for protonated toluene was observed and this dropped off slowly with time. This implies that, at any given time, protonation of pesticides can be done with either protonated toluene or by  $\text{H}_3\text{O}^+$ . The mechanism of protonation by two different ions is discussed in Chapter 8 (two-stage technique). If the proton affinity of the analyte of interest is higher than water or toluene, proton transfer will happen.

The pesticides are a complex compounds with different ionisable group attached to the main structure. These groups are responsible for either donating or accepting the proton during the proton transfer reaction. The proton affinity the different ionisable groups presented in the Table 2 is greater than the one for water and toluene and because of that, protonation of the pesticides at a given time can be done by

## Chapter 7

---

either protonated toluene or hydronium ion. The proton affinity for the different ionisable groups is presented in Table 2 for the reference purposes.

Table 7.2 Proton affinity of neutral molecules and anions

Base	Proton affinity
	(kJ/mol)
Neutral molecules	
Water	697
Toluene	784
Ionisable groups	
Trioxophosphate(1-)	1301
Iodide	1315
Pentacarbonylmanganate(1-)	1326
Trifluoroacetate	1350
Bromide	1354
Nitrate	1358
Pentacarbonylrhenate(1-)	1389
Chloride	1395
Nitrite	1415
Hydroselenide	1417
Formate	1444
Acetate	1458
Phenoxide	1470
Cyanide	1477
Hydrosulfide	1477
Cyclopentadienide	1490
Ethanethiolate	1495
Nitromethanide	1501
Arsinide	1502
Methanethiolate	1502
Germanide	1509
Trichloromethanide	1515
Formylmethanide	1533
Methylsulfonylmethanide	1534
Anilide	1536

---

Base	Proton affinity
	(kJ/mol)
Acetonide	1543
Phosphinide	1550
Silanide	1554
Fluoride	1554
Cyanomethanide	1557
Propoxide	1568
Acetylide	1571
Trifluoromethanide	1572
Ethoxide	1574
Phenylmethanide	1586
Methoxide	1587
Hydroxide	1635
Amide	1672
Hydride	1675
Methanide	1743

Taken from Jolly, WL [24]

### 7.3.2 Direct injection vs. Liquid-liquid extraction

Calibration standards for the comparison of the direct injection and liquid-liquid extraction technique were prepared as per section 2.1.

For the direct injection technique pesticides were detected at the desired concentration of 1.0 µg/ml and the highest level where pesticides were detected was at 20.0 µg/ml. For the liquid-liquid extraction technique, fenitrothion and triazophos were detected at 1.0 µg/ml, parathion, methylparathion and diazinon were detected at 2.0 µg/ml and phorate was detected at 10.0 µg/ml.

The direct injection technique is quicker than the liquid-liquid extraction approach but it suffers from poor sensitivity. When using rapid resolution liquid chromatography-electrospray tandem mass spectrometry Diaz *et al.* [20] reported a limit of

detection of 15.0 ng/l for 31 pesticides in water by injecting 100  $\mu\text{l}$  of sample, which compares with 20.0  $\mu\text{g}/\text{ml}$  from the liquid injection approach described here. The far better sensitivity achieved by Diaz *et al.* derives from the high sample volumes and chromatographic separation that could be used with their technique.

For liquid-liquid extraction, the lowest level at which pesticides were detected was at 1.00  $\mu\text{g}/\text{ml}$ . Maximum residue limit (MRL) *i.e.* maximum limit of pesticides is allowed in the food item available in UK, which was set by Health and Safety Executive (HSE) is in range of 0.1 to 5.00 mg/kg [25]. Even-though liquid-liquid extraction method requires sample pre-treatment, thus taking longer for analysis compared to direct injection and real time analysis is not possible, this technique is reasonably sensitive and cleaner than direct injection and the desired limit of quantification for multitude of different pesticides can be achieved.

### 7.3.3 Pesticides identification by PTR-MS

Mass spectra of the pesticides used in the experiments shown here are derived from standard solutions of each compound prepared at 10.0  $\mu\text{g}/\text{ml}$  in hexane. A small portion of the solution (10  $\mu\text{l}$ ) was injected into the HIS source to obtain the PTR-MS mass spectra. All the compounds were obtained as analytical reference standards and were specified as >99% pure and thus impurities should be negligible. Data obtained from the compound identification experiments are presented in Figure 7.2.

The pesticides compounds parathion, methyl parathion, fenthion, trizophos, Diazinon and primiphos-methyl produced a

protonated ion during a proton transfer reaction with hydronium.

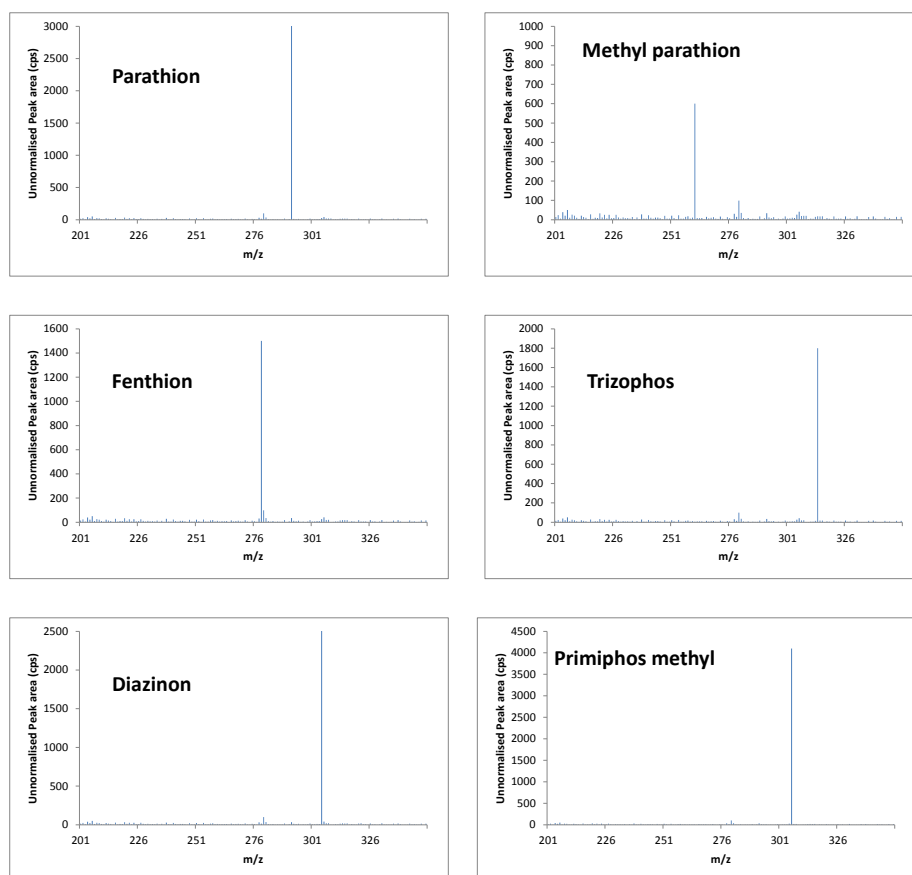


Figure 7.2 Compound identification data generated by injecting the reference standard solution prepared in hexane into HIS

As seen in Figure 7.2, all the pesticide samples used in the experiments were successfully identified by PTR-MS. A sensitive mass spectrum was observed at  $[M+H]^+$  for all the pesticides. After comparing the observed mass spectrum with the known fragment ion observed during the electron impact analysis in the NIST database, it was noted that no major fragmentation was observed with the PTR-MS mass spectrum. Prior to injecting the actual samples, blank sample *i.e.* pesticides free water and volatile solvent (hexane and toluene in this work) were injected to confirm that both sample/solvent and instrument is

contamination free at the relevant  $m/z$  for the different pesticides used in this work. The calibration samples prepared by adding the known amount of pesticides in the water prior to the extraction, the mass spectrum observed at relevant  $m/z$  was believed for the pesticide of the spiked compound.

### 7.3.4 Limit of Detection of Pesticides by PTR-MS

In this experiment, relatively low sensitivity was observed for methyl parathion when compared to parathion, pirimiphos methyl, diazinon, fenthion and trizophos. The possible reason for the observed low sensitivity for methyl parathion could be due to the low vapour pressure. Out of all the selected pesticides in the study, methyl parathion has the lowest vapour pressure. In spite of having a lower vapour pressure, acceptable sensitivity was observed for pirimiphos methyl. Therefore, low vapour pressure cannot be the only reason for low sensitivity. A second possible reason could be the higher fragmentation of the methyl parathion. After observing the fragmentation pattern of methyl parathion under electron impact ionisation showed that methyl parathion also produces the two considerable fragment ions at  $m/z$  110 and  $m/z$  126 and small sensitivity mass spectrum also observed at same  $m/z$  in the current experiments. The third possible explanation for low sensitivity could be due to preparation error, as same stock solution was used for the experiment.

The Limit of Detection (LoD) and limit of quantification (LoQ) for the different compound was also determined for different pesticides used in this study. The LoD is the lowest amount of the investigated compound in a sample that can be detected but not necessarily quantified. The limit of detection can be calculate by [26],

1). Signal-to-noise ratio method: Signal-to-noise ratio method is usually used for the calculation of LoD in separation and spectrometric method. The minimum signal/noise ratio of  $\geq 3$  is used in all the different experiments documented in this thesis.

2). Based on the calculation using the standard deviation of the response and the slope method: By using this method, the LoD can be calculated by using following equation,

$$C_{\text{LoD}} = \frac{3s}{m} \quad (2)$$

Where  $s$  is the standard deviation and  $m$  is the slope of related calibration line.

The achieved limit of quantification for each pesticide used in this study is discussed in section 7.3.5 to 7.3.10.

The calculated LOD from the experiments performed in this thesis and literature LOD is presented in Table 7.3.

Table 7.3 Limit of detection

Name	Calculated LOD ( $\mu\text{g/mL}$ )	Literature LOD ( $\mu\text{g/mL}$ )*
Pirimiphos-methyl	0.0479	0.004 [18]
Parathion	0.00131	0.004 [20]
Methyl-parathion	0.00302	0.000015 [28]
Diazinon	0.0318	0.000015 [28]
Fenitrothion	0.0278	0.0004 [22]
Triazophos	1.36	0.000001 [19]

In the publications, high amount of sample, in millilitres and extensive extraction procedures and chromatographic separation was used to achieve the low LoD compare to the sample in microliters with simple liquid-liquid extraction technique used in this study. One approach to achieve the low LoD for this work would be to use more samples, but as discussed in Chapter 3 of this thesis, with the higher injection

volume, HIS source is not capable to produce linear regression. The capillary inlet source (CIS) discussed in the Chapter 4 of this thesis is capable of handling more sample volume, thus there is a greater chance to achieve the low LoD.

### 7.3.5 Parathion and Methyl parathion

Parathion is a potent insecticide. Originally developed by IG Farben in the 1940s. It is highly toxic to non-target organisms, including humans. Its use is banned or restricted in many countries. When pure, parathion is a white crystalline solid; however, it is commonly distributed as a brown liquid that smells of rotting eggs or garlic. Parathion is stable, although it darkens when exposed to sunlight.

People can be exposed to parathion and methyl parathion primarily during a spray on the plant, inhalation while using and ingesting food containing parathion residue. Acute exposure may results in nausea, vomiting, abdominal cramps, diarrhoea, excessive salivation, headache, weakness, blurring, paralysis, coma and respiratory failure [27].

The structures of parathion and methyl parathion are shown in Figure 7.3.

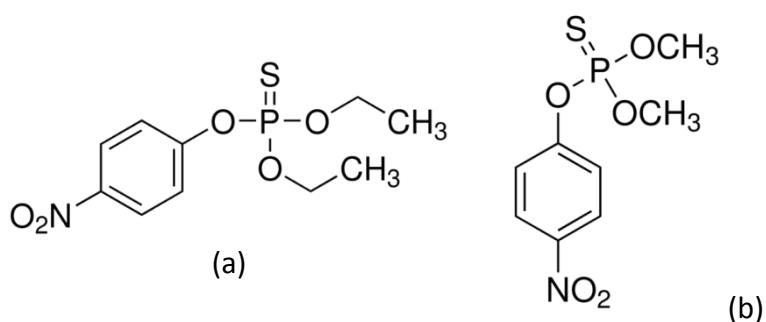


Figure 7.3 Chemical structure of (a) parathion and (b) methyl parathion

Initially, the direct injection technique was applied by injecting 20.0  $\mu\text{l}$  of calibration standard to the HIS source. When dilute solutions of up to 5.0  $\mu\text{g}/\text{ml}$  were used no compound could be detected in the mass spectrum for either parathion or methyl parathion. The threshold for quantification was 10.0  $\mu\text{g}/\text{ml}$ , which gave a signal-to-noise ratio of 3 for the protonated parent peak.

The liquid-liquid extraction technique also produced poor sensitivity for methyl parathion at 1.0, 2.0 and 5.0  $\mu\text{g}/\text{ml}$ , and thus calibration curve was not constructed. For parathion, with the liquid-liquid extraction technique poor sensitivity was observed at 1.0  $\mu\text{g}/\text{ml}$  (signal to noise: five to one) thus it was not included in the calibration curve. The calibration curve for parathion is shown in Figure 7.4.

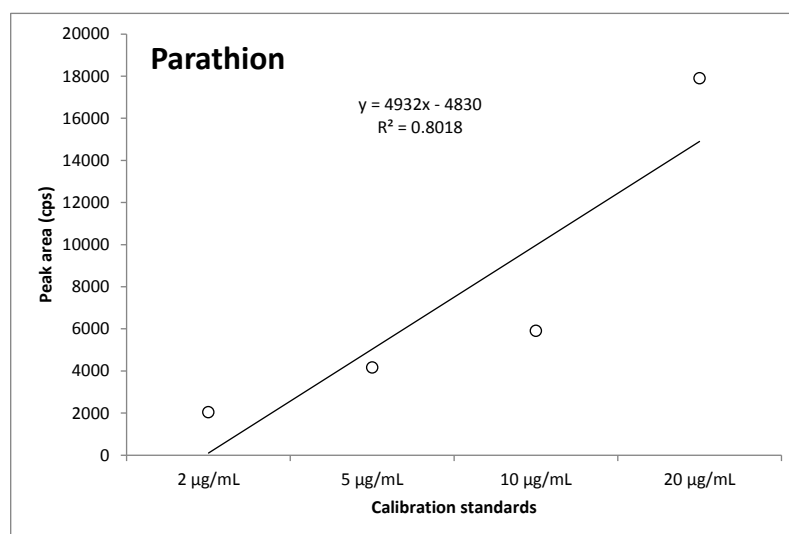


Figure 7.4 Calibration plot for parathion from the liquid-liquid extraction method

Even though the calibration curve appears to be non-linear, it was noted that the response for the 20.0  $\mu\text{g}/\text{ml}$  measurement was abnormally higher when compared to previous calibration points. This has caused the calibration curve to be non-linear. As

the calibration standards for the all the pesticides compounds used in these experiments were prepared in the same solution and linear responses were observed for the other compounds, the reason for the non-linear response here could not be due to the injection error. However, it could be due to the preparation error.

The Albanis *et al.* [28] used the solid phase extraction for the extraction and GC-MS for detection and they reported a linear response for parathion with the detection limit of 0.1 µg/l. The observed quantification limit of 2.0 µg/ml for parathion was not as low as the one reported by Albanis *et al.* One of the possible reasons could be the high sample volume used in [28] and also the solid phase extraction technique used in their work which produces the more cleaner extract thus allowing them to obtain sharper peak and less background noise to achieve low LoD.

### 7.3.6 Diazinon

Diazinon is a non-systemic insecticide used in agriculture to tackle and pests on a variety of fruits, vegetable, nut and field crops. Diazinon is a colourless to dark brown liquid and is a thiophosphoric acid ester developed in 1950 by Ciba-Geigy. Diazinon was one of the most widely used insecticides for household and agricultural pest control until it was outlawed in the U.S. in 2004 for household use.

Human's exposure to Diazinon is through absorption and, inhalation. Symptoms of acute diazinon exposure develop in minutes to hours following exposure. Initial symptoms include nausea, dizziness, salivation, headache, seating, lacrimation and rhinorrhoea. The symptoms can progress to vomiting, abdominal cramps, diarrhoea, muscle twitching, weakness and a lack of coordination [8]. Because diazinon is fat soluble, there is

potential for delayed toxicity if significant amounts of diazinon is stored in fatty tissue [29].

The chemical structure of Diazinon is shown in Figure 7.5.

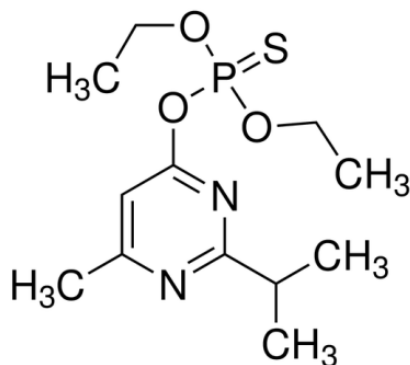


Figure 7.5 Chemical structure of Diazinon

Initially, the direct injection technique was applied in current work by injection of 20.0  $\mu$ l of calibration standard to the HIS source. The resulting mass spectrum was weak and for the protonated parent molecule peak a signal-to-noise of  $\geq 3$  was only observed at concentration  $> 10.0 \mu\text{g/ml}$ .

The liquid-liquid extraction method achieved a better sensitivity for diazinon. The calibration plot was drawn from 2.0  $\mu\text{g/ml}$  to 20.0  $\mu\text{g/ml}$  as poor sensitivity was observed at 1.0  $\mu\text{g/ml}$ . A calibration plot for diazinon at 2.00 to 20.0  $\mu\text{g/ml}$  is shown in Figure 7.6.

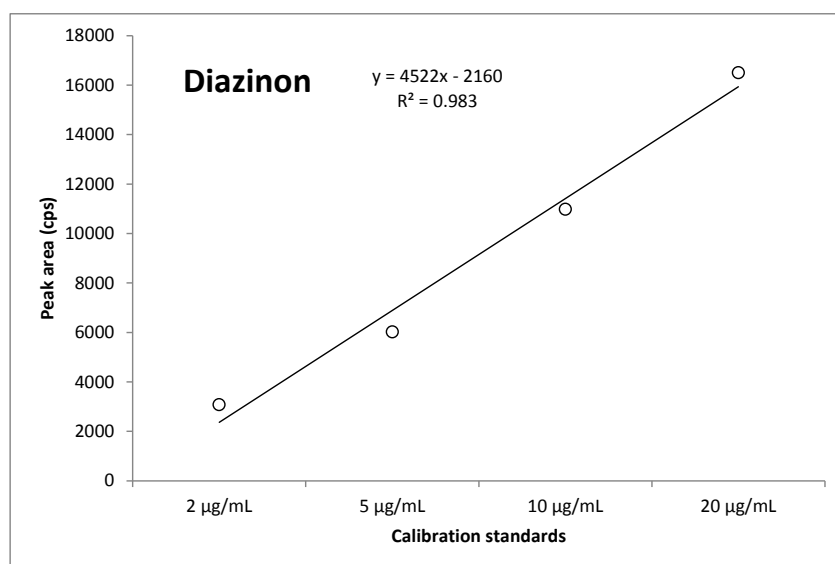


Figure 7.6 Calibration plot for diazinon from the liquid-liquid extraction method

A linear response was observed from 2.0 µg/ml to 20.0 µg/ml with the  $r^2$  value of 0.987 and limit of quantification is 2.0 µg/ml. Chen *et al.* [30] measured the diazinon from an aqueous sample by using dynamic hollow fibre-protected liquid-phase micro-extraction and GC-MS. They reported a linear response for the diazinon with the limit of quantification at 0.1 µg/ml and limit of detection of 0.006 µg/l based on a signal-to-noise ratio 3. The observed limit of quantification in the current study at 2.0 µg/ml is in agreement with [30].

### 7.3.7 Fenthion

Fenthion is an organothiophosphate insecticide also known as avicide or acaricide. Like most other organophosphates, its mode of action is via cholinesterase inhibition [31]. Fenthion is an oily liquid and is colourless with a mercaptan-like (slight garlic odour). The use of fenthion products is to control many sucking and biting pests in agricultural, commercial and domestic situations. It is use as a home veterinary treatment to control fleas on dogs, around commercial and industrial buildings, to

non-native birds and in domestic situations to control a number of insects [32]. Fenthion is listed as a moderately toxic compound in U.S. Environmental Protection Agency and World Health Organisation toxicity class [31].

Fenthion exposure to general population is quite limited based on its bioavailability. Common form of fenthion exposure is occupation related, and occurs through dermal contact or inhalation of dust and sprays [33]. Fenthion can cause cholinesterase inhibition in humans resulting in overstimulation of the nervous system and causing nausea, dizziness, and confusion. With very high exposure (*e.g.* accidents or major spills), respiratory paralysis and death can result.

The chemical structure of Diazinon is shown in Figure 7.7.

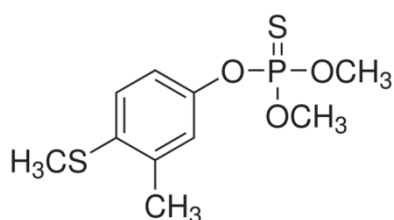


Figure 7.7 Chemical structure of fenthion

The direct injection technique showed acceptable detection sensitivity for the protonated parent molecule only at > 10.0 µg/ml. On the other hand, the liquid-liquid extraction technique produces acceptable sensitivity at 1.0 µg/ml and thus a calibration curve was constructed by using the usual five calibration points as shown in Figure 7.8.

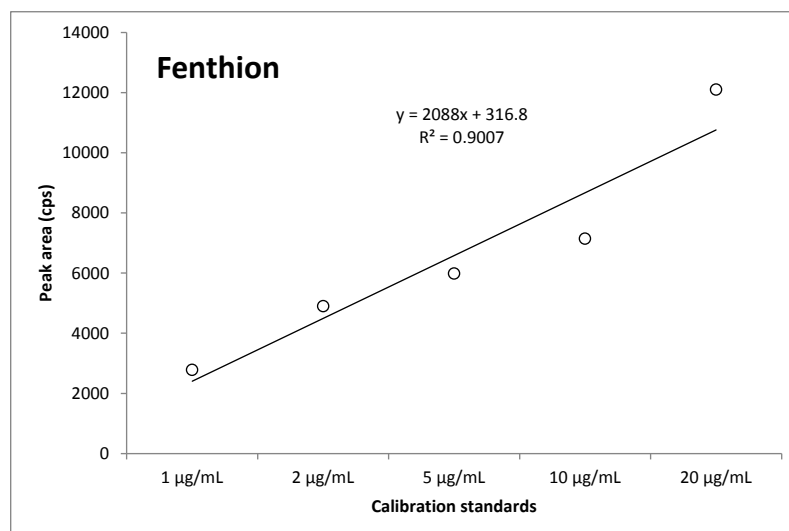


Figure 7.8 Calibration plot for fenthion from the liquid-liquid extraction method

A linear response was observed from 1.0 µg/ml to 20.0 µg/ml with the  $r^2$  value of 0.900 and a limit of quantification is 1.0 µg/ml. Chen *et al.* [30] measured the fenthion from the water sample by using dynamic hollow fibre-protected liquid-phase micro-extraction and GC-MS. They have reported the linear response for the fenthion with the limit of quantification of 0.5 µg/l and limit of detection at 0.042 µg/ml, based on a signal-to-noise ratio of three. The observed limit of quantification of 1.0 µg/ml is in agreement with [30].

### 7.3.8 Triazophos

Triazophos is an organophosphate pesticide effective against many insect pests on a wide range of crops. Triazophos is a cholinesterase inhibitor and acts on the central nervous system. In physical appearance, triazophos is a yellow liquid. Triazophos does not get broken down in the environment and does not bioaccumulate, unlike certain organochlorine insecticides *e.g.* DDT.

The structure of triazophos is shown in Figure 7.9.

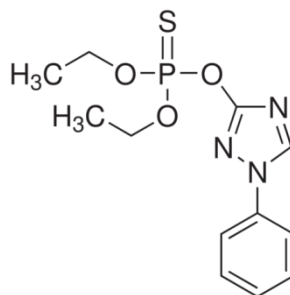


Figure 7.9 Chemical structure of Triazophos

The direct injection technique showed acceptable detection sensitivity for the protonate parent molecule only at > 10.0 µg/ml. On the other hand, the liquid-liquid extraction technique produces acceptable sensitivity at 1.0 µg/ml and thus a calibration curve was constructed by using the usual five calibration points as shown in Figure 7.10.

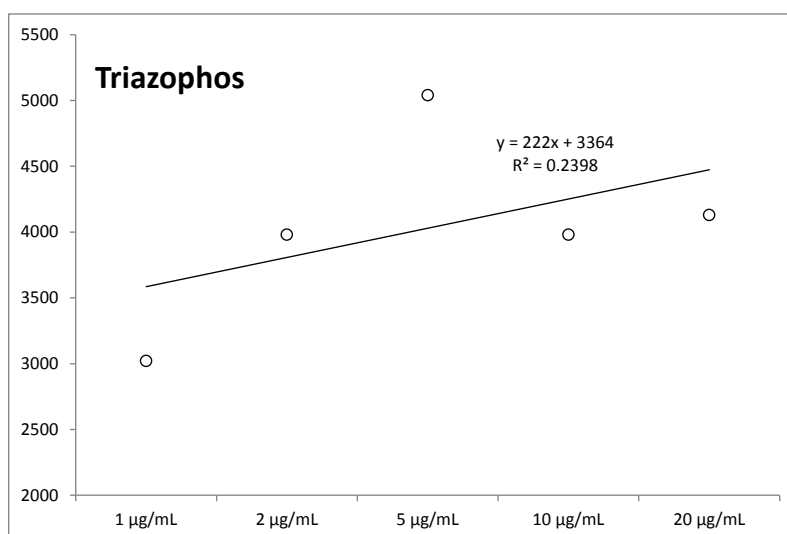


Figure 7.10 Calibration plot for triazophos from the liquid-liquid extraction method

It was observed from Figure 7.10 that a non-linear response was observed in the calibration plot for triazophos. After carefully observing the data, it was noted that a linear response was observed for the calibration standards at 1.0, 2.0 and 5.0 µg/ml

but the linearity was affected due to the low response for the calibration standards at 10.0 and 20.0 µg/ml. The possible cause for this could be the possible preparation error for calibration standard solution.

Fu *et al.* [34] used dispersive liquid-liquid micro-extraction with high performance liquid chromatography-fluorescence detection (HPLC-FLD) for the analysis of triazophos and carbaryl pesticides in water and fruit juice. They reported a linear curve with limit of quantification of 30 ng/ml. The observed limit of quantification of 1.0 µg/ml was not as low as reported in [34] but it was within limits set in [25]. In order to improve the LoD of the method Fu *et al.* [34] used dispersive liquid-liquid micro-extraction technique for the pre-concentration and HPLC for the chromatographic separation.

### 7.3.9 Pirimiphos-methyl

Pirimiphos-methyl is a broad-spectrum organophosphate insecticide, with both contact and fumigant action. In plants, it penetrates leaf tissue and exhibits translaminar action but is of short persistence. When applied to stored agricultural commodities such as grain and nuts, it provides longer-lasting pest control. Primiphos-methyl is used for controlling a wide range of chewing, sucking and boring insects and mites in warehouses, stored gain and domestic and industrial premises.

The structure of pirimiphos-methyl is shown in Figure 7.11.

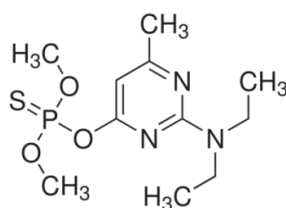


Figure 7.11 Chemical structure of pirimiphos-methyl

The direct injection technique showed acceptable sensitivity was observed at 20.0  $\mu\text{g}/\text{mL}$ . The liquid-liquid extraction technique produces acceptable sensitivity at 2.0  $\mu\text{g}/\text{ml}$ , thus calibration curve was plotted by using four calibration points. A calibration plot for primiphos-methyl at 2.0 to 20.0  $\mu\text{g}/\text{ml}$  is shown in Figure 7.12.

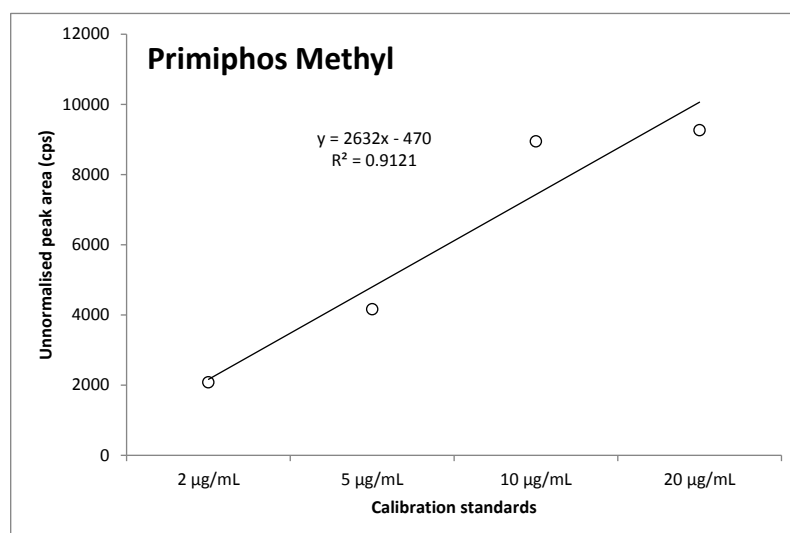


Figure 7.12 Calibration plot for primiphos-methyl from the liquid-liquid extraction method

A linear response was observed from 2.0  $\mu\text{g}/\text{ml}$  to 20.0  $\mu\text{g}/\text{ml}$  with the  $r^2$  value of 0.912 and limit of quantification is 2.0  $\mu\text{g}/\text{ml}$ . Patsias *et al.* [35] developed a multi-residue method to analyse 96 target pesticide compounds by using a solid phase extraction (SPE) as an extraction technique and ion trap mass-spectrometer as a detection technique. They have reported a linear response for primiphos-methyl with limit of detection 0.01  $\mu\text{g}/\text{l}$ . The observed limit of quantification of 1.0  $\mu\text{g}/\text{ml}$  was not as low as reported in [35] but it was within limits set in [25]. In order to improve the LoD of the method, Patsias *et al.* [35] has employed a solid phase extraction (SPE) technique for the pre-concentration and chromatographic separation was used.

## 7.3.10 Phorate and Atrazine

Phorate, atrazine and simazine are organophosphorus pesticides. At normal conditions, phorate is a yellow liquid which is poorly soluble in water but readily soluble in solvents. It is very toxic for both target organisms and for also for mammals including humans. It inhibits acetylcholinesterase and pseudocholinesterase [36].

Atrazine is an organic compound of the triazine class. At normal conditions, atrazine is a colourless crystalline powder with low vapour pressure. They are widely used as herbicides. Its use is controversial due to its impact on the aquatic ecosystem [37], widespread contamination in drinking water and its associations with birth defects and menstrual problems when consumed by humans at higher concentrations [38]. Atrazine use is banned in the European Union but it is still one of the most widely used herbicides in the world.

The chemical structures of phorate and atrazine are shown in Figure 7.13.

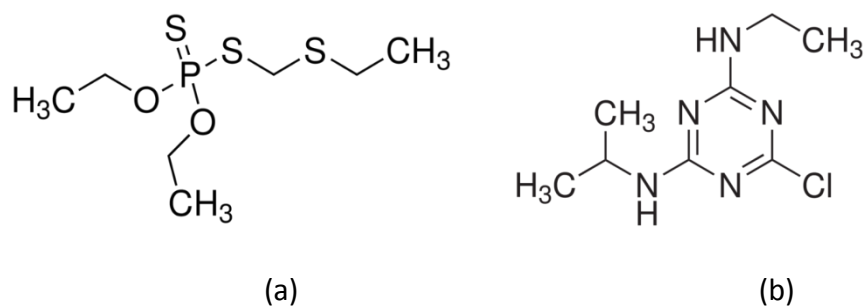


Figure 7.13 Chemical structure of (a) phorate, (b) atrazine

To identify the mass spectrum of the phorate, a solution was prepared in hexane at 10.0 µg/mL and then it was injected into the HIS source. A relatively small mass spectrum was observed at  $m/z$  261 (MW: 260). Fragmentation pattern was checked in the

NIST chemistry web-book for the mass spectrum obtained after electron impact ionisation. It was noted that strong fragment was observed at  $m/z$  75 but no fragment ion was observed in PTR-MS spectra. Even if fragment ion spectra was observed, it would be difficult to confirm that it was the fragment ion of phorate not any interference peak as PTR-ToF-MS was routinely used for the analysis of VOCs with molecular weight no higher than 100 amu. As observed sensitivity of phorate was poor, thus it was not used for further experiments.

Atrazine is available in crystalline powder form. To make the stock solution, first it was required to find the suitable solvent in which atrazine is readily soluble. Initially different solvents were tried e.g. methanol, hexane and ethyl acetate. Atrazine is not soluble in hexane. Even though it was soluble in methanol and ethyl acetate, they were not the ideal solvent as both solvents can be protonate in presence of  $H_3O^+$  and it can complicate the identification process. Atrazine is also readily soluble in water and as water is used in the PTR-ToF-MS system to generate hydronium ion, water was used as a preferred solvent. To identify the mass spectrum of atrazine, its stock solution prepared in water at 10.0  $\mu\text{g/mL}$  was injected into the HIS source but no mass spectrum was observed at  $m/z$  217 (MW: 215.7). A possible reason for this phenomenon is that atrazine might require a high temperature and/or high energy for the ionisation as it is readily identified in GC-MS which uses the electron impact for ionisation whereas PTR-ToF-MS is very soft ionisation technique.

## 7.4 CONCLUSION

In this chapter, it was established that it is possible to detect and analyse pesticides by the use of PTR-TOF-MS. Two techniques

were employed for adding the pesticide and the more sensitive one was based on a liquid-liquid extraction method. Even though it requires at least 10 minute for sample extraction, also no evaporation of solvent is required for further concentration of compound and to re-dissolving them to the mobile phase for the injection on HPLC or GC thus it is still relatively quicker than traditional liquid-liquid extraction methods. In addition, the amount of solvent required for extraction is also smaller to the traditional liquid-liquid extraction methods. It was observed during the course of the experiments that even though pesticides were also detected by direct injection of water samples, lower limit of quantification of 1.00 µg/ml was not achieved for all the pesticides. Then main reason for this low limit of quantification is a high sample volume is required compared to current 10 – 50 µL. However, with high injection volume, the current experimental setup suffers from the non-linearity, as discussed in Chapter 3. As discussed in the Chapter 3, to get a linear response by the use of HIS source, when injecting the water sample, it is important that 100% vaporisation is achieved at all time and with a high injection volume this is not achieved.

The PTR-ToF-MS is not able to detect all pesticides, for example, atrazine and phorate. There are two possible reasons for this. First, this may simply be a result of the low vapour pressure of the compound. Second, it could be that protonation does not occur using  $\text{H}_3\text{O}^+$  as the proton source or it might require different protonation reagent or high energy for ionisation.

For the non-volatile compounds in powder form, further work is required to investigate whether solubilised compounds comes out of the solution when injected into the HIS source set at 100 °C. This could have an impact on the limit of detection and

quantification of the compound and possible contamination issues.

Overall, the PTR-MS analysis time was less than 15 minutes per sample, which is considerably quicker than GC-MS analysis, which routinely requires 30 – 45 minutes run time per sample, without considering the sample preparation time. Less fragmentation was observed in the PTR-MS compared to GC-MS. GC-MS is able to analyse the majority of the pesticides available in the market. PTR-MS has limitations in this regard, as it is not able to analyse all the compounds, such as atrazine or a chlorinated pesticides. The possible reason for this could be that a different proton transfer reagent *e.g.*  $O_2^+$  might be required for successfully ionisation. The comparable limit of quantification for all pesticides analysed in this chapter is observed, as per the limit set in [25]. The observed limit of detection for pesticides was not as low as reported values. For example, for pirimiphos-methyl limit of quantification and detection is 2.0  $\mu\text{g}/\text{ml}$ . Diaz *et al.* [20] reported the limit of detection of 0.004  $\mu\text{g}/\text{ml}$ , which is considerably lower to the one achieved in this study.

Diaz *et al.* [20] and Pareja *et al.* [19] have developed a direct injection technique for analysing the pesticides compounds from the water. There is no sample pre-treatment is required and a total analysis time is less than 15 minutes, very similar to the PTR-MS. The limit of detection is also in the region of  $\text{ng}/\text{l}$  instead of  $\mu\text{g}/\text{ml}$  observed in this technique. In addition, wide range of pesticides can be analysed with these technique, compared to the technique demonstrated in this chapter, where only the organophosphates were analysed.

All the methods discussed here require sophisticated instruments for detection, auto-samplers for injection and

established extraction techniques to achieve a low limit of detection. The current technique was developed on a proof of principle basis to investigate whether semi-volatile compounds can be identified and measured by PTR-MS. The heated inlet source (HIS), used with PTR-MS for this work, which also requires the further research to improve the injection linearity with higher aqueous injection volume. In addition, manual injections were performed instead of using the auto-sampler, which also hampered the linearity of the experiments. The other limitations are that it cannot be applied to the analysis of compounds in powder form or the compounds that might require higher energy/temperature for the ionisation. Atrazine was one of the compounds used in the study that could not be detected successfully as discussed section 3.9. Although, even with this limitation, the experiments provided an excellent basis for the future work to achieve low limit of quantification and a linear regression for different semi-volatile compounds with high molecular weight.

In conclusion, it was established in this chapter that high molecular weight, semi-volatile compounds can be detected and measured by using PTR-TOF-MS. Linear response was observed from the calibration data of the pesticides used in the experiments and low limit of quantification was also observed with LLE technique. Further experiments with the use of a capillary inlet source (CIS) are required to increase the limit of detection for different compounds. The CIS is designed to be used for aqueous samples and a high sample volume can be injected throughout the course of the run to improve the sensitivity.

---

## 7.5 REFERENCES

1. Lindinger, W., A. Hansel, and A. Jordan, On-line monitoring of volatile organic compounds at pptv levels by means of proton-transfer-reaction mass spectrometry (PTR-MS) medical applications, food control and environmental research. *International Journal of Mass Spectrometry and Ion Processes*, 1998. 173(3): p. 191-241.
2. Prazeller, P., Palmer, P.T., Boscaini, E., Jobson, T., Alexander, M., Proton transfer reaction ion trap mass spectrometer. *Rapid Communications in Mass Spectrometry*, 2003. 17(14): p. 1593-1599.
3. Hansel, A., Jordan, A., Holzinger, R., Prazeller, P., Vogel, W., Lindinger, W., Proton transfer reaction mass spectrometry: on-line trace gas analysis at the ppb level. *International Journal of Mass Spectrometry and Ion Processes*, 1995. 149–150(0): p. 609-619.
4. Hewitt Cn Fau - Hayward, S., A. Hayward S Fau - Tani, and T. A, - The application of proton transfer reaction-mass spectrometry (PTR-MS) to the monitoring and analysis of volatile organic compounds in the atmosphere. *J Environ Monit*, 2003. 5(1): p. 1-7.
5. Willis, K.A., Development of Chemical Ionisation Reaction Time-of-Flight Mass Spectrometry for the Analysis of Volatile Organic Compounds in Exhaled Breath. Thesis: University of Leicester, 2009.
6. Araghipour, N., Colineau, J., Koot, A., Akkermans, W., Rojas, J.M.M., Beauchamp, J., Wisthaler, A., Mark, T.D., Downey, G., Guillou, C., Mannina, L., Ruth, S.V., Geographical origin classification of olive oils by PTR-MS. *Food Chemistry*, 2008. 108(1): p. 374-383.
7. Blake, R.S., P.S. Monks, and A.M. Ellis, Proton-Transfer Reaction Mass Spectrometry. *Chemical Reviews*, 2009. 109(3): p. 861-896.
8. Liebich, H.M., H.J. Buelow, and R. Kallmayer, Quantification of endogenous aliphatic alcohols in serum and urine. *Journal of Chromatography A*, 1982. 239(0): p. 343-349.
9. Gilden, R.C., K. Huffling, and B. Sattler, Pesticides and Health Risks. *Journal of Obstetric, Gynecologic, & Neonatal Nursing*, 2010. 39(1): p. 103-110.

10. Educational and Informational Strategies to Reduce Pesticide Risks. *Preventive Medicine*, 1997. 26(2): p. 191-200.
11. Driss, M.R., M.C. Hennion, and M.L. Bouguerra, Determination of carbaryl and some organophosphates pesticides in drinking water using on-line liquid chromatographic preconcentration techniques. *J Chromatogr.*, 1993. 639(2): p. 352-8.
12. Pawliszyn, J., Sample Preparation: Quo Vadis? *Analytical Chemistry*, 2003. 75(11): p. 2543-2558.
13. Barceló, D., Environmental Protection Agency and other methods for the determination of priority pesticides and their transformation products in water. *Journal of Chromatography A*, 1993. 643(1-2): p. 117-143.
14. Barnabas, I.J., J.R. Dean, and S.P. Owen, Supercritical fluid extraction of analytes from environmental samples. A review. *Analyst*, 1994. 119(11): p. 2381-2394.
15. Boyd-Boland, A.A., S. Magdic, and J.B. Pawliszyn, Simultaneous determination of 60 pesticides in water using solid-phase microextraction and gas chromatography-mass spectrometry. *Analyst*, 1996. 121(7): p. 929-937.
16. Dömötöróvá, M. and E. Matisová, Fast gas chromatography for pesticide residues analysis. *Journal of Chromatography A*, 2008. 1207(1-2): p. 1-16.
17. Mahara, B.M., J. Borossay, and K. Torkos, Liquid-Liquid Extraction for Sample Preparation prior to Gas Chromatography and Gas Chromatography-Mass Spectrometry Determination of Herbicide and Pesticide Compounds. *Microchemical Journal*, 1998. 58(1): p. 31-38.
18. Hernández, F., Sancho, J.V., Pozo, O., Lara, A., Pitarch, E., Rapid direct determination of pesticides and metabolites in environmental water samples at sub- $\mu\text{g/l}$  level by on-line solid-phase extraction-liquid chromatography-electrospray tandem mass spectrometry. *Journal of Chromatography A*, 2001. 939(1-2): p. 1-11.
19. Pareja, L., et al., Trace analysis of pesticides in paddy field water by direct injection using liquid chromatography-quadrupole-linear ion trap-mass spectrometry. *Journal of Chromatography A*, 2011. 1218(30): p. 4790-4798.
20. Díaz, L., J. Llorca-Pórcel, and I. Valor, Ultra trace determination of 31 pesticides in water samples by direct injection-rapid resolution liquid chromatography-

- electrospray tandem mass spectrometry. *Analytica Chimica Acta*, 2008. 624(1): p. 90-96.
21. Kalapos, M.P., On the mammalian acetone metabolism: from chemistry to clinical implications. *Biochimica et Biophysica Acta (BBA) - General Subjects*, 2003. 1621(2): p. 122-139.
  22. Lambropoulou, D.A. and T.A. Albanis, Optimization of headspace solid-phase microextraction conditions for the determination of organophosphates insecticides in natural waters. *Journal of Chromatography A*, 2001. 922(1-2): p. 243-255.
  23. Jia, C., Zhu, X., Wang, J., Zhao, E., He, M., Chen, L., Yu, P., Extraction of pesticides in water samples using vortex-assisted liquid-liquid microextraction. *Journal of Chromatography A*, 2010. 1217(37): p. 5868-5871.
  24. Jolly, W.L., *Modern Inorganic Chemistry*. 1989: McGraw-Hill.
  25. Eriksen, S., *New Scientist*, 381 (1964), p. 608.
  26. Alankar Shrivastava, V.B.G., Methods for the determination of limit of detection and limit of quantitation of the analytical methods. *Chron Young Sci* 2011. 2(1): p. 21-25.
  27. Alwis, K.U., et al., Simultaneous analysis of 28 urinary VOC metabolites using ultra high performance liquid chromatography coupled with electrospray ionization tandem mass spectrometry (UPLC-ESI/MSMS). *Analytica Chimica Acta*, (0).
  28. Albanis, T.A. and D.G. Hela, Multi-residue pesticide analysis in environmental water samples using solid-phase extraction discs and gas chromatography with flame thermionic and mass-selective detection. *Journal of Chromatography A*, 1995. 707(2): p. 283-292.
  29. Španěl, P. and D. Smith, Selected ion flow tube – mass spectrometry: detection and real-time monitoring of flavours released by food products. *Rapid Communications in Mass Spectrometry*, 1999. 13(7): p. 585-596.
  30. Chen, P.-S. and S.-D. Huang, Determination of ethoprop, diazinon, disulfoton and fenthion using dynamic hollow fiber-protected liquid-phase microextraction coupled with gas chromatography-mass spectrometry. *Talanta*, 2006. 69(3): p. 669-675.
  31. Pesticide information Profile for Fenthion. Cooperative Extension Offices of Cornell University, Michigan State

- University, Oregon State University, and University of California at Davis. . EXTOXNET., 2003.
32. Authority, A.P.V.M., The reconsideration of approvals of the active constituent fenthion, registrations of products containing fenthion and their associated labels December 2005.
  33. Rieder J Fau - Prazeller, P., et al., - Online monitoring of air quality at the postanesthetic care unit by proton-transfer-reaction mass spectrometry. *Anesth Analg*, 2001. 92(2): p. 389-92.
  34. Fu, L., et al., Application of dispersive liquid–liquid microextraction for the analysis of triazophos and carbaryl pesticides in water and fruit juice samples. *Analytica Chimica Acta*, 2009. 632(2): p. 289-295.
  35. Patsias, J. and E. Papadopoulou-Mourkidou, Rapid method for the analysis of a variety of chemical classes of pesticides in surface and ground waters by off-line solid-phase extraction and gas chromatography-ion trap mass spectrometry. *Journal of Chromatography A*, 1996. 740(1): p. 83-98.
  36. Yang, X. and T. Peppard, Solid-Phase Microextraction for Flavor Analysis. *Journal of Agricultural and Food Chemistry*, 1994. 42(9): p. 1925-1930.
  37. Graymore, M., F. Stagnitti, and G. Allinson, Impacts of atrazine in aquatic ecosystems. *Environment International*, 2001. 26(7–8): p. 483-495.
  38. Duhigg, C., Debating How Much Weed Killer Is Safe in Your Water Glass. *The New York Times*, August 22, 2009.

## **CHAPTER 8: TWO-STAGE PROTON TRANSFER REACTION TIME OF FLIGHT MASS SPECTROMETRY**

---

### **8.1 INTRODUCTION**

The proton-transfer-reaction mass spectrometry is a well-established technique for the measurement of trace volatile organic compounds (VOCs) in gases [1-4]. PTR-MS is discussed in detail in Chapter 2.

The strengths of the PTR-MS technique includes high detection sensitivity (down to approx. 10 pptV) coupled with high speed, the concentration of individual trace compounds often being measurable in minutes or even in seconds. However, one of the main weaknesses of PTR-MS is its reliance solely on mass spectrometry for discriminating between molecules, which means that isobaric species cannot be reliably distinguished. This is in sharp contrast to gas chromatography-mass spectrometry (GC-MS), where the chromatographic separation prior to mass spectrometry allows almost complete resolution of individual VOCs, albeit with a concomitant and dramatic loss of speed of measurement.

Solutions to the isobaric problem in PTR-MS have been proposed. One possibility is to employ an ion trap as the mass spectral device, which makes it possible to use energy-controlled collision-induced dissociation to selectively discriminate between isobaric species [5-9]. However, while certainly effective, this approach requires careful data analysis and the fact that most current PTR-MS instruments do not employ ion traps makes this of limited appeal. An alternative approach has been demonstrated by Wyche and co-workers in

which alternative chemical ionization (CI) reagents, including  $\text{NH}_4^+$  and  $\text{NO}^+$ , are employed [8, 10]. Many isobaric pairs, such as aldehyde and ketones, demonstrate quite different ion products with different CI reagents, which can potentially allow compound discrimination. However, this approach tends to rely on differences in ion fragmentation, which is not the best solution when working with complex mixtures of VOCs.

Recently, Inomata and Tanimoto have introduced a two-stage ion source for PTR-MS which makes it simple to use protonated VOCs as proton sources instead of  $\text{H}_3\text{O}^+$  [11]. This works by introducing an excess of a chosen VOC, referred to as  $\text{VOC}_1$ , into the drift tube upstream of the analyte gas inlet. Proton transfer from  $\text{H}_3\text{O}^+$  to  $\text{VOC}_1$  creates a new proton transfer reagent  $\text{H}^+ \text{VOC}_1$  with different characteristics. In particular, by using protonated VOCs as the proton source, one has the option of choosing a species for  $\text{VOC}_1$  with a proton affinity that can discriminate between two isobaric species providing that they possess substantially different proton affinities. This approach by Inomata and Tanimoto was demonstrated using ethyl acetate and 1,4-dioxane as the test species. Both of these molecules are protonated by  $\text{H}_3\text{O}^+$ , but switching to protonated acetone removed all signal due to ethyl acetate, leaving only contributions from 1,4-dioxane.

Inomata and Tanimoto also suggested that their two-stage source might provide effective discrimination between isobaric aldehydes and ketones. Aldehydes and ketones have a number of sources, both biogenic and anthropogenic, and it is sometimes important to be able to distinguish between isobaric pairs. For example, butanal is a well-known gaseous product found above many plants, including grasses [12, 13], whereas butanone has mainly man-made sources, such as vehicle emissions [14]. Methacrolein and methyl vinyl ketone (MVK)

represent another isobaric aldehyde/ketone pair, both of which are known isobaric oxidation products of isoprene in the atmosphere [15, 16] and therefore have significance in the production of tropospheric ozone through biogenic emissions. Consequently, the demonstration of a simple, quick and effective means of distinguishing between isobaric aldehyde/ketone pairs will strength the utility of PTR-MS in atmospheric VOC monitoring.

In the current study several isobaric aldehyde/ketone pairs including butanal/butanone and methacrolein/methyl vinyl ketone has been discriminated by the use of two-stage PTR-MS. Furthermore, this technique was applied to gain the first experimental information about the proton affinities of hexanal and 2-hexanone.

## 8.2 EXPERIMENTAL

The experimental work was carried out by using a PTR-ToF-MS instrument on loan from the University of York [17]. In contrast to the normal Leicester PTR-ToF-MS instrument, where radioactive generation of  $\text{H}_3\text{O}^+$  is employed, in the York instrument a discharge source is employed. The  $\text{H}_3\text{O}^+$  ions enter a drift tube and meet the incoming flow of  $\text{VOC}_1$ , efficiently transferring charge from  $\text{H}_3\text{O}^+$  to  $\text{VOC}_1$  to produce  $\text{VOC}_1 \cdot \text{H}^+$  in the upstream part of the drift tube (Reaction 1). The analyte gases  $\text{VOC}_2$  are added through a second entrance port further downstream where they encounter the flowing protonated  $\text{VOC}_1$  ions and produce some protonated  $\text{VOC}_2$  (Reaction 2). After flowing several further centimetres, the gas stream is sampled through a pinhole aperture and enters the source region of the time-of-flight mass spectrometer.





The significant point about the experiments was that further investigation was carried out to find the best location for adding  $\text{VOC}_1$ . One area considered was addition of  $\text{VOC}_1$  to the source drift region of the ion source, rather than in the upstream part of the drift tube. This was shown to yield highly effective protonation of VOCs in the analyte stream but there was an increased tendency for fragmentation of protonated  $\text{VOC}_1$ , as might be expected given the proximity to the highly energetic discharge region. An alternative choice was also explored, addition of excess  $\text{VOC}_1$  in the analyte inlet tube. This was the preferred operating configuration and benefits from the fact that no modification to the drift tube was required [11].

(A)

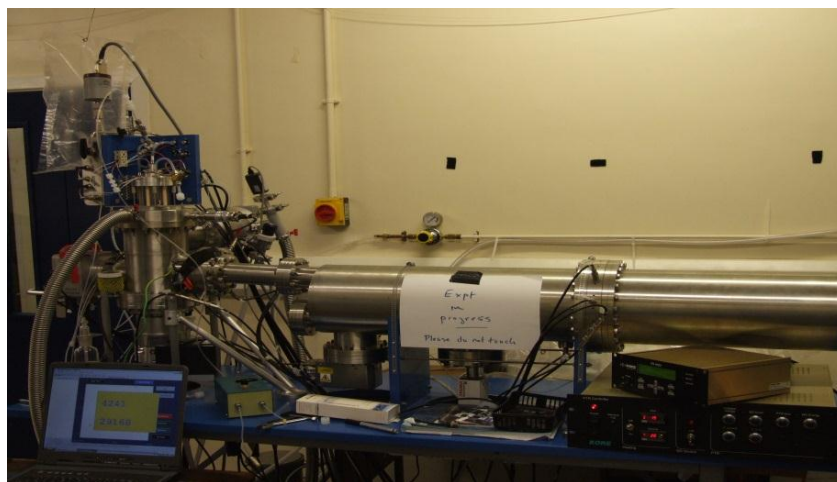


Figure 8.1 (A) University of York PTR-ToF-MS (B) Two stage PTR ion source

(B)

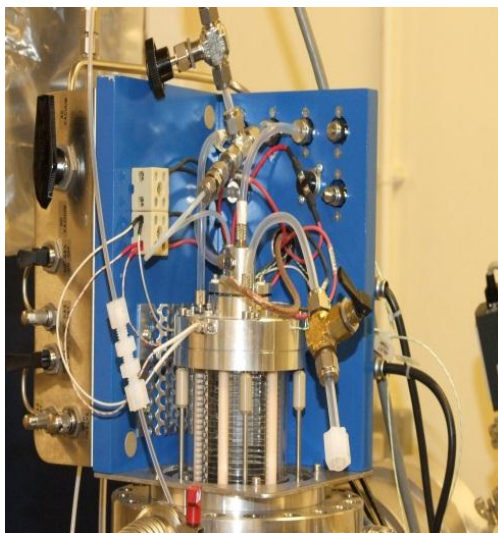


Figure 8.1 (A) University of York PTR-ToF-MS (B) Two stage PTR ion source

Typical drift tube conditions during experiments were as follows: pressure 1.5 mbar,  $E/N$  ratio = 100Td, and temperature 23 °C.

Analyte gases were delivered to the instruments via simple headspace extraction of the vapour above the chosen pure compound. For experiments where both  $VOC_1$  and  $VOC_2$  were delivered through the same inlet, mixtures of the two gases were prepared in Tedlar bags, with  $VOC_1$  in at least a 20-fold excess over  $VOC_2$ . Samples were produced by introducing microlitre ( $\mu$ l) quantities of the VOC material into 10 litre Tedlar bags, which were then inflated to atmospheric pressure with nitrogen (99.9999% pure). The initial mixtures were too concentrated (typically 200 ppmV) so a further (1000-fold) dilution was carried out by extracting 10 ml of the mixture with a gas syringe and introducing it into an empty 10 litre Tedlar bag. The ability to provide quantitative information on individual isomers in a two-compound mixture was explored via dynamic dilution. In these experiments a twin-oven diluter (Kintek 491M) was employed with appropriate permeation tubes for gas calibration.

## 8.3 RESULTS

### 8.3.1 Two-Stage PTR-MS

The proton affinity of water is  $691 \text{ kJ mol}^{-1}$  [18]. A wide variety of organic compounds possesses higher proton affinities than water, and so all are possible candidates for  $\text{VOC}_1$ . However, in practice more exacting criteria need to be applied to find a suitable  $\text{VOC}_1$ . In addition to an acceptable proton affinity, the chosen compound should be readily available, sufficiently volatile, and should produce little or no fragmentation when accepting a proton. Furthermore,  $\text{VOC}_1$  should also suppress the formation of  $\text{H}_3\text{O}^+(\text{H}_2\text{O})$  as well as  $\text{H}_3\text{O}^+$ , since the former cluster is also likely to be present in significant quantities in the drift tube, and it is not certain what role it would play in the presence of  $\text{VOC}_2$ .

Table 8.1 Comparison of aldehyde and ketone proton affinities relevant to this work.

Molecule	Proton affinity/kJ mol <sup>-1</sup>
H <sub>2</sub> O	691.0
Acetone (propanone)	812.0
Butanal	793
Butanone	827
Pentanal	797
2-Pentanone	833
3-Pentanone	837
Hexanal	-
2-Hexanone	-
3-Hexanone	843.2
Methacrolein	808.7
Methyl vinyl ketone	834.7

Taken from Hunter and Lias [19]

Crucial to the success of the experiments is the significant difference (where known) in the proton affinities of isobaric aldehyde/ketone pairs. Table 1 show that the ketone(s) possesses higher proton affinities than the corresponding aldehyde. Consequently, if a VOC with a proton affinity lying between that of the aldehyde and ketone is employed as  $\text{VOC}_1$  in an experiment with a two-stage source, the mass spectrum should, in principle, yield signal from the ketone only.

### 8.3.2 Butanal and Butanone

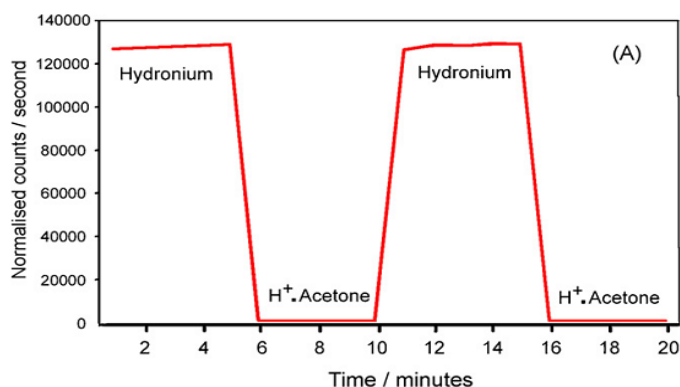
Butanone yields mainly the protonated parent molecule ( $m/z = 73$ ) in reactions with  $\text{H}_3\text{O}^+$ , whereas the major product for butanal is the dehydrated ion  $[\text{MH}-(\text{H}_2\text{O})]^+$  at  $m/z = 55$ .

Consequently, use of  $\text{H}_3\text{O}^+$  in PTR-MS already provides a means of potentially discriminating between the two isomers.

Nevertheless, the fact that butanal and butanone have distinct mass spectra is convenient for an initial test of the two-stage method. It should also be noted that mass channel 55 also coincides with the signal from  $[\text{H}_3\text{O}^+(\text{H}_2\text{O})]^2$ , which is always seen in spectra where  $\text{H}_3\text{O}^+$  is used as the proton source.

Consequently, distinguishing butanal and butanone in real gas mixtures using  $\text{H}_3\text{O}^+$  alone would be extremely difficult.

(A)



(B)

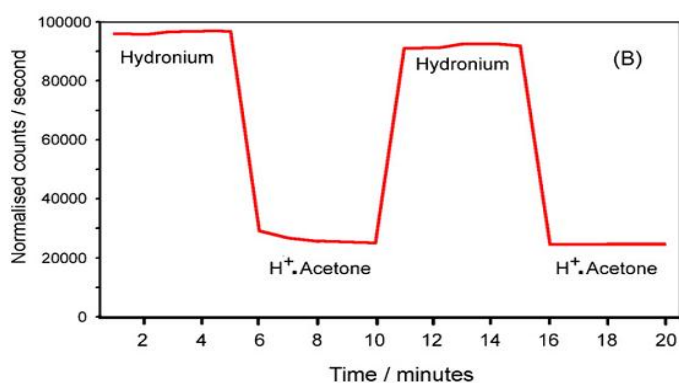


Figure 8.2 (a) Signal seen for protonated butanal (monitored at the fragment peak at  $m/z$  55) as the proton source is switched between  $\text{H}_3\text{O}^+$  and protonated acetone. (b) Corresponding results for butanone, in this case monitored at  $m/z$  73. The switch from  $\text{H}_3\text{O}^+$  to  $\text{H}^+$ .Acetone brings about a roughly threefold drop in the  $m/z$  73

According to Table 8.1, which shows only a very limited subset of possible compounds that could act as  $\text{VOC}_1$ , acetone should yield signal only from butanone since its proton affinity lies roughly midway between those of butanal and butanone. Experiments have confirmed this, showing almost complete disappearance of any signal from butanal at  $m/z$  = 55 when switching from  $\text{H}_3\text{O}^+$  to protonated acetone as reagent ion (see Figure 8.2 (a)). In the case of butanone, the switch to acetone as  $\text{VOC}_1$  retains a substantial protonated parent peak at  $m/z$  73, but this peak is much smaller than seen with  $\text{H}_3\text{O}^+$  as the proton

source (see Figure 8.2(b)). This is presumably due to a smaller rate constant for the reaction between protonated acetone and butanone when compared to the corresponding  $\text{H}_3\text{O}^+$  reaction. Nevertheless, a substantial protonated butanone signal remains and consequently this simple test demonstrates the feasibility of switching from  $\text{H}_3\text{O}^+$  to  $\text{VOC}_1 \cdot \text{H}^+$  in order to distinguish isobaric compounds. It is worth emphasizing that this switch can be achieved relatively rapidly (< 2 minutes).

### 8.3.3 Methacrolein and methyl vinyl ketone

In contrast to butanal and butanone, methacrolein (MA) and methyl vinyl ketone (MVK) both yield protonated parent molecules as the dominant signal in their PTR-MS spectra. Two-stage experiments with acetone as  $\text{VOC}_1$  yield good separation, but the MA signal does not completely disappear when switching from  $\text{H}_3\text{O}^+$  to protonated acetone, as can be seen from Figure 8.3. This incomplete separation is understandable given that the proton affinity of acetone is only 3 kJ mol<sup>-1</sup> above that of MA. Uncertainties in the measured proton affinities coupled with residual thermal energy can account for the non-zero signal from MA.

(A)

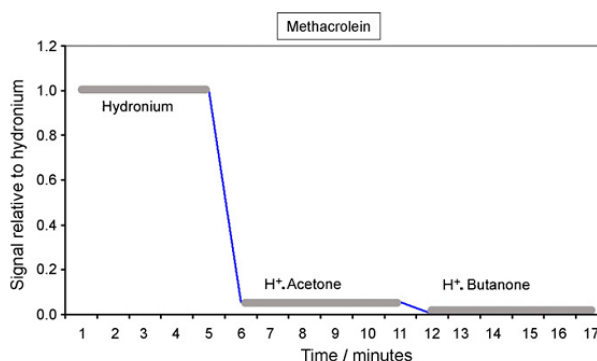


Figure 8.3 (A) Signal seen for protonated methacrolein as the proton source is switched between  $\text{H}_3\text{O}^+$ , protonated acetone and protonated butanone. (B) Signal levels seen for protonated methyl vinyl ketone (MVK) as the proton source is switched

between  $\text{H}_3\text{O}^+$ , protonated acetone and protonated butanone.

(B)

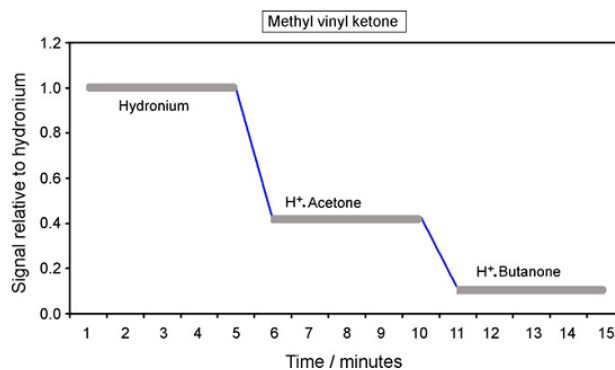


Figure 8.3 (A) Signal seen for protonated methacrolein as the proton source is switched between  $\text{H}_3\text{O}^+$ , protonated acetone and protonated butanone. (B) Signal levels seen for protonated methyl vinyl ketone (MVK) as the proton source is switched between  $\text{H}_3\text{O}^+$ , protonated acetone and protonated butanone.

From Table 1, butanone looks a better choice as  $\text{VOC}_1$  since it has a proton affinity some  $8 \text{ kJ mol}^{-1}$  below that of MVK and well above that of MA. Experiments on MA confirm this choice, almost completely removing all reaction products when using butanone as  $\text{VOC}_1$  (see Figure 8.3). The two-stage source is thus seen to be a highly effective means of discriminating between MA and MVK, but the downside is that when butanone is used as  $\text{VOC}_1$  this comes at the cost of a substantial loss in ion count rate.

#### 8.3.4 Hexanal/2-hexanone/3-hexanone

The proton affinities of hexanal and 2-hexanone have not been reported in the literature, although that of 3-hexanone is known ( $843.2 \text{ kJ mol}^{-1}$  [18]). However, on the basis of the known proton affinities for lighter aldehydes and ketones (see Table 8.1), we can estimate likely values for hexanal and 2-hexanone. For hexanal the expectation is a proton affinity near  $800 \text{ kJ mol}^{-1}$ ,

whereas the similarity of the proton affinities of 2-pentanone and 3-pentanone suggests that 2-hexanone should have a proton affinity just below that of 3-hexanone, most probably close to  $840 \text{ kJ mol}^{-1}$ . Based on these predictions it will prove impossible to choose a  $\text{VOC}_1$  that can completely discriminate between 2-hexanone and 3-hexanone, but the much lower proton affinity of hexanal should suffice to remove any trace of signal from this compound by suitable choice of  $\text{VOC}_1$ . Several candidates for  $\text{VOC}_1$  would be ideal in this regard, with proton affinities above that expected for hexanal but well below those of 2- and 3-hexanone.

Like butanal, proton transfer from  $\text{H}_3\text{O}^+$  and other proton sources, such as protonated acetone, to hexanal tends to result in ion dehydration, whereas the hexanones yield mainly protonated parent ions. The dehydration of hexanal is extensive, with the protonated parent peak at  $m/z$  101 accounting for only about 1% of the contribution to the mass spectrum. The dehydrated fragment ion at  $m/z$  83 was therefore used for monitoring hexanal in the current experiments.

The ability to vary  $\text{VOC}_1$  provides the opportunity to determine the proton affinity of hexanal through a bracketing procedure. Table 2 summarises the findings of these bracketing measurements. The proton affinity is found to lie within the range  $794.4 < \text{PA}(\text{hexanal}) < 797.0 \text{ kJ mol}^{-1}$ , providing the first experimental determination of the proton affinity of hexanal. Furthermore, the proton affinity of 2-hexanone was shown to be  $>812 \text{ kJ mol}^{-1}$  (the proton affinity of acetone), as expected.

Table 8.2 Outcome of hexanal proton affinity bracketing experiments

$\text{VOC}_1$	PA of $\text{VOC}_1/\text{kJ mol}^{-1}$	Product ion (s) seen?
Toluene	784.0	Yes
p-Xylene	794.4	Yes

VOC <sub>1</sub>	PA of VOC <sub>1</sub> /KJ mol <sup>-1</sup>	Product ion (s) seen?
Acrolein	797.0	No
Furan	803.4	No
Acetone	812.0	No

These limits provide a proton affinity of hexanal which is a little lower than that anticipated by extrapolation from the lighter aldehyde/ketone pairs, but which is broadly in line with expectations.

### 8.3.5 Quantification of isobaric components

The results presented above show that aldehydes can be distinguished from isobaric ketones by choice of an appropriate VOC<sub>1</sub>. However, for practical applications it is important that the aldehydes and ketones can be separately quantified.

Dynamic gas dilution was employed to produce known concentrations of MA and MVK separately, as well as a mixture of both. Calibration curves for each compound were obtained using both hydronium and protonated acetone as proton sources, in order to obtain compound sensitivities prior to analysing a mixture (Figure 8.4). These calibration curves were obtained by varying supply of nitrogen through temperature-regulated permeation tubes containing either MA or MVK. The MA permeation tube (KinTek) was specified for a leak rate of 92.9 ng min<sup>-1</sup> at an operating temperature of 60°C, while that for MVK (purchased from Metronics/Dynacal) gave a leak rate of 144 ng min<sup>-1</sup> at 50°C.

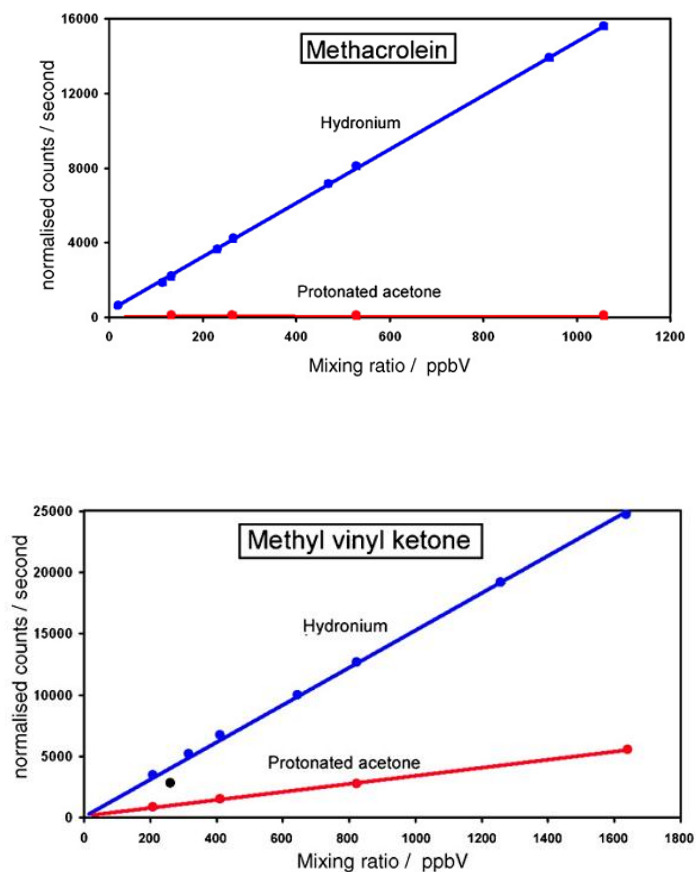


Figure 8.4 Calibration plots obtained for methacrolein (MA) and methyl vinyl ketone (MVK) using hydronium and protonated acetone as proton donors. Permeation tubes were used as VOC2 sources

Having obtained independent calibration curves, measurements were then carried out on a mixture of MA and MVK. Both permeation tubes were employed and a common oven temperature of 50°C was employed, which allowed the delivery of a pre-determined amount of MVK but an unknown amount of MA. The experiment to determine the composition of the mixture was carried out using two flow rates (0.3 and 0.6 l min<sup>-1</sup>) from the diluter, in effect giving two different concentrations of each compound in the mixture. Separate concentration determinations were then made using the same conditions but using one permeation tube only and using hydronium as the ion source. The sensitivities obtained from the initial calibrations provide reference concentrations of MA and

MVK that can be compared with those derived from the mixture. The concentrations determined in the mixture were obtained by measurements using protonated acetone and then  $\text{H}_3\text{O}^+$  as the ion source. The latter should give the combined MVK + MA concentration whereas the former should give MVK only.

Table 8.3 Quantitative experiment results on a mixture of MA and MVK

	[MA] (ppbv)		[MVK] (ppbv)	
	0.3	0.6	0.3	0.6
Flow rate (l min <sup>-1</sup> )	0.3	0.6	0.3	0.6
Single permeation tube	1220 ± 40	637 ± 30	1510 ± 50	801 ± 30
Mixture	1271 ± 50	619 ± 30	1620 ± 40	830 ± 40

The results obtained are shown in Table 8.3. The agreement between the reference concentrations (single permeation tubes) of MA and MVK and the values derived from the two mixtures are excellent, demonstrating that the switch between proton transfer sources can be used successfully to independently quantify MA and MVK.

## 8.4 CONCLUSION

The lower proton affinities of aldehydes relative to their isomeric ketone partners provides a means of distinguishing between and quantifying isomeric aldehydes and ketones by PTR-MS. Two-stage PTR-MS provides a simple and effective technique for achieving this. To separately quantify these compounds, an initial experiment using  $\text{H}_3\text{O}^+$  as the proton source is required to provide the total VOC concentration in a given mass channel. A subsequent experiment using a VOC with a proton affinity above that of the aldehyde but below that of the ketone switches off any aldehyde contribution and allows the ketone(s) to be quantified. Finally, these two measurements can be combined to provide separate quantification of the aldehyde and ketone. This ability to separate isobaric VOCs

based on differences in their proton affinities provides a valuable extra dimension to PTR-MS.

It is worth emphasizing that, while simple to implement, the two-stage approach does have its limitations. These include the possibility that a suitable choice of VOC for separating the contributions of two isomeric or isobaric compounds is unavailable. It is also possible that more than two compounds will contribute to a given mass channel. A good example of this is crotonaldehyde, which is isomeric with two of the compounds considered in the current study, methacrolein and methyl vinyl ketone. The proton affinity of crotonaldehyde lies at  $823 \text{ kJ mol}^{-1}$  [18], which is roughly midway between methacrolein and methyl vinyl ketone. Protonated acetone would switch off only the methacrolein contribution whereas protonated butanone would allow both methacrolein and crotonaldehyde signals to be removed from the mass spectrum. Consequently, by switching from  $\text{H}_3\text{O}^+$  to protonated acetone to protonated butanone, we would collect data sufficient to quantify all three compounds. Of course, such a quantification process would require prior compound calibration using known gas standards to allow for the changes in detection sensitivity, as the proton source is altered. Measurements can be combined to provide separate quantification of the aldehyde and ketone.

The ability to switch easily from  $\text{H}_3\text{O}^+$  to another proton source in the two-stage experiment also provides a means to estimate proton affinities of compounds. This bracketing approach has been used here to estimate the proton affinity of hexanal, which has not previously been reported and which is found to lie in the range  $794.5 < \text{PA}(\text{hexanal}) < 797.0 \text{ kJ mol}^{-1}$ .

## 8.5 REFERENCES:

1. Lindinger, W., A. Hansel, and A. Jordan, On-line monitoring of volatile organic compounds at pptv levels by means of

- proton-transfer-reaction mass spectrometry (PTR-MS) medical applications, food control and environmental research. *International Journal of Mass Spectrometry and Ion Processes*, 1998. 173(3): p. 191-241.
2. E. P. L. Hunter, S.G.L., Evaluated gas phase basicities and proton affinities of molecules: an update. *Journal of Physical and Chemical Reference Data*, 1998. 27(3): p. 413-656.
  3. Hewitt Cn Fau - Hayward, S., A. Hayward S Fau - Tani, and T. A., - The application of proton transfer reaction-mass spectrometry (PTR-MS) to the monitoring and analysis of volatile organic compounds in the atmosphere. *J Environ Monit*, 2003. 5(1): p. 1-7.
  4. de Gouw, J. and C. Warneke, Measurements of volatile organic compounds in the earth's atmosphere using proton-transfer-reaction mass spectrometry. *Mass Spectrometry Reviews*, 2007. 26(2): p. 223-257.
  5. Prazeller, P., et al., Proton transfer reaction ion trap mass spectrometer. *Rapid Communications in Mass Spectrometry*, 2003. 17(14): p. 1593-1599.
  6. Warneke, C., et al., Development of Proton-Transfer Ion Trap-Mass Spectrometry: On-line Detection and Identification of Volatile Organic Compounds in Air. *Journal of the American Society for Mass Spectrometry*, 2005. 16(8): p. 1316-1324.
  7. Steeghs, M.M.L., et al., Development of a proton-transfer reaction ion trap mass spectrometer: Online detection and analysis of volatile organic compounds. *International Journal of Mass Spectrometry*, 2007. 262(1-2): p. 16-24.
  8. Blake, R.S., et al., Chemical ionization reaction time-of-flight mass spectrometry: Multi-reagent analysis for determination of trace gas composition. *International Journal of Mass Spectrometry*, 2006. 254(1-2): p. 85-93.
  9. Warneke, C., et al., Two additional advantages of proton-transfer ion trap mass spectrometry. *Rapid Communications in Mass Spectrometry*, 2004. 18(1): p. 133-134.
  10. Wyche, K.P., et al., Differentiation of isobaric compounds using chemical ionization reaction mass spectrometry. *Rapid communications in mass spectrometry : RCM*, 2005. 19(22): p. 3356-3362.
  11. Inomata, S., Tanimoto, H., Kameyama, S., Tsunogai, U., Irie, H., Kanaya, Y., and Wang, Z.: Technical Note, Determination of formaldehyde mixing ratios in air with

- PTR-MS: laboratory experiments and field measurements. *Atmos. Chem. Phys.*, 2008. 8: p. 273-284.
12. Wildt, J., et al., Emissions of Oxygenated Volatile Organic Compounds from Plants Part II: Emissions of Saturated Aldehydes. *Journal of Atmospheric Chemistry*, 2003. 45(2): p. 173-196.
  13. H. Hellén, H.H., A. Reissell, and T. M. Ruuskanen, Carbonyl compounds in boreal coniferous forest air in Hyytiälä, Southern Finland. *Atmos. Chem. Phys.*, 2004. 4: p. 1771-1780.
  14. Grosjean, D., E. Grosjean, and A.W. Gertler, On-Road Emissions of Carbonyls from Light-Duty and Heavy-Duty Vehicles. *Environmental Science & Technology*, 2000. 35(1): p. 45-53.
  15. Atkinson, R. and J. Arey, Gas-phase tropospheric chemistry of biogenic volatile organic compounds: a review. *Atmospheric Environment*, 2003. 37, Supplement 2(0): p. 197-219.
  16. Paulson, S.E., R.C. Flagan, and J.H. Seinfeld, Atmospheric photooxidation of isoprene part II: The ozone-isoprene reaction. *International Journal of Chemical Kinetics*, 1992. 24(1): p. 103-125.
  17. Ennis, C.J., et al., A hollow cathode proton transfer reaction time of flight mass spectrometer. *International Journal of Mass Spectrometry*, 2005. 247(1-3): p. 72-80.
  18. Hunter, E.P.L. and S.G. Lias, Evaluated Gas Phase Basicities and Proton Affinities of Molecules: An Update. *Journal of Physical and Chemical Reference Data*, 1998. 27(3): p. 413-656.

## **CHAPTER 9:**

### **Summary and future direction**

---

#### **9.1 INTRODUCTION**

This thesis described the development and calibration of heated inlet source (HIS) and capillary inlet source (CIS) and the application of PTR-ToF-MS for the characterisation of different whisky, analysis of VOCs from headspace of human urine and analysis of semi-volatile compounds from water. The development of the PTR-ToF-MS instruments and its application has come a long way over the course covered in this thesis, from the design and calibration of the new inlet source for the use of the liquid and liquid headspace samples and development of the application by analysing the liquid samples and their headspace. Most of the work performed until now has been on a 'proof-of-principle' basis, which has provided some interesting results that could be used as a starting point to initiate further investigations.

#### **9.2 INLET SOURCES AND LIQUID INJECTION FOR PTR-MS**

The drift tube on PTR-MS operates under vacuum. Therefore, to analyse the liquid samples, they were first required to be vaporised. Initially the heated inlet source (HIS) was constructed to vaporise the liquid samples. The HIS is simple yet effective source made of heated glass tube. The first sets of experiments were performed to calibrate the HIS by preparing the calibration standards for acetone, 2-butanone, acetonitrile, methanol and acetaldehyde in water and organic solvent. In these experiments, the HIS was housed on the bottom plate between drift tube and ToF. The long expose Teflon tube used for the connection. The HIS temperature was set at 100°C for the experiments. It was noted that when samples were injected, there was a drop in the  $H_3O^+$  signal and it took considerable amount of time before it stabilised. It was

thought that long exposed tubing could be the reason for the delay in obtaining the stable  $\text{H}_3\text{O}^+$  signal. Therefore, it was decided to house the HIS on rod next to the drift tube. Because of this set-up, length of the expose Teflon tube was reduced considerably. When water sample was injected to the HIS with the new set-up, it was noted that stable  $\text{H}_3\text{O}^+$  signal was observed straight after the injection of the sample.

Three different matrixes were analysed with the HIS. These matrixes were water, organic solvent and headspace above aqueous. The limit of detection varied between different matrixes with lowest limit of detection was observed when headspace above the liquid sample was injected, followed by the calibration standards prepared in organic solvent and lastly for the calibration standards prepared in water. The similar pattern of changes in LoD from three matrixes used in the study was also observed for the sensitivity. The sensitivity and limit of detection were also investigated. It was observed that LoD was up to 100-fold better than DSI and sensitivity was up to 10-fold better than DAI when water sample was used. The different injection volumes were investigated to observe the improvement in the sensitivity and LoD of the technique. The improvement in both sensitivity and LoD was observed when injection volume was increased for organic solvent and headspace above the aqueous sample but it was not the case for the water. With water sample, when injection volume was increased, sensitivity was not increased in proportion to the injection volume and it affected the linearity of the standards. After observation of the injection volume, it was noticed that with the higher injection volume, vaporisation takes considerable longer and there was a possibility that 100% vaporisation could not be achieved within the experiment duration. In summary, for the HIS acceptable sensitivity, LoD and linearity was observed for the standard analysed in organic solvent and from the headspace above the aqueous sample, but further work is

required to improve the sensitivity, LoD and linearity with aqueous sample when higher injection volume is required. Additionally, in HIS sample was injected at a single time during the run therefore vaporised sample is introduced into the drift tube as a single pulse. The HIS technique will benefit greatly where new injection technique is developed which introduced the sample in a control manner through the run.

Due to the limitation with the higher injection volume, for the aqueous samples in the HIS, capillary inter source (CIS) was developed and constructed. The CIS allows the steady small flow of aqueous sample for the whole duration of the run. The source was made of stainless steel and heating was applied by external source *e.g.* halogen light. The CIS was housed vertically on top of the drift tube and sample was injected at a steady small flow by the use of the syringe pump. The distance between CIS sample outlet to drift tube sample inlet was only few centimetre therefore there was a less chance for vaporised samples to lose the temperature prior to entering the drift tube and steady  $\text{H}_3\text{O}^+$  signal was observed throughout the run. The calibration standards for acetone, 2-butanone, acetonitrile, methanol and acetaldehyde were prepared in water and they were injected at a steady small flow rate for the entire run. The improvement on the sensitivity and LoD was observed for acetonitrile when compared to the HIS data, whereas comparable data were observed for 2-butanone. However, poor sensitivity and LoD was observed for acetone. Further work is required to improve the heating of the CIS, as with current external head source temperature control is not possible. A thermostatic box as discussed in [2] might be a good starting point to control the temperature of the CIS.

A large background signal at the chosen  $m/z$  was observed. The water sample at a different concentration and injection volumes was used for different experiments during the course of the study. Therefore, either

the un-vaporised or a concentrated sample was the reason for the large background signal.

The sensitivity and LoD of the HIS and CIS was compared with dynamic solution injection (DSI) technique [1] and direct aqueous injection (DAI) technique [2]. The improved sensitivity and LoD for the similar compound (*e.g.* acetone) used in all studies was achieved with HIS and CIS compare to DSI and DAI. Only one compound was common between all four different techniques, therefore it cannot be claimed that either HIS or DSI technique is more sensitivity. Further work is required where more compounds are analysed by both HIS and CIS to assess the overall sensitivity and LoD of both techniques.

### **9.3 CHARACTERISATION OF WHISKY**

As the ultimate goal for the development of HIS and CIS was to open up a new field of applications for the PTR-MS where liquid samples can be used. The University of Leicester PTR-MS was used for the majority of the experiments in this thesis including the whisky characterisation work. As the Leicester PTR-MS employs the Time of Flight Mass Spectrometry, it allows the collection of complete mass profile. Advantage of this technique was used to collect the complete mass profile from the whisky analysis to discriminate between different blend and make of whiskies instead of relying on selected mass channels.

The whisky is an alcoholic beverage with ethanol content in the region of 40%. The high percentage of ethanol can influence the PTR-MS mass spectrum and it can also have an impact on the  $\text{H}_3\text{O}^+$  signal. Effect of ethanol was measured on  $\text{H}_3\text{O}^+$  signal and it was observed that due to a high residual moisture in the drift tube and only small amount of ethanol was injected at the start of the run, effect of ethanol on the  $\text{H}_3\text{O}^+$  signal was only limited to first 10-15s of the run. To further check the impact of the ethanol on the discrimination of whisky, direct

injection and headspace analysis was performed on two aliquots of the samples per brand of whisky. One aliquot of whisky sample was diluted with ethanol to make sure the ethanol was dominant in the sample, second aliquot of the sample was not diluted, and ethanol was treated as one of the VOCs from whisky.

It was observed that certain compounds were more sensitive in a sample where no dilution was performed to the sample which was diluted with ethanol. For example, mass spectrum at  $m/z$  106 was more sensitive for an undiluted whisky sample and mass spectrum at  $m/z$  60 was more sensitive for a diluted whisky sample. Even-though a difference in a sensitivity was observed with the dilution of whisky with the ethanol, but it was shown that it had no impact on the discrimination of the whiskies. The comparable separation was observed for the whiskies with and without the dilution with ethanol with both injection techniques.

Future work can be performed to discriminate the whiskies produced from the different breweries but within the same geographical locations. For example, discriminating the Scotch single malt made in the different breweries of the highlands.

#### **9.4 HEADSPACE AND DIRECT ANALYSIS OF URINE**

The objective of this study was to extend the application of PTR-MS by detecting and quantifying different VOCs from the urine samples by using HIS coupled with the Leicester PTR-MS. It was hoped that in future this technique would be used alongside the breath analysis in clinical setting to identify and analyse potential biomarkers for different diseases. In total five healthy volunteers within the Department of Chemistry at the University of Leicester were selected in the study. All the volunteers were on mixed diet and one of the volunteer was an occasional smoker. The effect of salt and pH on the VOCs was

investigated alongside the identification and quantification of different VOCs was also performed during the study.

In total 18 different VOCs were identified and quantified from of urine. These VOCs are different ketones, aldehydes, alcohol, aromatic hydrocarbons, nitrogen containing compounds and acetonitrile. Further four VOCs (3-hydroxybutyric acid, acetic acid, isoprene and ethyl acetate) were also tentatively identified by literature survey.

During the course of the study, it was noticed that when urine sample was injected directly, better sensitivity was observed compared to the headspace analysis. The urine is a complex mixture of water, electrolytes, organic acids, nitrogen-containing compounds, hormones and enzymes. During the early phase of the study, when direct injection of urine sample was made, instrumental problems were occurring mainly around the drop in the count rate. After the investigation, it was concluded that the urine is a complex mixture of different compounds, when directly injected; it blocks the orifice between drift tube and TOF-MS. Therefore, further research is required to find a suitable way to filter out the urine samples to prevent the blockage of the orifice without affecting the sensitivity of the method.

## **9.5 ANALYSIS OF SEMI-VOLATILE COMPOUNDS**

Historically, the PTR-MS is mainly used for the analysis of the volatile compounds with the molecular weight in the region of 25 – 150 g/mol. This study was performed by the use of the HIS to identify and analyse the semi-volatile compounds with the molecular weight in the region of 150 – 350 g/mol. After the careful consideration, compounds were selected based on their physical properties *e.g.* vapour pressure, physical appearance. It was decided to use semi-volatile organophosphate pesticides, which are in the liquid form and have a high vapour pressure. The pesticides used in the study were parathion,

methyl-parathion, pirimiphos-methyl, phorate, diazinon, fenthion, triazophos, atrazine and ethion.

The compound identification was performed by preparing the solution of >99% pure pesticides reference material in organic solvent. The portion of the solution was injected to the HIS source and data were collected. The mass spectrum for the protonated compounds was observed for all the compounds used in the study for analysis.

For the analysis, two methods were employed. First method was direct injection and second method was liquid-liquid extraction (LLE). For the direct injection technique, sample was directly injected to the HIS source. In the LLE method salt was added to the sample followed by the hexane/toluene mixture for the extraction. The sample and solvent mixture was mixed for at-least 8 – 10 minutes at 30°C and portion of organic solvent layer was injected.

Relatively poor sensitivity was observed with the direct injection technique in comparison to the LLE. Therefore, LLE was used for the future experiments in the study. The sensitivity and LoD of the technique was established. The observed LoD was sufficiently high to achieve maximum residue limit (MRL) set by the Health and Safety Executive (HSE) and European Parliament, but the sensitivity of the technique was lower compared to the established techniques. Numbers of different factors are possible for the lower sensitivity of the technique. For example, low sample and injection volume used in the study, temperature of the HIS, lack of pre-concentration step during the extraction and non-availability of the chromatographic separation. The sensitivity of the current study can be increased by the use of extraction technique such as solid phase micro extraction (SPME), QuEChERS (quick, easy, cheap, effective, rugged, and safe) [3] and by optimising the current LLE technique by finding the ideal solvent amount,

extraction time, extraction temperature and addition of pre-concentration step will also increase the sensitivity.

Even-though, lower sensitivity was observed in the current study, it establishes the good platform for the analysis of the semi-volatile and possibly non-volatile compounds by the use of PTR-MS. It is understood that this technique will not replace the established technique and will also lose the real-time analysis ability but hopefully it will be a good complementary technique where quick analysis is required.

## **9.6 TWO-STAGE PTR-MS**

The two-stage technique was established and discussed in this thesis. This technique was developed to provide an easier alternative to the currently available techniques, which requires either different reagent ion and extensive data analysis or the use of different mass analyser for the identification of the isobaric compounds.

## **9.7 FINAL COMMENTS**

The work covered here represents the exploratory studies that tested the capabilities of the PTR-ToF-MS for analysis of the liquid samples by discriminating the different whiskies, measuring and quantifying the VOCs from the urine headspace and analysis of the semi-volatile compounds. While a number of interesting preliminary results have been reported, follow-up investigations are required to substantiate these early findings. The good base has been established for the measurement of the semi-volatile compounds, where further research can lead to the new interesting application possibly for some clinical diagnostics or in the measurement of the environmental pollutants. Simultaneous study for the measurement of the potential biomarker from breath analysis and from urine headspace can complement and confirm the findings from the clinical research. As such, direct injection

analysis with PTR-MS is both a highly interesting and rewarding field of research.

## 9.8 REFERENCES

1. Jardine, K.J., et al., Dynamic Solution Injection: A new method for preparing pptv-ppbv standard atmospheres of volatile organic compounds. *Atmospheric Measurement Techniques*, 2010. 3(6): p. 1569-1576.
2. Jurschik, S., et al., Direct aqueous injection analysis of trace compounds in water with proton-transfer-reaction mass spectrometry (PTR-MS). *International Journal of Mass Spectrometry*. 289(2-3): p. 173-176.
3. <http://www.restek.com/pdfs/GNAN1097A.pdf>

---

**Conference/Meeting Presentation**

---

Two-stage Proton Transfer Reaction Time-of-Flight Mass Spectrometry	23 <sup>rd</sup> May 08
Analysis of semi-volatile compounds by PTR-TOF-MS	21 <sup>st</sup> June 10
Sensory Systems for Environment Monitoring	14 <sup>th</sup> October 10
60th ASMS Conference, Vancouver, British Columbia, Canada	19 <sup>th</sup> May 13 to 24 <sup>th</sup> May 13

---

---

**Publications**

---

R.S.Blake, M.Patel, P.S.Monks, A.M.Ellis, S.Inomata and H.Tanimoto (2008) Aldehyde and ketone discrimination and quantification using two-stage proton transfer reaction mass spectrometry, International Journal of Mass Spectrometry, 278 (1), 15-19

---